BULLETIN OF RUSSIAN STATE MEDICAL UNIVERSITY

BIOMEDICAL JOURNAL OF PIROGOV RUSSIAN NATIONAL RESEARCH MEDICAL UNIVERSITY

SUBMISSION http://vestnikrgmu.ru/login?lang=en
CORRESPONDENCE editor@vestnikrgmu.ru
COLLABORATION manager@vestnikrgmu.ru
ADDRESS ul. Ostrovityanova, d. 1, Moscow, Russia, 117997

Indexed in Scopus. CiteScoreTracker: 0.15

Indexed in WoS since 2018

Five-year h-index is 3

Indexed in RSCI. IF 2017: 0.326

Listed in HAC 27.01.2016 (no. 1760)

Open access to archive

Issue DOI: 10.24075/brsmu.2019-02
The mass media registration certificate no. 012769 issued on July 29, 1994
Founder and publisher is Pirogov Russian National Research Medical University (Moscow, Russia)

Approved for print 30.04.2019
Circulation: 100 copies. Printed by Print.Formula
www.print-formula.ru

ВЕСТНИК РОССИЙСКОГО ГОСУДАРСТВЕННОГО МЕДИЦИНСКОГО УНИВЕРСИТЕТА

НАУЧНЫЙ МЕДИЦИНСКИЙ ЖУРНАЛ РНИМУ ИМ. Н. И. ПИРОГОВА

ПОДАЧА РУКОПИСЕЙ http://vestnikrgmu.ru/login
ПЕРЕПИСКА С РЕДАКЦИЕЙ editor@vestnikrgmu.ru
СОТРУДНИЧЕСТВО manager@vestnikrgmu.ru
АДРЕС РЕДАКЦИИ ул. Островитянова, д. 1, г. Москва, 117997

Журнал включен в Scopus. CiteScoreTracker: 0,15

Журнал включен в WoS с 2018 г.

Индекс Хирша (h^5) журнала по оценке Google Scholar: 3

Журнал включен в РИНЦ. IF 2017: 0,326

Журнал включен в Перечень 27.01.2016 (№ 1760)

Здесь находится открытый архив журнала

DOI выпуска: 10.24075/vrgmu.2019-02
Свидетельство о регистрации средства массовой информации № 012769 от 29 июля 1994 г.
Учредитель и издатель — Российский национальный исследовательский медицинский университет имени Н. И. Пирогова (Москва, Россия)

Подписано в печать 30.04.2019
Тираж 100 экз. Отпечатано в типографии Print.Formula
www.print-formula.ru

BULLETIN OF RSMU **2, 2019**
ВЕСТНИК РГМУ

Contents
Содержание

PRECISION ONCOLOGY: MYTH OR REALITY?

Slavyanskaya TA[1,2] ✉, Salnikova SV[1,2]

[1] Peoples' Friendship University of Russia, Moscow, Russia

[2] Institute of Immunophysiology, Moscow, Russia

Cancer incidence rates are growing at an alarming pace pressing for the development of innovative personalized approaches to treating this disease. The absence of clinical symptoms in the early stages delays the onset of adequate treatment. Traditional therapies are not always as effective as they should be and do not guarantee long-lasting relapse-free survival. Metastatic cancers pose a particular challenge to healthcare professionals. This review touches upon the immunologic mechanisms underlying the development of malignancies, talks about conventional and innovative therapeutic modalities, such as targeted, gene or specific immunotherapies, and analyzes the literature on the use of different approaches that form a basis for precision oncology.

Keywords: cancer, nonspecific immunotherapy, cytokine therapy, targeted therapy, monoclonal antibodies, immune checkpoints, cancer vaccines, gene therapy, nanotechnologies, precision medicine

Author contribution: Slavyanskaya TA conceived and planned this review, collected, analyzed and interpreted literature data, reviewed the manuscript, provided images, and wrote conclusions. Salnikova SV collected and analyzed literature data and prepared the draft of the manuscript.

✉ **Correspondence should be addressed:** Tatiana A. Slavyanskaya
Miklouho-Maclay 6, Moscow, 117198; tslavyanskaya@gmail.com

Received: 24.08.2018 **Accepted:** 25.03.2019 **Published online:** 31.03.2019

DOI: 10.24075/brsmu.2019.018

ПРЕЦИЗИОННАЯ МЕДИЦИНА В ОНКОЛОГИИ: МИФ ИЛИ РЕАЛЬНОСТЬ?

Т. А. Славянская[1,2] ✉, С. В. Сальникова[1,2]

[1] Российский университет дружбы народов, Москва, Россия

[2] Институт иммунофизиологии, Москва, Россия

Бурный рост числа онкологических заболеваний во всем мире диктует необходимость разработки новых, инновационных и персонализированных подходов к их лечению. Отсутствие клинических проявлений на ранних стадиях болезни не позволяет своевременно назначить адекватную терапию. Традиционные методы лечения, не всегда обладающие удовлетворительной эффективностью, не предотвращают рецидивирование, не обеспечивают достаточную ремиссию и продолжительность жизни больного. Значительные трудности представляет собой лечение инвазивного, метастатического рака. В статье представлен краткий обзор иммунологических механизмов развития злокачественных новообразований, современных традиционных и инновационных методов лечения рака, а также анализ литературных данных по использованию методов таргетной, генной терапии, специфической иммунотерапии и других подходов, лежащих в основе прецизионной медицины в онкологии.

Ключевые слова: рак, неспецифическая иммунотерапия, цитокинотерапия, таргетная терапия, моноклональные антитела, иммунные чек-поинты, противоопухолевые вакцины, генная терапия, нанотехнологии, прецизионная медицина

Информация о вкладе авторов: Т. А. Славянская — идея и план написания обзора, сбор и анализ литературы, интерпретация данных, рецензирование статьи, подбор рисунков, написание выводов; С. В. Сальникова — сбор и анализ литературы, подготовка черновика рукописи.

✉ **Для корреспонденции:** Татьяна Александровна Славянская
ул. Миклухо-Маклая, д. 6, г. Москва, 117198; tslavyanskaya@gmail.com

Статья получена: 24.08.2018 **Статья принята к печати:** 25.03.2019 **Опубликована онлайн:** 31.03.2019

DOI: 10.24075/vrgmu.2019.018

Fighting cancer is still a top priority for global healthcare. The overall success achieved in treating a wide range of diseases [1–3], including malignancies [4–10], over the past few decades is indisputable. Advances in molecular biology, genetics and immunology have shed light on the immunogenetic and immunobiological features of tumors and expanded our knowledge of the protective role of the innate and adaptive immunity against cancer. There is convincing evidence that the efficacy of immunotherapy depends on the immunologic components of a tumor. Research into the mechanisms underlying cancer development and the processes unfolding in the tumor microenvironment [11] has paved the way to new strategies and integral approaches to treating malignancies [12–14]. The discovery of new therapeutic targets and the development of innovative methods for personalized therapy can improve treatment outcomes in patients with cancer [4, 5, 15, 16].

The role of the innate and adaptive immunities in anticancer defense

Rapid proliferation of cancer cells is caused, in the first place, by a breach in the immune defense (the cancer-immunity cycle) that allows cancer cells to evade the immune system. Three phases of immunoediting, a model of cancer development, include elimination, equilibrium and escape that either control or promote tumor growth. In the elimination phase, the initiated T-cell response is guided against malignant cells. During the equilibrium phase, limited immune control allows cancer cells to be in a state of dormancy and mutate. The inhibitory attacks of T cells drive the escape phase characterized by both local tumor growth and the spread of metastases [17–19].

Innate immunity

Malignant cells are eliminated by natural killers (NK), natural killer T cells (NKT), gamma-delta T cells (γδ-T), macrophages, and granulocytes.

NK play the key role in non-specific elimination of tumor cells. Their functions are regulated by cytokines (IL2, IL15), co-stimulatory molecules (CD40, CD70, CD80, CD86, ICOS) and killer activation receptors (NKp30, NKp44, NKp46, NKp80) that, apart from producing IFNγ and perforins, mediate the effector function of NK and inhibitory receptors (KIR, CD94) [18, 19].

NKT cells constitute a subset of lymphocytes expressing both NK markers and T-cell differentiation antigens. The effector function of NKT relies on the presence of granulocyte-macrophage colony-stimulating factor (GM-CSF) and IL12 [20]. NKT are crucial regulators of immune response that confer protection against tumor nascence, growth and metastasis.

γδ-T cells localized in the epithelium of the skin, gastrointestinal tract and urogenital system are a bridge between the innate and adaptive immunities. They can act as antigen-presenting cells (APC) [18].

It is impossible to estimate the contribution of granulocytes and macrophages in the early stages of carcinogenesis. In the advanced stages, macrophages promote tumor growth [18].

Adaptive immunity

Antigen presentation by APC is essential for activating the adaptive immunity. In most cases antigen presentation is done by dendritic cells (DC); however, endothelial cells, B lymphocytes and even cancer cells can also act as APC [19]. Apart from that, DC are involved in inducing and maintaining self-tolerance.

In healthy individuals, an adequate immune response is initiated by signal exchange between DC and T helper cells (Th) that can come into direct contact with each other or "communicate" at a distance. Their direct interaction is facilitated by a group of molecules on a T-cell membrane. Specifically, a number of consecutive interactions occur between CD2, MHC class II complexed to an antigen, CD40, ICAM I, CD 80/86, and CD 83 on the surface of APC and the following receptors on the Th surface: CD58, TCR, CD154, CD11a/CD18, CD28, and CD152.

The signal is transmitted into the cell by a group of second messengers, the most well studied being inositol trisphosphate, calmodulin and a group of kinases associated with T-cell receptors. The result of their direct and indirect interaction is the activation of Th1 and Th2 and, respectively, cellular and humoral immunity.

In terms of anticancer defense, the cell-mediated immune response is more important than the humoral immune component. T cells express a variety of receptors known for the ability to stimulate or inhibit the activation of their secretors (Fig. 1). The effect of T-cell activation is determined by how much those receptors are involved. Research into co-inhibitory T-cell receptors, as well as into monoclonal antibodies (mAb) that block inhibitory molecules on the surface of immunocompetent and tumor cells, seeks to improve the efficacy of the antitumor immune response.

A few *in vivo* studies have demonstrated that antibody-dependent cellular cytotoxicity also contributes to the elimination of cancer cells. In advanced stages of cancer, the humoral immunity prevents malignant cells from being killed [18, 19].

A tumor, especially a nascent one, does not produce antigens that would distinguish it from healthy tissue and is not recognized by the body as "foreign".

During the equilibrium phase, tumor cells that survived previous attacks continue to mutate and proliferate, and angiogenesis is activated. DC and macrophages emerge in the tumor microenvironment. A tumor clone is formed from the mutated cancer cells. In this phase, the immune system behaves like it did in the surveillance phase, but oncogenic processes prevail over protective immunological reactions, and the tumor gradually grows in size.

The escape phase is characterized by a shift towards immune suppression regulated by cytokines, an imbalance in the number of effector and suppressor immunocompetent cells, defective antigen recognition and presentation, and impaired signal transduction into the cell [19].

Cytokines are regulatory peptides secreted by the body. Transforming growth factor beta (TGF-β_{1-3}) is a regulatory peptide that participates in a variety of biological processes, including carcinogenesis, wound healing, and maintenance of immunological homeostasis. TGF-β_s exerts its biological functions via types I and II serine/threonine receptors (TGF-βRI, TGF-βRП). This cytokine promotes immunological tolerance by sending signals to $CD4^+$- and $CD8^+$-lymphocytes and NK cells. TGF-β guides the differentiation of $CD4^+$ cells into regulatory subpopulations ($CD4^+CD25^+$ T-regulatory cells or natural Tregs), inhibits the expression of perforins, granzyme B and FAS-ligand in $CD8^+$-lymphocytes, suppresses the IL12-induced production of IFN-r by NK [20–22].

Interleukin IL10 exerts its functions via IL10R1 and IL10R2 receptors localized on the surface of DC and Th cells. It inhibits the production of IL12 and co-stimulatory molecules, downregulates the expression of MHC class II antigens on DC, disrupting their maturation, and blocks cytokine secretion by $CD4^+$-cells [19]. The IL23 heterodimer consists of two subunits, one of which (p40) is identical to that of IL12. Both IL23 and IL12 are secreted by innate immunity cells but regulate the functions of adaptive immunity components. IL12 promotes T-cell maturation and triggers the production of IL6, IL15, IL18, TNFβ, and GM-CSF, while IL23 promotes the differentiation of immature cells into Th17 and stimulates the secretion of IL17, IL17F, IL6, and TNFα. Some studies have demonstrated that IL23 stimulates angiogenesis by upregulating the expression of matrix metalloproteinase 9 (MMP9) [18, 19, 22].

Vascular endothelial growth factor (VEGF) is a major proangiogenic factor produced by both tumors and immune competent cells. So far, 7 VEGF isoforms are known of which VEGF-α has the most significance for angiogenesis and immunomodulation. VEGF inhibits DC maturation and promotes the secretion of immature myeloid cells (iMC) that, in turn, suppress T-cell activity [19].

The tumor microenvironment is the main battlefield in the fight between the immune system and a tumor. In the escape phase, the proportion of immature DC and Tregs in the general cell population increases. Mature DC express on their surface CD40, CD80, CD83, and CD86 and secrete high levels of IL12. VEGF, IL6, TGF-β, IL10, COX-2, PGE2, and gangliosides found in the tumor microenvironment prevent DC from differentiating and maturing, rendering impossible an adequate immune response [19].

Regulatory T cells are components of the adaptive immunity. They are derived from immature T cells and suppress the effective immune response by regulating the functions of effector cells. At present, 3 Treg types are distinguished: $CD4^+CD25^+Foxp3^+$, Treg1 and Treg2 cells (formerly known as Th3); both Treg1 and Treg2 cells are induced Tregs. Besides them, there are suppressors with a $CD8^+$ phenotype but their function is still poorly understood. The major role in immune suppression in cancer patients is played by $CD4^+CD25^+$ Tregs originating in the bone marrow. Their concentrations are highly elevated in patients with breast, colorectal, lung, or pancreatic cancers. These cells arise from the same precursors as Th cells in the presence of the increased concentrations of TGF-β, IL10 and VEGF. The mechanism underlying the suppressor effect of $CD4^+CD25^+$ Tregs is associated with the secretion of suppressor cytokines (TGF-β, IL10), competition for ligands (IL2), induction of DC tolerance, and in some cases their direct lysis [23].

Molecular abnormalities in DC and lymphocytes are another important characteristic of the escape phase. Specifically, this phase is characterized by the loss of expression of MHC class I and II molecules, CD80, CD86, and CD154 on the surface of tumor cells, as well as low expression of Th TCR ξ-chain [23].

Not only the functional activity of lymphocytes is disrupted in cancer development; the expression of integrins on the surface of tumor cells and their composition also change. This can reduce the strength of cell-cell contacts and promote neoangiogenesis. The abnormal expression of selectins (CD44, ELAM-1) on the surface of cancer cells correlates with poor clinical outcome.

Gangliosides significantly contribute to the suppression of lymphocyte response in the tumor microenvironment. Among them are GD1a, GD2, GD3, GM1, and GM2 expressed on the surface of cancer cells and then shed into the extracellular matrix. They are capable of suppressing the function of tumor-infiltrating lymphocytes (TILs) by interfering with signal transduction. The impaired effector function of lymphocytes is reflected in the reduced expression of granzyme B and kinases complexed with TCR-p59fyn and ZAP-70.

A declining proliferative index, the reduced expression of α- and β-subunits of the IL2 receptor, and the low phosphorylation degree of the protein encoded by *Rb* all signal compromised immunity. Such changes typically affect peripheral lymphocytes and tumor-infiltrating cells but their severity varies. The expression levels of IL2 receptor, TCR ξ-chain, CD54, and some other molecules amount to about 80% for peripheral lymphocytes (relative to the norm observed in healthy individuals) and 30% for tumor-infiltrating lymphocytes [23]. The changes listed above are typical for patients with local or disseminated cancers.

Summing up, the immune system has a pivotal role in fighting malignancies. In patients with cancer, immunodepression is multifactorial; the situation is often exacerbated by the ability of a tumor clone to resist the attacks of effector cells. At the same time, the understanding of key mechanisms underlying tumor growth and its escape from immune surveillance has become a springboard for specific immunotherapy that forms a basis for precision oncology.

Innovative methods of treating malignancies

The idea of using nonspecific immunotherapy (NSIT) in patients with cancer is not new. The BCG vaccine alone or in combination with IL or anti-IL monoclonal antibodies (mAb against IL) has been long used to prevent recurrences in patients with urothelial cancer (UC) [6, 24]. It has been established that a combination of BCG-based NSIT and some *toll-like receptors* (TLR2, TLR4, TLR9, TRAIL) reduces the relapse rate. TLR7 and TLR9 agonists have also shown promise in a series of clinical trials [25].

At present, increasing attention is being paid to *adaptive immunotherapy*, a method based on inoculating the patient with his/her own immune cells activated in vitro [6].

Targeted therapy with mAb has become a real breakthrough in the management of cancer. mAb bind to the growth factors and receptors that are abundantly expressed by many human cancers and, therefore, can be regarded as a potential therapeutic target [26]. Researchers are currently studying the antitumor effect of therapeutic agents involved in angiogenesis, including VEGF, EGFR (epidermal growth factor receptor) and some others [27].

Angiogenesis inhibitors are also in the focus of scientific research. However, little is known about their effect on a tumor's blood vessels. Studies of VEGF inhibitors (AG013736 and VEGF-Trap) have shown that these molecules halt angiogenesis or cause the existing tumor vessels to regress. They induce early and persistent changes in endothelial cells, pericytes and the vascular basement membrane in RIP-Tag2 transgenic mice with spontaneous pancreatic islet cancer and in mice with subcutaneously transplanted Lewis lung

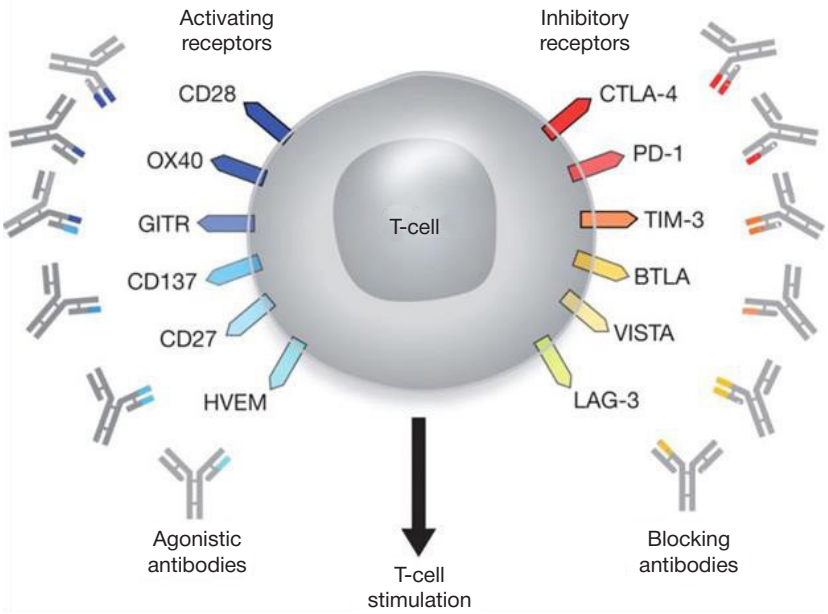

Fig. 1. T-cell activating and inhibitory receptors [21]. T cells express a variety of receptors known for the ability to stimulate or inhibit the activation of their secretors. The effect of T-cell activation is determined by how much those receptors are involved. *Inhibitory receptors*: CTLA-4 — cytotoxic T-lymphocyte antigen 4, a negative regulator of T-cell activation; PD-1 — programmed cell death 1 receptor. PD-1 plays an important role in the negative regulation of the immune system by preventing the activation of T cells, increasing self-tolerance and reducing autoimmunity; TIM — T-cell immunoglobulin mucin protein BTLA or B- and T-lymphocyte attenuator — an antigen that attenuates B- and T-cell functions; it participates in the regulation of T cells in the immune response. It is encoded by the BTLA gene. BTLA is expressed following T-cell activation and stays on the surface of Th1, but not Th2 cells. VISTA — V-domain Ig suppressor of T-cell activation; LAG-3 (CD223) — lymphocyte-activation gene. *Activating receptors*: CD28 — a co-stimulatory receptor; OX40 — a co-stimulatory receptor; GITR — a glucocorticoid-induced TNF receptor; CD137 — a co-stimulatory receptor; CD27 — a co-stimulatory receptor; HVEM — a membrane protein from a superfamily of tumor necrosis factor receptors 14 (TNFRSF14) and a herpes virus entry mediator

carcinomas. For example, an over 70% decline in vascular density was observed following treatment with angiogenesis inhibitors; the remaining endothelial cells acquired a normal phenotype and expressed less EGFT [27].

Integrins facilitate contacts between cells and the extracellular matrix, control cell proliferation, survival, migration, and adhesion [28]. The role of integrins in immune surveillance in general and their expression levels in particular are being studied extensively. At present, several integrin-targeting mAb are undergoing clinical trials, including etaracizumab and cilengitide [29, 30]. Although etaracizumab (a mAb that recognizes integrin αvβ3) demonstrated its efficacy against a range of tumors in phase I clinical trials, the results were not confirmed during phase II [29]. By contrast, the efficacy of cilengitide (a mAb that recognizes integrins αvβ3 and αvβ5) against glioblastomas and its good tolerance were confirmed in phase I and II clinical trials; in 69% of cases, 6-month relapse-free survival was observed [31].

Other molecules may also have a potential to become therapeutic targets, especially those participating in transmitting signals that suppress immune response in the tumor environment. Many leukocytes express an *integrin-associated protein* CD47 (membrane receptor protein) on their surface. It is capable of binding to beta-3-integrin, thrombospondin-1, signal-regulatory alpha protein (SIRP-α) and other signal proteins involved in the regulation of T-cell activation, cell migration, phagocytosis, and other activities of the immune system. CD47 is expressed by tumors and cancer stem cells, allowing the latter to survive and therefore leading to late relapses. A combination of CD47 and mAb has proved to be effective against acute lymphocytic leukemia, acute myeloid leukemia, and leiomyosarcoma in mouse models. At present, a phase I clinical trial is ongoing aimed at studying CD47 inhibition in patients with UC and acute myeloid leukemia [32].

Tumor necrosis factor receptors (TNF-R), such as glucocorticoid-induced TNF-R (GITR, CD357), CD27, OX40 (CD134) and 4-1BB (CD137), are a family of proteins responsible for transducing additional co-stimulatory signals required to activate T lymphocytes that participate in eliminating cancer cells. In order to use this important signaling cascade, agonistic mAb and specific ligand complexes were developed capable of interacting with TNF-R and initiating further reactions [33]. Varlilumab, a human IgG1 agonistic mAb targeting CD27 (aCD27), has already successfully completed a phase I clinical trial. Experimental studies in mice have shown that its combination with antiPD-1 leads to 100% elimination of tumor cells due to the ability of aCD27 to stimulate cytotoxic T lymphocytes. The response to varlilumab was stronger than to a combination therapy with aPD-1/aCTLA-4 [33].

The colony stimulating factor 1 receptor (CSF1R) is a cell surface receptor expressed by macrophages and monocytes. CSF1R signaling activates macrophages (M) and promotes their transformation into phenotype M2 (M2 macrophages participate in type 2 T-helper-mediated immune reactions and stimulate cell proliferation and angiogenesis). CSF1R blockade or depletion of cells expressing CSF1R facilitate macrophage differentiation into type M1; M1 macrophages stimulate the production of proinflammatory cytokines and cytotoxic molecules and are also involved in type 1 T-helper immune reactions. The efficacy of CSF1R inhibition has been demonstrated in the experiments conducted in animals [34]. Currently, a combination of a CSF1R inhibitor Plexxikon (PLX3397) and pembrolizumab is undergoing phase I and II clinical trials in patients with progressing malignancies. A few companies have synthesized mAb targeting CSF1R (FPA008, Five Prime Therapeutics; Emactuzumab, Hoffmann-La Roche).

Successful immunotherapy is impossible without understanding the processes occurring in the tumor microenvironment. The scope of tumor infiltration by T cells is a crucial factor, which can be estimated by studying macrophages, vascular endothelial cells, fibroblasts, and immunosuppressive metabolites, such as kynurenine, in the tumor microenvironment [7].

Tregs are potent *immunosuppressors* present in the tumor microenvironment. Experimental attempts were made to inhibit

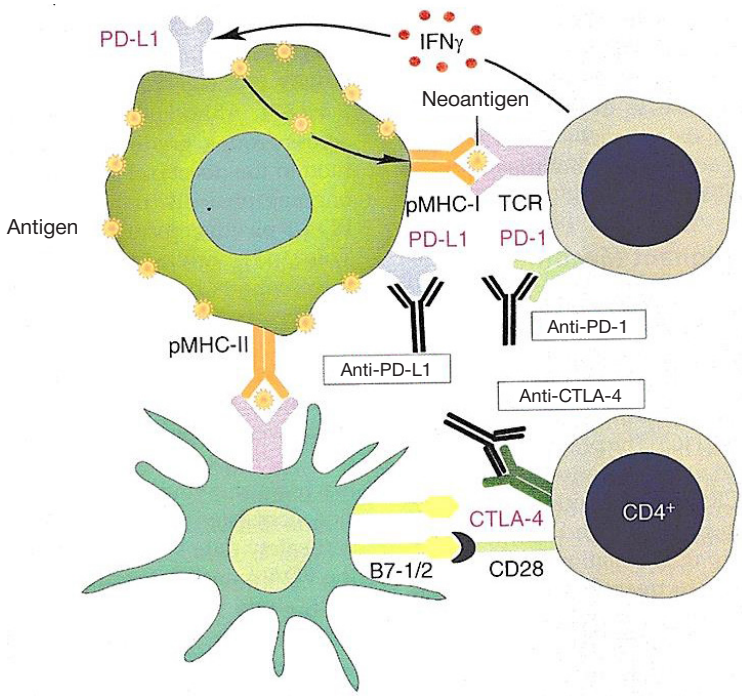

Fig. 2. The mechanism of neoantigen recognition and immune checkpoint blockade [42]. Anti-PD-1, anti-PDL-1 and anti-CTLA-4-antibodies block signaling pathways, facilitating neoantigen recognition and T cell activation. CD4+ — T cells expressing cluster of differentiation antigen 4 (CD4); recognizes MHC class II antigens; CD28 — T cells expressing cluster of differentiation antigen 28; CTLA-4 — antigen 4 associated with cytotoxic T lymphocytes; IFN — interferon; PD-L1 — programmed death-ligand 1; PD-1 — programmed cell death 1 receptor; pMHC — peptide-major histocompatibility complex receptor complementary to TCR; TCR — a T-cell receptor

Tregs by mAb and DC-based vaccines [7]. Tregs accumulate in the blood, ascitic fluid, metastases, and primary tumors. Clinical studies of daclizumab, sorafenib, sunitinib, and imatinib demonstrate that these mAb reduce Treg levels in patients with cancer, correlating with survival rates [7, 8]. A few research teams investigated the inhibitory effect of Tregs in combination with infiltrating myeloid-derived suppressor cells (MDSC) on the immune response to cancer progression in patients with renal cell carcinoma and soft tissue sarcoma [8]. In a preclinical study, MDSC exhibited sensitivity to a TRAIL-receptor 2 (TRAIL-R2) agonist. A phase I clinical trial has shown that TRAIL-R2 (DS-8273a) effectively lowers MDSC levels in 50% of patients with advanced UC, melanoma or hepatocellular carcinoma, but does not affect neutrophils, monocytes and other lymphoid and myeloid populations. A drop in MDSC negatively correlates with relapse-free survival [7, 8].

Low peripheral blood Tregs and a shift in the immune balance towards an effective immune response can be achieved by administering tyrosine kinase inhibitors (sorafenib). In a clinical study, neoadjuvant therapy with sorafenib caused a significant drop in the proportion of tumor-infiltrating Tregs in comparison with patients who did not receive the drug: 17.3% vs 28.1% on average (p = 0.046) [35]. The activity of Tregs in patients with renal cancer, leukemias, and gastrointestinal stromal tumors can be downregulated by daclizumab, sorafenib, sunitinib, and imatinib [36, 37].

Studies of the tumor microenvironment have stressed the role of intercellular adhesion molecules. Poor intercellular adhesion is typical for the majority of epithelial cancers. The key component of intercellular adhesion in epithelial tissue is *E-cadherin*. The loss of its expression is observed in almost 85% of lobular breast carcinomas; besides, its expression is extremely suppressed in esophageal, gastric and hepatocellular carcinomas [38]. Slowly growing and benign tumors preserve normal levels of E-cadherin expression. The suppression or the total loss of E-cadherin correlates with tumor invasiveness, metastatic spread and poor clinical outcome [39].

The discovery of regulatory molecules responsible for preventing the hyperactivation of T lymphocytes and their programmed death has paved the way to an innovative method of targeted immunotherapy called *immune checkpoint blockade* (ICPB). It has already received approval as a standard therapy for many types of cancer. There have been experiments with neoadjuvant and adjuvant ICPB regimens. Tumors with identical histological characteristics demonstrated suppressed the immune system in a variety of different ways. They modulated PD-1 expression or had different levels of infiltrating lymphocytes in their microenvironment [40, 41]. ICPB is used to block a tumor's systems of control and restore the anticancer immune response (Fig. 2). Among immune checkpoint blockers are anti-CTLA-4 (ipilimumab), anti-PD-1 (pembrolizumab and nivolumab) [43] and anti-PD-L1 (avelumab, atezolizumab). All of them have been proved to be highly effective against a number of malignancies, including advanced UC. The success of PD-1 and PD-L1 inhibitors reminds us of the versatility of immunotherapy as a cancer-treating modality. These drugs have become a standard therapeutic option for a few types of malignant tumors.

A combination of standard chemotherapy (CT) and ipilimumab stimulates the activity of $CD4^+$-and $CD8^+$-T-cells, as well as the production of proinflammatory cytokines (IL2, IL12) and GM-CSF [44]. However, since ipilimumab is very toxic, its use in patients with UC is limited. Pembrolizumab has been approved for first- and second-line treatment of metastatic UC, whereas nivolumab is recommended as a second-line therapy after platinum-based CT regimens have been exhausted [9].

Clinical trials show that PD-1 and CTLA-4 pathways have an irregular role in inhibiting the immune response to cancer growth [10, 45]. A combination of nivolumab and ipilimumab has proved to be more effective in patients with metastatic melanoma than monotherapy. In 2016, a combination therapy with these two drugs was approved for inoperable or metastatic melanoma [43]. Durvalumab and avelumab (antiPD-L1 inhibitors) have also been approved for clinical use [46].

Immunotherapy of malignancies with *4-1BB agonists* renders possible *in vivo* tumor elimination [33]. At present, two agonistic mAb against human 4-1BB (a4-1BB) are undergoing clinical trials (urelumab, IgG4 mAb, and utomilumab, IgG2 mAb) [33, 47]. To guide the immune response against tumor cells, a drug (PRS-343) has been developed consisting of agonistic mAb against 4-1BB and mAb against HER2 (trastuzumab) [33].

Another area of research looks at the possibility of inducing an antitumor immune response by *activating the genes involved in innate immunity signaling via STING* (a transmembrane protein 173 that contributes to immune response modulation by stimulating production of type I interferon, IFN-I) and TLR. In a preclinical trial, TLR boosted the secretion of cytokines inducing the immune response mediated by Langerhans cells, macrophages and lymphocytes, and stimulated proliferation of T cells via a protein kinase pathway. At the same time, TLR agonists inhibit tumor growth, averting the suppression of the anticancer immune response in the tumor microenvironment [48]. For example, Imiquimod (a TLR agonist) is reported to be effective against glioma, melanoma and breast cancer in 72% of patients [49]. In addition, some authors suggest that TLR agonists can be used as adjuvants for cancer vaccines [18, 49–51].

The T-cell chimeric antigen receptor (CAR) has recently been in the focus of scientific research. It is a membrane receptor capable of binding to a specific cancer antigen and containing an intracellular domain that activates a T cell in the presence of this antigen [52]. CAR-T cells can initiate co-stimulatory signaling (for CD28 or CD137) that activates T cells and entails a sustained immune response [53].

Another strategy is a *combination immunotherapy* involving the use of *oncolytic viruses*, such CD40L- or 4-1BBL-expressing adenoviruses. This type of treatment is intended to stimulate immunity against cancer by delivering specific agents into the tumor microenvironment that are capable of triggering T-cell reactions, alone or in combination with other immunologic drugs [54]. However, design of such combinations targeting the cells of a particular tumor poses a certain challenge.

A number of therapeutic combinations are being tested at the moment in prostate cancer and sarcoma models, including an agonistic mAb against OX40 with atezolizumab (aPD-L1); an agonistic mAb against OX40 with bevacizumab (the latter is a recombinant humanized anti-VEGF mAb); and an agonistic mAb against (PF-04518600) with an agonistic mAb against a4-1BB (NCT02315066) [55]. Avelumab (mAb against aPD-L1) can be used in a range of combinations, including avelumab + 4-1BB agonist (PF-05082566); avelumab + an agonistic mAb against OX40 (PF-04518600); avelumab + mAb against colony stimulating factor 1 (PD 0360324); Avelumab + mAb against 4-1BB and mAb against OX40 (NCT02554812). The combination therapy with mAb against OX40/CTLA-4 has been shown to improve survival and promote tumor regression [56, 57].

At the moment, there are ongoing phase I clinical trials of the following combination of drugs in patients with stage III/IV melanoma: humanized IgG1 mAb that do not contain aglycosyl (an agonist of the glucocorticoid-induced tumor necrosis factor receptor, GITR) + nivolumab or ipilimumab or both drugs [58].

GR-MD-02 is a constituent of another interesting therapeutic combination. It is a drug that specifically inhibits *Galectin-3*. Galectin-3 is a marker of tumor transformation that participates in the regulation of all processes involved in tumor progression. It is active in many different cancers, and its expression levels correlate with a tumor's metastatic potential and poor clinical prognosis. Besides, Galectin-3 can have a role in immune suppression. Preclinical trials have shown that GR-MD-02 combined with against OX40 or inhibiting checkpoints improves survival and causes tumor regression, as compared to the regimens based solely on immunotherapy [56]. These findings inspired a phase I clinical trial in patients with advanced cancer in which a combination of a GR-MD-02 inhibitor and ipilimumab or pembrolizumab was tested (NCT02117362, NCT02575404) [33].

Indoleamine 2,3-dioxigenase 1 (IDO1) is a promising therapeutic target. It causes T-cell proliferation to decline and promotes neovascularization, disrupting interferon gamma effects [59]. Currently, IDO1 inhibitors are being tested in combination with other immunomodulating agents; for example, a phase III trial of a PD-1 inhibitor (pembrolizumab) is being carried out in patients with melanoma [60].

Advanced cancer is normally associated with EGFR hyperexpression by cancer cells. The efficacy of cetuximab (C225) has been tested in phase II and III clinical trials. Cetuximab is a recombinant chimeric mAb exhibiting high specificity to an extracellular EGFR domain and capable of competing with natural ligands (EGF, TGF-a) for binding to the receptor. The drug was synthesized from a mouse mAb (M225) attached to a fragment of human IgG1 to reduce immunogenicity. This drug used alone or in combination with cisplatin was then tested for efficacy. Two of 52 patients with progressing head and neck tumors achieved partial remissions [61].

Although most patients benefit from targeted therapy, some of them fail to achieve a full therapeutic response. This dictates the need for developing other, more effective treatment modalities. The use of *cancer vaccines and oncolytic viruses* that boost antitumor immune response by facilitating the presentation of antigens to T cells is an innovative approach that can improve the efficacy of cancer treatment [33, 54].

In animal models, *whole-cell vaccines*, which are essentially cancer cells deprived of the ability to divide, induced a strong anticancer immune response, but their clinical trials were not successful [13, 62, 63].

Peptide vaccines based on the synthetic Survivin peptide (a complex of specific tumor-associated peptides and NY-ESO-1 + GM-CSF with a BCG-NSIT adjuvant) may also hold some promise. A few studies have shown that a personalized peptide vaccine (PPV) consisting of a combination of 4 peptides improves survival rates twofold [54, 63].

Attempts are being made to combine *DC vaccines with co-stimulatory agonists of anti OX40 or with mAb against anti 4-1BB*. The preliminary results of the studies conducted in mice demonstrate that combination vaccines ensure a better immune response in comparison with DC -based vaccines in transgenic Her-2/neu animals, leading to the complete elimination of the tumor [33, 64–67].

A phase II clinical trial of a DC-based Lapuleucel-T vaccine is ongoing. It is seeking to assess survival, safety and immune reactions in patients at a high risk for relapse (hypersecretion of HER-2 + bladder antigen UBC, NCT01353222) [68].

Autologous DC vaccines can initiate and enhance antigen-specific tumor reactions by activating both Th and cytotoxic T cells [67]. This approach is being actively studied in Russia in patients with advanced cancer who have no other therapeutic options left [4, 5, 69]. Autologous DC vaccines have already completed or are now undergoing phase II trials.

Because malignancies are sensitive to immunotherapy, *cancer vaccines* are seen as a promising therapeutic option [70]. Some of them are based on a *cancer-testis antigen* (NY-ESO-1), the *synthetic Survivin peptide* or its combination with IFN-α, and DC with supplemented blockade of the co-stimulatory B7-H1(PD-L1) molecule [71]. However, all those studies are few or still in the planning stage or have no clinical application yet.

Nanomedicine offers unique approaches to treating cancer with novel chemotherapy and immunotherapy drugs. Nanoparticles (NP) have been proposed to increase the therapeutic efficacy and mitigate the adverse effects of CT by directing chemotherapy agents towards cancer tissue and improving their bioavailability [72, 73].

Immunoswitch is a new technology, in which mAb and agonistic mAb bind to nanoparticles [73]. Immunoswitch NP are coated with two different antibodies capable of blocking the signal that inhibits the PD-L1 immune checkpoint and stimulating T cells via 4-1BB costimulatory pathways. *In vivo* research studies have demonstrated a significant delay in tumor growth and improved survival following administration of immunoswitch NP in mouse melanoma and colon cancer models in comparison with treatment with soluble antibodies and NP complexed with antibody inhibitors or stimulators. Immunoswitch NP are reported to improve the density, specificity and function of tumor-infiltrating cytotoxic lymphocytes [73].

Functionalized with specific mAb, NP can be used as a platform for targeted drug delivery to tumor cells, improving therapeutic outcomes and minimizing the side effects of treatment [73–76].

Nevertheless, molecular and cellular mechanisms underlying immune tolerance to tumors remain understudied. Today, NK cells are new promising therapeutic candidates, although their use is now limited to cases of hematological cancer. An experiment conducted in transgenic mice has revealed that natural killers can bind to a platelet-derived growth factor DD (PDGF-DD) via a NKp44 receptor and subsequently halt tumor growth [77].

Gene therapy, including CRISPR-technologies for genome editing, is another new and vigorously developing approach to anticancer therapy.

CONCLUSIONS

Precision (personalized) oncology is becoming a reality. Targeted therapy, nanotechnologies, immune checkpoint blockers, anticancer vaccines, molecular genetic research and the search for new promising targets and ways to overcome immunological tolerance will facilitate the diagnosis and treatment of cancer in its early stages, help oncologists to tailor a therapy to a specific patient and ultimately improve the patient's quality of life. Precision medicine based on a multidisciplinary approach to diagnosis, treatment and rehabilitation of cancer patients is gradually winning over conventional approaches. To benefit the patient, the advances of oncoimmunology should be used in combination with chemo- and immunotherapies. The most effective therapeutic options should be offered first, otherwise the patient will lose the chance to receive any treatment if all other therapies have been exhausted. Clinical efficacy (total survival rates, relapse-free survival and control of the disease), safety (toxicity control), efficiency, and the quality of life are essential components of successful therapy. Treatment strategies vary depending on cancer localization and its biological characteristics.

References

1. Kudryavceva IV, Slavyanskaya TA, Trunov AN, Trunova LA. Urovni autoantitel k jadernym DNK, laktoferrina i nekotorye immunologicheskie pokazateli u bol'nyh revmatoidnym artritom. Bjulleten' Sibirskogo otdelenija Rossijskoj akademii medicinskih nauk. 1999; 19 (3–4): 66–8.
2. Smipnova TA, Ponomapeva EP, Hanfepjan PA, Kolesnikov VV. Opyt primenenija ronkolejkina pri terapii jazvennoj bolezni zheludka, associirovannoj s Helicobacter Pylori, v ambulatornyh uslovijah. Terapevticheskij arhiv. 2009; 81 (2): 30–5.
3. Slavyanskaya TA, Sepiashvili RI, Vishnyakov MN, Chihladze MV. Immunologicheskij monitoring bol'nyh hronicheskim bronhitom v dinamike vosstanovitel'noj immunoreabilitacii. International Journal on Immunorehabilitation. 1999; (11): 70.
4. Slavyanskaya TA, Avdonkina NA, Salnikova SV. Optimizacija uslovij poluchenija zhiznesposobnoj pervichnoj kul'tury kletok urotelial'noj karcinomy. Allergologija i immunologija. 2016; 17 (3): 176–9.
5. Burger M, Thiounn N, Denzinger S, Kondas J, Benoit G, Chapado MS, et al. The application of adjuvant autologous antravesical macrophage cell therapy vs. BCG in non-muscle invasive bladder cancer: a multicenter, randomized trial. J Transl Med. 2010; (8): 54.
6. Camisaschi C, Vallacchi V, Vergani E, et al. Targeting immune regulatory networks to counteract immune suppression in cancer. Vaccines (Basel). 2016; 4 (4): pii: E38.
7. Dominguez G, Condamine TC, Mony S, et al. Selective targeting of myeloid-derived suppressor cells in cancer patients using DS-8273a, an agonistic TRAIL-R2 antibody. Clin Cancer Res. 2016; 23 (12): 2942–50.
8. Sharma P, Retz M, Seifker-Radtke A, et al. Nivolumab in metastatic urothelial carcinoma after platinum therapy (Check-Mate 275): a multicentre, single-arm, phase 2 trial. Lancet Oncol. 2017; 18 (3): 312–22.
9. Larkin J, Chiarion-Sileni V, Gonzalez R, Grob JJ, Cowey CL, Lao CD, et al. Combined nivolumab and ipilimumab or monotherapy in untreated melanoma. N Engl J Med 2015; (373): 23–34.
10. Sepiashvili RI, Beljaev AM. Immunoterapija raka: problemy i perspektivy. Allergologija i immunologija. 2015; 16 (4): 354–7.
11. Salnikova SV, Slavyanskaya TA, i dr. Innovacionnye tehnologii v lechenii raka mochevogo puzyrja. Allergologija i immunologija. 2016; 17 (1): 21–6.
12. Salnikova SV, Slavyanskaya TA, i dr. Sovremennye podhody i dostizhenija v lechenii raka mochevogo puzyrja. Allergologija i immunologija. 2016; 17 (1): 50–1.
13. Baldueva IA, Novik AV, Karickij AP, Kuleva SA, Nehaeva TL, Danilova AB, i dr. Immunoterapija raka: sovremennoe sostojanie problemy. Allergologija i immunologija. 2015; 16 (4): 354.
14. Slavyanskaya TA, Salnikova SV. Immunologicheskie kriterii i markery dlja diagnostiki i prognozirovanija raka mochevogo puzyrja. International Journal on Immunorehabilitation. 2009; 11 (1): 24.
15. Slavyanskaya TA, Salnikova SV. Immunologic criteria and markers for diagnostics and prognosis of urinary bladder cancer. Int J Immunoreh. 2009; 11 (2): 180.
16. Uhlen M, Zhang C, Lee S, Sjöstedt E, Fagerberg L, Bidkhori G, et al. A pathology atlas of the human cancer transcriptome. Science. 2017; 357 (6352). DOI: 10.1126/science.aan2507.
17. Svitich OA, Filina AB, Gankovskaja LV, Zverev VV. Rol' faktorov vrozhdennogo immuniteta v processe opuholeobrazovanija. Medicinskaja immunologija. 2018; 20 (2): 151–62.
18. Haitov RM, Kadagidze ZG. Immunitet i rak. M.: Geotar–Media, 2018. 256 c.
19. Crowe NY, Coquet JM, Berzins SP, et al. Differential Antitumor Immunity Mediated by NKT Cells Subsets in Vivo. J Exp Med. 2005; (202): 1279–88.
20. Brandes M, Willimann K, Moser B. Professional Antigen-presentation Function by Human Gammadelta T Cells. Science. 2005; (309): 264–8.
21. Mellman I, Coukos G, Dranoff G. Cancer immunotherapy comes of age. Nature. 2011; 480 (7378): 480–9.
22. Shevach EM. $CD4^+$, $CD25^+$ suppressor T-cells: More Questions than Answers. Nat Rev Immunol. 2002; (2): 389–400.
23. Lima L, Oliveira D, Tavares A, Amaro T, Cruz R, Oliveira MJ, et al. The predominance of M2-polarized macrophages in the stroma of low-hypoxic bladder tumors is associated with BCG immunotherapy failure. Urol Oncol. 2014; (32): 449–57.
24. LaRue H, Ayari C, Bergeron A, Fradet Y. Toll-like receptors in urothelial cells-targets for cancer immunotherapy. Nat Rev Urol. 2013; 10 (9): 537–45.
25. Diesendruck Y, Benhar I. Novel immune check point inhibiting antibodies in cancer therapy-opportunities and challenges. Drug Resist Updat. 2017; (30): 39–47.
26. Kavecansky J, Pavlick AC. Beyond Checkpoint Inhibitors: pii: E189The Next Generation of Immunotherapy in Oncology. AJHO. 2017; 13 (2): 9–20.
27. Ata R, Antonescu CN. Integrins and cell metabolism: an intimate relationship impacting cancer. Int J Mol Sci. 2017; 18 (1). DOI: 10.3390/ijms18010189.
28. Hadley GA, Higgins JM. Integrin αEβ7: molecular features and functional significance in the immune system. Adv Exp Med Biol. 2014; (819): 97–110.
29. Takimoto C. Forty Seven, Inc. Trial of Hu5F9-G4 in combination with cetuximab in patients with solid tumors and advanced colorectal cancer (NCT02953782). Accessed February 8, 2017; Clinicaltrials. gov website. Available from: https://clinicaltrials.gov/ct2/show/NCT02953782? ter-m=NCT02953782 & rank=1.
30. Desgrosellier JS, Cheresh DA. Integrins in cancer: biological implications and therapeutic opportunities. Nat Rev Cancer. 2010; 10 (1): 9–22.
31. Hersey P, Sosman J, O'Day S, et al. Etaracizumab Melanoma Study Group. A randomized phase 2 study of etaracizumab, a monoclonal antibody against integrin alpha(v)beta(3), + or – dacarbazine in patients with stage IV metastatic melanoma. Cancer. 2010; 116 (6): 1526–34.
32. Sturgill ER, Redmond WL. TNFR Agonists: A Review of Current Biologics Targeting OX40, 4-1BB, CD27, and GITR. AJHO. 2017; 13 (11): 4–15.
33. Stanley ER, Chitu V. CSF-1 receptor signaling in myeloid cells. Cold Spring Harb Perspect Biol. 2014; (6): 1–21.
34. Desar IM, Jacobs JH, Hulsbergen-vandeKaa CA, et al. Sorafenib reduces the percentage of tumour infiltrating regulatory T cells in renal cell carcinoma patients. Int J Cancer. 2011; 129 (2): 507–12. DOI: 10.1002/ijc.25674.
35. Adotevi O, Pere H, Ravel P, et al. A decrease of regulatory T cells correlates with overall survival after sunitinib-based antiangiogenic therapy in metastatic renal cancer patients. J Immunother. 2010; 33 (9): 991–8. DOI: 10.1097/CJI.0b013e3181f4c208.
36. Albeituni SH, Ding C, Yan J. Hampering immune suppressors: therapeutic targeting of myeloid-derived suppressor cells in cancer. Cancer J. 2013; 19 (6): 490–501. DOI: 10.1097/PPO.0000000000000006.
37. Ling ZQ, Li P, Ge MH, et al. Hypermethylation-modulated downregulation of CDH1 expression contributes to the progression of esophageal cancer. Int J Mol Med. 2011; (27): 625–35.
38. Glushankova NA, Zhitnjak IYu, Ajollo DV, Rubcova SN. Rol' E-kadherina v neoplasticheskoj jevoljucii jepitelial'nyh kletok. Uspehi molekuljarnoj onkologii. 2014; (1): 12–17.
39. Scognamiglio G, De Chiara A, Di Bonito M, et al. Variability in immunohistochemical detection of programmed death ligand 1 (PD-L1) in cancer tissue types. Int J Mol Sci. 2014; 17 (5): pii E790.
40. Abaza YM, Alemany C. Nanoparticle albumin-bound-paclitaxel in the treatment of metastatic urethral adenocarcinoma: the significance of molecular profiling and targeted therapy. Case Rep Urol. 2014; (2014): 1–3. DOI: 10.1155/2014/489686.
41. Gong J, Chehrazi-Raffle A. Development of PD-1 and PD-L1 inhibitors as a form of cancer immunotherapy: a comprehensive review of registration trials and future considerations. Journal for Immunotherapy of Cancer. 2018; (6): 8.
42. Velez MA, Wu Y, Dubinett SM, Dong Z, Wu S, Garon EB. Lung cancer. In: Butterfield LH, Kaufman HL, Marincola FM, editors. Cancer immunotherapy principles and practice. New York: Demosmedical, 2017; p. 728.
43. Bellmunt J, de Wit R, Vaughn DJ, et al. KEYNOTE-045 Investigators. Pembrolizumab as second-line therapy for advanced urothelial carcinoma. N Engl J Med. 2017; 376 (11): 1015–26.

44. Postow MA, Chesney J, Pavlick AC, Robert C, Grossmann K, McDermott D, et al. Nivolumab and ipilimumab versus ipilimumab in untreated melanoma. N Engl J Med. 2015; (372): 2006–17.
45. Massard C, Gordon MS, Sharma S, et al. Safety and efficacy of durvalumab (MEDI4736), an anti-programmed cell death ligand-1 immune checkpoint inhibitor, in patients with advanced urothelial bladder cancer. J Clin Oncol. 2016; 34 (26): 3119–25.
46. Segal NH, Logan TF, Hodi FS, et al. Results from an integrated safety analysis of urelumab, an agonist anti-CD137 monoclonal antibody. Clin Cancer Res. 2017; 23 (8): 1929–36.
47. Goding SR, Wilson KA, Xie Y, et al. Restoring immune function of tumor-specific $CD4^+$ T cells during recurrence of melanoma. J Immunol. 2013; 190 (9): 4899–909. DOI: 10.4049/jimmunol.1300271.
48. Ohkuri T, Ghosh A, Kosaka A, et al. STING contributes to antiglioma immunity via triggering type I IFN signals in the tumor microenvironment. Cancer Immunol Res. 2014; 2 (12): 1199–208. DOI: 10.1158/2326-6066.CIR-14-0099.
49. Lu H, Wagner WM, Gad E, et al. Treatment failure of a TLR- 7 agonist occurs due to self-regulation of acute inflammation and can be overcome by IL10 blockade. J Immunol. 2010; 184 (9): 5360–67. DOI: 10.4049/jimmunol.0902997.
50. Salmon H, Idoyaga J, Rahman A, et al. Expansion and activation of CD103(+) dendritic cell progenitors at the tumor site enhances tumor responses to therapeutic PD-L1 and BRAF inhibition. Immunity. 2016; 44 (4): 924–38. DOI: 10.1016/j.immuni.2016.03.012.
51. De Witte MA, Kierkels GJ, Straetemans T, Britten CM, Kuball J. Orchestrating an immune response against cancer with engineered immune cells expressing αβTCRs, CARs, and innate immune receptors: an immunological and regulatory challenge. Cancer Immunol Immunother. 2015; 64 (7): 893–902. DOI: 10.1007/s00262-015-1710-8.
52. Holzinger A, Barden M, Abken H. The growing world of CAR T cell trials: a systematic review. Cancer Immunol Immunother. 2016; 65 (12): 1433–50.
53. Eriksson E, Milenova I, Wenthe J, et al. Shaping the tumor stroma and sparking immune activation by CD40 and 4-1BB signaling induced by an armed oncolytic virus. Clin Cancer Res. 2017; 23 (19): 5846–57.
54. El-Khoueiry AB, Hamid O, Thompson JA, et al. The relationship of pharmacodynamics (PD) and pharmacokinetics (PK) to clinical outcomes in a phase I study of OX40 agonistic monoclonal antibody (mAb) PF-04518600 (PF-8600). J Clin Oncol. 2016; 35 (suppl; abst 3027).
55. Linch S, Kasiewicz MJ, McNamara M, Hilgart I, Farhad M, Redmond W. Galectin-3 inhibition using novel inhibitor GR-MD-02 improves survival and immune function while reducing tumor vasculature. J Immunother Cancer. 2015; 3 (suppl 2): 306.
56. Redmond WL, Linch SN, Kasiewicz MJ. Combined targeting of co-stimulatory (OX40) and co-inhibitory (CTLA-4) pathways elicits potent effector T cells capable of driving robust anti-tumor immunity. Cancer Immunol Res. 2014; 2 (2): 142–53. DOI: 10.1158/2326-6066.CIR-13-0031-T.
57. McHugh RS, Whitters MJ, Piccirillo CA, et al. CD4(+)CD25(+) immunoregulatory T cells: gene expression analysis reveals a functional role for the glucocorticoid-induced TNF receptor. Immunity. 2002; 16 (2): 311–23.
58. Tesaro A. Rhase I study of TSR-022, an anti-TIM-3 mono- clonal antibody, in patients with advanced solid tumors (NCT02817633). Accessed 2017 February 7; Available from: https://clinicaltrials.gov/ct2/show/NCT02817633?term=NCT02817633&rank =1.
59. Novartis. Safety and efficacy of MBG453 as single agent and in combination with PDR001 in patients with advanced malignancies (NCT02608268). Accessed 2017 February 7; Available from: https://clinicaltrials.gov/ct2/show/NCT02678338?term=NCT02678338& rank=1.
60. Cancer Immunotherapy Guidelines. Accessed 2017 March 8. Available from: http://www.sitcancer.org/research/cancer-immunotherapy-guidelines.
61. Slavyanskaya TA, Salnikova SV, i dr. Protivoopuholevye vakciny: potencial'nye misheni, sovremennye razrabotki i perspektivy ispol'zovanija. Rossijskij immunologicheskij zhurnal. 2016; 10 (19), (2–1): 498–500.
62. Melero I, Gaudernack G, Gerritsen W, Huber C, Parmiani G, Scholl S, et al. Therapeutic vaccines for cancer: an overview of clinical trials. Nat Rev Clin Oncol. 2014; (11): 509–24.
63. Palucka K, Banchereau J. Cancer immunotherapy via dendritic cells. Nat Rev Cancer. 2012; (12): 265–77.
64. Slavyanskaya TA, Salnikova SV, i dr. Celenapravlennaja terapija bol'nyh s urotelial'noj karcinomoj. Allergologija i immunologija. 2016; 17 (2): 153.
65. Beatty GL, O'Dwyer PJ, Clark J, et al. First-in-human phase I study of the oral inhibitor of indoleamine 2,3-dioxygenase-1epacadostat (INCB024360) in patients with advanced solid malignancies [ePub ahead of print]. Clin Cancer Res. 2017; pii: clincanres.2272.2016. DOI: 10.1158/1078-0432.CCR-16-2272.
66. Peethambaram PP, Melisko ME, Rinn KJ, Alberts SR, Provost NM, Jones LA, et al. A phase I trial of immunotherapy with lapuleucel-T (APC8024) in patients with refractory metastatic tumors that express HER-2/neu. Clin Cancer Res. 2009; (15): 5937–44.
67. Lowenfeld L, Mick R, Datta J, et al. Dendritic cell vaccination enhances immune responses and induces regression of HER2pos DCIS independent of route: results of randomized selection design trial [ePub ahead of print]. Clin Cancer Res. 2016; pii: clincanres: 1924; 2016.
68. Lesterhuis WJ, Schreibelt G, Scharenborg NM, et al. Wild-type and modified gp100 peptide-pulsed dendritic cell vaccination of advanced melanoma patients can lead to long-term clinical responses independent of the peptide used. Cancer Immunol Immunother. 2011; 60 (2): 249–60.
69. Chkadua GZ, Zabotina TN, Burkova AA, Tamaeva ZYe, Ogorodnikova EV, Zhordania KI. Adaptirovanie metodiki kul'tivirovanija dendritnyh kletok cheloveka iz monocitov periphericheskoj krovi dlja klinicheskogo primenenija. Rossijskij bioterapevticheskij zhurnal. 2002; (3): 56–62.
70. Sasada T, Suekane S. Variation of tumor-infiltrating lymphocytes in human cancers: controversy on clinical significance. Immunotherapy. 2011; 3 (10): 1235–51.
71. Eloy JO, Petrilli R, Trevizan LNF, Chorilli M. Immunoliposomes: a review on functionalization strategies and targets for drug delivery. Colloids Surf B: Biointerfaces. 2017; (159): 454–67.
72. Bilensoy E, Sarisozen C, Esendagli G, Dogan AL, Aktaş Y, Sen M, et al. Intravesical cationic nanoparticles of chitosan and polycaprolactone for the delivery of Mitomycin C to bladder tumors. Int J Pharm. 2009; (371): 170–6.
73. Kosmides AK, Sidhom JW, Fraser A, Bessell CA, Schneck JP. Dual targeting nanoparticle stimulates the immune system to inhibit tumor growth. ACS Nano. 2017; 11 (6): 5417–29.
74. Zhang Q, Neoh KG, Xu L, Lu S, Kang ET, Mahendran R, et al. Functionalized mesoporous silica nanoparticles with mucoadhesive and sustained drug release properties for potential bladder cancer therapy. Langmuir. 2014; (30): 6151–61.
75. Sudha T, Bharali DJ, Yalcin M, Darwish NH, Coskun MD, Keating KA, et al. Targeted delivery of cisplatin to tumor xenografts via the nanoparticle component of nano-diamino-tetrac. Nanomedicine. 2017; 12 (3): 195–205.
76. McKiernan JM, Barlow LJ, Laudano MA, Mann MJ, Petrylak DP, Benson MC. A phase I trial of intravesical nanoparticle albumin-bound paclitaxel in the treatment of bacillus Calmette-Guérin refractory nonmuscle invasive bladder cancer. J Urol. 2011; (186): 448–51.
77. Barrow AD, Edeling MA, Trifonov V, Luo J, Goyal P, Bohl B, et al. Natural killer cells control tumor growth by sensing a growth factor. Cell. 2018; 172 (3): 534–48.

Литература

1. Кудрявцева И. В., Славянская Т. А., Трунов А. Н., Трунова Л. А. Уровни аутоантител к ядерным ДНК, лактоферрина и некоторые иммунологические показатели у больных ревматоидным артритом. Бюллетень Сибирского отделения Российской академии медицинских наук. 1999; 19 (3–4): 66–8.
2. Смирнова Т. А., Пономарева Е. П., Ханферян Р. А., Колесников В. В. Опыт применения ронколейкина при терапии язвенной болезни желудка, ассоциированной с Helicobacter Pylori, в амбулаторных условиях. Терапевтический архив. 2009; 81 (2): 30–5.
3. Славянская Т. А., Сепиашвили Р. И., Вишняков М. Н., Чихладзе М. В. Иммунологический мониторинг больных хроническим бронхитом в динамике восстановительной иммунореабилитации. International Journal on Immunorehabilitation. 1999; (11): 70.
4. Славянская Т. А., Авдонкина Н. А., Сальникова С. В. Оптимизация условий получения жизнеспособной первичной культуры клеток уротелиальной карциномы. Аллергология и иммунология. 2016; 17 (3): 176–9.
5. Burger M, Thiounn N, Denzinger S, Kondas J, Benoit G, Chapado MS, et al. The application of adjuvant autologous antravesical macrophage cell therapy vs. BCG in non-muscle invasive bladder cancer: a multicenter, randomized trial. J Transl Med. 2010; (8): 54.
6. Camisaschi C, Vallacchi V, Vergani E, et al. Targeting immune regulatory networks to counteract immune suppression in cancer. Vaccines (Basel). 2016; 4 (4): pii: E38.
7. Dominguez G, Condamine TC, Mony S, et al. Selective targeting of myeloid-derived suppressor cells in cancer patients using DS-8273a, an agonistic TRAIL-R2 antibody. Clin Cancer Res. 2016; 23 (12): 2942–50.
8. Sharma P, Retz M, Seifker-Radtke A, et al. Nivolumab in metastatic urothelial carcinoma after platinum therapy (Check-Mate 275): a multicentre, single-arm, phase 2 trial. Lancet Oncol. 2017; 18 (3): 312–22.
9. Larkin J, Chiarion-Sileni V, Gonzalez R, Grob JJ, Cowey CL, Lao CD, et al. Combined nivolumab and ipilimumab or monotherapy in untreated melanoma. N Engl J Med. 2015; (373): 23–34.
10. Сепиашвили Р. И., Беляев А. М. Иммунотерапия рака: проблемы и перспективы. Аллергология и иммунология. 2015; 16 (4): 354–7.
11. Сальникова С. В., Славянская Т. А. и др. Инновационные технологии в лечении рака мочевого пузыря. Аллергология и иммунология. 2016; 17 (1): 21–6.
12. Сальникова С. В., Славянская Т. А. и др. Современные подходы и достижения в лечении рака мочевого пузыря. Аллергология и иммунология. 2016; 17 (1): 50–1.
13. Балдуева И. А., Новик А. В., Карицкий А. П., Кулева С. А., Нехаева Т. Л., Данилова А. Б. и др. Иммунотерапия рака: современное состояние проблемы. Аллергология и иммунология. 2015; 16 (4): 354.
14. Славянская Т. А., Сальникова С. В. Иммунологические критерии и маркеры для диагностики и прогнозирования рака мочевого пузыря. International Journal on Immunorehabilitation. 2009; 11 (1): 24.
15. Slavyanskaya TA, Salnikova SV. Immunologic criteria and markers for diagnostics and prognosis of urinary bladder cancer. Int J Immunoreh. 2009; 11 (2): 180.
16. Uhlen M, Zhang C, Lee S, Sjöstedt E, Fagerberg L, Bidkhori G, et al. A pathology atlas of the human cancer transcriptome. Science. 2017; 357 (6352). DOI: 10.1126/science.aan2507.
17. Свитич О. А., Филина А. Б., Ганковская Л. В., Зверев В. В. Роль факторов врожденного иммунитета в процессе опухолеобразования. Медицинская иммунология. 2018; 20 (2): 151–62.
18. Хаитов Р. М., Кадагидзе З. Г. Иммунитет и рак. М.: Геотар–Медиа, 2018. 256 с.
19. Crowe NY, Coquet JM, Berzins SP, et al. Differential Antitumor Immunity Mediated by NKT Cells Subsets in Vivo. J Exp Med. 2005; (202): 1279–88.
20. Brandes M, Willimann K, Moser B. Professional Antigen-presentation Function by Human Gammadelta T Cells. Science. 2005; (309): 264–8.
21. Mellman I, Coukos G, Dranoff G. Cancer immunotherapy comes of age. Nature. 2011; 480 (7378): 480–9.
22. Shevach EM. CD4+, CD25+ suppressor T-cells: More Questions than Answers. Nat Rev Immunol. 2002; (2): 389–400.
23. Lima L, Oliveira D, Tavares A, Amaro T, Cruz R, Oliveira MJ, et al. The predominance of M2-polarized macrophages in the stroma of low-hypoxic bladder tumors is associated with BCG immunotherapy failure. Urol Oncol. 2014; (32): 449–57.
24. LaRue H, Ayari C, Bergeron A, Fradet Y. Toll-like receptors in urothelial cells-targets for cancer immunotherapy. Nat Rev Urol. 2013; 10 (9): 537–45.
25. Diesendruck Y, Benhar I. Novel immune check point inhibiting antibodies in cancer therapy-opportunities and challenges. Drug Resist Updat. 2017; (30): 39–47.
26. Kavecansky J, Pavlick AC. Beyond Checkpoint Inhibitors: pii: E189The Next Generation of Immunotherapy in Oncology. AJHO. 2017; 13 (2): 9–20.
27. Ata R, Antonescu CN. Integrins and cell metabolism: an intimate relationship impacting cancer. Int J Mol Sci. 2017; 18 (1). DOI: 10.3390/ijms18010189.
28. Hadley GA, Higgins JM. Integrin αEβ7: molecular features and functional significance in the immune system. Adv Exp Med Biol. 2014; (819): 97–110.
29. Takimoto C. Forty Seven, Inc. Trial of Hu5F9-G4 in combination with cetuximab in patients with solid tumors and advanced colorectal cancer (NCT02953782). Accessed February 8, 2017; Clinicaltrials. gov website. Available from: https://clinicaltrials.gov/ct2/show/NCT02953782? ter-m=NCT02953782 & rank=1.
30. Desgrosellier JS, Cheresh DA. Integrins in cancer: biological implications and therapeutic opportunities. Nat Rev Cancer. 2010; 10 (1): 9–22.
31. Hersey P, Sosman J, O'Day S, et al. Etaracizumab Melanoma Study Group. A randomized phase 2 study of etaracizumab, a monoclonal antibody against integrin alpha(v)beta(3), + or – dacarbazine in patients with stage IV metastatic melanoma. Cancer. 2010; 116 (6): 1526–34.
32. Sturgill ER, Redmond WL. TNFR Agonists: A Review of Current Biologics Targeting OX40, 4-1BB, CD27, and GITR. AJHO. 2017; 13 (11): 4–15.
33. Stanley ER, Chitu V. CSF-1 receptor signaling in myeloid cells. Cold Spring Harb Perspect. Biol. 2014; (6): 1–21.
34. Desar IM, Jacobs JH, Hulsbergen-vandeKaa CA, et al. Sorafenib reduces the percentage of tumour infiltrating regulatory T cells in renal cell carcinoma patients. Int J Cancer. 2011; 129 (2): 507–12. DOI: 10.1002/ijc.25674.
35. Adotevi O, Pere H, Ravel P, et al. A decrease of regulatory T cells correlates with overall survival after sunitinib-based antiangiogenic therapy in metastatic renal cancer patients. J Immunother. 2010; 33 (9): 991–8. DOI: 10.1097/CJI.0b013e3181f4c208.
36. Albeituni SH, Ding C, Yan J. Hampering immune suppressors: therapeutic targeting of myeloid-derived suppressor cells in cancer. Cancer J. 2013; 19 (6): 490–501. DOI: 10.1097/PPO.0000000000000006.
37. Ling ZQ, Li P, Ge MH, et al. Hypermethylation-modulated downregulation of CDH1 expression contributes to the progression of esophageal cancer. Int J Mol Med. 2011; (27): 625–35.
38. Глушанкова Н. А., Житняк И. Ю., Айолло Д. В., Рубцова С. Н. Роль Е-кадхерина в неопластической эволюции эпителиальных клеток. Успехи молекулярной онкологии. 2014; (1): 12–17.
39. Scognamiglio G, De Chiara A, Di Bonito M, et al. Variability in immunohistochemical detection of programmed death ligand 1 (PD-L1) in cancer tissue types. Int J Mol Sci. 2014; 17 (5): pii E790.
40. Abaza YM, Alemany C. Nanoparticle albumin-bound-paclitaxel in the treatment of metastatic urethral adenocarcinoma: the significance of molecular profiling and targeted therapy. Case Rep Urol. 2014; (2014): 1–3. DOI: 10.1155/2014/489686.
41. Gong J, Chehrazi-Raffle A. Development of PD-1 and PD-L1 inhibitors as a form of cancer immunotherapy: a comprehensive review of registration trials and future considerations. Journal for Immunotherapy of Cancer. 2018; (6): 8.
42. Velez MA, Wu Y, Dubinett SM, Dong Z, Wu S, Garon EB. Lung cancer. In: Butterfield LH, Kaufman HL, Marincola FM, editors.

Cancer immunotherapy principles and practice. New York: Demosmedical, 2017; p. 728
43. Bellmunt J, de Wit R, Vaughn DJ, et al. KEYNOTE-045 Investigators. Pembrolizumab as second-line therapy for advanced urothelial carcinoma. N Engl J Med. 2017; 376 (11): 1015–26.
44. Postow MA, Chesney J, Pavlick AC, Robert C, Grossmann K, McDermott D, et al. Nivolumab and ipilimumab versus ipilimumab in untreated melanoma. N Engl J Med. 2015; (372): 2006–17.
45. Massard C, Gordon MS, Sharma S, et al. Safety and efficacy of durvalumab (MEDI4736), an anti-programmed cell death ligand-1 immune checkpoint inhibitor, in patients with advanced urothelial bladder cancer. J Clin Oncol. 2016; 34 (26): 3119–25.
46. Segal NH, Logan TF, Hodi FS, et al. Results from an integrated safety analysis of urelumab, an agonist anti-CD137 monoclonal antibody. Clin Cancer Res. 2017; 23 (8): 1929–36.
47. Goding SR, Wilson KA, Xie Y, et al. Restoring immune function of tumor-specific CD4+ T cells during recurrence of melanoma. J Immunol. 2013; 190 (9): 4899–909. DOI: 10.4049/jimmunol.1300271.
48. Ohkuri T, Ghosh A, Kosaka A, et al. STING contributes to antiglioma immunity via triggering type I IFN signals in the tumor microenvironment. Cancer Immunol Res. 2014; 2 (12): 1199–208. DOI: 10.1158/2326-6066.CIR-14-0099.
49. Lu H, Wagner WM, Gad E, et al. Treatment failure of a TLR- 7 agonist occurs due to self-regulation of acute inflammation and can be overcome by IL10 blockade. J Immunol. 2010; 184 (9): 5360–67. DOI: 10.4049/jimmunol.0902997.
50. Salmon H, Idoyaga J, Rahman A, et al. Expansion and activation of CD103(+) dendritic cell progenitors at the tumor site enhances tumor responses to therapeutic PD-L1 and BRAF inhibition. Immunity. 2016; 44 (4): 924–38. DOI: 10.1016/j.immuni.2016.03.012.
51. De Witte MA, Kierkels GJ, Straetemans T, Britten CM, Kuball J. Orchestrating an immune response against cancer with engineered immune cells expressing αβTCRs, CARs, and innate immune receptors: an immunological and regulatory challenge. Cancer Immunol Immunother. 2015; 64 (7): 893–902. DOI: 10.1007/s00262-015-1710-8.
52. Holzinger A, Barden M, Abken H. The growing world of CAR T cell trials: a systematic review. Cancer Immunol Immunother. 2016; 65 (12): 1433–50.
53. Eriksson E, Milenova I, Wenthe J, et al. Shaping the tumor stroma and sparking immune activation by CD40 and 4-1BB signaling induced by an armed oncolytic virus. Clin Cancer Res. 2017; 23 (19): 5846–57.
54. El-Khoueiry AB, Hamid O, Thompson JA, et al. The relationship of pharmacodynamics (PD) and pharmacokinetics (PK) to clinical outcomes in a phase I study of OX40 agonistic monoclonal antibody (mAb) PF-04518600 (PF-8600). J Clin Oncol. 2016; 35 (suppl; abst 3027).
55. Linch S, Kasiewicz MJ, McNamara M, Hilgart I, Farhad M, Redmond W. Galectin-3 inhibition using novel inhibitor GR-MD-02 improves survival and immune function while reducing tumor vasculature. J Immunother Cancer. 2015; 3 (suppl 2): 306.
56. Redmond WL, Linch SN, Kasiewicz MJ. Combined targeting of co-stimulatory (OX40) and co-inhibitory (CTLA-4) pathways elicits potent effector T cells capable of driving robust anti-tumor immunity. Cancer Immunol Res. 2014; 2 (2): 142–53. DOI: 10.1158/2326-6066.CIR-13-0031-T.
57. McHugh RS, Whitters MJ, Piccirillo CA, et al. CD4(+)CD25(+) immunoregulatory T cells: gene expression analysis reveals a functional role for the glucocorticoid-induced TNF receptor. Immunity. 2002; 16 (2): 311–23.
58. Tesaro A. Phase I study of TSR-022, an anti-TIM-3 mono-clonal antibody, in patients with advanced solid tumors (NCT02817633). Accessed 2017 February 7; Available from: https://clinicaltrials.gov/ct2/show/NCT02817633?term=NCT02817633&rank =1.
59. Novartis. Safety and efficacy of MBG453 as single agent and in combination with PDR001 in patients with advanced malignancies (NCT02608268). Accessed 2017 February 7; Available from: https://clinicaltrials.gov/ct2/show/NCT02678338?term=NCT02678338& rank=1.
60. Cancer Immunotherapy Guidelines. Accessed 2017 March 8. Available from:http://www.sitcancer.org/research/cancer-immunotherapy-guidelines.
61. Славянская Т. А., Сальникова С. В. и др. Противоопухолевые вакцины: потенциальные мишени, современные разработки и перспективы использования. Российский иммунологический журнал. 2016; 10 (19), (2-1): 498–500.
62. Melero I, Gaudernack G, Gerritsen W, Huber C, Parmiani G, Scholl S, et al. Therapeutic vaccines for cancer: an overview of clinical trials. Nat Rev Clin Oncol. 2014; (11): 509–24.
63. Palucka K, Banchereau J. Cancer immunotherapy via dendritic cells. Nat Rev Cancer. 2012; (12): 265–77.
64. Славянская Т. А., Сальникова С. В. и др. Целенаправленная терапия больных с уротелиальной карциномой. Аллергология и иммунология. 2016; 17 (2): 153.
65. Beatty GL, O'Dwyer PJ, Clark J, et al. First-in-human phase I study of the oral inhibitor of indoleamine 2,3-dioxygenase-1epacadostat (INCB024360) in patients with advanced solid malignancies [ePub ahead of print]. Clin Cancer Res. 2017; pii: clincanres.2272.2016. DOI: 10.1158/1078-0432.CCR-16-2272.
66. Peethambaram PP, Melisko ME, Rinn KJ, Alberts SR, Provost NM, Jones LA, et al. A phase I trial of immunotherapy with lapuleucel-T (APC8024) in patients with refractory metastatic tumors that express HER-2/neu. Clin Cancer Res. 2009; (15): 5937–44.
67. Lowenfeld L, Mick R, Datta J, et al. Dendritic cell vaccination enhances immune responses and induces regression of HER2pos DCIS independent of route: results of randomized selection design trial [ePub ahead of print]. Clin Cancer Res. 2016; pii: clincanres: 1924; 2016.
68. Lesterhuis WJ, Schreibelt G, Scharenborg NM, et al. Wild-type and modified gp100 peptide-pulsed dendritic cell vaccination of advanced melanoma patients can lead to long-term clinical responses independent of the peptide used. Cancer Immunol Immunother. 2011; 60 (2): 249–60.
69. Чкадуа Г. З., Заботина Т. Н., Буркова А. А., Тамаева З. Э., Огородникова Е. В., Жорданиа К. И. Адаптирование методики культивирования дендритных клеток человека из моноцитов периферической крови для клинического применения. Российский биотерапевтический журнал. 2002; (3): 56–62.
70. Sasada T, Suekane S. Variation of tumor-infiltrating lymphocytes in human cancers: controversy on clinical significance. Immunotherapy. 2011; 3 (10): 1235–51.
71. Eloy JO, Petrilli R, Trevizan LNF, Chorilli M. Immunoliposomes: a review on functionalization strategies and targets for drug delivery. Colloids Surf B: Biointerfaces. 2017; (159): 454–67.
72. Bilensoy E, Sarisozen C, Esendagli G, Dogan AL, Aktaş Y, Sen M, et al. Intravesical cationic nanoparticles of chitosan and polycaprolactone for the delivery of Mitomycin C to bladder tumors. Int J Pharm. 2009; (371): 170–6.
73. Kosmides AK, Sidhom JW, Fraser A, Bessell CA, Schneck JP. Dual targeting nanoparticle stimulates the immune system to inhibit tumor growth. ACS Nano. 2017; 11 (6): 5417–29.
74. Zhang Q, Neoh KG, Xu L, Lu S, Kang ET, Mahendran R, et al. Functionalized mesoporous silica nanoparticles with mucoadhesive and sustained drug release properties for potential bladder cancer therapy. Langmuir. 2014; (30): 6151–61.
75. Sudha T, Bharali DJ, Yalcin M, Darwish NH, Coskun MD, Keating KA, et al. Targeted delivery of cisplatin to tumor xenografts via the nanoparticle component of nano-diamino-tetrac. Nanomedicine. 2017; 12 (3): 195–205.
76. McKiernan JM, Barlow LJ, Laudano MA, Mann MJ, Petrylak DP, Benson MC. A phase I trial of intravesical nanoparticle albumin-bound paclitaxel in the treatment of bacillus Calmette-Guérin refractory nonmuscle invasive bladder cancer. J Urol. 2011; (186): 448–51.
77. Barrow AD, Edeling MA, Trifonov V, Luo J, Goyal P, Bohl B, et al. Natural killer cells control tumor growth by sensing a growth factor. Cell. 2018; 172 (3): 534–48.

CLINICAL AND MOLECULAR-GENETIC PROFILES OF PATIENTS WITH MORPHOLOGICAL INDICATIONS OF CONGENITAL MULTICORE MYOPATHY

Kozina AA[1,2,5] ✉, Shatalov PA[3,5], Baranich TI[1], Artemieva SB[3], Kupriyanova AG[3], Baryshnikova NV[1,5], Krasnenko AYu[1,5], Ilinsky VV[1,2,5], Sukhorukov VS[1,4]

[1] Pirogov Russian National Research Medical University, Moscow, Russia

[2] Orekhovich Institute of Biomedical Chemistry, Moscow, Russia

[3] Veltischev Research and Clinical Institute for Pediatrics, Pirogov Russian National Research Medical University, Moscow, Russia

[4] Research Center of Neurology, Moscow, Russia

[5] Genotek Ltd., Moscow, Russia

Congenital core myopathies are a clinically and genetically heterogenous group of congenital myopathies that share a specific histopathological feature: areas of reduced oxidative activity in muscle fibers. The relationship between clinical, genetic and morphological characteristics of this group of disorders remains understudied. The aim of this work was to compare clinical presentations and morphological phenotypes of patients with congenital myopathies/myodystrophy to the data yielded by massively parallel exome sequencing. Eight children were included in the study: 2 boys and 6 girls aged 3 to 14 years. Their biopsy material was analyzed by light and electron microscopy. Sequencing was performed on HiSeq2500. Mutations were detected in 7 (87.5%) of 8 participants. Six children had 8 mutations in the genes associated with congenital core myopathies; one patient had 2 mutations in the *LAMA2* gene implicated in merosin-deficient muscular dystrophy. The proportions of patients with mutations in *RYR1* and *SEPN1* were equal (42.86%). Of 10 detected mutations, 3 had not been previously described, including c.7561G>A in *RYR1*, c.485C>A in *SEPN1* and p.Cys1136Arg in *LAMA2*. The clinical and morphological features of core myopathies suggest that genetic causes of this group of disorders should not be limited to *RYR1* and *SEPN1* genes only. This necessitates the search for and the study of other genes implicated in congenital myopathies or myodystrophy using state-of-the-art molecular genetic tools.

Keywords: congenital central core disease, congenital multicore myopathies, *RYR1* gene, *SEPN1* gene, *LAMA2* gene, muscle biopsy, exome sequencing

Author contribution: Kozina AA — literature analysis, analysis and interpretation of exome sequencing data, manuscript preparation; Shatalov PA — data acquisition, microscopy, manuscript preparation; Baranich TI — microscopy; Artemieva SB — medical histories and neurological examinations; Kupriyanova AG — clinical data acquisition; Baryshnikova NV — literature analysis, analysis and interpretation of exome sequencing data, manuscript preparation; Krasnenko AYu — exome sequencing; Ilinsky VV — exome sequencing; Sukhorukov VS — study design, data acquisition.

Compliance with ethical standards: the study was approved by the Ethics Committee of Pirogov Russian National Research Medical University (Protocol № 172 dated February 19, 2018). All participants or their legal representatives gave informed consent to participate.

✉ **Correspondence should be addressed:** Anastasia A. Kozina
Nastavnichesky per. 17, bld. 1, Moscow, 105120; doctor@genotek.ru

Received: 07.02.2019 **Accepted:** 19.04.2019 **Published online:** 30.04.2019

DOI: 10.24075/brsmu.2019.034

КЛИНИЧЕСКИЕ И МОЛЕКУЛЯРНО-ГЕНЕТИЧЕСКИЕ ХАРАКТЕРИСТИКИ ПАЦИЕНТОВ С МОРФОЛОГИЧЕСКОЙ КАРТИНОЙ ВРОЖДЕННОЙ СТЕРЖНЕВОЙ МИОПАТИИ

А. А. Козина[1,2,5] ✉, П. А. Шаталов[3,5], Т. И. Баранич[1], С. Б. Артемьева[3], А. Г. Куприянова[3], Н. В. Барышникова[1,5], А. Ю. Красненко[1,5], В. В. Ильинский[1,2,5], В. С. Сухоруков[1,4]

[1] Российский национальный исследовательский медицинский университет имени Н. И. Пирогова, Москва, Россия

[2] Научно-исследовательский институт биомедицинской химии имени В. Н. Ореховича, Москва, Россия

[3] Научно-исследовательский клинический институт педиатрии имени академика Ю. Е. Вельтищева, Российский национальный исследовательский медицинский университет имени Н. И. Пирогова, Москва, Россия

[4] Научный центр неврологии, Москва, Россия

[5] ООО «Генотек», Москва, Россия

Врожденные стержневые миопатии — это клинически и генетически гетерогенная группа врожденных миопатий, общий гистопатологический признак которых — наличие участков с уменьшенной окислительной активностью при биопсии мышц. Взаимосвязь клинико-генетических, патогенетических и морфологических характеристик этой группы миопатий до конца не изучена. Целью исследования было проанализировать соответствие клинико-морфологических характеристик пациентов с врожденными миопатиями/миодистрофиями и результатов экзомного секвенирования, полученных методами массового параллельного секвенирования (MPS). В исследовании участвовали 8 детей (2 мальчика и 6 девочек 3–14 лет). Морфологический анализ проводили с помощью световой и электронной микроскопии. Молекулярно-генетический анализ проводили с помощью MPS на платформе HiSeq2500. Мутации были обнаружены в 87,5% случаев (у 7 из 8 обследованных): у 6 обследованных (8 мутаций) — в генах, ответственных за врожденные стержневые миопатии, и у одного пациента (2 мутации) — в гене *LAMA2*, ответственном за мерозин-негативную мышечную дистрофию. Доли пациентов с выявленными мутациями в гене *RYR1* и мутациями в гене *SEPN1* одинаковы и составили 42,86% среди пациентов с мутациями. Из 10 мутаций, выявленных у обследованных пациентов, 3 мутации описаны впервые: в гене *RYR1* — c.7561G>A; в гене *SEPN1* — c.485C>A; в гене *LAMA2* — p.Cys1136Arg. Совокупность клинических и морфологических признаков, характерных для стержневых миопатий, не позволяет ограничить молекулярно-генетический поиск причины заболевания генами *RYR1* и *SEPN1*, что приводит к необходимости исследовать другие гены, ответственные за развитие врожденных миопатий/миодистрофий, с использованием современных молекулярно-генетических методов.

Ключевые слова: врожденные миопатии центрального стержня, врожденные многостержневые миопатии, ген *RYR1*, ген *SEPN1*, ген *LAMA2*, мышечная биопсия, экзомное секвенирование

Информация о вкладе авторов: А. А. Козина — анализ литературы, интерпретация данных экзомного секвенирования, анализ данных, подготовка рукописи; П. А. Шаталов — сбор данных, проведение морфологического исследования, подготовка рукописи; Т. И. Баранич — проведение морфологического исследования; С. Б. Артемьева — сбор клинических данных, неврологический осмотр пациентов; А. Г. Куприянова — сбор клинических данных; Н. В. Барышникова — анализ литературы, интерпретация данных экзомного секвенирования, анализ данных, подготовка рукописи; А. Ю. Красненко — проведение экзомного секвенирования; В. В. Ильинский — проведение экзомного секвенирования; В. С. Сухоруков — планирование исследования, сбор данных.

Соблюдение этических стандартов: исследование одобрено этическим комитетом ФГБОУ ВО РНИМУ имени Н. И. Пирогова (протокол № 172 от 19 февраля 2018 г.); все участники исследования или их законные представители подписали добровольное информированное согласие.

✉ **Для корреспонденции:** Анастасия Александровна Козина
Наставнический переулок, д. 17, стр. 1, г. Москва, 105120; doctor@genotek.ru

Статья получена: 07.02.2019 **Статья принята к печати:** 19.04.2019 **Опубликована онлайн:** 30.04.2019

DOI: 10.24075/vrgmu.2019.034

Congenital myopathies constitute a clinically and genetically heterogenous group of neuromuscular disorders with complex pathogenesis, diverse symptoms and different inheritance patterns [1]. In the affected patients, the loss of muscle function is a result of structural pathology of muscle fibers in the absence of dystrophic changes in muscle tissue [2].

There are a few classic forms of congenital myopathies that can be distinguished histologically, the most common being central core disease, nemaline myopathy, multiminicore myopathy, and centronuclear myopathy [2].

Each of these forms has a number of genetic subtypes differing in the severity of presenting symptoms and the patterns of inheritance. This should be accounted for when deciding on an adequate treatment strategy or providing genetic counseling.

Because some congenital myopathies are quite rare, genetically heterogeneous and share symptoms with other neuromuscular disorders, their differential diagnosis and accurate classification pose a challenge, making it difficult to estimate the actual prevalence of these subtypes and their morphological phenotypes or to assess their contribution to the floppy baby syndrome. The limitations of existing sequencing methods complicate the situation even further.

Congenital myopathies have been studied since 1956 when central core disease was first described. However, the etiopathogenesis and the associations between clinical presentations and genetic phenotypes of congenital core myopathies are still not fully clear.

Morphologically, all core myopathies are characterized by areas of reduced oxidative enzyme activity in type 1 muscle fibers, sarcomere disorganization and almost complete depletion of mitochondria visible during a histochemical examination [3, 4].

Core myopathies can be broken down into two major types: central core disease and multiminicore myopathy.

According to the literature, hereditary core myopathies are largely caused by mutations in the genes coding for two proteins of the sarcoplasmic reticulum: the ryanodine receptor (*RYR1*) and selenoprotein N (*SEPN1*) [5, 6].

The ryanodine receptor gene (*RYR1*) is located on chromosome 19q13.1 and comprises 106 exons. The receptor itself is a calcium release channel of the endoplasmic reticulum membrane. In skeletal muscles, this receptor is embedded in the sarcoplasmic reticulum membrane, where it interacts with the dihydropyridine receptor located on plasma membrane invaginations known as transverse tubules. Electrical signals that travel along the sarcolemma activate calcium release from the sarcoplasmic reticulum following the coupling of the two receptors, and the muscle contracts [7–9]. Mutations tend to occur more often in the ryanodine receptor gene (*RYR1*) than in the gene coding for selenoprotein N (*SEPN1*). Mutant *RYR1* variants are associated with a few pathological conditions, such as an autosomal dominant or autosomal recessive central core disease, in the first place (OMIM entry #117000), and, less often, multiminicore disease (OMIM entry #255320) with an autosomal pattern of inheritance [10, 11]. Mutations in *RYR1* are associated with an increased susceptibility to autosomal dominant malignant hyperthermia (OMIM entry #145600), a predisposition to severe and potentially lethal adverse reactions to volatile anesthetics and/or muscle relaxants [12].

Central core disease is driven by ultrastructural changes and the loss of enzyme activity (exerted by mitochondrial enzymes, in particular) in the center of skeletal muscle fibers. Histologically, these “cores” differ from the peripheral areas of the fibers, so their morphology is the major diagnostic criterion for this disorder [13] (Fig. 1 and 2). Central core disease usually has an onset in early infancy. Among its typical symptoms are motor development delay, low muscle tone, and weakness of proximal muscles (facial muscles are spared). Skeletal manifestations are not rare, including congenital hip dislocation and scoliosis. Hypotonia does not progress with age.

The *SEPN1* gene is located on chromosome 1p36-p35, comprises 13 exons and codes for selenoprotein N, a glycoprotein of the endoplasmic reticulum and a selenium mediator. Selenoprotein is an important component of many metabolic pathways and antioxidant systems. It also helps to maintain calcium homeostasis in muscle tissue by stimulating oxidative enzymes and regulating the oxidative state of ryanodine receptors. Deficit in selenoprotein N promotes oxidation in myotubes and entails deregulation of superoxide dismutase and catalase. This causes oxidative stress; dysfunctional ryanodine receptors can no longer control calcium release from the endoplasmic reticulum, disrupting calcium homeostasis in muscle tissue [9, 11, 14]. Mutations in *SEPN1* are associated with multicore myopathies (OMIM entry #602771) and congenital rigid spine muscular dystrophy (OMIM entry #602771), which has a similar phenotype [15]. The inheritance pattern here is autosomal recessive.

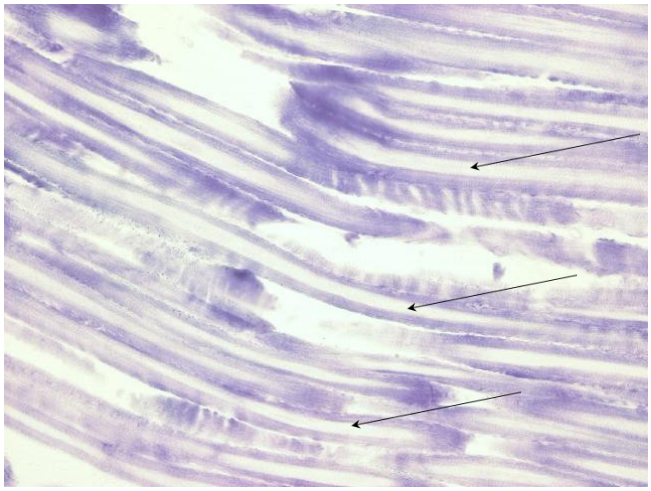

Fig. 1. Skeletal muscle tissue of a 21-year-old patient with congenital central core myopathy. Histochemical analysis of succinate dehydrogenase activity in frozen sections (×200; the method was proposed by Sukhorukov VS) using the nitro BT method by Nachlass et al. (1957). The total absence of enzyme activity is observed in almost all longitudinal sections of the examined muscle fibers (*the arrows*)

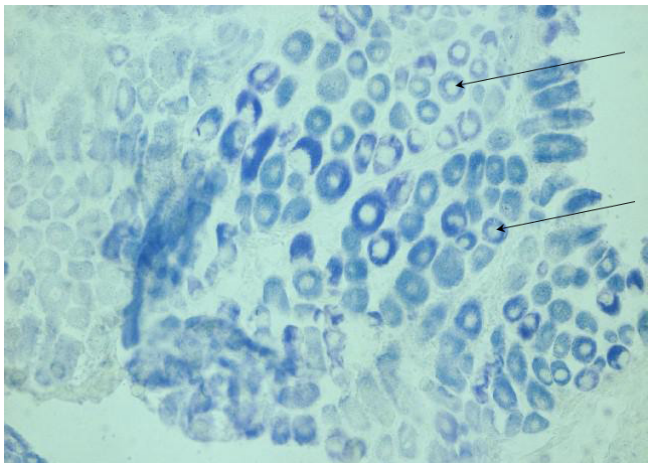

Fig. 2. Skeletal muscle tissue of a 1-year-old patient with congenital central core myopathy Histochemical analysis of succinate dehydrogenase activity in frozen sections (×200; the method was proposed by Sukhorukov VS) using the nitro BT method by Nachlass et al. (1957). The total absence of enzyme activity is observed in almost all cross-sections of the examined muscle fibers (*the arrows*)

Histologically, multicore myopathies are characterized by the presence of multiple cores in skeletal muscle fibers that do not necessarily affect the center of the fiber (Fig. 3). In *RYR1*-associated multiminicore myopathy, the cores are quite massive [9, 11]. In *SEPN1*-associated myopathy, minicores are abundantly present in the muscle tissue [9, 11].

Multiminicore myopathy is a congenital myopathy that develops in infancy and manifests itself as a floppy baby syndrome. The symptoms include low muscle tone, delayed motor development, proximal muscle weakness, spinal deformities, early onset of scoliosis, and chest deformities. Facial muscle weakness is also typical.

The similarity of clinical presentations between core myopathies and other congenital myopathies, the complexity of these diseases, and the existence of different combinations of muscle tissue abnormalities complicate the differential diagnosis. The diagnosis of congenital myopathy is based on the assessment of both clinical and morphological presentations and the results of molecular-genetic tests. Patients with structural myopathies do not always share the same clinical and morphological phenotype. Although such myopathies are linked to the mutations in the *RYR1* and *SEPN1* genes, there is a hypothesis suggesting that other genes may also be involved; some authors also hypothesize the polygenic nature of these neuromuscular conditions [2]. In light of this, it may be relevant to explore clinical, morphological and genetic aspects of congenital core myopathies in parallel.

The aim of this study was to compare clinical and morphological features and the results of massively parallel exome sequencing in patients with clinical symptoms and histological evidence of congenital core myopathies.

METHODS

The study was carried out in 8 children (2 boys and 6 girls) aged 3 to 14 years. The study included patients of both sexes with no family history of neurological disorders who were diagnosed with congenital myopathy and whose histological samples suggested core myopathy; the patients also underwent molecular genetic testing. The following exclusion criteria were applied: the absence of morphological signs of core myopathies in biopsy samples.

The patients' medical records were analyzed. Biopsy samples were studied by light and electron microscopy following the protocols supplied by the manufacturers. Prior to light microscopy, the samples were either paraffinized or frozen and then stained.

1. Fresh tissue sections were prepared by immersing the samples in liquid nitrogen and then slicing them on a Microm HM 505 N cryostat microtome (Microm Tech.; USA). Paraffin sections were prepared by fixing biopsy material in 10% neutral (pH 7.4) buffered formalin following the manufacturer's protocol and then slicing it on the microtome.

2. Hematoxylin-eosin staining of both frozen and paraffinized sections was performed according to the standard protocol. Succinate dehydrogenase activity in the frozen sections was measured using the standard nitro blue tetrazolium-based technique proposed by Nachlass in 1957 [16].

3. Prior to electron microscopy, the samples less than 1 mm^3 in size were prefixed in a 2.5% solution of glutaraldehyde in a phosphate buffer (pH 7.4) at 0 °C. After being washed in a phosphate buffer (pH 7.4), the samples were fixed in 1% osmium tetroxide at 2–4 °C for 1 h. Then, the samples were dehydrated in a series of ascending ethanol concentrations, washed in acetone 3 times and embedded in Epon resin using a technique proposed by Luft [17]. The slices were prepared on the REICHERT Nr. 321850/E ultratome (Reichert tech.; Austria) and stained with lead citrate and sodium uranyl acetate as proposed by Reynolds in [18]. The sections were examined under a transmission electron microscope JEOL JEM-100B (Jeol LTD; Japan).

Exome sequencing was performed using the HiSeq2500 platform (Illumina; USA) according to the manufacturer's protocol.

1. Amplification products were labeled using the BigDye Terminator v3.1 Cycle Sequencing Kit (Thermo Fisher Scientific; USA) according to the manufacturer's protocol. Sanger sequencing was carried out on an ABI PRISM 3500 Genetic Analyzer (Applied Biosystems; USA) according to the manufacturer's protocol.

2. Sequencing data was processed in Cutadapt ver. 1.14 (Cutadapt; USA), BWA ver. 1.14 (Illumina; USA), FastQC ver. 0.11.5 (Illumina; USA), GATK HaplotypeCaller ver. 3.7 (GATK HaplotypeCaller; USA), and snpEff ver. 4.3p (SnpEff; USA). Pathogenicity and conservation of mutations were assessed based on the data extracted from dbNSFP, Clinvar, OMIM, and HGMD databases. SIFT 1.03 (SIFT; USA) and Polyphen2 ver. 2.2.2 (Polyphen2; USA) utilities were used to predict potential pathogenicity of the detected mutations. Information about the frequency of the mutations was obtained from the 1000Genomes project, ExAC and other databases. The annotations and pathogenicity of the detected mutations were predicted as proposed by the Standards and Guidelines for the interpretation of sequence variants developed by ACMG, AMP and CAP [19].

3. Clinical interpretation of sequencing data was aided by OMIM (https://omim.org/), Varsome (https://varsome.com/), ClinVar (https://www.ncbi.nlm.nih.gov/clinvar/), The Human Gene Mutation Database (http://www.hgmd.cf.ac.uk/ac/index.php), and some other genetic databases according to the guidelines for MPS data interpretation [20].

RESULTS

The patients had similar clinical symptoms typical of congenital structural myopathies: the floppy baby syndrome in infancy and delayed motor development. Gait was also affected: some patients were unable to walk on their own; spinal deformities were observed. Neurological symptoms included low muscle tone and strength, weak or absent tendon reflexes in the upper and lower limbs. Biochemistry tests revealed normal creatine

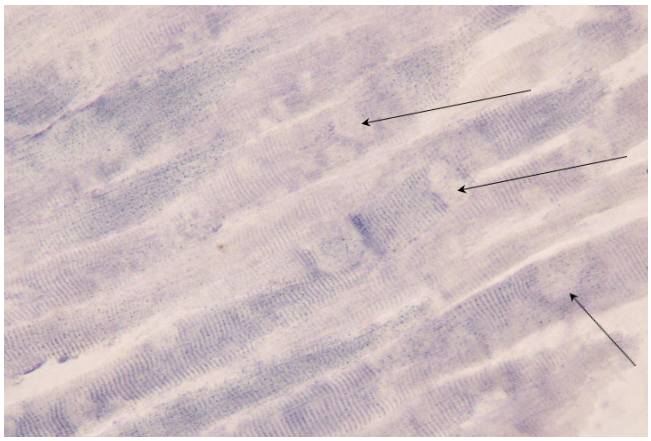

Fig. 3. Skeletal muscle tissue of a 3.5-year-old patient with congenital multiminicore myopathy Histochemical analysis of succinate dehydrogenase activity in frozen sections (×200; the method was proposed by Sukhorukov VS) using the nitro BT method by Nachlass et al. (1957). Cores are abundant in almost all longitudinal sections of the examined muscle fibers (*the arrows*)

phosphokinase (CPK) levels in 3 children under 5 years of age; in 5 children aged 7 to 14 years CPK was either high but within the reference range or slightly elevated above the norm (Table 1). Cores were observed in the biopsy samples of 5 patients (patients 1, 2, 3, 7, and 8) diagnosed with central core disease; histological analysis suggested multiminicore myopathy in 3 patients (patients 4, 5, and 6).

Mutations were detected in 87.5% of cases (7 of 8 examined patients). Six children had mutant variants of *RYR1* and *SEPN1* implicated in congenital myopathy. One patient had a mutation in *LAMA2* associated with merosin-deficient muscular dystrophy (Table 2).

DISCUSSION

Sequencing data are well-correlated with the clinical presentations and morphological features of the patients: in 3 patients with a morphological phenotype of central core disease (patients 1, 2 and 3), mutations were observed in gene *RYR1*; 3 patients with a morphological phenotype of multicore myopathy (patients 4,5 and 6) had mutations in gene *SEPN1* (Table 2). The proportions of patients with mutations in *RYR1* and *SEPN1* were equal and amounted to 42.86 % each relative to all the examined patients with mutations.

Three patients had 4 mutations in *RYR1*. Of those mutant variants, 3 were not described previously, including c.11798A>G, c.14387A>G and c.14581C>T [21, 22, 23].

According to the literature, mutations c.11798A>G and c.14387A>G are associated with sporadic central core disease; our patients who carried them (patients 1 and 2, respectively) were also heterozygous.

Patient 3 had 2 mutations (c.14581C>T and c.7561G>A) in the *RYR1* gene that were presumably compound heterozygous, which suggests an autosomal recessive pattern of inheritance. Mutation c.14581C>T is known to occur in patients with sporadic central core disease but can also be recessive [27]. Mutation c.7561G>A was not described previously. The presence of 2 mutations in one patient suggests an autosomal recessive pattern of inheritance.

Three patients had 4 mutations in the *SEPN1* gene. Mutations c.611dupA, c.713dupA, and c.583G>A were described previously [24, 25]

C.611dupA is a frameshift mutation that produces a shortened dysfunctional protein. This mutation was homozygous in patient 5, which is consistent with an autosomal recessive pattern of inheritance.

Another frameshift mutation c.713dupA was detected in a compound heterozygous patient 4. It is described as a cause of *rigid spine muscular dystrophy* (OMIM entry #602771) in homo- and heterozygous French patients [24]. Genetic variant c.583G>A carried by patient 4 was characterized by the prediction software as likely pathogenic; genetic databases refer to it as benign. Therefore, its role in the disease still needs to be elucidated.

Mutation c.485C>A is a previously unknown mutation that was heterozygous in patient 6. This means that multicore myopathy diagnosed in this patient cannot be confirmed by the genetic test, although morphological and clinical findings suggest otherwise. At the same time, we cannot rule out *SEPN1*- associated multicore myopathy because mutations in the second allele of the gene might have been overlooked due to the technical limitations of massive parallel sequencing.

Sequencing revealed the absence of *RYR1* and *SEPN1* mutations in 2 patients (patients 7 and 8) who had been diagnosed with myopathy/myodystrophy before the genetic test and had a morphological phenotype of central core disease.

Table 1. Symptoms of the patients with morphological signs of core myopathies revealed by histological analysis

Symptoms / Patient	1	2	3	4	5	6	7	8
Weight and height at birth (g/cm)	3310/50	3540/55	2480/48	2800/49	3780/53	3060/50	2859/50	3500/54
Congenital hip dislocation/dysplasia	–	–	+ (dislocation)	–	–	–	+ (dysplasia)	–
Delayed motor development	–	+	+	+	+	–	++	+
Muscle strength	4 points	4 points	4 points	2–3 points	4 points	2–3 points	1–2 points	3–4 points
Gait	Myopathic	Cannot walk at the moment	Myopathic	Myopathic	Myopathic	Has not walked since 9 years of age	Was never able to walk	Myopathic
Spinal deformities	Thoracic hyperkyphosis	Thoracic hyperkyphosis	Curvature of the spine	Thoracic and lumbar spine scoliosis	Rigid spine	Kyphoscoliosis	Scoliosis	Scoliosis
Joint contractures	Ankle joint	–	–	Hip, knee and ankle joints	Ankle joint	Hip, knee and ankle joint	Hip, knee, ankle, elbow and wrist joints	Hip, knee and ankle joint
Reduced reflexes in upper and lower limbs	+	+	+	++	+	++	++	++
Breathing problems	+	+–	N/A	+++	+	+	N/A	+
Reduced intellectual capacity	–	+	+ –	–	–	–	–	–
Additional symptoms	–	–	–	Severe malnutrition	–	Ptosis of the upper eyelid, chronic hypoventilation syndrome	Weak facial muscles, occipital epilepsy	–
CPK levels, un/L (normal range of 15–190)	78	66	79	188	284	174	290	194

Note: 1 — boy, 4 years; 2 — girl, 3 years; 3 — girl, 5 years; 4 — girl, 8 years; 5 — boy, 7 years; 6 — girl, 11 years; 7 — girl, 14 years; 8 — girl, 7 years.

Table 2. A list of mutations detected in the patients with morphological signs of core myopathy

Patient	Diagnosis before the genetic test	Gene	Detected mutations and genotypes					Reference
			Exon №	Transcript №	Nucleotide	Amino acid substitution	Genotype	
1	Congenital structural myopathy. Central core disease	*RYR1*, 19q13.2	86	NM_000540.2	c.11798A>G	p.Tyr3933Cys	Heterozygous	[21]
2	Congenital myopathy	*RYR1*, 19q13.2	100	NM_000540.2	c.14387A>G	p.Tyr4796Cys	Heterozygous	[22]
3	Congenital structural myopathy	*RYR1*, 19q13.2	101	NM_000540.2	c.14581C>T	p.Arg4861Cys	Heterozygous	[23]
			47	NM_000540.2	c.7561G>A	p.Val2521Met	Heterozygous	Not described
4	Congenital myopathy	*SEPN1*, 1p36.11	5	NM_020451.2	c.713dupA	p.Asn238fs	Heterozygous	[24]
			5	NM_020451.2	c.583G>A	p.Ala195Thr	Heterozygous	[25]
5	Congenital myopathy	*SEPN1*, 1p36.11	4	NM_206926.1	c.611dupA	p.Asn204fs	Homozygous	[24]
6	Congenital myopathy	*SEPN1*, 1p36.11	4	NM_206926.1	c.485C>A	p.Ser162*	Heterozygous	Not described
7	Congenital structural myopathy	*LAMA2*, 6q22.33	50	NM_000426.3	c.7147C>T	p.Arg2383*	Heterozygous	[26, 28]
			23	NM_000426.3	c.3406T>C	p.Cys1136Arg	Heterozygous	Not described
8	Congenital muscular dystrophy	–	–	–	Undetected	Undetected	Unknown	–

Note: 1 — boy, 4 years; 2 — girl, 3 years; 3 — girl, 5 years; 4 — girl, 8 years; 5 — boy, 7 years; 6 — girl, 11 years; 7 — girl, 14 years; 8 — girl, 7 years; * — a stop codon.

Patient 7 had 2 presumably compound heterozygous mutations in the *LAMA2* gene (14.28% of total detected mutations). Mutant *LAMA2* variants are associated with type 23 limb-girdle muscular dystrophy (OMIM entry #618138) and congenital merosin-deficient muscular dystrophy (OMIM entry #607855) that follow a dominant recessive pattern of inheritance.

The *LAMA2* mutation c.7147C>T (p.Arg2383*) detected in patient 7 results in the synthesis of a shortened dysfunctional protein. Its homozygous variant was previously described in a 4-year-old girl [28] who had typical symptoms of type A merosin-deficient muscular dystrophy, including congenital hypotonia, muscle weakness, elevated CPK of 1,556 IU/L and white matter abnormalities seen on MRI. Besides, patients afflicted with this disorder can have seizures and structural brain abnormalities. In patients with congenital laminin alpha 2 deficient muscular dystrophy, severity of the clinical symptoms varies, but the causes underlying this phenomenon are not fully understood and might be associated with RNA missplicing [26].

The second detected mutation in the LAMA2 gene is a nonsynonymous substitution c.3406T>C (p.Cys1136Arg) that was not described previously. Nonsynonymous substitutions can result in the formation of alternative splice sites, synthesis of new protein isoforms and conformational changes to the protein structure that affect its function. Therefore, the role of the detected mutation in the development of the disease needs to be elucidated.

The symptoms observed in patient 7 were different from those described above. The differential diagnosis included Werdnig-Hoffmann disease and congenital structural myopathy. Epilepsy was benign and was not considered a symptom. Histological findings suggested central core disease. However, the clinical, morphological and genetic data collected from the patient should not be regarded as controversial. The mechanism underlying the formation of cores in muscle fibers and the time it takes remain understudied [2]. Formation of cores might be the result of disrupted mitochondrial activity. The study of muscle tissue biopsy samples obtained from patients with different forms of congenital myopathy/myodystrophy at different stages of the disease will broaden our knowledge of the interactions and the order of involvement of proteins and muscle tissue components into the pathological process.

No clinically relevant genetic variants associated with neuromuscular disorders were detected in patient 8. However, this might have been due to the technical limitations of massive parallel sequencing.

The absence of mutations in the *RYR1* gene in 2 patients (7 and 8) with a preliminary diagnosis of congenital myopathy/myodystrophy and a morphological phenotype of central core disease confirms the need for extensive molecular genetic testing in such patients. At the same time, in the presence of additional clinical symptoms rarely seen in a particular condition (in our case, patient 7 had seizures) the probability of detecting other molecular-genetic abnormalities increases. This also speaks for the necessity of research into the mechanisms underlying congenital myopathies and myodystrophy and their morphological manifestations.

We have also discovered correlations between CPK activity and the detected mutations. As a rule, CPK levels suggest the location of lesions in patients with neuromuscular disorders, their acuteness and duration. *RYR1* mutations were present only in the patients with normal CPK levels. The highest CPK was observed in the patient with a homozygous *SEPN1* mutation and also in the patient who carried mutations in the *LAMA2* gene associated with the most severe form of congenital myopathy. Perhaps, CPK can be used to measure pathogenicity of a molecular-genetic abnormality (the presence/absence of a protein or the loss of its function) that leads to the disease and causes secondary myodystrophy.

CONCLUSIONS

Our findings confirm that myopathies characterized by the presence of cores in muscle fibers are genetically heterogenous. Mutations in the *RYR1* and *SEPN1* genes are the major genetic cause of core myopathies in Russian patients, which is consistent with the findings of our foreign colleagues. The majority (75%, 6 of 8 patients) of *RYR1* and *SEPN1* mutant variants carried by our patients were described previously. Two previously unknown mutations need to be studied further in order to elucidate their clinical relevance. Our work shows that histological findings cannot be used as the only criterion for the differential diagnosis of congenital myopathies. Morphological phenotypes typical for core myopathies can also be seen in other congenital myopathies

or myodystrophy. This means that clinical, morphological and genetic correlations should be studied in-depth to understand the mechanisms underlying the development of the disease and to come up with effective therapies in the case of complications. The absence of mutations in the genes implicated in congenital myopathies in patients with clinical symptoms and morphological signs of core myopathies requires further investigation.

References

1. Bonne G, Rivier F, Hamroun D. The 2019 version of the gene table of neuromuscular disorders (nuclear genome). Neuromuscul Disord. 2018 Dec; 28 (12): 1031–63. DOI: 10.1016/j.nmd.2018.09.006.
2. Suhorukov VS, Harlamov DA. Vrozhdennye miopatii. M.: OOO Press-Art, 2010; 155 s.
3. Jungbluth H, Sewry CA, Muntoni F. Core Myopathies. Semin Pediatr Neurol. 2011 Dec; 18 (4): 239–49. DOI: 10.1016/j.spen.2011.10.005.
4. Harlamov DA, Baranich TI, Glinkina VV, Brydun AV. Mitohondrial'nye narushenija pri vrozhdennyh miopatijah. Rossijskij vestnik perinatologii i pediatrii. 2014; 59 (3): 32–38.
5. MacLennan DH, Zorzato F, Fujii J, Otsu K, Phillips M, Lai FA, et al. Cloning and localization of the human calcium release channel (ryanodine receptor) gene to the proximal long arm (cen-q13.2) of human chromosome 19. (Abstract) Am J Hum Genet [Internet]. 1989; 45 (suppl.).
6. Moghadaszadeh B, Petit N, Jaillard C, Brockington M, Roy SQ, Merlini L, et al. Mutations in SEPN1 cause congenital muscular dystrophy with spinal rigidity and restrictive respiratory syndrome. Nature Genet. 2001; (29): 17–8.
7. Melnikov KN. Raznoobrazie i svojstva kal'cievyh kanalov vozbudimyh membran. Psihofarmakologija i biologicheskaja narkologija. 2006; (1–2): 1139–51.
8. Chen W, Koop A, Liu Y, Guo W, Wei J, Wang R, et al. Reduced threshold for store overload-induced Ca^{2+} release is a common defect of RyR1 mutations associated with malignant hyperthermia and central core disease. Biochem J. 2017 Aug 7; 474 (16): 2749–61. DOI: 10.1042/BCJ20170282. PMID: 28687594.
9. Suhorukov VS, Harlamov DA, Shatalov PA, Harabadze MN, Yablonskaya MI, Brydun AV i dr. Vrozhdennaja «mnogosterzhnevaja» miopatija. Rossijskij vestnik perinatologii i pediatrii. 2012; 57 (4–1): 90–3.
10. Jungbluth H, Zhou H, Hartley L, Halliger-Keller B, Messina S, Longman C, et al. Minicore myopathy with ophthalmoplegia caused by mutations in the ryanodine receptor type 1 gene. Neurology. 2005 Dec 27; 65 (12): 1930–5. PMID: 16380615.
11. Jungbluth H. Multi-minicore Disease. Orphanet J Rare Dis. 2007; (2): 31–45.
12. McCarthy EJ. Malignant hyperthermia: pathophysiology, clinical presentation, and treatment. AACN Clin Issues. 2004 Apr–Jun; 15 (2): 231–7. PMID: 15461040.
13. Suhorukov VS, Shatalov PA, Harlamov DA, Brydun AV. Izmenenija mitohondrij pri vrozhdennoj miopatii «central'nogo sterzhnja» u detej. Rossijskij vestnik perinatologii i pediatrii. 2011; 56 (4): 84–7.
14. Lescure A, Rederstorff M, Krol A, et al. Selenoprotein function and muscle disease. Biochim Biophys Acta. 2009; (1790): 1569–74.
15. Engel AG, Gomes MR. Congenital myopathy associated with multifocal degeneration of muscle fibers. Trans Am Neurology Assoc. 1966; (91): 222–3.
16. Pirs A. Gistohimiya. M.: Izd-vo inostrannoj literatury, 1962; 963 s.
17. Luft JH. Improvements in epoxy resin embedding methods. J Biophys Biochem Cytol. 1961; (9): 409–14.
18. Reynolds ES. The use of lead citrate at high pH as an electron-opaque stain in electron microscopy. J Cell Biol. 1963; (17): 208–12.
19. Richards S, Aziz N, Bale S, Bick D, Das S, Gastier-Foster J. et al. Standards and guidelines for the interpretation of sequence variants: a joint consensus recommendation of the American College of Medical Genetics and Genomics and the Association for Molecular Pathology. Genet Med. 2015;17 (5): 405–23.
20. Ryzhkova OP, Kardymon OL, Prohorchuk EB, Konovalov FA, Maslennikov AB, Stepanov VA i dr. Rukovodstvo po interpretacii dannyh, poluchennyh metodami massovogo parallel'nogo sekvenirovanija (MPS). Medicinskaja genetika. 2017; 16 (7): 4–17.
21. Duarte ST, Oliveira J, Santos R, Pereira P, Barroso C, Conceição I, et al. Dominant and recessive RYR1 mutations in adults with core lesions and mild muscle symptoms. Muscle Nerve. 2011 Jul; 44 (1): 102–8. DOI: 10.1002/mus.22009. PMID: 21674524.
22. Monnier N, Romero NB, Lerale J, Nivoche Y, Qi D, MacLennan DH, et al. An autosomal dominant congenital myopathy with cores and rods is associated with a neomutation in the RYR1 gene encoding the skeletal muscle ryanodine receptor. Hum Mol Genet. 2000 Nov 1; 9 (18): 2599–608. PMID: 11063719.
23. Davis MR, Haan E, Jungbluth H, Sewry C, North K, Muntoni F, et al. Principal mutation hotspot for central core disease and related myopathies in the C-terminal transmembrane region of the RYR1 gene. Neuromuscul Disord. 2003 Feb; 13 (2): 151–7. PMID: 12565913.
24. Ferreiro A, Quijano-Roy S, Pichereau C, Moghadaszadeh B, Goemans N, Bönnemann C, et al. Mutations of the seleno-protein N gene, which is implicated in rigid spine muscular dystrophy, cause the classical phenotype of multiminicore disease: reassessing the nosology of early-onset myopathies. Am J Hum Genet. 2002 Oct; 71 (4): 739–49. PMID: 12192640.
25. Tajsharghi H, Darin N, Tulinius M, Oldfors A. Early onset myopathy with a novel mutation in the Selenoprotein N gene (SEPN1). Neuromuscul Disord. 2005 Apr; 15 (4): 299–302. PMID: 15792869.
26. Pegoraro E, Fanin M, Trevisan CP, Angelini C, Hoffman EP. A novel laminin alpha 2 isoform in severe laminin alpha 2 deficient congenital muscular dystrophy. Neurology. 2000 Oct 24; 55 (8): 1128–34. PMID: 11071490.
27. Kossugue PM, Paim JF, Navarro MM, Silva HC, Pavanello RC, Gurgel-Giannetti J, et al. Central core disease due to recessive mutations in RYR1 gene: is it more common than described? Muscle Nerve. 2007 May; 35 (5): 670–4. PMID: 17226826.
28. He Z, Luo X, Liang L, Li P, Li D, Zhe M. Merosin-deficient congenital muscular dystrophy type 1A: A case report. Exp Ther Med. 2013 Nov; 6 (5): 1233–6. PMID: 24223650.

Литература

1. Bonne G, Rivier F, Hamroun D. The 2019 version of the gene table of neuromuscular disorders (nuclear genome). Neuromuscul Disord. 2018 Dec; 28 (12): 1031–63. DOI: 10.1016/j.nmd.2018.09.006.
2. Сухоруков В. С., Харламов Д. А. Врожденные миопатии. М.: ООО Пресс-Арт, 2010; 155 с.
3. Jungbluth H, Sewry CA, Muntoni F. Core Myopathies. Semin Pediatr Neurol. 2011 Dec; 18 (4): 239–49. DOI: 10.1016/j.spen.2011.10.005.
4. Харламов Д. А., Баранич Т. И., Глинкина В. В., Брыдун А. В. Митохондриальные нарушения при врожденных миопатиях. Российский вестник перинатологии и педиатрии. 2014; 59 (3): 32–38.

5. MacLennan DH, Zorzato F, Fujii J, Otsu K, Phillips M, Lai FA, et al. Cloning and localization of the human calcium release channel (ryanodine receptor) gene to the proximal long arm (cen-q13.2) of human chromosome 19. (Abstract) Am J Hum Genet [Internet]. 1989; 45 (suppl.).
6. Moghadaszadeh B, Petit N, Jaillard C, Brockington M, Roy SQ, Merlini L, et al. Mutations in SEPN1 cause congenital muscular dystrophy with spinal rigidity and restrictive respiratory syndrome. Nature Genet. 2001; (29): 17–8.
7. Мельников К. Н. Разнообразие и свойства кальциевых каналов возбудимых мембран. Психофармакология и биологическая наркология. 2006; (1–2): 1139–51.
8. Chen W, Koop A, Liu Y, Guo W, Wei J, Wang R, et al. Reduced threshold for store overload-induced Ca^{2+} release is a common defect of RyR1 mutations associated with malignant hyperthermia and central core disease. Biochem J. 2017 Aug 7; 474 (16): 2749–61. DOI: 10.1042/BCJ20170282. PMID: 28687594.
9. Сухоруков В. С., Харламов Д. А., Шаталов П. А., Харабадзе М. Н., Яблонская М. И., Брыдун А. В. и др. Врожденная «многостержневая» миопатия. Российский вестник перинатологии и педиатрии. 2012; 57 (4–1): 90–3.
10. Jungbluth H, Zhou H, Hartley L, Halliger-Keller B, Messina S, Longman C, et al. Minicore myopathy with ophthalmoplegia caused by mutations in the ryanodine receptor type 1 gene. Neurology. 2005 Dec 27; 65 (12): 1930–5. PMID: 16380615.
11. Jungbluth H. Multi-minicore Disease. Orphanet J Rare Dis. 2007; (2): 31–45.
12. McCarthy EJ. Malignant hyperthermia: pathophysiology, clinical presentation, and treatment. AACN Clin Issues. 2004 Apr–Jun; 15 (2): 231–7. PMID: 15461040.
13. Сухоруков В. С., Шаталов П. А., Харламов Д. А., Брыдун А. В. Изменения митохондрий при врожденной миопатии «центрального стержня» у детей. Российский вестник перинатологии и педиатрии. 2011; 56 (4): 84–7.
14. Lescure A, Rederstorff M, Krol A, et al. Selenoprotein function and muscle disease. Biochim Biophys Acta. 2009; (1790): 1569–74.
15. Engel AG, Gomes MR. Congenital myopathy associated with multifocal degeneration of muscle fibers. Trans Am Neurology Assoc. 1966; (91): 222–3.
16. Пирс Э. Гистохимия. М.: Изд-во иностранной литературы, 1962; 963 с.
17. Luft JH. Improvements in epoxy resin embedding methods. J Biophys Biochem Cytol. 1961; (9): 409–14.
18. Reynolds ES. The use of lead citrate at high pH as an electron-opaque stain in electron microscopy. J Cell Biol. 1963; (17): 208–12.
19. Richards S, Aziz N, Bale S, Bick D, Das S, Gastier-Foster J. et al. Standards and guidelines for the interpretation of sequence variants: a joint consensus recommendation of the American College of Medical Genetics and Genomics and the Association for Molecular Pathology. Genet Med. 2015;17 (5): 405–23.
20. Рыжкова О. П., Кардымон О. Л., Прохорчук Е. Б., Коновалов Ф. А., Масленников А. Б., Степанов В. А. и др. Руководство по интерпретации данных, полученных методами массового параллельного секвенирования (MPS). Медицинская генетика. 2017; 16 (7): 4–17.
21. Duarte ST, Oliveira J, Santos R, Pereira P, Barroso C, Conceição I, et al. Dominant and recessive RYR1 mutations in adults with core lesions and mild muscle symptoms. Muscle Nerve. 2011 Jul; 44 (1): 102–8. DOI: 10.1002/mus.22009. PMID: 21674524.
22. Monnier N, Romero NB, Lerale J, Nivoche Y, Qi D, MacLennan DH, et al. An autosomal dominant congenital myopathy with cores and rods is associated with a neomutation in the RYR1 gene encoding the skeletal muscle ryanodine receptor. Hum Mol Genet. 2000 Nov 1; 9 (18): 2599–608. PMID: 11063719.
23. Davis MR, Haan E, Jungbluth H, Sewry C, North K, Muntoni F, et al. Principal mutation hotspot for central core disease and related myopathies in the C-terminal transmembrane region of the RYR1 gene. Neuromuscul Disord. 2003 Feb; 13 (2): 151–7. PMID: 12565913.
24. Ferreiro A, Quijano-Roy S, Pichereau C, Moghadaszadeh B, Goemans N, Bönnemann C, et al. Mutations of the seleno-protein N gene, which is implicated in rigid spine muscular dystrophy, cause the classical phenotype of multiminicore disease: reassessing the nosology of early-onset myopathies. Am J Hum Genet. 2002 Oct; 71 (4): 739–49. PMID: 12192640.
25. Tajsharghi H, Darin N, Tulinius M, Oldfors A. Early onset myopathy with a novel mutation in the Selenoprotein N gene (SEPN1). Neuromuscul Disord. 2005 Apr; 15 (4): 299–302. PMID: 15792869.
26. Pegoraro E, Fanin M, Trevisan CP, Angelini C, Hoffman EP. A novel laminin alpha 2 isoform in severe laminin alpha 2 deficient congenital muscular dystrophy. Neurology. 2000 Oct 24; 55 (8): 1128–34. PMID: 11071490.
27. Kossugue PM, Paim JF, Navarro MM, Silva HC, Pavanello RC, Gurgel-Giannetti J, et al. Central core disease due to recessive mutations in RYR1 gene: is it more common than described? Muscle Nerve. 2007 May; 35 (5): 670–4. PMID: 17226826.
28. He Z, Luo X, Liang L, Li P, Li D, Zhe M. Merosin-deficient congenital muscular dystrophy type 1A: A case report. Exp Ther Med. 2013 Nov; 6 (5): 1233–6. PMID: 24223650.

ADENOSINE-TO-INOSINE RNA EDITING MAY BE IMPLICATED IN HUMAN PATHOGENESIS

Kliuchnikova AA ✉, Moshkovskii SA

Institute of Biomedical Chemistry, Moscow, Russia

Pirogov Russian National Research Medical University, Moscow, Russia

Adenosine-to-inosine (A-to-I) RNA editing is a common mechanism of post-transcriptional modification in many metazoans including vertebrates; the process is catalyzed by adenosine deaminases acting on RNA (ADARs). Using high-throughput sequencing technologies resulted in finding thousands of RNA editing sites throughout the human transcriptome however, their functions are still poorly understood. The aim of this brief review is to draw attention of clinicians and biomedical researchers to ADAR-mediated RNA editing phenomenon and its possible implication in development of neuropathologies, antiviral immune responses and cancer.

Keywords: RNA-specific adenosine deaminase (ADAR), RNA editing, immune resistance, malignant tumour, neurodegenerative disease

Funding: the work was performed within The Programme for fundamental scientific research of state science academies for 2013–2020.

Author contribution: both authors have contributed equally to manuscript writing.

✉ **Correspondence should be addressed:** Anna A. Kliuchnikova
Pogodinskaya 10, bld. 8, Moscow, 119121; a.kliuchnikova@gmail.com

Received: 13.08.2018 **Accepted:** 06.04.2019 **Published online:** 16.04.2019

DOI: 10.24075/brsmu.2019.028

ПРИРОДНОЕ РЕДАКТИРОВАНИЕ РНК С ЗАМЕНОЙ АДЕНОЗИНА НА ИНОЗИН МОЖЕТ УЧАСТВОВАТЬ В ПАТОГЕНЕЗЕ БОЛЕЗНЕЙ ЧЕЛОВЕКА

А. А. Ключникова ✉, С. А. Мошковский

Научно-исследовательский институт биомедицинской химии имени В. Н. Ореховича, Москва, Россия

Российский национальный исследовательский медицинский университет имени Н. И. Пирогова, Москва, Россия

Редактирование РНК с заменой аденина на инозин является наиболее распространенным природным механизмом посттранскрипционной модификации у разных многоклеточных организмов, включая позвоночных, и катализируется ферментами семейства РНК-зависимых аденозиндезаминаз ADAR. Недавние исследования с использованием высокопроизводительного секвенирования нуклеиновых кислот позволили выявить тысячи участков такого редактирования и у человека, однако функция многих из них остается не до конца ясной. Мы хотим привлечь внимание клиницистов и специалистов по биомедицине к ADAR-опосредованному редактированию мРНК и его возможному участию в развитии болезней нервной системы, противовирусных иммунных реакций и злокачественных опухолей.

Ключевые слова: РНК-зависимая аденозиндезаминаза (ADAR), редактирование РНК, иммунитет, злокачественная опухоль, нейродегенеративные заболевания

Финансирование: работа выполнена в рамках Программы фундаментальных научных исследований государственных академий наук на 2013–2020 гг.

Информация о вкладе авторов: оба автора в равной степени участвовали в написании текста статьи.

✉ **Для корреспонденции:** Анна Алексеевна Ключникова
ул. Погодинская, д. 10, стр. 8, г. Москва, 119121; a.kliuchnikova@gmail.com

Статья получена: 13.08.2018 **Статья принята к печати:** 06.04.2019 **Опубликована онлайн:** 16.04.2019

DOI: 10.24075/vrgmu.2019.028

RNA editing is one of mechanisms of post-transcriptional modification of nucleotide chemical structure. Here we review RNA editing as a natural phenomenon distinguished from programmable genome editing tools such as RNA editing with CRISPR-Cas systems in bacteria. The most common type of natural RNA editing is adenosine to inosine (A-to-I) deamination catalyzed by RNA-specific adenosine deaminases (ADARs). The process is called “editing” as such modifications in many cases lead to changing the informational content of the RNA.

In humans, three genes encoding ADAR proteins are found; ADAR1 (encoded by adar gene) and ADAR2 (encoded by adarb1 gene) proteins have enzymatic activity while ADAR3 (encoded by adarb2) acts as an inhibitor of editing [1]. Active ADAR enzymes are binding to dsRNA and converting adenosine (A) to inosine (I) by deamination. Codon changes can arise from such editing. Deamination in coding regions of RNA may result in recoding of proteins as inosine typically mimicks guanosine during translation [2].

ADAR-mediated RNA editing was unknown till 1987; recently, the process was shown to be widespread in genomes of most animals and associated with different functions. Thus, RNA editing was reported to be particularly common in some Protostomia — cephalopods, in particular — as compared to other invertebrates and was supposed to sustain molecular plasticity under changing environmental conditions and the evolutionary conservatism at the same time [3].

In mammals, RNA editing occurs as well. In a recent large-scale transcriptome research, the process was investigated comprehensively and more than 20,000 editing sites in human and mouse were identified. More than two thousand human editing sites were reported to lead to amino acid substitutions in the encoded proteins [1]. A variety of transcriptome editing sites is called "RNA editome" similarly to other molecular "-omes".

Until recently, RNA editing role was unclear. However, using knockout rodent models allowed to demonstrate that ADAR1 was mainly associated with control of innate immune responses

while ADAR2 regulated signal transmission and excitability in the central nervous system [4]. ADARs edit various substrates including matrix RNA, short and long non-coding RNA as well as viral RNA, that have only one thing in common: double stranded RNA. The scale of the phenomenon was estimated only recently, and due to its complexity the data on RNA editing functions in different objects are accumulated slowly.

Let us consider the significance of phenomenon of natural editing RNA observed at the proteome level in humans and laboratory animals as a process possibly contributing to development of antiviral immune responses, nervous system diseases and cancer.

RNA editing in the central nervous system

RNA editing occurs actively in the central nervous system (CNS). It is associated mainly with ADAR2 enzyme [1]. Such editing is known to make point substitutions in related sequences of voltage-gated ion channels and G protein-coupled receptors of the nervous system. RNA editing events in GluK and GluA glutamate receptors are well studied. Normally, RNA editing results in an amino acid substitution of glutamine for arginine in one of the glutamate receptor subunits during development of the nervous system. The receptors containing the edited subunit become Ca^{2+}-impermeable while channels containing unedited subunits are Ca^{+}-permeable. Neurons with such subunits are subject to a "physiological" excitotoxicity due to an increase of glutamate content in synapses. It is known to result in neuronal death and be an important factor of development of some neurodegenerative disorders, a spinal neurodegeneration at amyotrophic lateral sclerosis (ALS), in particular [5]. Mutations in adarb1 could contribute to epilepsy and diseases involving neuronal plasticity defects such as autism and Martin-Bell syndrome [4]. In mice, the ADAR2 knockout resulting in appearance of unedited glutamate receptors is lethal as it causes overexcitement in brain cells with strong epileptic seizures.

RNA editing and virus-induced immunity

Some findings point to ADAR1 implication in immunity including immune responses to infection with RNA viruses. It was shown that ADAR1 enzyme can play a role in mechanisms of protection against viral infections and inflammation. Thus, ADAR1 can edit the hepatitis C virus RNA limiting its replication [6]. The adenosinedeaminase was shown to edit influenza virus to a greater extent compared to measles virus — on the one hand, this can make influenza virus nonfunctional, while on the other hand, can promote mutagenesis and evasion from immunity [7].

Type I interferon is known to induce ADAR1 increasing synthesis of its long p150 form however, such activity interferes with formation of stress granules against measles virus. Thus, ADAR1 is considered to be a suppressor of innate immune responses in this case [8].

Missens mutations leading to amino acid substitutions in ADAR1 reduce activity of RNA editing and cause Aicardi-Goutières syndrome (AGS). AGS is characterized by progressing encephalopathy and interferonopathy mimicking a viral infection [9] that demonstrates the involvement of ADAR1 into immune response.

RNA editing and cancer

The results of the recent research performed within The Cancer Genome Atlas (TCGA) project facilitated systematization of data on genomes and transcriptomes in different tumor types [10]. The use of available sequencing data made it possible to obtain RNA editing libraries. Significant RNA editing differences have been observed between cancerous and normal tissues. For most of the tested cancer types including head and neck cancer, breast cancer and thyroid carcinoma, the increased RNA editing levels were reported that was associated with high ADAR1 expression levels in tumors [11].

Occurrence of RNA editing events in brain cells becomes higher with age however, may decrease in glioblastoma [12]. Similar to cancer driver somatic mutations, RNA editing events can promote tumor progression. Thus, both in vitro and in vivo experiments provided data on a protein playing an important role in cell growth and proliferation due to maintaining the homeostasis of polyamine in cells. RNA editing of AZIN1 (encoding antizyme inhibitor 1) by ADAR1 results in a serine-to-glycine substitution at residue 367 of AZIN1. The edited form has a stronger affinity to antizyme and induces a cytoplasmic-to-nuclear AZIN1 translocation resulting in a more aggressive behavior of tumor [13]. Thus, the edited protein can be considered a potential therapeutic target.

Some RNA editing events can be used as predictive markers and have an effect on tissue response in cancer therapy. For example, a glycine-to-arginine substitution at position 764 (R764G) in glutamate receptor *GRIA2* and an isoleucine to valine substitution (I635V) at *COG3* protein responsible for vesicle-mediated transport between the Golgi complex and endoplasmic reticulum, increase sensitivity of mitogen-activated protein kinase kinase (MAPKK) to kinase inhibitors [14]. ADAR2 onco-supressing properties are of particular interest in studying glioblastoma. ADAR2-mediated editing the CDC14B phosphatase responsible for DNA damage can modulate a cell cycle pathway involving the Skp2/p21/p27 proteins and inhibit growth of glioblastoma [12].

Although a large amount of information on ADARs and RNA editing has been already accumulated, the biological significance of RNA editing remains largely unknown. In most cases it is not clear whether the editing events are implicated in transcriptome regulation or provide proteome functional plasticity or perhaps related to molecular noise. ADARs are known to edit a variety of dsRNA substrates such as matrix RNA, short and long non-coding RNA as well as viral RNA. The scale of this phenomenon becomes recently clear with a progress in studying RNA modifications at a genome-wide scale [1] that however require further functional confirmation.

Thus, ADAR1 activity is known to be connected with antiviral immune responses as well as regulation of cellular responses to Type I interferon. The general opinion is that ADAR1 activity has a proviral impact and in case of viral absence it suppresses undesirable cellular immune responses (for example, mutations in adar gene cause Aicardi-Goutières syndrome with a childhood encephalitis and interferonopathy). The activity of ADAR2 was reported to be involved in regulation of the central nervous system, for example, in the form of excitatory stimuli (Fig. 1).

It was also reported that RNA editing events can play a crucial role in development of cancer. The activity of ADAR1 is likely to have oncogenic effect. The edited AZIN1 protein can be considered a potential therapeutic target. The edited form of COG3 protein can serve as a predictive marker and have an effect on cellular response in cancer therapy [15]. In case of CDC14B, PODXL, GABRA3 and IGFBP7 proteins, ADAR2 editing may probably have oncosupressing effects [4].

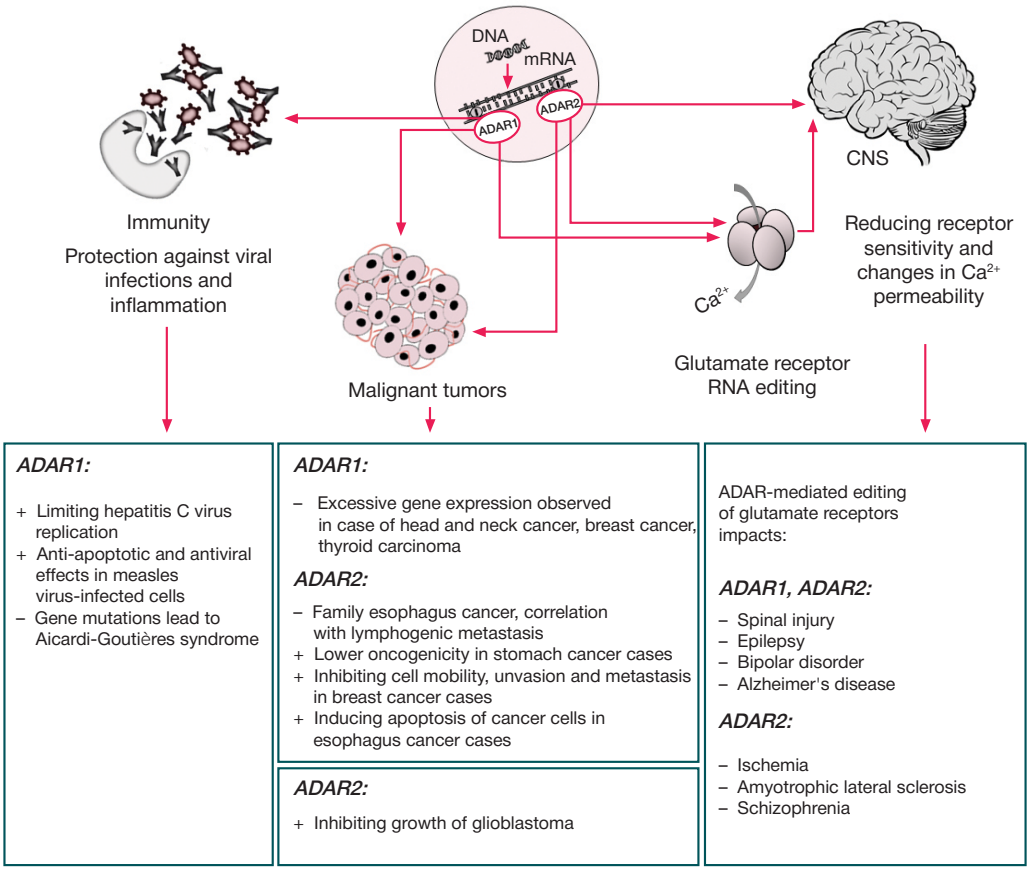

Fig. 1. ADAR effects associated with human diseases. Changes in ADAR1 activities are assiciated with immune protection against viral infections and inflammation and with certain types of cancer; RNA editing in glutamate receptors normally occurs in CNS. ADAR2 effects are associated with both positive and negative impacts on tumor progression while its deficiency may cause various CNS disorders

CONCLUSIONS

Based on the above-referenced examples, ADAR-mediated RNA editing is an evolutionarily ancient mechanism having various, yet understudied, functions in embryonic development of the central nervous system in particular. In pathological conditions such as neurodegenerative diseases and malignant tumors, levels of editing of many transcripts are changed. It is necessary to further investigate the mechanisms of cellular and histological effects of RNA editing. It is also important to distinguish significant editing events from the molecular noise and to find out whether it is possible to consider ADAR enzymes and related products as predictive biomarkers and molecular targets for therapeutic strategies.

References

1. Tan MH, Li Q, Shanmugam R, Piskol R, Kohler J, Young AN, et al. Dynamic landscape and regulation of RNA editing in mammals. Nature. 2017; (550): 249–54.
2. Basilio C, Wahba AJ, Lengyel P, Speyer JF, Ochoa S. Synthetic polynucleotides and the amino acid code. V Proc Natl Acad Sci USA. 1962; (48): 613–6.
3. Liscovitch-Brauer N, Alon S, Porath HT, Elstein B, Unger R, Ziv T, et al. Trade-off between Transcriptome Plasticity and Genome Evolution in Cephalopods. Cell. 2017; (169): 191–202.e11.
4. Gallo A, Vukic D, Michalík D, O'Connell MA, Keegan LP. ADAR RNA editing in human disease; more to it than meets the I. Hum Genet. 2017; (136): 1265–78.
5. Young PE, Kum Jew S, Buckland ME, Pamphlett R, Suter CM. Epigenetic differences between monozygotic twins discordant for amyotrophic lateral sclerosis (ALS) provide clues to disease pathogenesis. PLoS One. 2017; (12): e0182638.
6. Taylor DR, Puig M, Darnell MER, Mihalik K, Feinstone SM. New antiviral pathway that mediates hepatitis C virus replicon interferon sensitivity through ADAR1. J Virol. 2005; (79): 6291–8.
7. Suspène R, Petit V, Puyraimond-Zemmour D, Aynaud MM, Henry M, Guétard D, et al. Double-stranded RNA adenosine deaminase ADAR-1-induced hypermutated genomes among inactivated seasonal influenza and live attenuated measles virus vaccines. J Virol. 2011; (85): 2458–62.
8. John L, Samuel CE. Induction of stress granules by interferon and down-regulation by the cellular RNA adenosine deaminase ADAR1. Virology. 2014; (454–455): 299–310.
9. Crow YJ. Aicardi-Goutières syndrome. Handb Clin Neurol. 2013; (113): 1629–35.
10. Tomczak K, Czerwińska P, Wiznerowicz M. The Cancer Genome Atlas (TCGA): an immeasurable source of knowledge. Contemp Oncol (Poznan, Poland). 2015; (19): A68–77.
11. Peng X, Xu X, Wang Y, Hawke DH, Yu S, Han L, et al. A-to-I RNA Editing Contributes to Proteomic Diversity in Cancer. Cancer Cell. 2018; (33): 817–828.e7.
12. Galeano F, Rossetti C, Tomaselli S, Cifaldi L, Lezzerini M, Pezzullo M, et al. ADAR2-editing activity inhibits glioblastoma growth through the modulation of the CDC14B/Skp2/p21/p27 axis. Oncogene. 2013; (32): 998–1009.
13. Chen L, Li Y, Lin CH, Chan THM, Chow RKK, Song Y, et al. Recoding RNA editing of AZIN1 predisposes to hepatocellular carcinoma. Nat Med. 2013; (19): 209–16.

14. Han L, Diao L, Yu S, Xu X, Li J, Zhang R, et al. The Genomic Landscape and Clinical Relevance of A-to-I RNA Editing in Human Cancers. Cancer Cell. 2015; (28): 515–28.

15. Xu X, Wang Y, Liang H. The role of A-to-I RNA editing in cancer development. Curr Opin Genet Dev. 2018; (48): 51–6.

Литература

1. Tan MH, Li Q, Shanmugam R, Piskol R, Kohler J, Young AN, et al. Dynamic landscape and regulation of RNA editing in mammals. Nature. 2017; (550): 249–54.
2. Basilio C, Wahba AJ, Lengyel P, Speyer JF, Ochoa S. Synthetic polynucleotides and the amino acid code. V Proc Natl Acad Sci USA. 1962; (48): 613–6.
3. Liscovitch-Brauer N, Alon S, Porath HT, Elstein B, Unger R, Ziv T, et al. Trade-off between Transcriptome Plasticity and Genome Evolution in Cephalopods. Cell. 2017; (169): 191–202.e11.
4. Gallo A, Vukic D, Michalík D, O'Connell MA, Keegan LP. ADAR RNA editing in human disease; more to it than meets the I. Hum Genet. 2017; (136): 1265–78.
5. Young PE, Kum Jew S, Buckland ME, Pamphlett R, Suter CM. Epigenetic differences between monozygotic twins discordant for amyotrophic lateral sclerosis (ALS) provide clues to disease pathogenesis. PLoS One. 2017; (12): e0182638.
6. Taylor DR, Puig M, Darnell MER, Mihalik K, Feinstone SM. New antiviral pathway that mediates hepatitis C virus replicon interferon sensitivity through ADAR1. J Virol. 2005; (79): 6291–8.
7. Suspène R, Petit V, Puyraimond-Zemmour D, Aynaud MM, Henry M, Guétard D, et al. Double-stranded RNA adenosine deaminase ADAR-1-induced hypermutated genomes among inactivated seasonal influenza and live attenuated measles virus vaccines. J Virol. 2011; (85): 2458–62.
8. John L, Samuel CE. Induction of stress granules by interferon and down-regulation by the cellular RNA adenosine deaminase ADAR1. Virology. 2014; (454–455): 299–310.
9. Crow YJ. Aicardi-Goutières syndrome. Handb Clin Neurol. 2013; (113): 1629–35.
10. Tomczak K, Czerwińska P, Wiznerowicz M. The Cancer Genome Atlas (TCGA): an immeasurable source of knowledge. Contemp Oncol (Poznan, Poland). 2015; (19): A68–77.
11. Peng X, Xu X, Wang Y, Hawke DH, Yu S, Han L, et al. A-to-I RNA Editing Contributes to Proteomic Diversity in Cancer. Cancer Cell. 2018; (33): 817–828.e7.
12. Galeano F, Rossetti C, Tomaselli S, Cifaldi L, Lezzerini M, Pezzullo M, et al. ADAR2-editing activity inhibits glioblastoma growth through the modulation of the CDC14B/Skp2/p21/p27 axis. Oncogene. 2013; (32): 998–1009.
13. Chen L, Li Y, Lin CH, Chan THM, Chow RKK, Song Y, et al. Recoding RNA editing of AZIN1 predisposes to hepatocellular carcinoma. Nat Med. 2013; (19): 209–16.
14. Han L, Diao L, Yu S, Xu X, Li J, Zhang R, et al. The Genomic Landscape and Clinical Relevance of A-to-I RNA Editing in Human Cancers. Cancer Cell. 2015; (28): 515–28.
15. Xu X, Wang Y, Liang H. The role of A-to-I RNA editing in cancer development. Curr Opin Genet Dev. 2018; (48): 51–6.

HIGH-SPEED BRAIN-COMPUTER COMMUNICATION INTERFACE BASED ON CODE-MODULATED VISUAL EVOKED POTENTIALS

Grigoryan RK[1] ✉, Filatov DB[1,2], Kaplan AY[1]

[1] Faculty of Biology, Lomonosov Moscow State University, Moscow, Russia

[2] Department of Mechanics and Mathematics, Lomonosov Moscow State University, Moscow, Russia

Brain-computer interface (BCI) technologies are actively used in clinical practice to communicate with patients unable to speak and move. Such interfaces imply identifying potentials evoked by stimuli meaningful to the patient in his/her EEG and interpreting these potentials into inputs for the communication software. The stimuli can take form of highlighted letters on a screen, etc. This study aimed to investigate EEG indicators and assess the command input performance of a promising type of BCI utilizing the so-called code-modulated visual evoked potentials (CVEP) appearing in response to a certain sequence of highlights of the desired letter. The operation of the interface was studied on 15 healthy volunteers. During the experiments, we changed the speed of stimuli demonstration and inverted the order of flashing. It was established that the optimal speed of stimulation significantly depends on individual traits of the person receiving the stimuli, and inversion of their sequence does not affect operation of the interface. The median accuracy of selection of commands was as follows: 1 s stimulation cycle mode — 0.96 and 0.95 (information transfer rate 142 and 141 bit per minute); 2 s stimulation cycle mode — 1; 0.5 s cycle — 0.33. The evoked potentials were most expressed at the Oz site. It was assumed that CVEP-based brain-computer interfaces can be optimized through individualization of the set of stimulation parameters.

Keywords: neurocomputer interfaces, evoked potentials, EEG, Electroencephalogram, BCI, brain-computer interfaces, speech disorders, CVEP, code-modulated visual evoked potentials

Author contribution: Grigoryan RK — experiment planning and conducting, data processing, article authoring; Filatov DB — experiment planning, software development, article authoring; Kaplan AY — task setting, experiment planning, general research effort management, article authoring.

Compliance with ethical standards: the study was approved by the ethical commission of the Lomonosov Moscow State University's Faculty of Biology (Protocol № 29-ch of December 11 2015); the participants signed a voluntary informed consent.

✉ **Correspondence should be addressed:** Rafael K. Grigoryan
Leninskie Gory 1, bld. 12, Moscow, 119234; grraph.bio@gmail.com

Received: 29.07.2018 **Accepted:** 24.03.2019 **Published online:** 04.04.2019

DOI: 10.24075/brsmu.2019.019

ВЫСОКОСКОРОСТНОЙ КОММУНИКАЦИОННЫЙ ИНТЕРФЕЙС МОЗГ-КОМПЬЮТЕР НА ОСНОВЕ КОДИРОВАННЫХ ЗРИТЕЛЬНЫХ ВЫЗВАННЫХ ПОТЕНЦИАЛОВ

Р. К. Григорян[1] ✉, Д. Б. Филатов[1,2], А. Я. Каплан[1]

[1] Биологический факультет, Московский государственный университет имени М. В. Ломоносова, Москва, Россия

[2] Механико-математический факультет, Московский государственный университет имени М. В. Ломоносова, Москва, Россия

Технологии интерфейсов мозг-компьютер (ИМК) активно используют в клинической практике для обеспечения коммуникации с пациентами, не способными к речи и движениям. Ввод команд в компьютер посредством таких интерфейсов осуществляют на основе выделения в ЭЭГ вызванных потенциалов в ответ на значимые для пользователя стимулы, например подсвеченные на экране буквы. Целью работы было исследовать показатели ЭЭГ и эффективность ввода команд в перспективном типе ИМК на основе так называемых кодированных вызванных потенциалов, возникающих в ответ на определенную последовательность подсветок нужной буквы. На 15 здоровых добровольцах изучали работу такого интерфейса на разных скоростях подачи стимульных последовательностей при их инвертировании, когда подсветку и ее отсутствие меняли местами. Показано, что оптимальное значение скорости стимуляции имеет значительную индивидуальную вариабельность, а инверсия стимульной последовательности не оказывает влияния на работу интерфейса. Медианная точность выбора команд составила: в режимах с циклом стимуляции 1 с — 0,96 и 0,95 (скорость передачи информации 142 и 141 бит/мин); в режиме со стимульным циклом 2 с — 1; с циклом 0,5 с — 0,33. Максимальную выраженность вызванных потенциалов наблюдали в отведении Oz. Сделано предположение о том, что оптимизация нейроинтерфейсов на основе кодированных вызванных потенциалов возможна на основе индивидуального подбора параметров стимуляции.

Ключевые слова: нейроинтерфейсы, вызванные потенциалы, ЭЭГ, электроэнцефалограмма, ИМК, интерфейс мозг-компьютер, нарушения речи, КЗВП, кодированные зрительные вызванные потенциалы

Информация о вкладе авторов: Р. К. Григорян — планирование и проведение эксперимента, обработка данных, подготовка статьи; Д. Б. Филатов — планирование эксперимента, разработка программного обеспечения (ПО), подготовка статьи; А. Я. Каплан — постановка задачи, планирование эксперимента, руководство проведением исследования, подготовка статьи.

Соблюдение этических стандартов: исследование одобрено этической комиссией Биологического факультета МГУ имени М. В. Ломоносова (протокол № 29-ч от 11 декабря 2015 г.); испытуемые подписали добровольное информированное согласие на участие в исследовании.

✉ **Для корреспонденции:** Рафаэль Каренович Григорян
ул. Ленинские горы, д. 1, стр. 12, г. Москва, 119234; grraph.bio@gmail.com

Статья получена: 29.07.2018 **Статья принята к печати:** 24.03.2019 **Опубликована онлайн:** 04.04.2019

DOI: 10.24075/vrgmu.2019.019

Brain-computer interface (BCI) is a technology that allows patients with speech and movement disorders to control a computer through the analysis of correlates of their neuronal activity. BCI requires the user to focus attention either on internal images, e.g., limb movements, or on objects on the screen, like letters needed at the given moment. BCI systems translate such mental efforts into computer input commands by registering specific EEG markers peculiar to such efforts [1–3]. Interfaces that make use of visual potentials evoked, for example, by flashing objects on the screen, offer a wide range

of EEG-detectable commands, their amount being the same as that of on-screen stimuli. P300 component is the traditional EEG marker signaling of the user's attention to a specific event, like flashing a certain letter [4, 5]. Such interfaces have lately been actively introduced into the medical rehabilitation practice to enable communication with patients suffering from severe speech and movement disorders [6]. Their reliability in translating commands given by cognitively intact patients is sufficient, but the speed of operation is quite low, which is a drawback. For example, a comparison of BCI capabilities as used by healthy people and patients with amyotrophic lateral sclerosis has revealed that the text typing rate does not exceed 2–3 letters per minute with each target object shown 14 times. With the accuracy in both groups exceeding 95%, such a rate translates to 11–14 bits per minute (bpm) [7], which makes BCI using P300 as marker uncomfortable even for healthy people. Code-modulated visual evoked potentials (CVEP) promise to speed up BCI transfer rates. CVEP is a joint EEG-detectable response to the special irregular frequency sequences of flashes of the required on-screen object. Such sequences stimulate a steady state visually evoked potential (SSVEP) registered by EEG, which is phase-locked with stimulation. Phase synchronization, which is also peculiar to SSVEP-enabled BCI featuring regular frequency stimulation, allows the evoked potential to retain the properties of the stimuli sequence to a certain degree, in particular — its cyclicity, autocorrelation and spectral characteristics. Presenting a number of visual stimuli through a number of different sequences that correlate with each other at least minimally allows distinguishing between the evoked potentials brought by different stimuli through a correlation analysis. There are various sets of binary sequences with suitable cross-correlation properties, such as the Gold codes, Barker codes and m-sequences. They are used to identify signals carried on the same frequency in various spheres, like mobile communications and satellite navigation.

M-sequence is a pseudo-random binary sequence that has a single peak of autocorrelation function at zero shift. With a cyclic shift, one m-sequence can produce several sequences not correlated with each other, which facilitates its application in BCI featuring a large number of stimuli, as it shortening the classifier learning period. To distinguish between the potentials evoked by different stimuli, it is necessary to assemble a learning sample. Such a sample should contain potentials corresponding to each stimulus. With each stimulus using its own binary sequence generated by a single m-sequence, it is enough to get the reference evoked potential peculiar only to that binary sequence. Then, it is possible to detect the target stimulus by shift of the correlation function's peak between spatially filtered sections of the recorded EEG and that reference evoked potential. As a result, the duration of learning does not depend on the number of different stimuli, which allows using the amount of stimuli sufficient to print a text.

Canonical correlation analysis of EEG allows reliable detection of short instances of code-modulated evoked potentials synchronous with the flashes of the currently needed on-screen object. The number of stimuli activation repetition cycles therein can be as low as 2 or 3. Thus enabled BCI offer information transfer rates in excess of 100 bpm [8]. Both EEG and electrocorticogram [9] allow registering code-modulated evoked potentials; they can be used to optimize BCI operation to adjust to error-related potentials and to utilize color gamut in the stimulus environment [11].

Seeking to find the optimal modes of code-modulated on-screen object flashing for BCI, we tested operation with different sequences and rates of stimuli flashes.

METHODS

Participants

Fifteen healthy volunteers (7 female and 8 male) aged 18–30 years participated in the study. The inclusion criteria were: no history of neurological diseases, including epilepsy; normal or corrected vision. The exclusion criteria were: age different from the required; history of neurological diseases; vision problems.

EEG registration

We used the Neurovisor-BMM 40 EEG amplifier (Meditsinskiye Computerniye Systemy; Russia) to record biopotentials, and 22 channels (FCz, C3, C1, Cz, C2, C4, CP3, CP1, CPz, CP2, CP4, P5, P3, Pz, P4, P6, PO3, POz, PO4, O1, Oz, O2) with AFz as a grounding electrode and two averaged ear electrodes as reference. Before recording, we checked the interelectrode impendance; the recording was started after the resistance was brought to the values below 10 kOhm. The sampling rate was 500 Hz.

Experimental rig

The experiment was controlled from a computer using custom software developed by the authors in C++. The stimuli were shown to participants on a 24-inch display with a refresh rate of 120 Hz. The participants sat in a chair approximately 60 cm away from the display. A photosensor was used to ensure synchronization of EEG recording and stimuli presentation.

Stimuli presentation

The objects were presented in 32 square cells (4 by 8 table) containing letters on a black background. The stimulation was effected through changing the color of the cell from black to white.

The color change algorithm was determined by a 63-bit m-sequence. Each cell changed color in accordance with its own m-sequence derived from the basis sequence through 2-bit cyclic shifts. Thus, activation of the first cell followed the basis sequence, that of the second cell was shifted by 2 bits, of the 10th — by 18 bits, etc. Overall, we used two basis m-sequences: basis — [0, 0, 0, 0, 0, 1, 1, 1, 1, 1, 0, 1, 1, 1, 1, 0, 0, 1, 1, 1, 0, 1, 0, 1, 1, 0, 0, 0, 1, 0, 1, 1, 1, 0, 0, 0, 1, 1, 0, 1, 1, 0, 1, 0, 0, 1, 0, 0, 0, 1, 0, 0, 1, 1, 0, 0, 1, 0, 1, 0, 1, 0] and inverted — [1, 1, 1, 1, 1, 0, 0, 0, 0, 0, 1, 0, 0, 0, 0, 1, 1, 0, 0, 0, 1, 0, 1, 0, 0, 1, 1, 1, 1, 0, 1, 0, 0, 0, 1, 1, 1, 0, 0, 1, 0, 0, 1, 0, 1, 1, 0, 1, 1, 1, 0, 1, 1, 0, 0, 1, 1, 0, 1, 0, 1, 0, 1].

There are no other 63-bit m-sequences that are not cyclic shifts of these. The inverted sequence is similar to the basis one in terms of autocorrelation properties, but it generates a significantly different visual stimulation.

In the course of our experiment, we tested four modes of BCI, each with its own m-sequence and stimulation rate. The first two modes featured basis and inverted sequences, respectively. The period was 1 second. Parameters of the third, "slow" mode — basis sequence and 2-second period, those of the fourth, "fast" mode — period of 500 ms.

Thus, the duration of one bit in white and black colors in standard, fast and slow modes were approximately 16, 8 and 32 ms, respectively.

Structure of the study

Each volunteer participated in 4 experimental sessions. The order of modes was selected at random after briefing and electrodes

placement. Each mode session began with the classifier learning from the participant's viewing one of the stimuli for 40 full sequence presentation periods. After that, the participant had to enter 32 commands following a predetermined order of concentration on stimuli. Entering a command took a careful look at a particular letter while concentrating on its flashes. After a few seconds, the system produces an answer, which could be correct or wrong. Then the stimulation is stopped. Following a break of several seconds, the stimulation resumed and the participant had to try to enter another command.

The command was considered entered when the classifier reached a certain threshold. The accuracy of the choice of commands was determined as the ratio of correctly entered commands to the total number of input attempts.

Pattern classification

Canonical correlation analysis allows obtaining the weights of channels used to spatially filter EEG and to isolate a significant response to the sequence of stimuli. Weights obtained through analyzing EEG readings recorded while learning were used to decrease the signal's dimension. Learning yielded a single-channel m-sequence response signal averaged over 40 full periods. During actual operation, a one-dimensional signal peculiar to demonstration of the m-sequence in full triggers compilation of the function describing its correlation with the signal obtained during learning. The command selected by the user is determined by the shift of peak of this correlation function. Determining the number of the target stimulus takes division of the correlation function's time shift maximum by the time of one bit implementation and the shift between successive stimuli.

Data analysis

We used the scipy 1.1.0 package [12] to process the results, normalized cross-correlation to build correlation maps and applied the Wilcoxon test (Holm-Sidak multiple comparison correction) to pairwise comparisons.

RESULTS

Assessment of classification accuracy and information transfer rate

In slow mode, with the m-sequence period of 2 s, the median accuracy of command selection reached 1 (Fig. 1). In basis and inverted m-sequence modes the accuracy was 0.96 and 0.95, respectively. In the fast mode the median accuracy was 0.33, which makes it the only mode the accuracy of which is significantly different from that of all other modes with the multiple comparison correction applied ($p < 0.05$). However, one participant showed the accuracy of 0.96 in this mode, a result that cannot be explained by random reasons since it was preceded by input of 32 commands.

The command input rate is another important property of BCI. In the modes with m-sequence period of 1 s, the median time required to identify one command was 2 s. In the slow mode, the figure was 3.5 s, in the fast mode — 1.2 s.

Information transfer rate is an integrative indicator of the BCI quality: it combines both the rate and the accuracy of command selection. We used the Shannon definition as applied to neurocomputer interfaces [13] to calculate the indicator. The median information transfer rate in the basis and inverted sequence modes was 141 and 142 bpm, in the slow mode — 93 bpm, while the fast mode yielded the smallest value: 37 bpm, which is the result of low accuracy in command selection. In the latter mode, however, one user was able to enter commands accurately and showed the highest transfer rate of 287 bpm, with the command input time being 1 second and accuracy of 0.96. The information transfer rate at the m-sequence period of 1 second was significantly different from the slow mode ($Z = 2.7$; $p = 0.019$).

The shape of evoked potentials and topographic distribution of evoked activity

Figure 2 shows the shape of code-modulated evoked potentials averaged relative to the first bit of the sequence, restored for the zero-shift m-sequence.

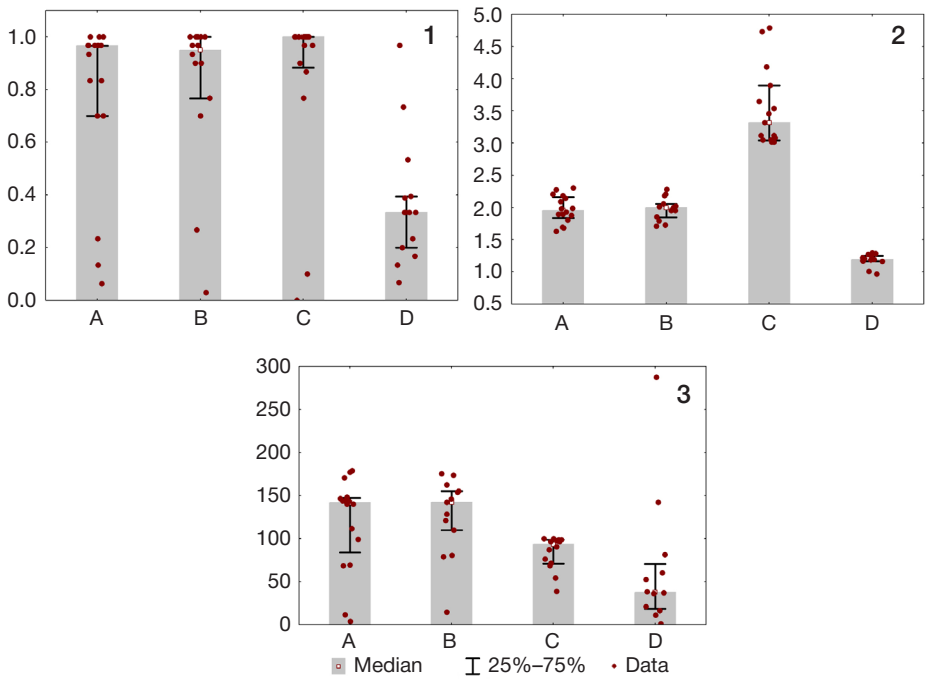

Fig. 1. Neurointerface utilization by users: indicators. **1** — command input accuracy; **2** — average command input time (in seconds); **3** — information transfer rate, bpm; A — basis stimulus sequence; B — inverted; C — slow mode; D — fast mode

As a quantitative characteristic, we used the correlation between the averaged evoked potential and single potentials corresponding to single m-sequences. Figure 3 shows the maps of maximum values of normalized cross-correlations between averaged evoked potentials and responses to single sequences.

According to the figure, the degree of similarity between evoked potentials reaches its maximum in occipital channels. All modes that allowed a high accuracy of command selection had the highest correlation degree at the Oz site. The maximum correlation was registered in 8 channels: P4, P6, PO3, POz, PO4, O1, O2, Oz. The absolute values of the cross-correlation maxima do not differ significantly between the modes when compared in corresponding channels. In the fast mode, localization of evoked potentials was less pronounced, which is probably one of the reasons behind the poorest results shown by the participants.

DISCUSSION

Research of the CVEP-enabled BCI reveals a number of interesting patterns that play a role in the development of a high-quality medical neurocommunicator for a wide range of patients. First of all, it is the ratio between rate, accuracy of input and the overall information transfer rate peculiar to a specific modification of the interface. Obviously, from the user's viewpoint, the main property of a BCI is the information transfer rate. The data obtained indicate that this type of interface is capable of a transfer rate severalfold greater than that of the traditional BCI making use of P300, which makes the new interface a promising tool in the clinical practice. In the first three modes, the information transfer rate is within the limits usual for interfaces of this type [8, 14]. However, one participant managed to reach the rate of 287 bpm in the fast mode, which proved impossible for the majority of other participants. This is an important fact; being unique for the sample, this result substantiates the development of a BCI that would allow fine tuning the parameters to individual characteristics of its user with the aim to find their optimal combination (stimulation rate in particular). Such an approach can help overcome the known problems associated with adaptation of results of laboratory research involving healthy participants to clinical practice [15]. Another problem it would solve is the so-called BCI-illiteracy, i.e. inability of patients to learn to operate a brain-computer interface [16]. There are different approaches to tackling these problems, including modification of the training stage [17] and

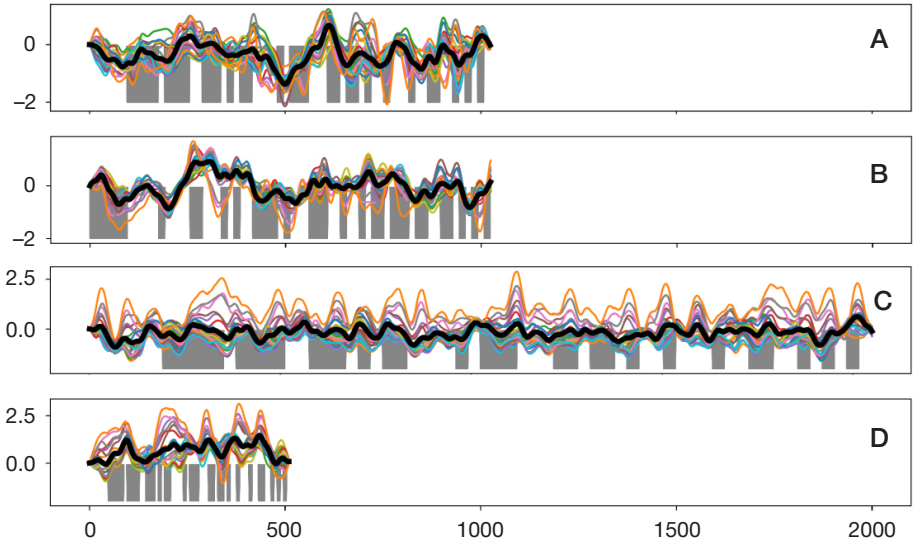

Fig. 2. Averaged evoked potentials registered during stimulation, all channels, shifted to zero shift relative to the basis m-sequence. The stimulus sequence is given in gray. One curve — one channel of the averaged EEG. The potential averaged between all channels is given in black

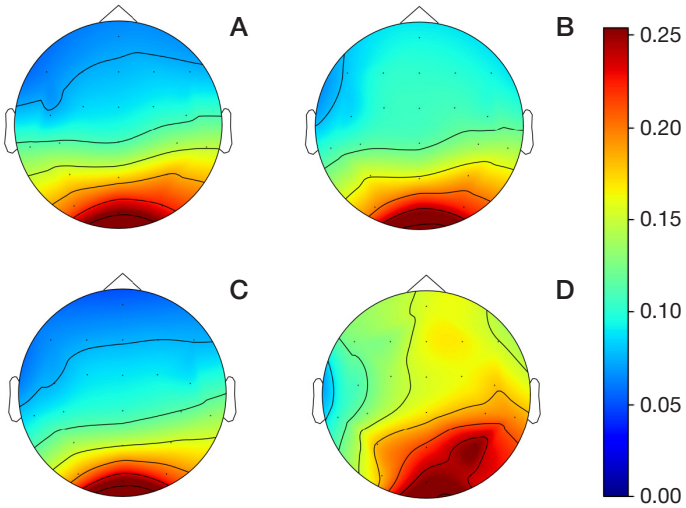

Fig. 3. Correlation function's maximum value maps, averaged for all participants, for averaged evoked potential of each channel (Fig. 2) and individual evoked potentials for single m-sequences. This indicator allows assessing the intensity of potential in all channels

the individualization of interfaces. Fine tuning the m-sequence carrier frequency and its period could help find optimal values that maximize the information transfer rate for each specific user. In fact, this is a routine already practiced when tuning P300-based BCI [18]. Unfortunately, modern displays, even those with high refresh rates, do not allow sufficient flexibility in adjustment of the stimulus sequence period frequency for CVEP BCI. For example, in the context of this study we were unable to demonstrate a sequence with the period of 0.8 seconds, which suggests that designing a special device for such purpose would be feasible. Several such attempts have already been made (based on evoked potentials) [19], but the specific implementations presented offer a low information transfer rate due to the small number of stimuli.

CONCLUSIONS

The results of this study suggest that optimizing BCI operation for a user requires fine tuning the parameters depending on the individual characteristics of each such user. We have shown that inverting the coding stimulus sequence does not affect the accuracy of selection of commands by BCI users, which translates into equal applicability of both direct and inverted stimulation modes. At the same time, faster modes of BCI operation with the sequences twice shorter proved to be suboptimal for the majority of participants of the experiment. The significant individual differences in accuracy and information transfer rate revealed by this study suggest that it is possible to optimize BCI through its fine-tuning to the specifics of the given patient.

References

1. Kaplan AY. Neurophysiological foundations and practical realizations of the brain–machine interfaces in the technology in neurological rehabilitation. Hum Physiol. 2016 Jan 23; 42 (1): 103–10.
2. Wolpaw JR, Birbaumer N, McFarland DJ, Pfurtscheller G, Vaughan TM. Brain-computer interfaces for communication and control. Clin Neurophysiol [Internet]. 2002 Jun; 113 (6): 767–91. Available from: http://www.ncbi.nlm.nih.gov/pubmed/12048038.
3. Jeunet C, Lotte F, Batail J-M, Philip P, Micoulaud Franchi J-A. Using Recent BCI Literature to Deepen our Understanding of Clinical Neurofeedback: A Short Review. Neuroscience [Internet]. 2018 May 15 [cited 2018 Jul 24]; (378): 225–33. Available from: https://www.sciencedirect.com/science/article/pii/S0306452218302045.
4. Akram F, Han H-S, Kim T-S. A P300-based brain computer interface system for words typing. Comput Biol Med [Internet]. 2014 Feb [cited 2014 Jun 1]; (45): 118–25. Available from: http://www.ncbi.nlm.nih.gov/pubmed/24480171.
5. Yeom SK, Fazli S, Ller KRM, Lee SW. An efficient ERP-based brain-computer interface using random set presentation and face familiarity. PLoS One. 2014; 9 (11): 1–13.
6. Guger C, Allison BZ, Edlinger G. Emerging BCI Opportunities from a Market Perspective. In Springer, Dordrecht; 2014 [cited 2018 Jul 16]: 85–98. Available from: http://link.springer.com/10.1007/978-94-017-8996-7_7.
7. McCane LM, Heckman SM, McFarland DJ, Townsend G, Mak JN, Sellers EW, et al. P300-based brain-computer interface (BCI) event-related potentials (ERPs): People with amyotrophic lateral sclerosis (ALS) vs. age-matched controls. Clin Neurophysiol [Internet]. 2015 Nov 1 [cited 2018 Jul 16]; 126 (11): 2124–31. Available from: https://www.sciencedirect.com/science/article/pii/S138824571500067X.
8. Bin G, Gao X, Wang Y, Li Y, Hong B, Gao S. A high-speed BCI based on code modulation VEP. J Neural Eng. 2011; 8 (2): 025015.
9. Kapeller C, Kamada K, Ogawa H, Prueckl R, Scharinger J, Guger C. An electrocorticographic BCI using code-based VEP for control in video applications: a single-subject study. Front Syst Neurosci [Internet]. 2014 Aug 7 [cited 2018 Jul 17]; (8): 139. Available from: http://journal.frontiersin.org/article/10.3389/fnsys.2014.00139/abstract.
10. Spüler M, Rosenstiel W, Bogdan M. Online Adaptation of a c-VEP Brain-Computer Interface(BCI) Based on Error-Related Potentials and Unsupervised Learning. Baumert M, editor. PLoS One [Internet]. 2012 Dec 7 [cited 2018 Jul 17]; 7 (12): e51077. Available from: http://dx.plos.org/10.1371/journal.pone.0051077.
11. Nezamfar H, Salehi SSM, Erdogmus D. Stimuli with opponent colors and higher bit rate enable higher accuracy for C-VEP BCI. In: 2015 IEEE Signal Processing in Medicine and Biology Symposium (SPMB) [Internet]. IEEE; 2015 [cited 2018 Jul 17]: 1–6. Available from: http://ieeexplore.ieee.org/document/7405476/.
12. Jones E, Oliphant T, Peterson P. {SciPy}: Open source scientific tools for {Python}. 2001.
13. Yuan P, Gao X, Allison B, Wang Y, Bin G, Gao S. A study of the existing problems of estimating the information transfer rate in online brain–computer interfaces. J Neural Eng [Internet]. 2013 Apr 1 [cited 2018 Jul 16]; 10 (2): 026014. Available from: http://stacks.iop.org/1741-2552/10/i=2/a=026014?key=crossref.0e89a1992040af23792558b5b8301c22.
14. Wei Q, Gong H, Lu Z. Grouping modulation with different codes for improving performance in cVEP-based brain–computer interfaces. Electron Lett. 2017 Jan 10; 53 (4): 214–6.
15. Kleih SC, Kaufmann T, Zickler C, Halder S, Leotta F, Cincotti F, et al. Out of the frying pan into the fire—the P300-based BCI faces real-world challenges. Prog Brain Res [Internet]. 2011 Jan 1 [cited 2018 Jul 16]; (194): 27–46. Available from: https://www.sciencedirect.com/science/article/pii/B9780444538154000194.
16. Spezialetti M, Cinque L, Tavares JMRS, Placidi G. Towards EEG-based BCI driven by emotions for addressing BCI-Illiteracy: a meta-analytic review. Behav Inf Technol [Internet]. 2018 Aug 3 [cited 2018 Jul 16]; 37 (8): 855–71. Available from: https://www.tandfonline.com/doi/full/10.1080/0144929X.2018.1485745.
17. Jeunet C, Cellard A, Subramanian S, Hachet M, N'Kaoua B, Lotte F. How Well Can We Learn With Standard BCI Training Approaches? A Pilot Study. 2014 [cited 2018 Jul 16]; Available from: https://hal.archives-ouvertes.fr/hal-01052692/.
18. Carabalona R. The Role of the Interplay between Stimulus Type and Timing in Explaining BCI-Illiteracy for Visual P300-Based Brain-Computer Interfaces. Front Neurosci [Internet]. 2017 Jun 30 [cited 2018 Jul 16]; (11): 363. Available from: http://journal.frontiersin.org/article/10.3389/fnins.2017.00363/full.
19. Aminaka D, Rutkowski TM. A Sixteen-Command and 40 Hz Carrier Frequency Code-Modulated Visual Evoked Potential BCI. In Springer, Cham; 2017 [cited 2018 Jul 16]: 97–104. Available from: http://link.springer.com/10.1007/978-3-319-64373-1_10.

Литература

1. Kaplan AY. Neurophysiological foundations and practical realizations of the brain–machine interfaces in the technology in neurological rehabilitation. Hum Physiol. 2016 Jan 23; 42 (1): 103–10.
2. Wolpaw JR, Birbaumer N, McFarland DJ, Pfurtscheller G, Vaughan TM. Brain-computer interfaces for communication and control. Clin Neurophysiol [Internet]. 2002 Jun; 113 (6): 767–91. Available from: http://www.ncbi.nlm.nih.gov/pubmed/12048038.
3. Jeunet C, Lotte F, Batail J-M, Philip P, Micoulaud Franchi J-A.

Using Recent BCI Literature to Deepen our Understanding of Clinical Neurofeedback: A Short Review. Neuroscience [Internet]. 2018 May 15 [cited 2018 Jul 24]; (378): 225–33. Available from: https://www.sciencedirect.com/science/article/pii/S0306452218302045.
4. Akram F, Han H-S, Kim T-S. A P300-based brain computer interface system for words typing. Comput Biol Med [Internet]. 2014 Feb [cited 2014 Jun 1]; (45): 118–25. Available from: http://www.ncbi.nlm.nih.gov/pubmed/24480171.
5. Yeom SK, Fazli S, Ller KRM, Lee SW. An efficient ERP-based brain-computer interface using random set presentation and face familiarity. PLoS One. 2014; 9 (11): 1–13.
6. Guger C, Allison BZ, Edlinger G. Emerging BCI Opportunities from a Market Perspective. In Springer, Dordrecht; 2014 [cited 2018 Jul 16]: 85–98. Available from: http://link.springer.com/10.1007/978-94-017-8996-7_7.
7. McCane LM, Heckman SM, McFarland DJ, Townsend G, Mak JN, Sellers EW, et al. P300-based brain-computer interface (BCI) event-related potentials (ERPs): People with amyotrophic lateral sclerosis (ALS) vs. age-matched controls. Clin Neurophysiol [Internet]. 2015 Nov 1 [cited 2018 Jul 16]; 126 (11): 2124–31. Available from: https://www.sciencedirect.com/science/article/pii/S138824571500067X.
8. Bin G, Gao X, Wang Y, Li Y, Hong B, Gao S. A high-speed BCI based on code modulation VEP. J Neural Eng. 2011; 8 (2): 025015.
9. Kapeller C, Kamada K, Ogawa H, Prueckl R, Scharinger J, Guger C. An electrocorticographic BCI using code-based VEP for control in video applications: a single-subject study. Front Syst Neurosci [Internet]. 2014 Aug 7 [cited 2018 Jul 17]; (8): 139. Available from: http://journal.frontiersin.org/article/10.3389/fnsys.2014.00139/abstract.
10. Spüler M, Rosenstiel W, Bogdan M. Online Adaptation of a c-VEP Brain-Computer Interface(BCI) Based on Error-Related Potentials and Unsupervised Learning. Baumert M, editor. PLoS One [Internet]. 2012 Dec 7 [cited 2018 Jul 17]; 7 (12): e51077. Available from: http://dx.plos.org/10.1371/journal.pone.0051077.
11. Nezamfar H, Salehi SSM, Erdogmus D. Stimuli with opponent colors and higher bit rate enable higher accuracy for C-VEP BCI. In: 2015 IEEE Signal Processing in Medicine and Biology Symposium (SPMB) [Internet]. IEEE; 2015 [cited 2018 Jul 17]: 1–6. Available from: http://ieeexplore.ieee.org/document/7405476/.
12. Jones E, Oliphant T, Peterson P. {SciPy}: Open source scientific tools for {Python}. 2001.
13. Yuan P, Gao X, Allison B, Wang Y, Bin G, Gao S. A study of the existing problems of estimating the information transfer rate in online brain–computer interfaces. J Neural Eng [Internet]. 2013 Apr 1 [cited 2018 Jul 16]; 10 (2): 026014. Available from: http://stacks.iop.org/1741-2552/10/i=2/a=026014?key=crossref.0e89a1992040af23792558b5b8301c22.
14. Wei Q, Gong H, Lu Z. Grouping modulation with different codes for improving performance in cVEP-based brain–computer interfaces. Electron Lett. 2017 Jan 10; 53 (4): 214–6.
15. Kleih SC, Kaufmann T, Zickler C, Halder S, Leotta F, Cincotti F, et al. Out of the frying pan into the fire—the P300-based BCI faces real-world challenges. Prog Brain Res [Internet]. 2011 Jan 1 [cited 2018 Jul 16]; (194): 27–46. Available from: https://www.sciencedirect.com/science/article/pii/B9780444538154000194.
16. Spezialetti M, Cinque L, Tavares JMRS, Placidi G. Towards EEG-based BCI driven by emotions for addressing BCI-Illiteracy: a meta-analytic review. Behav Inf Technol [Internet]. 2018 Aug 3 [cited 2018 Jul 16]; 37 (8): 855–71. Available from: https://www.tandfonline.com/doi/full/10.1080/0144929X.2018.1485745.
17. Jeunet C, Cellard A, Subramanian S, Hachet M, N'Kaoua B, Lotte F. How Well Can We Learn With Standard BCI Training Approaches? A Pilot Study. 2014 [cited 2018 Jul 16]; Available from: https://hal.archives-ouvertes.fr/hal-01052692/.
18. Carabalona R. The Role of the Interplay between Stimulus Type and Timing in Explaining BCI-Illiteracy for Visual P300-Based Brain-Computer Interfaces. Front Neurosci [Internet]. 2017 Jun 30 [cited 2018 Jul 16]; (11): 363. Available from: http://journal.frontiersin.org/article/10.3389/fnins.2017.00363/full.
19. Aminaka D, Rutkowski TM. A Sixteen-Command and 40 Hz Carrier Frequency Code-Modulated Visual Evoked Potential BCI. In Springer, Cham; 2017 [cited 2018 Jul 16]: 97–104. Available from: http://link.springer.com/10.1007/978-3-319-64373-1_10.

ADAPTING THE P300 BRAIN-COMPUTER INTERFACE TECHNOLOGY TO ASSESS CONDITION OF ANOREXIA NERVOSA PATIENTS

Ganin IP[1]✉, Kosichenko EA[1], Sokolov AV[2,3], Ioannisyanc OM[2], Arefev IM[2], Basova AYa[2,3], Kaplan AYa[1]

[1] Faculty of Biology, Lomonosov Moscow State University, Moscow, Russia

[2] Scientific-practical Children's and Adolescents Mental Health Center n.a. G. Sukhareva, Moscow, Russia

[3] Pirogov Russian National Research Medical University, Moscow, Russia

Brain-computer interface based on the P300 wave (P300 BCI) allows activating a given command according to the electroencephalogram (EEG) response to a predetermined relevant stimulus. The same algorithm enables detecting a subjectively important item (i.e., one triggering emotional response) in an environment even without actively drawing attention to it. Such systems allow assessing the personal significance of certain information, which can be used in the diagnostics of disorders of emotional perception or value system, e.g., eating disorders. This study aimed to investigate the EEG responses of anorexia nervosa patients (diagnosis F50.0, *n* = 12, age 11–16 years) to the stimuli with different perceived emotional significance, as well as to validate application of P300 BCI to detect the focus of attention to subjectively important stimuli. The inclusion criteria were: diagnosed anorexia nervosa (diagnosis F50.0); active rehabilitation. We registered the EEG while presenting images with different content to the patients. The event-related potentials (ERP) were detected and analyzed with the help of MATLAB 7.1 (MathWorks; USA). Statistica 7.0 software (StatSoft; USA) was used for statistical analysis of the data. We have discovered that in passive viewing paradigm, images of body parts of emaciated people among other images caused ERP with higher amplitude than images of food. Moreover, the accuracy of detection was higher for images of body parts: 89% against 59%, respectively. Thus, we have proven the validity of applying P300 BCI to detect covert emotional foci of attention and added to the existing knowledge about the mechanisms of development of anorexia nervosa.

Keywords: brain-computer interface (BCI), electroencephalogram (EEG), event-related potentials (ERP), visual attention, P300 wave, eating disorders, anorexia nervosa

Author contribution: all authors participated in the experiment planning; Ganin IP — immediate research activities, data analysis and interpretation, literature analysis, manuscript authoring; Kosichenko EA — immediate research activities, literature analysis, data analysis; Sokolov AV — immediate research activities, data interpretation, text editing; Ioannisyanc OM — diagnosing and selection of patients for the study; Arefev IM — support of experiments, data interpretation; Basova AYa — data interpretation, text editing; Kaplan AYa — data interpretation.

Compliance with ethical standards: the study was approved by the ethical committee of Scientific-practical Children's and Adolescents Mental Health Center n.a. G. Sukhareva (Protocol No. 1 of 2017.09.21). The legal representatives of children signed a voluntary informed consent allowing them to participate in the study.

✉ **Correspondence should be addressed:** Ilya P. Ganin
Leninskie Gory 1, bld. 12, ap. 246, Moscow, 119234; ipganin@mail.ru

Received: 08.10.2018 **Accepted:** 27.03.2019 **Published online:** 10.04.2019

DOI: 10.24075/brsmu.2019.022

АДАПТАЦИЯ ТЕХНОЛОГИИ ИНТЕРФЕЙСОВ МОЗГ-КОМПЬЮТЕР НА ВОЛНЕ P300 ДЛЯ ОЦЕНИВАНИЯ СОСТОЯНИЯ БОЛЬНЫХ НЕРВНОЙ АНОРЕКСИЕЙ

И. П. Ганин[1]✉, Е. А. Косиченко[1], А. В. Соколов[2,3], О. М. Иоаннисянц[2], И. М. Арефьев[2], А. Я. Басова[2,3], А. Я. Каплан[1]

[1] Биологический факультет, Московский государственный университет имени М. В. Ломоносова, Москва, Россия

[2] Научно-практический центр психического здоровья детей и подростков имени. Г. Е. Сухаревой, Москва, Россия

[3] Российский национальный исследовательский медицинский университет имени Н. И. Пирогова, Москва, Россия

Интерфейс мозг-компьютер на основе волны P300 (ИМК-P300) позволяет с помощью показателей электроэнцефалограммы (ЭЭГ), полученных при реакции на заданный заранее стимул, активировать соответствующую целевую команду. С помощью аналогичного алгоритма можно выделить из окружающего контекста субъективно выделяющийся по эмоциональным характеристикам стимул даже без привлечения к нему активного внимания. Такие системы позволят оценивать значимость для человека определенной информации, что можно использовать при диагностике нарушений эмоционального восприятия или системы ценностей, например, при нарушениях пищевого поведения. Целью исследования было изучить ЭЭГ-реакции на предъявление стимулов различной эмоциональной значимости больным с диагнозом F50.0 «Нервная анорексия» (*n* = 12, возраст 11–16 лет) и проверить гипотезу о возможном детектировании фокуса внимания к субъективно значимым стимулам на основе ИМК-P300. Критерии включения пациентов в исследование: наличие диагноза F50.0 «Нервная анорексия»; период реабилитации. Регистрировали ЭЭГ на фоне предъявления изображений различного содержания. Выделяли и анализировали потенциалы, связанные с событиями (ПСС) с помощью среды MATLAB 7.1 (MathWorks; США). Статистический анализ данных выполняли с помощью пакета программ STATISTICA 7.0 (StatSoft; США). Как показало исследование, предъявление в условиях пассивного внимания изображений частей тела истощенных людей на фоне прочих изображений вызывало более высокие амплитуды ПСС, чем при предъявлении изображений пищи. Алгоритм позволил также распознавать реакции внимания в ЭЭГ пользователя на оба типа изображений среди остальных стимулов, при этом точность распознавания для изображений частей тела была существенно выше (89% против 59%). Это доказывает возможность использования ИМК-P300 для распознавания неявных эмоциональных фокусов внимания и дополняет существующие знания о механизмах развития нервной анорексии.

Ключевые слова: интерфейс мозг-компьютер (ИМК), электроэнцефалограмма (ЭЭГ), потенциалы, связанные с событиями (ПСС), зрительное внимание, волна P300, нервная анорексия, нарушение пищевого поведения, расстройство приема пищи

Информация о вкладе авторов: все авторы участвовали в планировании эксперимента; И. П. Ганин — проведение исследования, анализ и интерпретация данных, анализ литературы, подготовка текста рукописи; Е. А. Косиченко — проведение исследования, анализ литературы, анализ данных; А. В. Соколов — проведение исследования, интерпретация данных, редактирование текста; О. М. Иоаннисянц — диагностика и подбор пациентов для исследования; И. М. Арефьев — обеспечение экспериментов, интерпретации данных; А. Я. Басова — интерпретация данных, редактирование текста; А. Я. Каплан — интерпретация данных.

Соблюдение этических стандартов: исследование одобрено этическим комитетом ГБУЗ «НПЦ ПЗДМ им. Г. Е. Сухаревой ДЗМ» (протокол № 1 от 21 сентября 2017 г.). Законные представители детей подписали добровольное информированное согласие на участие в исследовании.

✉ **Для корреспонденции:** Илья Петрович Ганин
Ленинские горы, д. 1, стр. 12, к. 246, г. Москва,119234; ipganin@mail.ru

Статья получена: 08.10.2018 **Статья принята к печати:** 27.03.2019 **Опубликована онлайн:** 10.04.2019

DOI: 10.24075/vrgmu.2019.022

Brain-computer interface technology (BCI) is currently being accepted as a standard research tool by more and more neurophysiology laboratories in the world [1]. BCI is a system developed and designed to enable people with lost or damaged motor functions to command external devices by decoding specific electroencephalogram (EEG) patterns [2]. There is a high demand for such interfaces in medicine: they are used to control auxiliary units [3, 4], for rehabilitation purposes [5], and also for communication [6]. Therefore, BCI is the subject of many research efforts.

At its current level, in certain conditions BCI allow highly accurate interpretation of the operator's commands as analyzed from EEG, which signals of the possible extension of the technology's potential sphere of application. First of all, the approaches and algorithms used in BCI can be used not only to recognize specific commands resulting from an arbitrary concentration of attention, but also to detect implicit foci of attention to external stimuli or one's own internal states. Such involuntary shifts of attention or, on the contrary, absence of attention markers in the EEG readings under certain conditions, can help diagnose various mental disorders in the context of instrument-assisted examinations.

There is a number of BCI versions that would allow designing a system for this purpose; the most appropriate of them is the interface enabling interpretation of the P300 wave, the P300 BCI [2, 6, 7], which offers external stimuli-commands and thus enables its operator to select commands. Determining such commands takes sequential activation of the stimuli (e.g., flashing letters on a display) and analysis of the response thereto. If the amplitude of the event-related potentials (ERP) is high, the stimuli is considered to be important for the operator, which translates into selection of the corresponding command. P300, a well-studied wave, is the main component of ERP: its amplitude is highest in response to rare and important stimuli.

EEG registers a specific response to an external stimulus in case the BCI user actively concentrates on the relevant command. However, the P300 wave and other EEG-detectable signs of attention to an event may be caused by stimuli that attract the person's attention indirectly, i.e. they are not immediately and clearly interesting to that person but probably possess some significance due to subjective experience, current psycho-emotional status [8, 9], which justifies the involuntary attention. Thus, the P300 BCI stimuli presentation paradigm also allows deriving the peculiarities of perception of specific information from the person's EEG readings, as well as detecting the focus of implicit interest to the certain classes of external stimuli. The patients would not have to react to a specific class of stimuli; rather, such a system would simply require them to look at the presented sequences of stimuli [10], thus exploiting the so-called passive attention paradigm. The feasibility of such an approach is based on the fact that even without a conscious response to a stimulus, biological or emotional, it can anyway trigger a reaction [11] because it is of significance to the person. Therefore, for the BCI purposes such a stimulus can be considered a "target" stimulus, which allows further classification based on the analysis of EEG readings.

The most logical option for such examination methods is to use emotional content in a mix with neutral content [12]. The systems making use of these methods would automatically detect overexcitement in people whose job implies high emotional load [13]. They would also enable instrument-assisted diagnosing of the emotion perception disorders, such as autism [14, 15].

Applying the methods exploiting P300 BCI to assess the state of patients with eating disorders is as interesting. In particular, they can be shown a number of visual stimuli related to anorexia, and their EEG readings, analyzed, can serve as an additional indicator of treatment effectiveness. Earlier, it was shown that anorexia nervosa patients fail to perceive emotional stimuli normally [16], and that failure is EEG-detectable. Besides, the P300 wave and other ERP components registered in such patients feature some specific characteristics if recorded when they solve a task requiring concentration of attention, which signals of deterioration of some brain functions [17].

Some previous research efforts aimed to identify the peculiarities of EEG readings resulting from presentation of visual stimuli in various conditions. However, to date, there is no prototype of a system that would recognize the focus of interest to certain classes of stimuli based on the EEG signal. Therefore, this study aimed to find the specific features of ERP triggered by presenting the stimuli of varying emotional value to anorexia nervosa patients whose attention is in the passive mode, as well as to validate application of P300 BCI to detect the focus of attention to subjectively important stimuli.

METHODS

Twelve adolescent girls (11–16 years old), patients at the Scientific-practical Children's and Adolescents Mental Health Center n.a. G. Sukhareva, participated in the study. The inclusion criteria were: diagnosed anorexia nervosa (diagnosis F50.0); active rehabilitation. The exclusion criteria were: severe somatic pathology; high degree of protein and energy deficiency; strict bed rest. We recorded EEG of the participants while they were looking at the screen showing sets of photographic images.

The angular dimensions of the images were 12.9 × 9.6°; they were presented against a gray background following the oddball paradigm: the stimuli appeared sequentially in the center of the screen, which remained empty otherwise. The stimuli were shown for 200 ms, the interval between them was 500 ms. There were two types of images: pictures of food and body parts of emaciated people. As for the neutral ("insignificant") stimuli, they were images of objects, animals, geometric figures, landscapes, etc., taken from the IAPS database [18], which was also the source of some images of food. The majority of the significant stimuli was selected following the analysis of online channels covering anorexia. Before being shown to the patients, all images were assessed by the doctor that treated them. The sets included 6 images, 5 insignificant and 1 significant. Each set of stimuli presented was covered by a single EEG recording lasting less than a minute; the recordings were separated by short pauses. The presentation took form of the sequences of stimuli, each showing the images once, in a random order. One EEG recording consisted of 10 sequences of stimuli. Each participant received the sets in a pseudo-random order; the records with the stimuli (food and body parts) were rotated. The total number of "food" and "body parts" stimuli records usually equaled 10 and 12, respectively (each patient).

The EEG registration was monopolar, sites Cz, P3, Pz, P4, PO7, PO8, O1, O2, reference electrode on the lobe of the left ear. We used the NVX52 amplifier with a sampling frequency of 500 Hz. BCI2000 software (www.bci2000.org) enabled data recording and stimuli presentation control.

MATLAB 7.1 (MathWorks; USA) was used to isolate and analyze ERP. We bandpass filtered the EEG signal in the range of 0.5–20 Hz (Butterworth filter), and then divided it into epochs relative to the moment the stimulus was presented with boundaries from 0.1 to 0.7 s. After removing the epochs containing oculomotor artifacts from the array, we divided the epochs into target ("significant") and non-target ("insignificant").

The type of the image (food or body part) was another criterium for division. The number of target and non-target epochs was equalized through eliminating some of the latter. The epochs for target and non-target stimuli were equalized separately. Thus, for each participant we received target and non-target ERP in all EEG channels and in two blocks. Besides, the difference ERP were determined through subtracting non-target curves from target curves.

The amplitudes of P300, N1 and LPP components were measured as a maximum or a minimum value in time window selected individually for each participant. The P300 component amplitudes were measured in the Cz and Pz channels, those of the N1 and LPP components — in channels PO7, PO8, O1 and O2. Not all participants had the entire range of components registered in all channels, therefore the results contain the number of patients (*n*) that underwent this or that analysis.

Using the Fisher's linear discriminant, we modeled an approach to classification of the P300 BCI target commands with the aim to assess the effectiveness of EEG-enabled identification of special responses to significant stimuli. The classifier learned and was tested through cross-validation of two classes, target and non-target stimuli. In each testing attempt, the classifier was tasked with identifying one most prominent stimulus out of six. If the identified stimulus was significant, the attempts was deemed successful.

Based on the ERP amplitude calculations and the level of accuracy of classification, we calculated the averages of each value in both blocks by processing the data in STATISTICA 7.0 software (StatSoft; USA). When the samples distribution was normal, we used the paired samples t-tests, when it was not — Wilcoxon signed-rank test.

RESULTS

The individual difference curves of the majority of anorexia nervosa patients had peaking N1 (latency 120–180 ms), P300 (350–450 ms), and LPP (550–700 ms). These peaks are also seen on the target and non-target ERP averaged over the entire group, as well as on difference curves (Fig. 1). The ratio of amplitudes of target and non-target ERP seen on the difference curves allows deducing the intensity with which significant stimuli attracted attention compared to insignificant stimuli. Since the individual latency of peaks varied and not all participants had all peaks in their EEG readings, some ERP components in the averaged picture appear blurred and poorly pronounced, so Fig. 1 is the reflection of the situation on the whole. Table below contains the average values of all analyzed components in the target, non-target and difference curves.

In both blocks, the amplitude of the P300 component was higher on target curves than on non-target ones both in the Cz ($p < 0.01$; $n = 11$ and $p < 0.01$, $n = 12$, paired samples t-tests) and Pz ($p < 0.01$, $n = 12$ and $p < 0.01$, $n = 11$) channels, food and body parts images, respectively (table). Comparison of the P300 amplitudes of two difference curves describing two types of stimuli did not reveal significant differences (Fig. 2).

The N1 component target ERP amplitudes were higher than non-target for both food images ($p < 0.05$, $n = 9$; $p < 0.05$, $n = 10$; $p < 0.05$, $n = 9$; $p < 0.05$, $n = 11$, in sites PO7, PO8, O1, O2, respectively, paired samples t-tests) and images of body parts ($p < 0.01$, $n = 9$; $p < 0.01$, $n = 12$; $p < 0.01$, $n = 12$; $p < 0.01$, $n = 11$, Wilcoxon test). Despite the fact that body part images triggered higher average N1 difference curves amplitudes than food images (Fig. 1 and Table), only P08 site has shown significant differences between the two types of stimuli ($p < 0.05$, $n = 10$; Wilcoxon test) (Fig. 2).

The LPP component had the greatest amplitude in the occipital sites. Its target ERP amplitudes were higher than non-target for both food images ($p < 0.01$, $n = 8$; $p < 0.01$, $n = 9$; $p < 0.05$, $n = 8$; $p < 0.01$, $n = 9$, in sites PO7, PO8, O1, O2, respectively, paired samples t-tests) and images of body parts ($p < 0.01$, $n = 9$; $p < 0.01$, $n = 10$; $p < 0.01$, $n = 10$; $p < 0.01$, $n = 10$). On average, the images of body parts caused higher

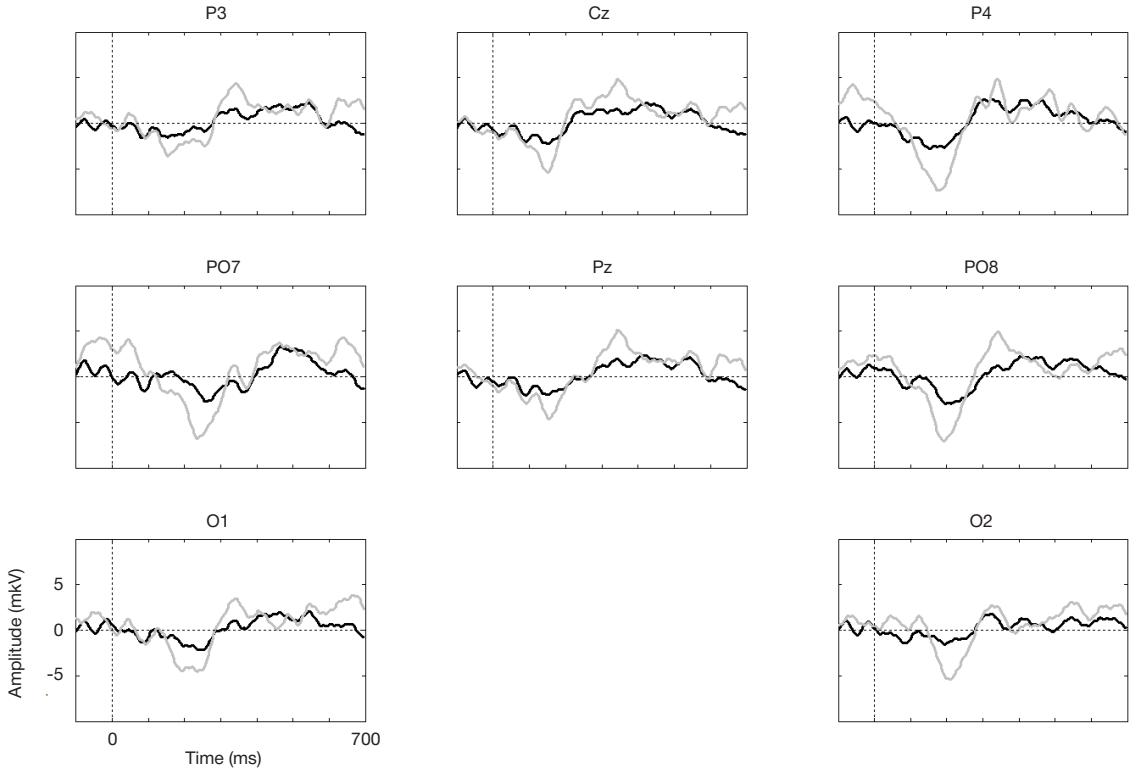

Fig. 1. Group mean differential ERP ($n = 10$). Stimuli: black line — images of food, gray line — images of body parts of emaciated people. Vertical — amplitude (mkV), horizontal — time (ms). Vertical dashed line (0 ms) reflects the time of stimulus presentation. Above each curve — name of EEG site

Table. P300, N1 and LPP amplitude values, response to presentation of stimuli (images of food and images of body parts of emaciated people). Mean ± standard error of mean, mkV

	Images of food			Images of body parts		
P300						
Site	Target	Non-target	Differential	Target	Non-target	Differential
Cz	4.5 ± 1.1	1.4 ± 0.7	5.8 ± 0.9	4.1 ± 0.6	0.6 ± 0.4	5.9 ± 0.9
Pz	5.0 ± 0.6	2.1 ± 0.6	5.5 ± 0.9	5.7 ± 0.8	2.2 ± 0.8	6.0 ± 0.8
N1						
PO7	–6.1 ± 1.6	–3.0 ± 0.9	–3.9 ± 1.0	–4.5 ± 1.8	0.5 ± 0.9	–7.3 ± 1.6
PO8	–5.8 ± 2.1	–2.7 ± 1.4	–4.7 ± 1.1	–6.6 ± 1.6	–2.2 ± 1.8	–8.7 ± 1.6
O1	–4.6 ± 2.2	–1.7 ± 1.6	–4.5 ± 1.1	–4.1 ± 1.8	0.1 ± 1.7	–6.3 ± 0.7
O2	–4.8 ± 2.3	–2.4 ± 1.8	–4.0 ± 0.8	–4.3 ± 1.9	–0.3 ± 2.2	–6.4 ± 0.6
LPP						
PO7	0.7 ± 0.8	–2.1 ± 0.9	4.2 ± 0.6	6.8 ± 2.7	–1.6 ± 0.8	10.9 ± 2.4
PO8	0.4 ± 1.2	–2.1 ± 0.9	4.1 ± 0.8	4.9 ± 1.0	–0.8 ± 1.0	8.0 ± 1.3
O1	–0.4 ± 1.3	–3.6 ± 1.2	4.4 ± 0.9	2.5 ± 1.4	–2.9 ± 0.8	8.4 ± 1.4
O2	–1.5 ± 1.0	–4.5 ± 1.1	4.5 ± 0.8	1.8 ± 1.2	–2.9 ± 0.9	8.5 ± 1.4

LPP amplitudes than food images, however, the differences were significant only at sites PO7 and PO8 ($p < 0.05$, $n = 7$; $p < 0.05$, $n = 8$, respectively) (Fig. 2).

Figure 3 shows the average accuracy of significant stimuli classification among the neutral ones (both blocks). The average classifier recognition accuracy for the food image stimuli was 59.1 ± 5.3%, which is lower than that for the emaciated body parts images that equaled 89.1 ± 2.3% ($p = 0.0002$, $n = 12$, paired samples t-tests).

DISCUSSION

The main result of this study is identification of a number of features of ERP peculiar to passive perception of emotionally significant images, as well as the proven possibility to use EEG readings to detect attention to such stimuli when mixed with neutral content, the accuracy of such detection being close to that of the current BCI systems.

It is known that people running a high risk of eating disorders are sensitive to emotionally significant stimuli associated with the body shape weight [19]. This level of sensitivity is subjective; in case of anorexia nervosa, it can be explained by the special attitude the patients have towards their bodies, including development of the dysmorphophobia / dysmorfomania syndrome against the background of low self-esteem [19, 20]. We have discovered that food or emaciated body part images result in higher ERP amplitudes, which means such images are important to the patients, although the intensity of response was different for the two types considered.

Based on the available literature, we could explain the higher ERP amplitude associated with the significant stimuli by the fact that they are presented rarely compared to the neutral stimuli in the mix, i.e., as the oddball paradigm has it, rare target stimuli provoke a more intense response [21]. At the same time, the oddball paradigm we utilized in our study was modified: its classic version implies using two greatly different simple classes of stimuli, whereas we had the stimuli equally heterogeneous both within the significant/insignificant classes and between the classes. This fact suggests that the differences registered in the present study result not from the specific features of the images but solely from the subjective significance of the semantic content of this group of stimuli. Thus, presentation

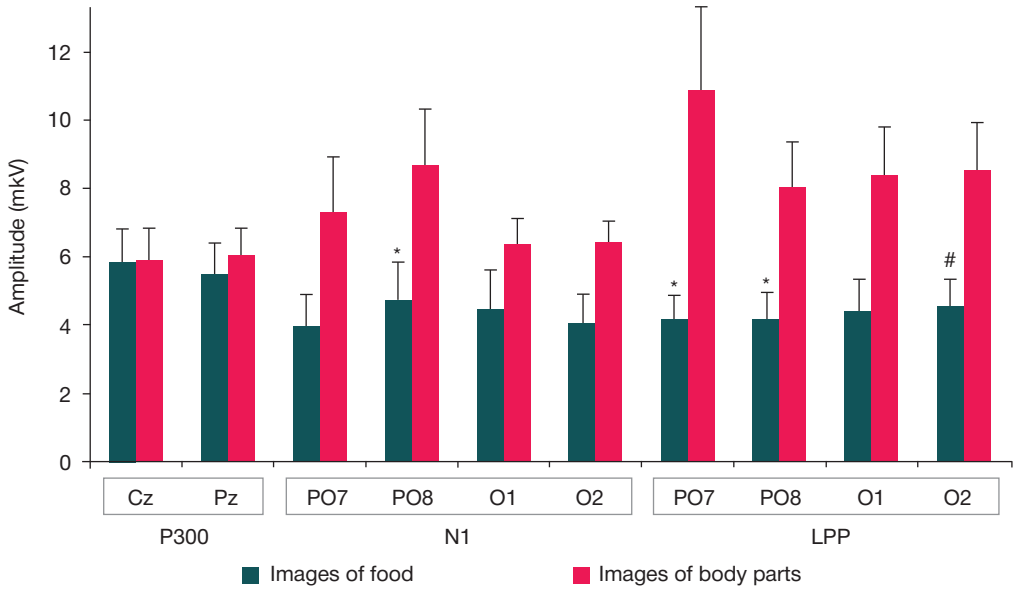

Fig. 2. Group mean P300, N1 and LPP component amplitude, two types of stimuli (images of food and images of body parts of emaciated people). Mean and standard error of mean. Difference between blocks: * — $p < 0.05$, # — $p < 0.1$

of the images of body parts caused a significantly stronger reaction (as reflected by ERP) than those of food, although both such stimuli were equally likely to be important to the participants. An assumption based thereon is that the stimulus that is unlike the majority of other stimuli shown triggers intense response because it is of special emotional value to the patient and not solely because it is a rare component of the given mix. This assumption is further confirmed by the fact that the P300 wave amplitude that reflects the frequency characteristics of the stimulus was the same for the two types of images, while all other ERP components and classifier accuracy depended on the type of stimulus.

One of the most important results of this work is the extremely high accuracy of classification of subjectively significant images based on the EEG-detectable response: for food images it was 59%, for images of body parts — 89%. It should be noted here that the tasks set before the participants did not require them to actively concentrate on the stimuli shown. This level of accuracy is far higher than the 16.7% random recognition rate, when participants select one of the 6 stimuli at random. Moreover, it is close to the values achieved with the help of P300 BCI, the use of which implies active concentration on the target stimulus-command and disregard of all other stimuli [22, 23].

The research described in this paper is largely a pilot study; its practical value is the effort to adapt the existing BCI approaches to the purposes of development of methods and systems to detect subjective foci of attention. Therefore, one of the limitations of this work is the absence of a control group of healthy subjects. At the same time, we can consider mixes with food images to be the control component compared to mixes with body part images: the two produced different ERP components, although they were equally likely to prove significant to the patients and featured the same set of insignificant stimuli (see above). The results are comparable to those attained by the authors in the context of another recent study that had healthy people performing a similar task: they were passively viewing various images on a screen, the mix featured some that were emotionally different from the rest but not subjectively significant to the participants [12]. The component amplitudes reflecting response to the different stimuli were lower than in this work, and the accuracy of classification was 40–45%. Some data suggest that anorexia nervosa patients respond weaker (as revealed by ERP) to the food-related visual stimuli than healthy people [24]. We have discovered that images of body parts of emaciated people triggered a significantly more intense EEG-detectable response than images of food. This may mean that the latter can attract attention better and are especially important to anorexia nervosa patients.

The N1 component reflects the processes of fixation on a certain stimulus; it is associated with emotional perception [25], which allows deducing the level of attention the patients pay to the images of food and body parts, as well as assuming that the significance of such stimuli is the result of an emotional reaction. The LPP component is associated with the late stages of emotional processing of visual stimuli [26], which is another fact supporting the statement that the special EEG-detectable response to the significant images used herein is the result of actual cognitive processing and not just a reaction to a stimulus that looks out of context. Overall, the higher N1 and LPP component amplitudes together with the high accuracy of classification registered for the emaciated body part images versus food images support the assumption that anorexia can largely be caused by the person's specific attitude to his/her body, faulty perception of its shape and size, obsessive desire to meet certain physical standards, while the actual denial to consume food may be only one of the secondary reasons [19].

CONCLUSIONS

The applied method of identification of involuntary attention to images of food and body parts of emaciated people shown to anorexia nervosa patients allowed receiving highly accurate results of classification of involuntary attention reactions to emotionally significant stimuli. Further development of this method can contribute to the design of systems to detect emotional foci of attention with the help of EEG readings. Such systems could be used to determine peculiarities of the patients' emotional perception (as part of diagnosing their overall condition) at different stages of treatment. We have registered a stronger response to the images of body parts of emaciated people than to the images of food; this result was confirmed by EEG experiments. On the one hand, this can support the known patterns of development of anorexia nervosa, and on the other hand, suggests applying the relevant stimuli materials in the above-mentioned systems.

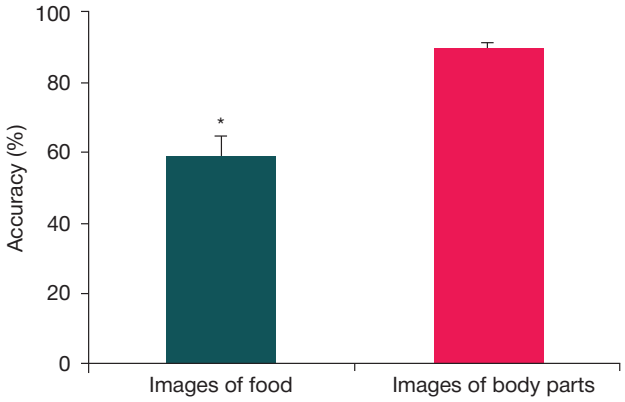

Fig. 3. Group mean classification accuracy, BCI algorithm, identification of significant stimuli among neutral ones in two blocks (images of food and images of body parts of emaciated people). Mean and standard error of mean. Difference between blocks: * — $p < 0.05$

References

1. McFarland DJ, Vaughan TM. BCI in practice. Progress in brain research. 2016; 228: 389404. Available from: https://doi.org/10.1016/bs.pbr.2016.06.005.
2. Wolpaw JR. Brain-computer interfaces as new brain output pathways. J Physiol. 2007; 579 (3): 613–9. Available from: https://doi.org/10.1113/jphysiol.2006.125948.
3. Alqasemi R, Dubey R. A 9-DoF Wheelchair-Mounted Robotic Arm System: Design, Control, Brain-Computer Interfacing, and Testing. Journal of Advances in Robot Manipulators In Tech. 2010: 51–78. Available from: https://doi.org/10.5772/9678.
4. Lopes AC, Pires G, Vaz L, Nunes U. Wheelchair navigation assisted by human-machine shared-control and a P300-based

brain computer interface. International Conference on Intelligent Robots and Systems (IROS). 2011: 2438–44. Available from: https://doi.org/10.1109/iros.2011.6094748.
5. Vidaurre C, Klauer C, Schauer T, Ramos-Murguialday A, Müller KR. EEG-based BCI for the linear control of an upper-limb neuroprosthesis. Medical Engineering & Physics. 2016; 38 (11): 1195–204. Available from: https://doi.org/10.1016/j.medengphy.2016.06.010.
6. Rezeika A, Benda M, Stawicki P, Gembler F, Saboor A, Volosyak I. Brain–Computer Interface Spellers: A Review. Brain Sciences. 2018; 8 (4): 57. Available from: https://doi.org/10.3390/brainsci8040057.
7. Farwell LA, Donchin E. Talking off the top of your head: toward a mental prosthesis utilizing event-related brain potentials. Electroencephalography and Clinical Neurophysiology. 1988; 70: 510–23. Available from: https://doi.org/10.1016/0013-4694(88)90149-6.
8. Asmaro D, Jaspers-Fayer F, Sramko V, Taake I, Carolan P, Liotti M. Spatiotemporal dynamics of the hedonic processing of chocolate images in individuals with and without trait chocolate craving. Appetite. 2012; 58 (3): 790–9. Available from: https://doi.org/10.1016/j.appet.2012.01.030.
9. Asmaro D, Carolan PL, Liotti M. Electrophysiological evidence of early attentional bias to drug-related pictures in chronic cannabis users. Addict Behav. 2014; 39 (1): 114–21. Available from: https://doi.org/10.1016/j.addbeh.2013.09.012.
10. Olofsson, JK, Nordin S, Sequeira H, Polich J. Affective picture processing: an integrative review of ERP findings. Biological psychology. 2008; 77 (3): 247–65. Available from: https://doi.org/10.1016/j.biopsycho.2007.11.006.
11. Ohman A, Flykt A, Esteves F. Emotion drives attention: detecting the snake in the grass. Journal of experimental psychology: general. 2001; 130 (3): 466–78. Available from: https://doi.org/10.1037//0096-3445.130.3.466.
12. Ganin IP, Kosichenko EA, Kaplan AYa. Osobennosti jelektrojencefalograficheskih reakcij na jemocional'no znachimye stimuly v tehnologii interfejsa mozg-komp'juter na volne P300. Zhurn vyssh nerv dejat. 2017; 67 (4): 453–63. Available from: https://doi.org/10.7868/s0044467717040074.
13. Singh M, Singh M, Goyal M. Selection of attribute combinations of ERP's for classification of emotions along arousal axis. International Journal of Information Technology & Knowledge Management. 2015; 8 (2): 142–9. Available from: https://doi.org/10.141079/IJITKM.2015.801.
14. Liu TL, Wang PW, Yang YC, Hsiao RC, Su YY, Shyi GC, Yen CF. Deficits in facial emotion recognition and implicit attitudes toward emotion among adolescents with high functioning autism spectrum disorder. Compr Psychiatry. 2019; (90): 7–13. Available from: https://doi.org/10.1016/j.comppsych.2018.12.010.
15. Stavropoulos KK, Viktorinova M, Naples A, Foss-Feig J, McPartland JC. Autistic traits modulate conscious and nonconscious face perception. Soc Neurosci. 2016; (10): 1–12. Available from: https://doi.org/10.1080/17470919.2016.1248788.
16. Hatch A, Madden S, Kohn MR, Clarke S, Touyz S, Gordon E et al. Emotion brain alterations in anorexia nervosa: a candidate biological marker and implications for treatment. Journal of psychiatry & neuroscience: JPN. 2010; 35 (4): 267–74. Available from: https://doi.org/10.1503/jpn.090073.
17. Bradley SJ, Taylor MJ, Rovet JF, Goldberg E, Hood J, Wachsmuth R, et al. Assessment of brain function in adolescent anorexia nervosa before and after weight gain. Journal of Clinical and Experimental Neuropsychology. 1997; 19 (1): 20–33. Available from: https://doi.org/10.1080/01688639708403833.
18. Lang PJ, Bradley MM, Cuthbert BN. International affective picture system (IAPS): Affective ratings of pictures and instruction manual. Technical Report A-8. University of Florida, Gainesville, FL. 2008.
19. Meijboom A, Jansen A, Kampman M, Schouten E. An experimental test of the relationship between self–esteem and concern about body shape and weight in restrained eaters. International Journal of Eating Disorders. 1999; 25 (3): 327–34. Available from: https://doi.org/10.1002/(sici)1098-108x(199904)25:3<327::aid-eat11>3.0.co;2-5.
20. Blechert J, Ansorge U, Beckmann S, & Tuschen-Caffier B. The undue influence of shape and weight on self-evaluation in anorexia nervosa, bulimia nervosa and restrained eaters: a combined ERP and behavioral study. Psychological Medicine. 2011; 41 (1): 185–94. Available from: https://doi.org/10.1017/s0033291710000395.
21. Squires NK, Squires KC, Hillyard SA. Two Varieties of Long-latency positive Waves Evoked by Unpredictavle Audiatory Stimuli in Man. Electroencephalography and Clinical Neurophysiology. 1975; (38): 387–401. Available from: https://doi.org/10.1016/0013-4694(75)90263-1.
22. Guger C, Daban S, Sellers E, Holzner C, Krausz G, Carabalona R, et al. How many people are able to control a P300-based brain-computer interface (BCI)? Neurosci Lett. 2009; 462 (1): 94–8. Available from: https://doi.org/10.1016/j.neulet.2009.06.045.
23. Ganin IP, Kaplan AYa. Interfejs mozg-komp'juter na osnove volny P300: pred"javlenie kompleksnyh stimulov «podsvetka + dvizhenie». Zhurnal vysshej nervnoj dejatel'nosti. 2014; 64 (1): 32–40. Dostupno po ssylke: https://doi.org/10.7868/s0044467714010067.
24. Nikendei C, Friederich HC, Weisbrod M, Walther S, Sharma A, Herzog W, et al. Event-related potentials during recognition of semantic and pictorial food stimuli in patients with anorexia nervosa and healthy controls with varying internal states of hunger. Psychosomatic medicine. 2012; 74 (2): 136–145. Available from: https://doi.org/10.1097/psy.0b013e318242496a.
25. Sprengelmeyer R, Jentzsch I. Event related potentials and the perception of intensity in facial expressions. Neuropsychologia. 2006; (44): 2899–06. Available from: https://doi.org/10.1016/j.neuropsychologia.2006.06.020.
26. Foti D, Hajcak G, Dien J. Differentiating neural responses to emotional pictures: Evidence from temporal-spatial PCA. Psychophysiology. 2009; 46 (3): 521–30. Available from: https://doi.org/10.1111/j.1469-8986.2009.00796.x.

Литература

1. McFarland DJ, Vaughan TM. BCI in practice. Progress in brain research. 2016; 228: 389404. Available from: https://doi.org/10.1016/bs.pbr.2016.06.005.
2. Wolpaw JR. Brain-computer interfaces as new brain output pathways. J Physiol. 2007; 579 (3): 613–9. Available from: https://doi.org/10.1113/jphysiol.2006.125948.
3. Alqasemi R, Dubey R. A 9-DoF Wheelchair-Mounted Robotic Arm System: Design, Control, Brain-Computer Interfacing, and Testing. Journal of Advances in Robot Manipulators In Tech. 2010: 51–78. Available from: https://doi.org/10.5772/9678.
4. Lopes AC, Pires G, Vaz L, Nunes U. Wheelchair navigation assisted by human-machine shared-control and a P300-based brain computer interface. International Conference on Intelligent Robots and Systems (IROS). 2011: 2438–44. Available from: https://doi.org/10.1109/iros.2011.6094748.
5. Vidaurre C, Klauer C, Schauer T, Ramos-Murguialday A, Müller KR. EEG-based BCI for the linear control of an upper-limb neuroprosthesis. Medical Engineering & Physics. 2016; 38 (11): 1195–204. Available from: https://doi.org/10.1016/j.medengphy.2016.06.010.
6. Rezeika A, Benda M, Stawicki P, Gembler F, Saboor A, Volosyak I. Brain–Computer Interface Spellers: A Review. Brain Sciences. 2018; 8 (4): 57. Available from: https://doi.org/10.3390/brainsci8040057.
7. Farwell LA, Donchin E. Talking off the top of your head: toward a mental prosthesis utilizing event-related brain potentials. Electroencephalography and Clinical Neurophysiology. 1988; 70: 510–23. Available from: https://doi.org/10.1016/0013-4694(88)90149-6.
8. Asmaro D, Jaspers-Fayer F, Sramko V, Taake I, Carolan P, Liotti M. Spatiotemporal dynamics of the hedonic processing of chocolate images in individuals with and without trait chocolate craving.

Appetite. 2012; 58 (3): 790–9. Available from: https://doi.org/10.1016/j.appet.2012.01.030.
9. Asmaro D, Carolan PL, Liotti M. Electrophysiological evidence of early attentional bias to drug-related pictures in chronic cannabis users. Addict Behav. 2014; 39 (1): 114–21. Available from: https://doi.org/10.1016/j.addbeh.2013.09.012.
10. Olofsson, JK, Nordin S, Sequeira H, Polich J. Affective picture processing: an integrative review of ERP findings. Biological psychology. 2008; 77 (3): 247–65. Available from: https://doi.org/10.1016/j.biopsycho.2007.11.006.
11. Ohman A, Flykt A, Esteves F. Emotion drives attention: detecting the snake in the grass. Journal of experimental psychology: general. 2001; 130 (3): 466–78. Available from: https://doi.org/10.1037//0096-3445.130.3.466.
12. Ганин И. П., Косиченко Е. А., Каплан А. Я. Особенности электроэнцефалографических реакций на эмоционально значимые стимулы в технологии интерфейса мозг-компьютер на волне Р300. Журн. высш. нерв. деят. 2017; 67 (4): 453–63. Available from: https://doi.org/10.7868/s0044467717040074.
13. Singh M, Singh M, Goyal M. Selection of attribute combinations of ERP's for classification of emotions along arousal axis. International Journal of Information Technology & Knowledge Management. 2015; 8 (2): 142–9. Available from: https://doi.org/10.141079/IJITKM.2015.801.
14. Liu TL, Wang PW, Yang YC, Hsiao RC, Su YY, Shyi GC, Yen CF. Deficits in facial emotion recognition and implicit attitudes toward emotion among adolescents with high functioning autism spectrum disorder. Compr Psychiatry. 2019; (90): 7–13. Available from: https://doi.org/10.1016/j.comppsych.2018.12.010.
15. Stavropoulos KK, Viktorinova M, Naples A, Foss-Feig J, McPartland JC. Autistic traits modulate conscious and nonconscious face perception. Soc Neurosci. 2016; (10): 1–12. Available from: https://doi.org/10.1080/17470919.2016.1248788.
16. Hatch A, Madden S, Kohn MR, Clarke S, Touyz S, Gordon E et al. Emotion brain alterations in anorexia nervosa: a candidate biological marker and implications for treatment. Journal of psychiatry & neuroscience: JPN. 2010; 35 (4): 267–74. Available from: https://doi.org/10.1503/jpn.090073.
17. Bradley SJ, Taylor MJ, Rovet JF, Goldberg E, Hood J, Wachsmuth R, et al. Assessment of brain function in adolescent anorexia nervosa before and after weight gain. Journal of Clinical and Experimental Neuropsychology. 1997; 19 (1): 20–33. Available from: https://doi.org/10.1080/01688639708403833.
18. Lang PJ, Bradley MM, Cuthbert BN. International affective picture system (IAPS): Affective ratings of pictures and instruction manual. Technical Report A-8. University of Florida, Gainesville, FL. 2008.
19. Meijboom A, Jansen A, Kampman M, Schouten E. An experimental test of the relationship between self–esteem and concern about body shape and weight in restrained eaters. International Journal of Eating Disorders. 1999; 25 (3): 327–34. Available from: https://doi.org/10.1002/(sici)1098-108x(199904)25:3<327::aid-eat11>3.0.co;2-5.
20. Blechert J, Ansorge U, Beckmann S, & Tuschen-Caffier B. The undue influence of shape and weight on self-evaluation in anorexia nervosa, bulimia nervosa and restrained eaters: a combined ERP and behavioral study. Psychological Medicine. 2011; 41 (1): 185–94. Available from: https://doi.org/10.1017/s0033291710000395.
21. Squires NK, Squires KC, Hillyard SA. Two Varieties of Long-latency positive Waves Evoked by Unpredictavle Audiatory Stimuli in Man. Electroencephalography and Clinical Neurophysiology. 1975; (38): 387–401. Available from: https://doi.org/10.1016/0013-4694(75)90263-1.
22. Guger C, Daban S, Sellers E, Holzner C, Krausz G, Carabalona R, et al. How many people are able to control a P300-based brain-computer interface (BCI)? Neurosci Lett. 2009; 462 (1): 94–8. Available from: https://doi.org/10.1016/j.neulet.2009.06.045.
23. Ганин И. П., Каплан А. Я. Интерфейс мозг-компьютер на основе волны Р300: предъявление комплексных стимулов «подсветка + движение». Журнал высшей нервной деятельности. 2014; 64 (1): 32–40. Доступно по ссылке: https://doi.org/10.7868/s0044467714010067.
24. Nikendei C, Friederich HC, Weisbrod M, Walther S, Sharma A, Herzog W, et al. Event-related potentials during recognition of semantic and pictorial food stimuli in patients with anorexia nervosa and healthy controls with varying internal states of hunger. Psychosomatic medicine. 2012; 74 (2): 136–145. Available from: https://doi.org/10.1097/psy.0b013e318242496a.
25. Sprengelmeyer R, Jentzsch I. Event related potentials and the perception of intensity in facial expressions. Neuropsychologia. 2006; (44): 2899–06. Available from: https://doi.org/10.1016/j.neuropsychologia.2006.06.020.
26. Foti D, Hajcak G, Dien J. Differentiating neural responses to emotional pictures: Evidence from temporal-spatial PCA. Psychophysiology. 2009; 46 (3): 521–30. Available from: https://doi.org/10.1111/j.1469-8986.2009.00796.x.

INFLUENCE OF DENTAL PROSTHETICS TECHNOLOGY ON THE DYNAMICS OF EARLY PREDICTORS OF DESTRUCTIVE INFLAMMATORY PROCESS IN THE PERIIMPLANT ZONE

Tlustenko VP, Bayrikov IM, Trunin DA, Gusyakova OA, Komlev SS ✉

Samara State Medical University, Samara, Russia

An objective assessment of the morphofunctional characteristics of the state of soft tissues and bone structures adjacent to the dental implant allows to control the dynamics of the processes of osseointegration in the jaw-dental implant system. The aim of the work was to investigate the level of the β-CrossLaps, C-reactive protein (CRP), osteocalcin markers after orthopedic treatment of patients using dental implant supported advanced dental restoration technologies, to perform a biochemical analysis of the oral fluid of patients after restoration using dental implants and new two-part dental implants. In patients of the index group (52 people), the removable prostheses with metal frame and fixing elements or the commercially available dental implant supported removable prostheses were installed. For the patients of the control group (12 people), the commercially available dental implant supported removable prostheses of acrylic plastics were constructed. For all the patients after 6 months the level of β-CrossLaps, CRP, osteocalcin markers in the oral fluid was analysed. In patients of the index group, the average content of β-CrossLaps was 0.0126 ± 0.002 ng/ml, in the control group it was 0.0147 ± 0.002 ng/ml. The average content of the CRP in patients of the index group was 0.358 ± 0.019 mg/l, in patients of the control group it was 0.78 ± 0.01 mg/l. In patients of the index group, the average content of osteocalcin was 1.46 ± 0.25 ng/ml, in the control group it was 1.98 ± 0.31 ng/ml. It has been shown that biochemical markers of the oral fluid can be used to predict complications after the dental implants installation. Restoration with two-part dental implants of modern design is associated with fewer complications.

Keywords: removable dental prostheses, two-part dental implant, β-CrossLaps, CRP, osteocalcin metabolic markers

Author contribution: Tlustenko VP, Bayrikov IM, Trunin DA, Komlev SS — concept and research design, surgical and orthopedic treatment of patients; Gusyakova OA, Bayrikov IM, Komlev SS — collection and processing of material, biochemical analysis of oral fluid, statistical processing of results.

Compliance with ethical standards: the study was approved by the Ethics Committee of Samara State Medical University (protocol № 2018/196). All patients signed a voluntary informed consent to participate in the study (dental implantation and orthopedic treatment, collection of oral fluid samples).

✉ **Correspondence should be addressed:** Sergey S. Komlev
Chapayevskaya 89, Samara, 443099; stomat.ks@mail.ru

Received: 27.11.2018 **Accepted:** 03.04.2019 **Published online:** 13.04.2019

DOI: 10.24075/brsmu.2019.025

ВЛИЯНИЕ ТЕХНОЛОГИИ ПРОТЕЗИРОВАНИЯ ЗУБОВ НА ДИНАМИКУ РАННИХ ПРЕДИКТОРОВ ВОСПАЛИТЕЛЬНО-ДЕСТРУКТИВНОГО ПРОЦЕССА В ПЕРИИМПЛАНТАТНОЙ ЗОНЕ

В. П. Тлустенко, И. М. Байриков, Д. А. Трунин, О. А. Гусякова, С. С. Комлев ✉

Самарский государственный медицинский университет, Самара, Россия

Объективная оценка морфофункциональных характеристик состояния мягких тканей и костных структур, прилежащих к дентальному имплантату, позволяет контролировать динамику процессов остеоинтеграции в системе челюсть — дентальный имплантат. Целью работы было исследовать уровни маркеров β-CrossLaps, С-реактивный белок (СРБ), остеокальцина после ортопедического лечения пациентов с применением усовершенствованных технологий протезирования зубов с опорой на дентальные имплантаты. Провести биохимический анализ ротовой жидкости пациентов после протезирования на дентальных имплантатах и новых разборных дентальных имплантатах. Пациентам основной группы (52 человека) изготовили съемные ортопедические конструкции с металлическим каркасом и фиксирующими элементами с опорой на разборные дентальные имплантаты и съемные ортопедические конструкции с опорой на серийно выпускаемые дентальные имплантаты. Для пациентов контрольной группы (12 человек) были изготовлены съемные ортопедические конструкции из акриловых пластмасс с опорой на дентальные имплантаты, выпускаемые серийно. Всем пациентам через 6 месяцев исследовали уровни маркеров β-CrossLaps, СРБ, остеокальцина в ротовой жидкости. У пациентов основной группы содержание β-CrossLaps в среднем составило 0,0126 ± 0,002 нг/мл, в контрольной группе — 0,0147 ± 0,002 нг/мл. Содержание СРБ у пациентов основной группы в среднем составило 0,358 ± 0,019 мг/л, у пациентов контрольной группы — 0,78 ± 0,01 мг/л. В основной группе содержание остеокальцина в среднем составило 1,46 ± 0,25 нг/мл, в контрольной группе пациентов — 1,98 ± 0,31 нг/мл. Показано, что биохимические маркеры ротовой жидкости можно использовать для прогнозирования осложнений после установки дентальных имплантатов. Протезирование усовершенствованными конструкциями на разборных дентальных имплантатах сопряжено с меньшим количеством осложнений.

Ключевые слова: съемные ортопедические конструкции, разборный дентальный имплантат, метаболические показатели β-CrossLaps, СРБ, остеокальцин

Информация о вкладе авторов: В. П. Тлустенко, И. М. Байриков, Д. А. Трунин, С. С. Комлев — разработка концепции и дизайна исследования, хирургическое и ортопедическое лечение пациентов; О. А. Гусякова, И. М. Байриков, С. С. Комлев — сбор и обработка материала, биохимическое исследование ротовой жидкости, статистическая обработка результатов.

Соблюдение этических стандартов: исследование одобрено этическим комитетом Самарского государственного медицинского университета (протокол № 2018/196). Все пациенты подписали информированное согласие на участие в исследовании (проведение операции дентальной имплантации и ортопедическое лечение, сбор образцов ротовой жидкости).

✉ **Для корреспонденции:** Сергей Сергеевич Комлев
ул. Чапаевская, д. 89, г. Самара, 443099; stomat.ks@mail.ru

Статья получена: 27.11.2018 **Статья принята к печати:** 03.04.2019 **Опубликована онлайн:** 13.04.2019

DOI: 10.24075/vrgmu.2019.025

When treating patients with partial and complete absence of teeth using dental implant supported prostheses, it is important to plan the surgical intervention, select the implant system and the prosthesis, predict the outcome of the chosen set of measures. An objective assessment of the morphological and functional characteristics of the state of soft tissues and bone structures adjacent to the dental implant is essential. It allows to prevent errors that can lead to disruption of the processes

of osseointegration in the jaw — dental implant system and contribute to the development of early and late destructive inflammatory complications [1].

After installation of commercially available dental implants, two-part dental implants and orthopedic treatment with improved prostheses, it is necessary to study the factors that serve as indicators of the preclinical stage of development of inflammatory destructive disorders. For this purpose, the studies of the oral fluid as a biological media that provides homeostasis of the tissues in the periimplant zone are conducted [2–4].

The regeneration of bone tissue around the implant after a dental implantation operation is a combination of processes of structural and functional recovery after damage. The process of ossification is based on the mechanisms of transformation of undifferentiated cells into osteoblasts, the process of osteoinduction, as well as the emergence of a matrix that ensures the deposition of bone stock. Indicators reflecting the processes of destruction and the state of mineralization–demineralization of bone tissue include osteocalcin, C-reactive protein (CRP), the cleavage product of C-telopeptide of the I type collagen (β-CrossLaps) [5–8].

Osteocalcin is a non-collagen calcium-binding protein of the bone matrix, consisting of 49 amino acid residues. It is synthesized almost exclusively by osteoblasts and is involved in the processes of mineralization, it is a marker of bone remodeling. β-CrossLaps is a bone resorption marker. CRP is a typical protein of the acute phase of inflammation, which is considered to be the most sensitive laboratory marker of infection, inflammation and tissue damage. In its structure, the CRP consists of five identical polypeptide subunits, forming a cyclic disc-shaped pentameric structure. Synthesis of CRP occurs in hepatocytes and is regulated by anti-inflammatory cytokines. In presence of inflammation, infection, or traumatic injury, the CRP levels quickly increase. In the oral fluid, the level of CRP reaches its maximum 24 hours after activation of its synthesis in hepatocytes, [9–12].

Complications of dental implantation occur in 6–23% of cases. According to epidemiological studies data, in patients who use dental implant supported prostheses for a long time, the signs of mucositis are present in 80% of cases, and the signs of periimplantitis are present in 28–56% cases. Clinical manifestations of dental periimplantitis are predicated by the presence of the destructive inflammatory process. A significant number of publications shows the great informative value of the qualitative and quantitative assessment of indicators of the oral fluid of patients, and the ability to use indicators of oral fluid as a prognostic instruments for dental implantation [13–15].

The aim of the work was to determine the levels of the β-CrossLaps, CRP, osteocalcin markers after orthopedic treatment of patients using advanced implant supported restoration techniques.

METHODS

The study included 52 patients of the index group and 12 patients of the control group. Criteria for inclusion of patients in the study: any gender; partial absence of teeth, Kennedy class I and II. Exclusion criteria: dentofacial anomalies; the presence of diseases of the endocrine system and of the gastrointestinal tract.

Patients of the index group were divided into two subgroups: index group 1 and index group 2. Index group 1 included 12 patients: 4 men and 8 women aged 45–65 years. In the patients of this group, the removable prostheses with a metal frame and fixing elements were installed. Telescopic crowns and clasps were used. 28 two-part dental implants of our design (Patent of Russian Federation № 2593349) were installed.

Index group 2 included 40 patients: 15 men and 25 women aged 45–65 years. In patients of this group, the commercially available dental implant supported removable prostheses (85 dental implants) were installed. The fixing elements were located in the metal frame of the removable prosthesis.

For the patients of the index group, the removable prostheses were constructed of thermoplastics, nylon with a metal frame (Patent of Russian Federation № 2588488). Introduction of molded frame into thermoplastic made it possible to evenly distribute the load on the abutment teeth and dental implants, to obtain the possibility of stabilization along the plane, to improve the fixation of the prosthesis.

The control group included 12 patients: 3 men and 9 women aged 45–65 years, for whom the commercially available dental implant supported removable prostheses made of acrylic plastics were constructed. The fixing elements were located in the basis of a removable prosthesis; depending on the defect of the dental arcade, 2–3 dental implants were installed.

When examining patients, the dental status was assessed. All participants were subjected to biochemical analysis of oral fluid samples by determining the following metabolic parameters: β-CrossLaps, CRP, osteocalcin. Study of the metabolic processes of oral homeostasis is a non-invasive research method. Evaluation of metabolic processes in the bone tissue of patients of control and index groups was performed 6 months after orthopedic treatment. At the stage of biochemical analysis of saliva, patients did not have signs of acute somatic diseases.

The quantitative analysis of β-CrossLaps and osteocalcin in the oral fluid was performed by the solid-phase tube method with ECL reaction on the basis of the streptavidin-biotin technology with ruthenium label using the Elecsys-2010 (F. Hoffmann-La Roche; Switzerland) automatic ECL laboratory unit. Evaluation of CRP was performed on the Cobas Integra 400 plus (F. Hoffmann-La Roche; Switzerland) biochemical analyzer. The following diagnostic kits (F. Hoffmann-La Roche; Switzerland) were used: a set of calibrators for evaluation of β-CrossLaps, N-MID osteocalcin, a reagent kit for quantitative analysis of β-CrossLaps, N-MID osteocalcin, C-reactive protein Lx.

Statistical processing of the obtained data was performed using Student's t-test on a personal computer running the Microsoft Windows 10 operating system using the SPSS Statistics 21.0 (license № 20130626-3; USA) statistical software package.

The parametric Student's t-test was used, as well as the Kruskal–Wallis one-way analysis of variance and the Mann–Whitney U-test.

RESULTS

The table presents the values of metabolic parameters of samples of oral fluid from patients of the control and index groups taken 6 months after orthopedic treatment.

In the index group, the average content of β-CrossLaps in the oral fluid was 0.0126 ± 0.002 ng/ml, in the control group it was 0.0147 ± 0.002 ng/ml. During the bone resorption, telopeptides with remnants of collagen molecules enter the oral fluid.

In the index group, the average content of CRP was 0.358 ± 0.019 mg/l, in the control group it was 0.78 ± 0.01 mg/l.

To assess the metabolic processes in the bone tissue of patients after orthopedic treatment, we evaluated the osteocalcin content in the oral fluid. In the index group, the

Table 1. β-CrossLaps, CRP, osteocalcin metabolic markers in patients of the control and index groups 6 months after dental implantation

Parameters	Reference values	Index group		Control group
		1	2	
β-CrossLaps (ng/ml)	0.01 ± 0.001	0.0123 ± 0.002*	0.0128 ± 0.002*	0.0147 ± 0.002
CRP (mg/l)	0.1 ± 0.001	0.241 ± 0.013*	0.476 ± 0.024*	0.78 ± 0.01
Osteocalcin (ng/ml)	1.11 ± 0.11	1.33 ± 0.26*	1.58 ± 0.24	1.98 ± 0.31

Note: * — the significance of differences compared to the data of the control group ($p < 0.05$).

average value was 1.46 ± 0.25 ng/ml, in the control group the average value was 1.98 ± 0.31 ng/ml. Osteocalcin, the bone matrix protein, containing the γ-carboxyglutamic acid, promotes the fixation of calcium ions and enables mineralization. Osteocalcin exhibits chemotactic properties in relation to the precursor cells of osteoblasts and osteoclasts, attracting them to the osteogenesis zone.

In the index group, the biochemical parameters in 3 patients had the following values: β-CrossLaps — 0.0295 ± 0.002 ng/ml, CRP — 1.17 ± 0.03 mg/l, osteocalcin — 2.92 ± 0.11 ng/ml. In the control group, in 3 patients there were the following values: β-CrossLaps — 0.0463 ± 0.002 ng/ml, CRP — 1.49 ± 0.01 mg/l, osteocalcin — 3.11 ± 0.17 ng/ml. The obtained values of metabolic parameters of patients of the control group indicate presence of characteristic for periimplantitis destructive processes in the bone tissue. The number of complications in the index and control groups of patients was 5.8 and 16.7%, respectively.

DISCUSSION

The state of oral homeostasis after the dental implantation operation was studied by determining indicators of the metabolism of the oral fluid of patients in the control and index groups, reflecting the presence of destruction processes, the state of mineralization and demineralization of bone tissue. The study of early predictors [2, 6, 11] of the destructive inflammatory process in the periimplant zone allows to control the dynamics of the processes of osseointegration in the jaw — dental implant system. Metabolic indices of β-CrossLaps, CRP, osteocalcin reflected the intensity of the inflammatory response characteristic of the traumatic process during the dental implantation operation.

CRP analysis is an objective method of screening the inflammatory activity in patients of the control and index groups after dental implantation using commercially available dental implants, two-part dental implants and after orthopedic treatment using improved prostheses.

To assess the metabolic processes in the bone tissue of patients after dental implantation, we evaluated the osteocalcin content.

The method of studying oral fluid as the main homeostatic environment of the oral cavity objectively reflected the response of oral tissues during destructive inflammatory processes that occurred in patients of the control and index groups after the dental implantation operation. In the presence of minor inflammatory events, changes in the metabolic indices of the oral fluid occurred associated with the delivery of the destroyed protein macromolecules fragments, the insufficiently oxidized metabolic products.

An increase in the level of osteocalcin in the oral fluid indicated a decrease in the mineralization in the periimplant zone and the plastic resources of the bone tissue in patients of the control group. The increased content of CRP reflects the severity of the inflammatory response, which allows to obtain additional evaluation criteria for characterizing the pathological process. Patients in the control group after 3 months of anti-inflammatory and antimicrobial therapy experienced a decrease in the level of biochemical parameters.

Lower levels of inflammation in patients of the index group compared to the control group are attributed to the use of improved prostheses and fixing elements supported by titanium abutments of the two-part dental implants.

When analyzing the results of osteomatrix protein content in saliva, a rapid increase in β-CrossLaps decay fragments and an increase in the concentration of osteocalcin and CRP were found. These data indicate the specificity of the revealed violations of the biochemical composition of the oral fluid during the acceleration of osteoclastic processes in patients with complications.

A characteristic indicator of enhanced bone resorption is an established increase of the content of collagen fragments (β-CrossLaps), osteocalcin, CRP.

CONCLUSION

The results of our research confirmed that metabolic markers such as β-CrossLaps, CRP, osteocalcin, in patients after dental implantation are informative for predicting complications when using different types of dental implants. A lower percentage of complications and a smaller deviation from normal level of the inflammation indicators in patients of the index group compared to the control group are presumably associated with the use of improved prostheses and fixing elements supported by titanium abatments of the two-part dental implants.

References

1. Aziz S. Hard and soft tissue surgical complications in dental implantology. Oral Maxillofac. Surg Clin North Am. 2015; 27 (2): 313–8.
2. Guobis Z, Pacauskiene I, Astramskaite I. General diseases influence on peri-implantitis development: a systematic review. J Oral Maxillofac Res. 2016; 7 (5): 9–14.
3. Lohmann CH, Rampal S, Lohrengel M, Singh G. Imaging in peri-prosthetic assessment: an orthopaedic perspective. EFORT Open Rev. 2017; 2 (5): 117–25.
4. Greenstein G, Carpentieri J, Cavallaro J. Nerve damage related to implant dentistry: incidence, diagnosis, and management. Compend Contin Educ Dent. 2015; 36 (9): 652–9.

5. Alikhasi M, Alsharbaty MHM, Moharrami M. Digital Implant Impression Technique Accuracy: A Systematic Review. Implant Dent. 2017; 26 (6): 929–35. DOI: 10.1097/ID.0000000000000683.
6. Atrushkevich VG, Shkolnaya KD. Osobennosti mineral'nogo i kostnogo obmena u pacientov v zavisimosti ot haraktera techenija parodontita. Lechenie i profilaktika. 2017; 2 (22): 85–92.
7. Alrabeah GO, Brett P, Knowles JC, Petridis H. The effect of metal ions released from different dental implant-abutment couples on osteoblast function and secretion of bone resorbing mediators. J Dent. 2017; 66: 91–101. DOI: 10.1016/j.jdent.2017.08.002.
8. Boronat-Catala M, Catala-Pizarro M, Bagan Sebastian J. Salivary and crevicular fluid interleukins in gingivitis. J Clin Exp Dent. 2014; 6 (1): 175–9.
9. Casado PL, Aguiar DP, Costa LC. Different contribution of BRINP3 gene in chronic periodontitis and periimplantitis: a cross-sectional study. BMC Oral. Health. 2015; (15): 33. DOI 10.1186/s12903-015-0018-6.
10. Plyuhin DV. Soderzhanie produktov svobodnoradikal'nogo okislenija v kostnoj tkani i ishod dental'noj implantacii. Medicinskaja nauka i obrazovanie Urala. 2016; 1 (85): 105–7.
11. Kozlova MV, Mkrtumyan AM, Belyakova AS. Reguljacija metabolicheskih processov kosti pri dental'noj implantacii. Kremlevskaja medicina. Klinicheskij vestnik. 2018; (2): 30–9.
12. Riega-Torres JC, Villarreal-Gonzalez AJ, Ceceñas-Falcon LÁ, Salas-Alanis JC. Sjögren's syndrome (SS), a review of the subject and saliva as a diagnostic method. Gac Med Mex. 2016; 152 (3): 371–80.
13. Modi A, Morou-Bermudez E, Vergara J, et al. Validation of two point-of-care tests against standard lab measures of NO in saliva and in serum. Nitric Oxide. 2017; (64): 16–21. DOI: 10.1016/j.niox.2017.01.009.
14. Alkan EA, Tüter G, Parlar A, et al. Evaluation of peri-implant crevicular fluid prostaglandin levels in augmented extraction sockets by different biomaterials. Acta Odontol Scand. 2016; 74 (7): 532–8.
15. Fernandes MH, Gomes PS. Bone Cells Dynamics during Peri-Implantitis: a Theoretical Analysis. J Oral Maxillofac Res. 2016; 7 (3): e6.

Литература

1. Aziz S. Hard and soft tissue surgical complications in dental implantology. Oral Maxillofac. Surg Clin North Am. 2015; 27 (2): 313–8.
2. Guobis Z, Pacauskiene I, Astramskaite I. General diseases influence on peri-implantitis development: a systematic review. J Oral Maxillofac Res. 2016; 7 (5): 9–14.
3. Lohmann CH, Rampal S, Lohrengel M, Singh G. Imaging in peri-prosthetic assessment: an orthopaedic perspective. EFORT Open Rev. 2017; 2 (5): 117–25.
4. Greenstein G, Carpentieri J, Cavallaro J. Nerve damage related to implant dentistry: incidence, diagnosis, and management. Compend Contin Educ Dent. 2015; 36 (9): 652–9.
5. Alikhasi M, Alsharbaty MHM, Moharrami M. Digital Implant Impression Technique Accuracy: A Systematic Review. Implant Dent. 2017; 26 (6): 929–35. DOI: 10.1097/ID.0000000000000683.
6. Атрушкевич В. Г., Школьная К. Д. Особенности минерального и костного обмена у пациентов в зависимости от характера течения пародонтита. Лечение и профилактика. 2017; 2 (22): 85–92.
7. Alrabeah GO, Brett P, Knowles JC, Petridis H. The effect of metal ions released from different dental implant-abutment couples on osteoblast function and secretion of bone resorbing mediators. J Dent. 2017; 66: 91–101. DOI: 10.1016/j.jdent.2017.08.002.
8. Boronat-Catala M, Catala-Pizarro M, Bagan Sebastian J. Salivary and crevicular fluid interleukins in gingivitis. J Clin Exp Dent. 2014; 6 (1): 175–9.
9. Casado PL, Aguiar DP, Costa LC. Different contribution of BRINP3 gene in chronic periodontitis and periimplantitis: a cross-sectional study. BMC Oral. Health. 2015; (15): 33. DOI 10.1186/s12903-015-0018-6.
10. Плюхин Д. В. Содержание продуктов свободнорадикального окисления в костной ткани и исход дентальной имплантации. Медицинская наука и образование Урала. 2016; 1 (85): 105–7.
11. Козлова М. В., Мкртумян А. М., Белякова А. С. Регуляция метаболических процессов кости при дентальной имплантации. Кремлевская медицина. Клинический вестник. 2018; (2): 30–9.
12. Riega-Torres JC, Villarreal-Gonzalez AJ, Ceceñas-Falcon LÁ, Salas-Alanis JC. Sjögren's syndrome (SS), a review of the subject and saliva as a diagnostic method. Gac Med Mex. 2016; 152 (3): 371–80.
13. Modi A, Morou-Bermudez E, Vergara J, et al. Validation of two point-of-care tests against standard lab measures of NO in saliva and in serum. Nitric Oxide. 2017; (64): 16–21. DOI: 10.1016/j.niox.2017.01.009.
14. Alkan EA, Tüter G, Parlar A, et al. Evaluation of peri-implant crevicular fluid prostaglandin levels in augmented extraction sockets by different biomaterials. Acta Odontol Scand. 2016; 74 (7): 532–8.
15. Fernandes MH, Gomes PS. Bone Cells Dynamics during Peri-Implantitis: a Theoretical Analysis. J Oral Maxillofac Res. 2016; 7 (3): e6.

A PROGNOSTIC MODEL FOR THE PREDICTION OF GENERALIZED CHRONIC PERIODONTITIS IN PATIENTS WITH METABOLIC SYNDROME

Petrukhina NB[1,2], Zorina OA[1,2], Shikh EV[1], Kartysheva EV[1]✉, Kudryavtsev AV[2]

[1] Sechenov First Moscow State Medical University, Moscow, Russia

[2] Central Research Institute of Dentistry and Maxillofacial Surgery, Moscow, Russia

The pathogenesis of periodontitis involves a complex inflammatory cascade initiated by biofilm bacteria. The susceptibility to or the risk of developing the disease is determined by the body's response to the invasion, specifically, by the strength of the inflammatory response and the differential activation of immune pathways. In this paper, we propose a model for predicting the risk of severe chronic generalized periodontitis (GCP) in patients with metabolic syndrome based on the levels of tumor necrosis factor alpha (TNF-α) in the periodontal pocket exudate. The analysis of oral cavity cytokine profiles conducted in 537 patients with GCP and comorbid metabolic syndrome showed that increased TNF-α correlated with the severity of GCP: higher levels of TNF-α were observed in patients whose condition was more severe. The prognostic model built in Statistica. 10 allowed us to use TNF-α as a prognostic criterium for GCP severity. We determined the cut-off point above which a high risk of severe GCP can be concluded with 91.2% sensitivity and 70.8% specificity. The spreadsheet in Microsoft Excel 2010 automatically computed the risk of severe GCP from a patient's TNF-α concentrations in the PP, which makes the model convenient for routine clinical use in dentistry.

Keywords: periodontitis, metabolic syndrome, cytokines, tumor necrosis factor, TNF, prognostic model

Author contribution: Petrukhina NB and Shikh EV conceived the study, analyzed and interpreted the obtained data; Zorina OA analyzed and interpreted the obtained data; Kartysheva EV collected the samples, analyzed the literature and interpreted the obtained data; Kudryavtsev AV prepared the manuscript draft and analyze the literature.

Compliance with ethical standards: the study was approved by the Ethics Committee of I.M.Sechenov First Moscow State Medical University (Protocol No. 10–15 dated November 18, 2015). All patients gave informed consent to participate.

✉ **Correspondence should be addressed:** Ekaterina V. Kartysheva,
Bolshaya Pirogovskaya 2, bld. 4, Moscow, 119991; 89057676464@mail.ru

Received: 24.09.2018 **Accepted:** 31.03.2019 **Published online:** 14.04.2019

DOI: 10.24075/brsmu.2019.026

ПРОГНОСТИЧЕСКАЯ МОДЕЛЬ ДЛЯ ОЦЕНКИ ХРОНИЧЕСКОГО ГЕНЕРАЛИЗОВАННОГО ПАРОДОНТИТА У ПАЦИЕНТОВ С МЕТАБОЛИЧЕСКИМ СИНДРОМОМ

Н. Б. Петрухина[1,2], О. А. Зорина[1,2], Е. В. Ших[1], Е. В. Картышева[1]✉, А. В. Кудрявцев[2]

[1] Первый Московский государственный медицинский университет имени И. М. Сеченова (Сеченовский Университет), Москва, Россия

[2] Центральный научно-исследовательский институт стоматологии и челюстно-лицевой хирургии, Москва, Россия

Патогенез пародонтита включает сложный иммунный воспалительный каскад, который инициируется бактериями биопленки, а восприимчивость или вероятность развития заболевания определяется реакцией организма человека, в частности, величиной воспалительного ответа и дифференциальной активацией иммунных путей. Цель исследования — разработать прогностическую модель для оценки риска развития тяжелой степени хронического генерализованного пародонтита в зависимости от содержания фактора некроза опухоли-α (ФНО-α) в экссудате пародонтального кармана (ПК) пациента. При клинико-инструментальном обследовании 537 пациентов с хроническим генерализованным пародонтитом и метаболическим синдромом установлено, что уровень повышения ФНО-α в содержимом ПК коррелировал со степенью тяжести хронического генерализованного пародонтита (ХГП): более высокие значения цитокина соответствовали более тяжелой степени. Разработанная в программе Statistica.10 прогностическая модель дала возможность использовать уровень ФНО-α в содержимом ПК пациента в качестве прогностического критерия течения ХГП. Определено критическое значение, при превышении которого с диагностической чувствительностью 91,2% и специфичностью 70,8% можно заключить о высоком риске развития тяжелой степени ХГП. Созданное окно в программе Microsoft Excel 2010 позволяет автоматически рассчитывать риск развития тяжелой степени ХГП в зависимости от индивидуального значения концентрации ФНО-α в содержимом ПК пациента, что делает данную модель удобной для применения врачами-стоматологами.

Ключевые слова: пародонтит, метаболический синдром, цитокины, фактор некроза опухоли, ФНО, прогностическая модель

Информация о вкладе авторов: Н. Б. Петрухина; Е. В. Ших — планирование исследования, анализ и интерпретация данных; О. А. Зорина — анализ и интерпретация данных; Е. В. Картышева — сбор данных, анализ и интерпретация данных; А. В. Кудрявцев — черновик рукописи, анализ литературы.

Соблюдение этических стандартов: этический комитет Первого МГМУ им. И. М. Сеченова (Сеченовский Университет) (протокол № 10–15 от 18 ноября 2015 г.); все пациенты подписали добровольное согласие на участие в исследовании.

✉ **Для корреспонденции:** Екатерина Владимировна Картышева,
ул. Большая Пироговская, д. 2, стр. 4, г. Москва, 119991; 89057676464@mail.ru

Статья получена: 24.09.2018 **Статья принята к печати:** 31.03.2019 **Опубликована онлайн:** 14.04.2019

DOI: 10.24075/vrgmu.2019.026

Tumor necrosis factor alpha (TNF-α) is one of the early proinflammatory cytokines that plays a key role in periodontal tissue destruction [1]. Clinical studies have demonstrated that elevated TNF-α is a risk factor for the progression of periodontal diseases. TNF-α mediates periodontal tissue destruction via at least two different pathways. Firstly, it stimulates production of osteoclasts that cause alveolar bone resorption [2, 3]. Secondly, TNF-α promotes the body's early immune response to periodontal pathogens and regulates synthesis of matrix metalloproteinases (MMP) capable of damaging connective tissue. Besides, it is reported that TNF-α levels are increased systemically in patients with obesity or metabolic syndrome [4]. Adipose tissue cells secrete TNF-α; therefore, accumulation of excess fat leads to chronic systemic inflammation [5, 6]. It has been shown that TNF-α levels also correlate with insulin resistance [7]. TNF-α is a paracrine mediator: its local activity is aimed at reducing sensitivity of adipocytes to insulin [8]. There is a reciprocal connection between periodontal disease and

metabolic syndrome. The severity of systemic inflammation in patients with metabolic syndrome can affect local inflammation in the periodontium, while the products of periodontal inflammation can stimulate secretion of systemic cytokines. In this study we propose a prognostic model for predicting the risk of severe generalized chronic periodontitis based on TNF-α concentrations in the exudate from a periodontal pocket (PP).

METHODS

We examined 537 patients (243 females and 294 males; 45.25% vs. 54.75%, respectively) aged 35 to 65 years with clinically diagnosed generalized chronic periodontitis (GCP) and metabolic syndrome. The patients were distributed into 3 age groups: group 1 included patients aged 35–44 years, with the mean age of 41.7 ± 2.1; group 2 consisted of patients aged 45–54 years, with the mean age of 52.2 ± 1.2; group 3 comprised individuals aged 55–65 years, with the mean age of 63.4 ± 1.1. Our study included patients of both sexes aged 35 to 65 years, with clinically diagnosed GCP, comorbid metabolic syndrome and a body mass index ≥ 25 kg/m^2, who gave written informed consent to participate. The following exclusion criteria were applied: age under 35 years; hematologic disorders; diseases of the central nervous system, both congenital and acquired; malignancies (cancers, sarcomas); decompensated chronic conditions (myocardial infarction, systemic thromboembolism); pregnancy.

Exudate samples were collected onto filter paper strips introduced into the PP for 30 s. Then, the strips were transferred into Eppendorf tubes containing 1 ml of sterile normal saline and left there for 40 min. After that, the strips were taken out with tweezers, and the content of the Eppendorf tubes was analyzed. TNF-α levels were measured using ELISA kits by BIOSOURCE (Europe S. A.; Belgium); spectrophotometry was done by a microplate reader at 450 nm wavelength. Cytokine concentrations were determined from a standard curve and expressed as pg/ml.

The next step was to create a prognostic model for predicting the risk of developing severe GCP based on TNF-α concentrations. A primary data matrix was generated in Statistica.10 (StatSoft; USA). Model coefficients were calculated in the output spreadsheet and included into the mathematical expression. Then, a ROC curve was constructed and a cut-off point was determined. The cut-off point allows using the model for practical tasks: new data can be assigned to one of the 2 classes depending on their position relative to the cut-off point. Besides, we applied the ROC-curve analysis to assess the diagnostic efficacy of our model by calculating the AUC value (Area Under Curve) using a trapezoidal rule.

RESULTS

Based on the obtained TNF-α concentrations (Table 1), a prognostic model was built for predicting the risk of developing severe GCP.

The mathematical expression below can be used to calculate the risk of severe periodontal tissue destruction based on the TNF-α concentrations in the PP. The measured TNF-α concentrations should be plugged into the following formula:

$$W = -3.2 + 1.2 \cdot \log_{10}(Y),$$

where W is a risk of developing severe GCP calculated from the cytokine profile of the oral cavity and Y is a TNF-α concentration in the PP expressed as pg/ml.

Table 1. Levels of the key proinflammatory cytokine TNF-α in the PP exudate in patients with GCP and comorbid metabolic syndrome

Parameter	35–44 years		45–54 years		55–65 years	
Sex	M	F	M	F	M	F
	Mild GCP					
TNF-α (pg/ml)	576.80 ± 19.49	584.96 ± 21.54	611.78 ± 21.67	634.57 ± 23.5	645.67 ± 23.7	678.45 ± 24.9
	Moderate GCP					
TNF-α (pg/ml)	845.44 ± 32.76	876.5 ± 33.7	848.34 ± 24.5	998.56 ± 21.5*	945.81 ± 32.33	1045.33 ± 31.56
	Severe GCP					
TNF-α (pg/ml)	878.93 ± 32.11	911.23 ± 31.67	905.78 ± 35.6	1145.87 ± 35.11*	1234.56 ± 33.17	1341.54 ± 33.98

Note: * — shows that the difference is significant.

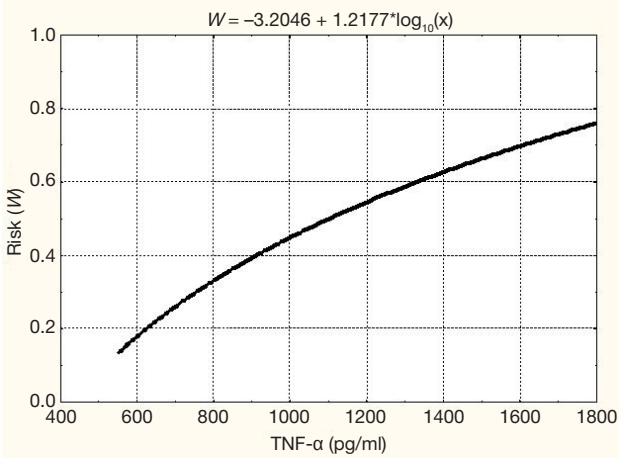

Fig. 1. The graph shoes the relationship between the risk of developing severe GCP and the TNF-α concentrations in the PP

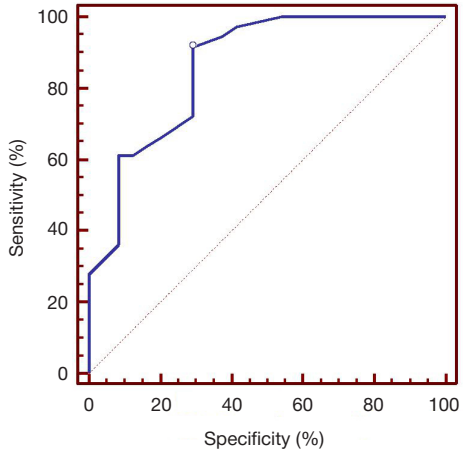

Fig. 2. The ROC-curve represents a relationship between the diagnostic sensitivity and specificity in predicting the risk of severe GCP from the cytokine profile of the oral cavity

Fig. 1 is the graphic representation of the relationship between the risk of developing severe GCP and the TNF-α concentrations in the PP. The risk for severe GCP increases as TNF-α levels grow in the PP.

The risk *W* for developing severe GCP was calculated for each study participant from TNF-α concentrations in the PP. Then, the ROC analysis was conducted to determine a critical (cut-off) value for *W* (0.3), above which a high risk for severe GCP could be predicted with maximum specificity and sensitivity.

$W \geq 0.3$ means that the risk for severe GCP is high; $W < 0.3$ means it is low. The diagnostic sensitivity of the method is 91.2%, whereas its specificity is 70.8%.

Fig. 2 features a ROC curve for different values of the prognostic coefficient *W*. Table 2 shows sensitivity and specificity of the method at which $W = 0.3$ had the highest sensitivity and specificity.

The AUC value of 0.862 ± 0.05 ($z = 7.3$; $p < 0.001$) and the confidence interval of 0.765–0.959 suggest that *W* has a high diagnostic significance in predicting severe GCP based on the cytokine profile of the oral cavity.

W was computed in Microsoft Excel 2010; individual TNF-α concentrations were entered into the highlighted cell (Fig. 3).

DISCUSSION

TNF-α plays a key role in the pathogenesis of periodontal diseases. When bacterial lipopolysaccharides permeate periodontal tissue, macrophages assisted by CD14-lymphocytes activate a number of innate and adaptive immunity mechanisms through specific receptors. An inadequately strong immune response leads to chronic inflammation and periodontal tissue destruction [9, 10]. Prostaglandin E2, IL1β and TNF-α are key proinflammatory mediators that activate tissue metalloproteinases and thereby stimulate bone resorption by osteoclasts and induce damage to the periodontium [11]. A number of nonimmune periodontal cells, such as epithelial cells and fibroblasts, can recognize and respond to proinflammatory IL1β and TNF-α. Tissue metalloproteinases produced by neutrophils, macrophages, fibroblasts, and osteoclasts promote proteolysis of collagen, gelatin and elastin, destroying the connective tissue components of tooth-supporting structures. Among the members of the TNF superfamily are osteotropic factors, such as the receptor activator of NF-kB ligand (RANKL) and RANK themselves that are synthesized by osteoclasts and promote bone resorption [12]. The binding of the RANK ligand to the RANK receptor is accompanied by a fusion of a few precursor cells into a mature multinucleated osteoclast that immediately starts to destroy bone tissue (Fig. 4).

In light of this, the study of TNF-α levels in the PP of patients opens new possibilities for predicting the severity of GCP.

CONCLUSIONS

We have found that elevated TNF-α concentrations in the PP correlate with the severity of GCP in patients with metabolic syndrome: higher TNF-α levels are associated with a more

Table 2. Sensitivity and specificity of the method at different values of the prognostic coefficient *W* used to predict the risk of severe GCP from the cytokine profile of the oral cavity

Parameter *W*	Diagnostic sensitivity	CI for DSn	Diagnostic. specificity	CI for DSp
> 0.29	94.44	81.3 – 99.3	62.5	40.6 – 81.2
> 0.3*	91.67	77.5 – 98.2	70.83	48.9 – 87.4
> 0.32	86.11	70.5 – 95.3	70.83	48.9 – 87.4
> 0.33	83.33	67.2 – 93.6	70.83	48.9 – 87.4
> 0.34	80.56	64.0 – 91.8	70.83	48.9 – 87.4
> 0.35	72.22	54.8 – 85.8	70.83	48.9 – 87.4
> 0.36	69.44	51.9 – 83.7	75	53.3 – 90.2
> 0.38	66.67	49.0 – 81.4	79.17	57.8 – 92.9
> 0.4	63.89	46.2 – 79.2	83.33	62.6 – 95.3
> 0.41	61.11	43.5 – 76.9	87.5	67.6 – 97.3
> 0.45	61.11	43.5 – 76.9	91.67	73.0 – 99.0
> 0.46	55.56	38.1 – 72.1	91.67	73.0 – 99.0
> 0.5	44.44	27.9 – 61.9	91.67	73.0 – 99.0
> 0.51	36.11	20.8 – 53.8	91.67	73.0 – 99.0
> 0.52	27.78	14.2 – 45.2	100	85.8 – 100.0

Note: * — marks the cut-off point.

Fig. 3. A spreadsheet in Microsoft Excel 2010 used for automatic calculations of the risk for severe GCP based on the oral cavity cytokine profile

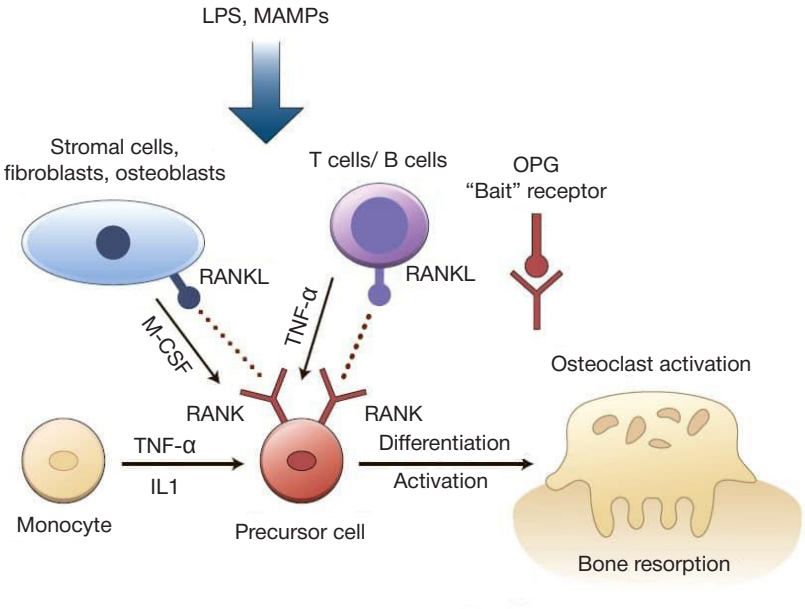

Fig. 4. Integration of proinflammatory and osteotropic factors in bone resorption

severe course of the disease. The proposed prognostic model based on the TNF-α concentrations in the PP is a promising and informative noninvasive method that can be used to predict the progression of the disease. The advantages of our model include low costs, availability, fast results, and the simplicity of use, which is crucial for routine dental practice.

References

1. Graves D, Cochran D. The contribution of interleukin-1 and tumor necrosis factor to periodontal tissue destruction. J Periodontol. 2003; 74 (3): 391–401.
2. Aganov DS, Tyrenko VV, Cygan EN, Toporkov MM, Bologov SG. Rol' citokinovoj sistemy RANKL/RANK/OPG v regulyacii mineral'nogo obmena kostnoj tkani. Geny i kletki. 2014; (4): 50–2. Russian.
3. Hotamisligil GS, Shargill NS, Spiegelman BM. Adipose expression of tumor necrosis factor-alpha: direct role in obesity-linked insulin resistance. Science. 1993; 259 (5091): 87–91.
4. Petrukhina NB, Rabinovich IM, Zorina OA. Narushenie mikrobiocenoza rta u pacientov s metabolicheskim sindromom (chast'1). Institut stomatologii. 2014; 1 (62): 54–7. Russian.
5. Hivert MF, Sullivan LM, Fox CS, Nathan DM, D'Agostino RB Sr, Wilson PW et al. Associations of adiponectin, resistin, and tumor necrosis factor-alpha with insulin resistance. J Clin Endocrinol Metab. 2008; 93 (8): 3165–72.
6. Hotamisligil GS, Arner P, Caro JF, Atkinson RL, Spiegelman BM. Increased adipose tissue expression of tumor necrosis factor-alpha in human obesity and insulin resistance. J Clin Invest. 2005; 95 (5): 2409–15.
7. Gregor MF, Hotamisligil GS. Inflammatory mechanisms in obesity. Annu Rev Immunol. 2011; (29): 415–45.
8. Kobayashi K, Takahashi N, Jimi E, Udagawa N, Takami M, Kotake S. et al. Tumor necrosis factor alpha stimulates osteoclast differentiation by a mechanism independent of the ODF/RANKL-RANK interaction. J Exp Med. 2000; 191 (2): 275–86.
9. Lau DC, Dhillon B, Yan H, Szmitko PE, Verma S. Adipokines: molecular links between obesity and atheroslcerosis. Am J Physiol Heart Circ Physiol. 2005; 288 (5): 2031–41.
10. Zorina OA, Rabinovich IM, Petrukhina NB, Kudryavtseva EV. Sravnitel'nye rezul'taty antropometrii i bioimpedansnogo issledovaniya u pacientov s hronicheskim generalizovannym parodontitom i metabolicheskim sindromom. Stomatologiya. 2016; 95 (2): 91–2. Russian.
11. Barer G, Grigoryan S, Postnova N. Rol' interferona i drugih citokinov v vozniknovenii i razvitii zabolevanij parodonta. Cathedra. 2006; 5 (3): 54–60. Russian.
12. Sagalovsky S, Schönert M. RANKL-RANK-OPG system and bone remodeling: a new approach on the treatment of osteoporosis. Clin Exptl Pathol. 2011; 2 (10): 146–53.

Литература

1. Graves D, Cochran D. The contribution of interleukin-1 and tumor necrosis factor to periodontal tissue destruction. J Periodontol. 2003; 74 (3): 391–401.
2. Аганов Д. С., Тыренко В. В., Цыган Е. Н., Топорков М. М., Бологов С. Г. Роль цитокиновой системы RANKL/RANK/OPG в регуляции минерального обмена костной ткани. Гены и клетки. 2014; (4): 50–2.
3. Hotamisligil GS, Shargill NS, Spiegelman BM. Adipose expression of tumor necrosis factor-alpha: direct role in obesity-linked insulin resistance. Science. 1993; 259 (5091): 87–91.
4. Петрухина Н. Б., Рабинович И. М., Зорина О. А. Нарушение микробиоценоза рта у пациентов с метаболическим синдромом (часть 1). Институт стоматологии. 2014; 1 (62): 54–7.
5. Hivert MF, Sullivan LM, Fox CS, Nathan DM, D'Agostino RB Sr, Wilson PW et al. Associations of adiponectin, resistin, and tumor necrosis factor-alpha with insulin resistance. J Clin Endocrinol Metab. 2008; 93 (8): 3165–72.
6. Hotamisligil GS, Arner P, Caro JF, Atkinson RL, Spiegelman BM. Increased adipose tissue expression of tumor necrosis factor-alpha in human obesity and insulin resistance. J Clin Invest. 2005; 95 (5): 2409–15.
7. Gregor MF, Hotamisligil GS. Inflammatory mechanisms in obesity. Annu Rev Immunol. 2011; (29): 415–45.
8. Kobayashi K, Takahashi N, Jimi E, Udagawa N, Takami M, Kotake S. et al. Tumor necrosis factor alpha stimulates osteoclast differentiation by a mechanism independent of the ODF/RANKL-

RANK interaction. J Exp Med. 2000; 191 (2): 275–86.
9. Lau DC, Dhillon B, Yan H, Szmitko PE, Verma S. Adipokines: molecular links between obesity and atheroslcerosis. Am J Physiol Heart Circ Physiol. 2005; 288 (5): 2031–41.
10. Зорина О. А., Рабинович И. М., Петрухина Н. Б., Кудрявцева Е. В. Сравнительные результаты антропометрии и биоимпедансного исследования у пациентов с хроническим генерализованным пародонтитом и метаболическим синдромом. Стоматология. 2016; 95 (2): 91–2.
11. Барер Г., Григорян С., Постнова Н. Роль интерферона и других цитокинов в возникновении и развитии заболеваний пародонта. Cathedra. 2006; 5 (3): 54–60.
12. Sagalovsky S, Schönert M. RANKL-RANK-OPG system and bone remodeling: a new approach on the treatment of osteoporosis. Clin Exptl Pathol. 2011; 2 (10): 146–153.

ANALYSIS OF DIVERGENCE BETWEEN THE AXES OF DENTAL IMPLANTS INSTALLED USING A CLASSIC FREEHAND TECHNIQUE

Ivaschenko AV, Yablokov AE ✉, Fedyaev IM, Tlustenko VP, Rotin NE, Tugushev VV

Samara State Medical University, Samara, Russia

Accuracy is a common challenge in dental implant placement. A successful clinical outcome is largely determined by accurate positioning of the implant at the prepared site and proper angulation. This study aimed to compare the divergence between the axes of the implants installed using a classic freehand technique. Cartesian coordinates of implant necks were determined on the CT images of 34 patients in the XOY (horizontal) plane, followed by the coordinates of implant apices. The obtained data were submitted to the original software developed by the authors (patent 2018661716) that automatically computed an angle between the insertion axes of the installed implants. We found that in 87% of cases, this angle was significantly greater (up to 27°) than recommended by implantation dentistry guidelines (7°). In 100% of the studied cases, the implants were not parallel; in sector 1, the deviation was 27° 4`.

Keywords: dental implantation, navigation system, freehand placement

Author contribution: Ivaschenko AV — study design, data acquisition, manuscript draft; Yablokov AE — data acquisition and analysis, manuscript draft; Fedyaev IM — study design, manuscript editing; Tlustenko VP — data analysis, manuscript editing; Rotin NE — study design, data acquisition; Tugushev VV — study design, manuscript editing.

Compliance with ethical standards: this study was conducted in compliance with the ethical standards for specialized medical care (Order 1525n of the Ministry of Healthcare of the Russian Federation, dated December 2012) and approved by the Ethics Committee of Samara State Medical University (Protocol 673/17 dated September 11, 2018). The patients gave written informed consent to participate.

✉ **Correspondence should be addressed:** Alexey E. Yablokov
Chapaevskaya 89, Samara, 443099; s1131149@yandex.ru

Received: 26.10.2018 **Accepted:** 04.04.2019 **Published online:** 15.04.2019

DOI: 10.24075/brsmu.2019.027

АНАЛИЗ УГЛОВЫХ ОТКЛОНЕНИЙ МЕЖДУ ОСЯМИ ДЕНТАЛЬНЫХ ИМПЛАНТАТОВ, УСТАНОВЛЕННЫХ ПО КЛАССИЧЕСКОЙ МЕТОДИКЕ

А. В. Иващенко, А. Е. Яблоков ✉, И. М. Федяев, В. П. Тлустенко, Н. Е. Ротин, В. В. Тугушев

Самарский государственный медицинский университет, Самара, Россия

Наиболее распространенной сложностью при постановке имплантатов является затрудненный выбор пространственного положения имплантатов. При интеграции имплантатов в полость рта две трети успеха операции зависят от того, насколько точно врач выберет позицию и угол наклона имплантата. Одной из важных проблем при установке имплантатов является их позиционирование в костном ложе. Целью работы было провести сравнительный анализ угловых отклонений дентальных имплантатов, установленных по классической методике, по «методу свободной руки» («free hand»). Использовали следующий алгоритм исследования. В декартовой системе координат на КТ-снимке в плоскости XOY (горизонтальная плоскость) определяли координаты шеек сравниваемых имплантатов у 34 исследуемых пациентов. Затем находили координаты апикальных частей всех исследуемых имплантатов. Полученные координаты помещали в разработанную нами программу ЭВМ № 2018661716 «Программа расчета угловых отклонений дентальных имплантатов», которая автоматически вычисляла угловое отклонение между осями установленных имплантатов. Расчет угловых отклонений между осями дентальных имплантатов у пациентов в послеоперационном периоде показал в 87% случаев значительное отклонение угла (до 27°) между осями имплантатов по сравнению с общепринятыми в дентальной имплантологии пределами (до 7°). В 100% изучаемых случаев не было отмечено параллельной установки дентальных имплантатов; анализ результатов дентальной имплантации в 1-м секторе выявил угловые отклонения в 27° 4`.

Ключевые слова: дентальная имплантация, навигационная платформа, метод свободной руки

Информация о вкладе авторов: А. В. Иващенко — написание статьи, разработка дизайна исследования, подбор клинического материала; А. Е. Яблоков — написание статьи, подбор клинического материала, анализ полученных данных; И. М. Федяев — разработка дизайна исследования, редактирование статьи; В. П. Тлустенко — редактирование, анализ полученных данных; Н. Е. Ротин — разработка дизайна исследования, подбор клинического материала; В. В. Тугушев — разработка дизайна исследования, редактирование.

Соблюдение этических стандартов: исследование проведено в соответствии с этическими стандартами оказания специализированной медицинской помощи (Приказ Министерства здравоохранения России от 24 декабря 2012 г. № 1525н) и одобрено этическим комитетом Самарского государственного медицинского университета (протокол № 673/17 от 11 сентября 2018 г.). Все пациенты подписали информированное согласие на участие в исследовании.

✉ **Для корреспонденции:** Алексей Евгеньевич Яблоков
ул. Чапаевская, д. 89, г. Самара, 443099; s1131149@yandex.ru

Статья получена: 26.10.2018 **Статья принята к печати:** 04.04.2019 **Опубликована онлайн:** 15.04.2019

DOI: 10.24075/vrgmu.2019.027

Accurate positioning and proper angulation of a dental implant determine successful treatment outcomes and contribute to the durability of an implant prosthesis. In Russia, the freehand approach has become a gold standard in implant dentistry [1]. The decision about implant positioning is guided by a surgeon's professional expertise. A misangled implant poses a serious problem for further treatment. According to the official guidelines, the maximum acceptable divergence between the implants is 7° [1]. A few researchers report that in some cases the freehand technique can result in a substantial divergence of up to 35° [2].

Angulation can be significantly improved by using surgical navigation systems that guide the placement of a dental implant [3, 4]. Such systems minimize angular deviation from an implant's axis, bringing it to the acceptable 7° [5–7]. However, these platforms are not widely applied in clinical routine because they are too costly and can be only used by specially trained surgeons [8–11]. In light of this, freehand surgery still remains

one of the most popular methods of implant placement that, unfortunately, can negatively affect treatment outcome if performed unskillfully [12–15].

Stability of dental implants can be evaluated by measuring osseointegration of the installed implant using such systems as Periotest or Osstell ISQ [16, 17].

The aim of this study was to compare divergence between the insertion axes of dental implants installed using a classic freehand technique.

METHODS

The study was carried out at the facilities of the Maxillofacial Surgery Unit of Samara State Medical University between 2015 and 2018. All patients underwent clinical examination. Their medical histories were also taken; complaints, unhealthy habits and comorbidities that could cause postoperative complications or be regarded as contraindications for dental implantation were noted down. The study included 32 partially edentulous patients of both sexes, aged 18 to 65 years, with no comorbidities. The majority of the participants (53.1%) were females aged 26 to 66 years (Table 1). Dental implantation was performed using a classic freehand technique. Postoperatively, the patients underwent a CT scan (Vatech Pax Duo scanner; Vatech; Korea).

RESULTS

A follow-up clinical examination was conducted in the postoperative period. The patients' complaints (including those of pain) and body temperature were taken; facial configuration, tissue condition at the site of surgery, implant excursion, sutures and gingiva formers were evaluated.

The MISS and DENTIUM dental implants (Israel) were installed following a conventional two-step protocol. The procedure was carried out by a dental surgeon specialized in implant dentistry. The number and size the installed implants are given in Table 2.

Ten patients were randomly selected for a CT scan (Vitech Pax Duo) in order to estimate the average divergence between the axes of the installed implants. The angles were calculated using the following algorithm (software patent 2018661716):

$$\alpha = arc\cos\frac{\left|(\vec{a},\vec{b})\right|}{\left|\vec{a}\right|\bullet\left|\vec{b}\right|} = arc\cos\frac{\left|a_x\bullet b_x + a_y\bullet b_y + a_z\bullet b_z\right|}{\sqrt{a_x^2+a_y^2+a_z^2},\bullet\sqrt{b_x^2+b_y^2+b_z^2},},$$

$$\vec{a} = (a_x, a_y, a_z) \text{ and } \vec{b} = (b_x, b_y, b_z),$$

$$\cos\alpha = \frac{\left|(\vec{a},\vec{b})\right|}{\left|\vec{a}\right|\bullet\left|\vec{b}\right|} = \frac{\left|a_x\bullet b_x + a_y\bullet b_y + a_z\bullet b_z\right|}{\sqrt{a_x^2+a_y^2+a_z^2},\bullet\sqrt{b_x^2+b_y^2+b_z^2}}.$$

A total of 22 implants were analyzed in 10 patients.

Briefly, Cartesian coordinates of necks of the compared implants were determined on the CT image in the XOY (horizontal) plane (Fig. 1A) followed by the coordinates of apices (Fig. 1B). The obtained data were fed to the software developed by the authors of this study (patent 2018661716 issued September 12, 2018); the software computed the angle between the axes of the installed implants.

Then, the data were structured and analyzed, and the dynamics of angular deviations were determined.

In 100% of the studied cases, the implants were not parallel. In sector 4, the implants were minimally divergent. On average, the angle between the insertion axes ranged from 2° 58' to 5° 4', falling into the accepted range of deviations. In sectors 2 and 3, the angles between the insertion axes of the installed implants varied from 3° 4' and 17° 96' (sector 3) and from 1° 83' to 17° 75' (sector 2), suggesting an unsatisfactory implantation result. In sector 1, the deviation reached 27° 4', which might have resulted from difficult anatomy. Summing up, the most significant divergence was observed in sector 1.

DISCUSSION

The divergence between the insertion axes of the installed dental implants was significant (27° 4') in 87% of cases, falling outside of the acceptable values (Fig. 2). In this study, the axis was defined as a geometric center of an implant shaped as a regular cylinder.

The most significant divergence was observed in the projection of sector 1, which is consistent with the findings of

Table 1. Demographic characteristics of the patients

Age \ Sex	18–25	26–44	45–65	Total	Number of patients, %
Males	1	3	4	8	25
Females	1	17	6	24	75
Total	2	20	10	32	100

Table 2. The number and size of the installed implants

Diameter \ Number	1 implant	2 implants	3 implants	Total	Number, %
3.3 • 10.0 («MISS»)	4	2	0	6	16.2
3.6 • 7.0 («Dentium»)	0	1	0	1	2.7
3.75 • 8.0 («MISS»)	6	2	0	8	21.6
3.75 • 10.0 («MISS»)	2	2	0	4	10.8
3.75 • 11.5 («MISS»)	5	1	0	6	16.2
4.0 • 10.0 («MISS»)	0	0	1	1	2.7
4.2 • 8.0 («MISS»)	4	1	0	5	13.5
4.2 • 10.0 («MISS»)	3	0	0	3	8.1
4.2 • 11.5 («MISS»)	3	0	0	3	8.1
Total	27	9	1	37	100.0

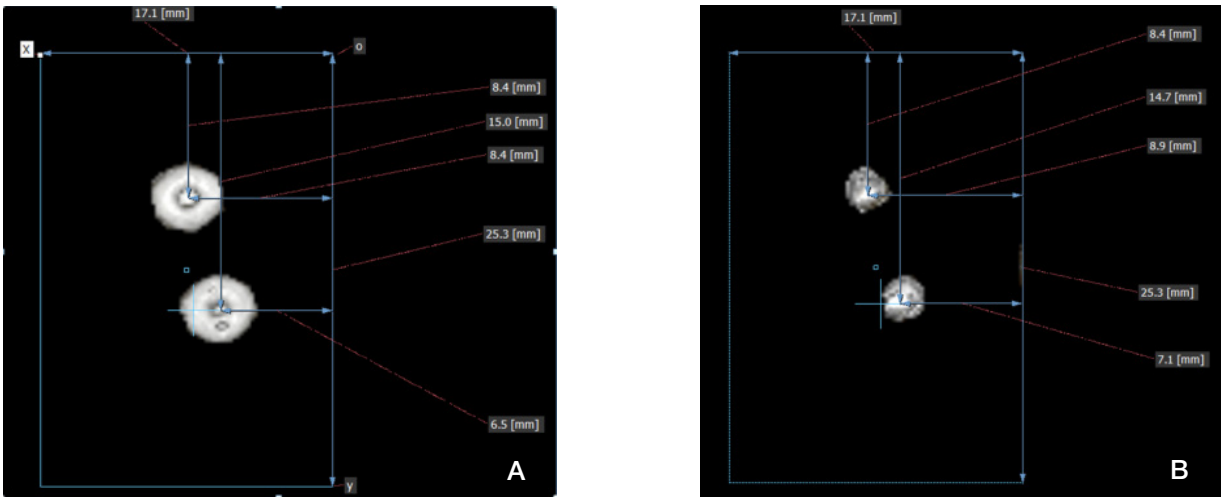

Fig. 1. A schematic representation of measurements performed by the original software developed by the authors. **A**. Neck coordinates of the implants. **B**. Apical coordinates of the implants

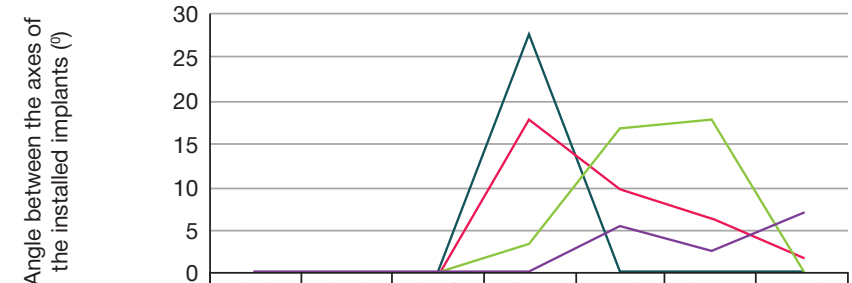

	1.–2	2.–3	3.–4	4.–5	5.–6	6.–7	7.–8
Sector 1	0	0	0	27,4	0	0	0
Sector 2	0	0	0	17.75	9.82	6.39	1.83
Sector 3	0	0	0	3.4	16.88	17.96	0
Sector 4	0	0	0	0	5.4	2.58	6.93

Fig. 2. Statistic values of divergence between the axes of the installed implants

other researchers [6, 12, 15]. The lowest statistically significant values were ± 0.5°. In the present study, the teeth were assigned to 4 sectors, according to the WHO classification: sector 1, teeth 1.1 to 1.8; sector 2, teeth 2.1 to 2.8; sector 3, teeth 3.1 до 3.8; sector 4, teeth 4.1 to 4.8.

Understanding the effects of divergence between the installed implants on treatment outcomes and the importance of accurate implant placement is critical for the health of the entire dentofacial system.

CONCLUSIONS

In this work we studied the angles between the axes of the implants installed during a freehand surgical procedure. The freehand approach should be further improved by using mechanical devices and semi- or fully automatic systems for guiding dental implant placement. We recommend our mathematical model as a tool for measuring divergence between the axes of dental implants.

References

1. Klinicheskie rekomendacii (protokoly lechenija) pri diagnoze polnoe otsutstvie zubov (polnaja vtorichnaja adentija, poterja zubov vsledstvie neschastnogo sluchaja, udalenija ili lokalizovannogo parodontita). Utverzhdeny postanovleniem # 15 soveta associacii obshhestvennyh ob"edinenij «Stomatologicheskaja associacija Rossii» ot 30 sentjabrja 2014 g. Dostupno po ssylke: www.e-stomatology.ru.
2. Potapov IV, Ivashhenko AV, Bajrikov AI, Monakov DV, Monakov VA. Obosnovanie ispol'zovanija navigacionnoj sistemy v dental'noj implantologii. Institut stomatologii. 2014; (4): 83–5.
3. Amhadova MA, Ignatov AYu. Dental'naja implantacija s primeneniem navigacionnogo implantologicheskogo shablona, izgotovlennogo po tehnologii CAD/CAM. Stomatologija. 2011; (2): 49–52.
4. Olesova VN, Kashenko PV, Bronshtejn DA, Magamedhanov MYu, Havkin VA. Komp'juternoe planirovanie vnutrikostnoj dental'noj implantacii. Stomatologija. 2011; (2): 43–8.
5. Fedyaev IM, Hamadeeva AM, Nikolskij VYu, Ganzha IR. Vtorichnaja adentija pri dental'noj implantacii (jepidemiologicheskoe i sociologicheskoe issledovanie s pomoshh'ju metoda telefonnogo interv'ju). Stomatologija. 2004; 83 (6): 65–8.
6. Nesterov AP, Lepilin AV, Nesterov AV, Ulyanova SP. Vzaimosvjaz' polozhenija implantatov v nizhnej cheljusti. Vestnik medicinskogo stomatologicheskogo instituta. 2016; 2 (37): 17–20.

7. Fazullin FZ, Galieva Yel, Rjabyh LA. Snizhenie riska razvitija oslozhnenij dental'noj implantacii. V sbornike: Materialy HHIV Mezhdunarodnogo simpoziuma «Innovacionnye tehnologii v stomatologii», posvjashhennogo 60-letiju stomatologicheskogo fakul'teta Omskogo gosudarstvennogo medicinskogo universiteta. Omsk: Izdatel'skij centr «KAN», 2017; 501–5.
8. Kan IV, Karerov MR, Samotesov PA, Shevchenko DP, Martynchuk DV. Vybor optimal'nogo diametra implantata pri neposredstvennoj stomatologicheskoj implantacii. Zhurnal anatomii i gistopatologii. 2018; 7 (1): 47–52.
9. Ushakov RV, Korkin VV, Ushakov AR, Lyahovich AA. Kompleksnaja reabilitacija pacientov s polnym otsutstviem zubov. Rossijskij medicinskij zhurnal. 2011; (1): 34–7.
10. Ahmadova AM, Mohov AV, Muzaeva ZR. Ozdemirov MI, Shalabaeva KZ. Sposob uvelichenija keratinizirovannoj desny v oblasti implantatov s ispol'zovaniem nebnogo soedinitel'notkannogo transplantata. Medicinskij alfavit. 2015; 3 (13): 28–30.
11. Saakjan ShH, Kalamkarov AYe. Struktura izmenenij v al'veoljarnoj kosti pri ortopedicheskom lechenii pacientov s defektami zubnyh rjadov s ispol'zovaniem. Vestnik stomatologii i vnutrikostnyh implantatov. Rossijskij stomatologicheskij zhurnal. 2014; (2): 13–16.
12. Matveeva AI, Frolov VA, Gvetadze RSh, AG. Borisov Vlijanie implantata parametrov na naprjazhenno-deformirovannoe sostojanie kostnoj tkani zony implantacii. Stomatologija. 2010; (1): 54–5.
13. Chuyko AN i dr. Terminy: fiksacija i stabilizacija s pozicii biohimicheskogo analiza. Molodoy uchenyy. 2013; (9): 98–108.
14. Konchakovskiy AV, Konchakovskiy AA. Odnomomentnaja implantacija v lunku udalennogo zuba i neposredstvennoe predvaritel'noe implantacionnoe protezirovanie akrilovymi konstrukcijami. Sovremennaja nauka: aktual'nye problemy teorii i praktiki. Serija: Estestvennye i tehnicheskie nauki. 2018; (7): 199–204.
15. Bayrikov IM, Ivashhenko AV, Layva OV, Kondrashin DV, Fedyaev IM, Nesterov AM. Klinicheskie vozmozhnosti navigacionnoj sistemy pri ustanovke dental'nyh implantatov. V sbornike: Aktual'nye voprosy stomatologii. Sbornik nauchnyh trudov, posvjashhennyj 50-letiju stomatologicheskogo obrazovanija v SamGMU. 2016; 124–134.
16. Sarmento HR, Dantas RVF, Pereira-Cenci T, Faot F. Elements of implant-supported rehabilitation planning in patients with bruxism. Journal of Craniofacial Surgery. 2012; 23 (6): 1905–9.
17. Eroshin VA, Dzhalalova MV, Arutjunov SD, Stepanov AG, Bagdasarjan GG. Podvizhnost' i kriterii gotovnosti dental'nyh implantatov k funkcional'nym nagruzkam. Sovremennye problemy nauki i obrazovanija. 2018; (2): 53.

Литература

1. Клинические рекомендации (протоколы лечения) при диагнозе полное отсутствие зубов (полная вторичная адентия, потеря зубов вследствие несчастного случая, удаления или локализованного пародонтита). Утверждены постановлением № 15 совета ассоциации общественных объединений «Стоматологическая ассоциация России» от 30 сентября 2014 г. Доступно по ссылке: www.e-stomatology.ru.
2. Потапов И. В., Иващенко А. В., Байриков А. И., Монаков Д. В., Монаков В. А. Обоснование использования навигационной системы в дентальной имплантологии. Институт стоматологии. 2014; (4): 83–5.
3. Амхадова М. А., Игнатов А. Ю. Дентальная имплантация с применением навигационного имплантологического шаблона, изготовленного по технологии CAD/CAM. Стоматология. 2011; (2): 49–52.
4. Олесова В. Н., Кашенко П. В., Бронштейн Д. А., Магамедханов М. Ю., Хавкин В. А. Компьютерное планирование внутрикостной дентальной имплантации. Стоматология. 2011; (2): 43–8.
5. Федяев И. М., Хамадеева А. М., Никольский В. Ю., Ганжа И. Р. Вторичная адентия при дентальной имплантации (эпидемиологическое и социологическое исследование с помощью метода телефонного интервью). Стоматология. 2004; 83 (6): 65–8.
6. Нестеров А. П., Лепилин А. В., Нестеров А. В., Ульянова С. П. Взаимосвязь положения имплантатов в нижней челюсти. Вестник медицинского стоматологического института. 2016; 2 (37): 17–20.
7. Фазуллин Ф. З., Галиева Э. И., Рябых Л. А. Снижение риска развития осложнений дентальной имплантации. В сборнике: Материалы XXIV Международного симпозиума «Инновационные технологии в стоматологии», посвященного 60-летию стоматологического факультета Омского государственного медицинского университета. Омск: Издательский центр «КАН», 2017; 501–5.
8. Кан И. В., Кареров М. Р., Самотесов П. А., Шевченко Д. П., Мартынчук Д. В. Выбор оптимального диаметра имплантата при непосредственной стоматологической имплантации. Журнал анатомии и гистопатологии. 2018; 7 (1): 47–52.
9. Ушаков Р. В., Коркин В. В., Ушаков А. Р., Ляхович А. А. Комплексная реабилитация пациентов с полным отсутствием зубов. Российский медицинский журнал. 2011; (1): 34–7.
10. Ахмадова А. М., Мохов А. В., Музаева З. Р. Оздемиров М. И., Шалабаева К. З. Способ увеличения кератинизированной десны в области имплантатов с использованием небного соединительнотканного трансплантата. Медицинский алфавит. 2015; 3 (13): 28–30.
11. Саакян Ш. Х., Каламкаров А. Э. Структура изменений в альвеолярной кости при ортопедическом лечении пациентов с дефектами зубных рядов с использованием. Вестник стоматологии и внутрикостных имплантатов. Российский стоматологический журнал. 2014; (2): 13–16.
12. Матвеева А. И., Фролов В. А., Гветадзе Р. Ш., Борисов А. Г. Влияние имплантата параметров на напряженно-деформированное состояние костной ткани зоны имплантации. Стоматология. 2010; (1): 54–5.
13. Чуйко А. Н. и др. Термины: фиксация и стабилизация с позиции биохимического анализа. Молодой ученый. 2013; (9): 98–108.
14. Кончаковский А. В., Кончаковский А. А. Одномоментная имплантация в лунку удаленного зуба и непосредственное предварительное имплантационное протезирование акриловыми конструкциями. Современная наука: актуальные проблемы теории и практики. Серия: Естественные и технические науки. 2018; (7): 199–204.
15. Байриков И. М., Иващенко А. В., Лайва О. В., Кондрашин Д. В., Федяев И. М., Нестеров А. М. Клинические возможности навигационной системы при установке дентальных имплантатов. В сборнике: Актуальные вопросы стоматологии. Сборник научных трудов, посвященный 50-летию стоматологического образования в СамГМУ. 2016; 124–134.
16. Sarmento HR, Dantas RVF, Pereira-Cenci T, Faot F. Elements of implant-supported rehabilitation planning in patients with bruxism. Journal of Craniofacial Surgery. 2012; 23 (6): 1905–9.
17. Ерошин В. А., Джалалова М. В., Арутюнов С. Д., Степанов А. Г., Багдасарян Г. Г. Подвижность и критерии готовности дентальных имплантатов к функциональным нагрузкам. Современные проблемы науки и образования. 2018; (2): 53.

EFFECT OF VARIOUS TYPES OF REMOVABLE APPLIANCES AND DENTAL IMPLANTS ON THE ORAL MICROBIOCENOSIS DURING ORTHOPEDIC TREATMENT

Tlustenko VP, Bairikov IM, Trunin DA, Komlev SS ✉, Zhestkov AV, Lyamin AV

Samara State Medical University, Samara, Russia

The problem of complications arising after dental implantation is still relevant. The aim of the work was to investigate the effect of various types of removable appliances and dental implants on the oral microbiocenosis during orthopedic treatment of 64 people: 12 patients of the first index group, 40 patients of the second index group and 12 people of the control group. 6 months after the implants were installed, as a result of a microbiological study of the oral cavity, the differences were found in the qualitative composition of the microflora of the mucous membrane around the neck of the dental implant. In the first index group representatives of normal microflora prevailed. In 100% of cases *Streptococcus vestibularis* was isolated, from more than half patients *S. oralis*, *S. mitis*, *Rothia mucilaginosa* were isolated, *S. gordonii* was isolated from one patient. In the second index group, a significant diversity of microbial species was observed, including enterobacteria, which were isolated from 22.5% of the examined patients. In the control group, in addition to representatives of the normal microflora of the oral mucosa *S. vestibularis* (75.5%), *S. oralis* (50.0%), *Neisseria subflava* (66.7%) and *Haemophylus parainfluenzae* (50.0%) were found. From all patients of the control groups *S. gordonii* was isolated, as well as the other potentially pathogenic streptococci species, *S. anginosus* and *S. constellatus* by 66.7%. The type of removable appliances and dental implants used affects the microflora composition of the oral cavity, and, consequently, the further prognosis and the risk of complications. Collapsible dental implant supported removable prosthetic appliances with a metal frame and fixing elements, telescopic crowns and clasps less than other types of prosthetic appliances change the qualitative composition of the microflora of the oral mucosa around the neck of the dental implant.

Keywords: microbiocenosis, implantation, collapsible dental implant, removable prosthetic appliances

Author contribution: Tlustenko VP, Bairikov IM, Trunin DA, Komlev SS — concept and research design, surgical and orthopedic treatment of patients; Bairikov IM, Komlev SS, Zhestkov AV, Lyamin AV — collection and processing of material, microbiological investigation of clinical material, statistical processing of results.

Compliance with ethical standards: the study was approved by the Ethics Committee of Samara State Medical University (protocol № 2018/197). All patients signed a voluntary informed consent for the dental implantation operation, orthopedic treatment and participation in the study.

✉ **Correspondence should be addressed:** Sergey S. Komlev
Chapayevskaya 89, Samara, 443099; stomat.ks@mail.ru

Received: 27.01.2019 **Accepted:** 08.04.2019 **Published online:** 18.04.2019

DOI: 10.24075/brsmu.2019.029

ВЛИЯНИЕ РАЗЛИЧНЫХ ВИДОВ СЪЕМНЫХ КОНСТРУКЦИЙ И ДЕНТАЛЬНЫХ ИМПЛАНТАТОВ НА МИКРОБИОЦЕНОЗ ПОЛОСТИ РТА ПРИ ОРТОПЕДИЧЕСКОМ ЛЕЧЕНИИ

В. П. Тлустенко, И. М. Байриков, Д. А. Трунин, С. С. Комлев ✉, А. В. Жестков, А. В. Лямин

Самарский государственный медицинский университет, Самара, Россия

Проблема осложнений, возникающих после проведения дентальной имплантации, остается актуальной. Целью работы было исследовать влияние различных видов съемных конструкций и дентальных имплантатов на микробиоценоз полости рта при ортопедическом лечении 64 человек: 12 пациентов 1-й основной группы, 40 пациентов 2-й основной группы и 12 человек группы контроля. Через 6 месяцев после установки имплантатов в результате микробиологического исследования полости рта были выявлены различия в качественном составе микрофлоры слизистой оболочки вокруг шейки дентального имплантата. В основной группе 1 преобладали представители нормальной микрофлоры. В 100% случаев выделен *Streptococcus vestibularis*, более чем у половины пациентов выделены *S. oralis*, *S. mitis*, *Rothia mucilaginosa*, *S. gordonii* выделен у одного пациента. В основной группе 2 отмечено значительное разнообразие видов микроорганизмов, включая энтеробактерии, которые были выделены у 22,5% обследованных. В контрольной группе помимо представителей нормальной микрофлоры слизистой оболочки полости рта обнаружены *S. vestibularis* (75,5%), *S. oralis* (50,0%), *Neisseria subflava* (66,7%) и *Haemophylus parainfluenzae* (50,0%). У всех пациентов контрольной группы были выделены *S. gordonii*, а также другие виды потенциально патогенных стрептококков — *S. anginosus* и *S. constellatus* по 66,7%. Вид используемых съемных конструкций и дентальных имплантатов влияет на состав микрофлоры полости рта, а, следовательно, на дальнейший прогноз и риск развития осложнений. Съемные ортопедические конструкции с металлическим каркасом и фиксирующими элементами, телескопическими коронками и замковыми креплениями с опорой на разборные дентальные имплантаты менее других видов конструкций изменяют качественный состав микрофлоры слизистой оболочки полости рта вокруг шейки дентального имплантата.

Ключевые слова: микробиоценоз, дентальная имплантация, разборный дентальный имплантат, съемные ортопедические конструкции

Информация о вкладе авторов: В. П. Тлустенко, И. М. Байриков, Д. А. Трунин, С. С. Комлев — разработка концепции и дизайна исследования, хирургическое и ортопедическое лечение пациентов; И. М. Байриков, С. С. Комлев, А. В. Жестков, А. В. Лямин — сбор и обработка материала, микробиологическое исследование клинического материала, статистическая обработка.

Соблюдение этических стандартов: исследование одобрено этическим комитетом Самарского государственного медицинского университета (протокол № 2018/197). Все пациенты подписали информированное согласие на проведение операции дентальной имплантации и ортопедическое лечение и участие в исследовании.

✉ **Для корреспонденции:** Сергей Сергеевич Комлев
ул. Чапаевская, д. 89, г. Самара, 443099; stomat.ks@mail.ru

Статья получена: 27.01.2019 **Статья принята к печати:** 08.04.2019 **Опубликована онлайн:** 18.04.2019

DOI: 10.24075/vrgmu.2019.029

Despite significant achievements in solving technical issues, the problem of complications after the dental implants installation is still relevant in modern dental implantology [1]. The most common are mucositis and periimplantitis, in the development of which microorganisms take an active part, both normally presented in the oral cavity and colonizing surfaces of materials of which dental implants and removable appliances are constructed [2–5].

In literature, the ability of microorganisms to adhere to the surface of dental implant abutments and removable prosthetic

appliances is described. As test microorganisms, bacteria are most often evaluated, which are not fundamental in terms of the development of pathological processes associated with the use of dental implants [6–8].

Additional difficulties in evaluating oral microbiota when using removable prosthetic appliances and dental implants arise from the imperfection of the applied laboratory diagnostics methods and improperly constructed research design. Researchers are most commonly limited to a general assessment of anaerobic and/or aerobic microflora without regard to its species diversity; to using nothing but methods based on the detection of DNA of microorganisms, representatives of pathogenic complexes; in some cases, methods which are obviously unacceptable for purposes of assessment of oral cavity microflora are used, for example, test systems developed to evaluate microflora of other loci of the human body [9–11].

This approach can lead to contradictory results when assessing the qualitative and quantitative composition of oral microflora, and also make it difficult to evaluate the role of microflora representatives in the development of complications associated with the dental implants installation; qualitative and quantitative composition of microflora when comparing the influence of similar prosthetic appliances constructed of various materials. Moreover, pathogenicity factors and complex architectonics of the interaction of various types of microorganisms during the colonization of the surfaces of dental implants and removable prosthetic appliances by normal, pathogenic and transient microflora are not taken into account.

The aim of the work was to investigate the effect of various types of dental implants on the oral cavity microbiocenosis.

METHODS

Microbiological investigation was performed in 64 patients with various types of dental implants (22 men and 42 women aged 45–65): 12 patients of the first index group, 40 patients of the second index group, the control group was formed of 12 people. Criteria for inclusion in the study: presence of unilateral and bilateral free-end edentulous spaces. Exclusion criteria: presence of diseases of the circulatory system; presence of cancer.

The collection and transportation of biological material was carried out in accordance with the requirements of the 4.2.2039-05 «Method of collecting and transporting of biomaterials in microbiological laboratories» guidelines. Samples of material for microbiological investigation were collected from the mucous membrane of the oral cavity around the neck of a dental implant with sterile cotton swabs, which were placed into transport media for aerobic and anaerobic microorganisms immediately after collection. The material was transported to the laboratory in 2 hours under isothermal conditions at 22–24 °C.

In the laboratory, the material was inoculated on the solid media: blood agar, HiCrome universal differentiation medium (HiMedia; India), agar for anaerobic microorganisms (HiMedia; India), selective media for isolation of staphylococci — mannitol salt agar (HiMedia; India), for isolation of fungi — Sabouraud agar (HiMedia; India), for enterobacteria — Endo agar (HiMedia; India), for non-fermenting gram-negative bacteria — cetrimide agar (HiMedia; India). Cultivation was performed under aerobic and anaerobic conditions using the anaerobic culture jars and the BD GasPak™ EZ Container Systems commercial gas generating pouches (BD; USA) for 48–72 hours at 35–37 °C.

The microorganisms isolated were identified using MALDI-ToF mass-spectrometry with the Microflex LT unit (MALDI Biotyper 3.1, Bruker Daltonik GmbH; Germany).

The material was collected 6 months after the orthopedic treatment of patients. The qualitative composition of the isolated microflora was assessed taking into account the grouping of microorganisms depending on their potential pathogenetic effects on the oral mucosa and bone tissue.

In total, 328 strains of microorganisms of 26 genera were isolated and identified.

Evaluation of the microflora composition of the oral mucosa around the neck of the dental implant was performed in 64 patients. Depending on the design of the dental implant and the removable prosthetic appliance, all patients who underwent a microbiological study were divided into three groups.

1. The 1st subgroup of the index group (index group 1) included 12 patients for whom the collapsible dental implants supported removable prosthetic appliances with a metal frame and fixing elements, using telescopic crowns and clasps were constructed (patent of Russian Federation № 2593349). After the operation of implantation and irreversible bone resorption with the proposed implant design, it became possible to detach the intermediate part from the osseointegrated apical part and use the apical part to fix the abutment, the removable prosthetic appliance.

2. The 2nd subgroup of the index group (index group 2) included 40 patients, for whom the commercial dental implants supported removable prosthetic appliances were constructed, the fixing clasps were located in the metal frame of the removable prosthesis.

3. The control group included 12 patients, for whom the commercial dental implants supported removable prosthetic appliances of acrylic plastics were constructed, the fixing elements were located in the basis of a removable prosthetic appliance.

RESULTS

All microorganisms colonizing the mucous membranes of the oral cavity may have a certain pathogenic potential, but in some of them it is more pronounced, in others it seldom occurs. Thus, we conditionally divided the isolated microorganisms into representatives of the normal biota of the oral mucosa (*Streptococcus salivarius, Streptococcus vestibularis, Streptococcus parasanguinis, Streptococcus oralis, Streptococcus sanguinis, Streptococcus mitis, Rothia dentocariosa, Rothia mucilaginosa, Neisseria macacae, Neisseria subflava, Neisseria flavescens, Haemophilus parainfluenzae, Lactobacillus salivarius, Gemella haemolysans*), microflora that participates in pathogenic processes at various levels (*Streptococcus anginosus*, *Streptococcus gordonii*, *Streptococcus constellatus*), microflora, less characteristic for the oral mucosa, but usually not involved in pathological processes (*Acinetobacter junii*, *Staphylococcus capitis*, *Staphylococcus epidermidis*, *Staphylococcus warnerii*, *Streptococcus pneumoniae*), microflora with high pathogenic potential that is not typical for the oral cavity (*Enterobacter cloacae*, *Citrobacter freundii*, *Escherichia coli*). A separate group consisted of the *Candida* genus fungi.

During the qualitative composition analysis of the microflora of the oral mucosa around the dental implant in patients of the studied groups the data were obtained presented in the following table.

The analysis of the obtained data revealed the following features of the qualitative composition of microorganisms in the microbiocenosis structure of the oral mucosa around the dental implant neck.

A distinctive feature of the microflora of the 1st index group patients was the predominance of normal flora in a

significant part of the patients examined. In 100% of cases *Streptococcus vestibularis* was isolated, from more than half patients *Streptococcus oralis*, *Streptococcus mitis*, *Rothia mucilaginosa* were isolated. *Enterobacteria* and *Candida* fungi were not isolated in this group of patients. However, a rather frequent isolation of saprophytic microflora, uncharacteristic for the oral mucosa, should be noted, which was found in half of the patients.

The 2nd index group was characterized by a significant variety of microorganisms. In patients, the dominant group of microorganisms had not been revealed. Nevertheless, the microflora was more often represented by normal microorganisms characteristic for the oral mucosa, among which *Streptococcus vestibularis* prevailed. From one-third of the patients potentially pathogenic microorganisms were isolated. But, in our opinion, the fact that from 9 patients enterobacteria, which are uncharacteristic for this locus and possess significant pathogenic potential, were isolated, had the greatest value in this group, both for production of proteolytic enzymes, and for direct participation in the development of infectious complications of various localization.

Streptococcus vestibularis and *Streptococcus oralis*, as well as *Neisseria subflava* and *Haemophilus parainfluenzae* as representatives of the normal oral microflora prevailed in the control group. The other representatives of the normal flora were isolated from less than 50% of the examined patients in the control group. A distinctive feature of the microflora in patients of the control group was the wide distribution of microorganisms that play an important role as triggers in the pathogenic microflora colonization. *Streptococcus gordonii* was isolated from all patients of the control group, having an increased adhesive ability, which is realized by microorganisms with pronounced pathogenic potential. Besides, *Streptococcus anginosus* and *Streptococcus constellatus* were isolated from more than a half of the control group patients. Only in the control group the *Candida* genus fungi were isolated, represented by the one single *Candida albicans* species (it was isolated from one third of the patients).

Thus, in patients of the 1st index group, the implantological treatment carried out using collapsible dental implants and the orthopedic treatment demonstrate the smallest change in the qualitative composition of the microflora of the oral mucosa around the neck of the dental implant. It should be noted that no representatives of the "red" paradontopathogenic complex were isolated from patients of all groups.

In addition to the qualitative composition, the frequency of isolation of microorganisms by groups and genera was analyzed taking into account their potential participation in the pathological process. Due to the significant influence of certain types of streptococci on pathogenic processes, it was decided to divide them into two groups: "having potential pathogenic significance" and "normal flora representatives".

Data on the frequency of isolation of representatives of different groups of microorganisms from patients are presented in Fig 1.

The following microflora features were identified. In the 1st index group, when analyzing the frequency of isolation of various groups of microorganisms representatives, the significant

Table. Qualitative composition of the microflora of the mucous membrane around the dental implant (number of strains in absolute numbers and proportion of strains of the total number of microorganisms isolated from the group)

Microorganism species	Control group	Index group 1	Index group 2
Streptococcus salivarius	2 (16.7%)	2 (16.7%)	12 (30.0%)
Streptococcus vestibularis	9 (75.0%)	12 (100%)	24 (60.0%)
Streptococcus parasanguinis	0	2 (16.7%)	8 (20.0%)
Streptococcus oralis	6 (50.0%)	10 (83.3%)	12 (30.0%)
Streptococcus sanguinis	3 (25.0%)	0	15 (37.5%)
Streptococcus mitis	4 (33.3%)	6 (50.0%)	12 (30.0%)
Streptococcus anginosus	8 (66.7%)	0	0
Streptococcus gordonii	12 (100%)	1 (8.3%)	9 (22.5%)
Streptococcus constellatus	8 (66.7%)	0	0
Streptococcus pneumoniae	3 (25.0%)	4 (33.3%)	4 (10.0%)
Rothia dentocariosa	3 (25.0%)	2 (16.7%)	3 (7.5%)
Rothia mucilaginosa	0	8 (66.7%)	18 (45.0%)
Neisseria macacae	3 (25.0%)	0	3 (7.5%)
Neisseria subflava	8 (66.7%)	2 (16.7%)	18 (45.0%)
Neisseria flavescens	0	2 (16.7%)	4 (10.0%)
Haemophilus parainfluenzae	6 (50.0%)	1 (8.3%)	8 (20.0%)
Lactobacillus salivarius	2 (16.7%)	4 (33.3%)	3 (7.5%)
Gemella haemolysans	0	2 (16.7%)	4 (10.0%)
Acinetobacter junii	0	1 (8.3%)	0
Staphylococcus capitis	0	2 (16.7%)	0
Staphylococcus epidermidis	4 (33.3%)	2 (16.7%)	8 (20.0%)
Staphylococcus warnerii	3 (25.0%)	2 (16.7%)	0
Enterobacter cloacae	0	0	6 (15.0%)
Citrobacter freundii	0	0	2 (5.0%)
Escherichia coli	0	0	1 (2.5%)
Candida albicans	4 (33.3%)	0	0

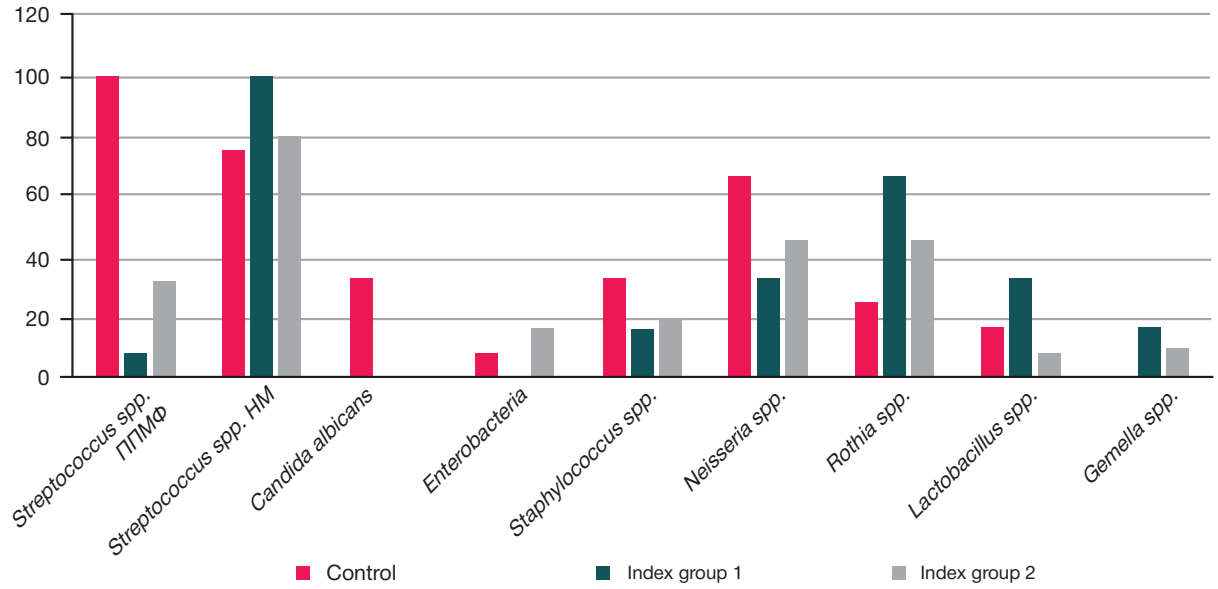

Fig. 1. Frequency of isolation of microorganisms from patients of different groups (%). ППМФ — potentially pathogenic microflora, НМ — normal microflora

predominance of normal microflora was observed, represented by streptococci, lactobacteria, representatives of the *Rothia*, *Gemella* genera. Opportunistic pathogenic Neisseria were less common than in the control group, and staphylococci were also less common.

In the 2nd index group, streptococci — representatives of normal microflora, Neisseria, as well as bacteria of the *Rothia* genus were the leaders by their incidence rate. However, it should be noted that this was the only group of patients from which enterobacteria were isolated.

In the control group, potentially pathogenic streptococci were found in 100% of the patients, which, of course, may have a negative effect in relation to the risk of complications in the early period after the implant is installed. Streptococci — representatives of normal flora were isolated from more than 70% of patients. There was a decrease in the frequency of isolation of other normal microflora representatives, which were detected in less than 50% of the examined patients from the control group, with the exception of the *Neisseria* genus representatives. As described above, *Candida* fungi were isolated from one-third of the patients.

DISCUSSION

When analyzing the incidence degree of representatives of various microorganisms groups on the mucous membrane of the oral cavity around the neck of a dental implant, certain patterns were identified. In the control group, potentially pathogenic microorganisms prevailed characterized by increased adhesive activity, as well as the *Candida* genus fungi, which may be due to the specific location of the fixing elements in the basis of acrylic prostheses supported by cobalt-chrome abutments of commercial dental implants. The absence of complications in patients included in the study is due to the fact that, along with the potentially aggressive microflora, the normal microflora representatives were also rather common in the control group. In the index group 1, the optimal microbiological relationships were identified, both in terms of the qualitative composition of microflora and of the inoculation frequency of oral mucosa normal microbiota inhabitants. In this group, there was the lowest isolation frequency of potentially pathogenic streptococci, there was no candida and enterobacteria inoculation. The index group 2 was characterized by the maximum variety of both qualitative composition and isolation frequency of various microorganisms groups. Together with normal microflora, the potentially pathogenic streptococci as well as enterobacteria were identified, which, in our opinion, is the greatest threat in relation to the post-implantation complications formation [4, 7, 9–11].

It should be noted that almost all microorganisms having pathogenic potential were isolated under strict anaerobic conditions, which may be an indirect indicator of their active participation in the process of adaptation to the altered conditions on the mucous membranes around the neck of the dental implant. Significant changes in the qualitative composition of microflora and in the isolation frequency of various groups of microorganisms among patients in the control and index groups demonstrate the need for careful selection of the design of a dental implant, of an abutment, of a removable prosthetic appliance. In this case the main goals are minimization of the negative impact of a “foreign” object (dental implant) on intermicrobial interactions that can lead to the predominance of potentially pathogenic microorganisms with pronounced adhesive properties in the microbiocenosis, as well as the elimination of mucus membranes colonization with transient microflora with a high pathogenic potential, which can act as a trigger of the mucositis and peri-implantitis development. The negative impact of implants was confirmed by data obtained during the study: the predominance of microorganisms with high adhesive potential among the control group patients; a wide variety of transient microflora and enterobacteria in the index group 2.

The oral cavity microflora is a complex association of microorganisms, the qualitative and quantitative composition of which is influenced by various external and internal factors. Prosthetics using dental implants supported removable prosthetic appliances inevitably affects the mucous membranes microbiota. These changes can be conditionally “neutral” in relation to the prevailing groups of microorganisms, or they can lead to significant changes in the microflora composition, when representatives of normal microbiota are displaced by transient microorganisms, the number of which increases significantly on the mucous membranes of the oral cavity due to the use of removable prosthetic appliances.

It should be noted that the material of which dental implant abutments, fixing mechanisms and removable prosthetic appliances are constructed can influence the redistribution of

the prevailing groups of microorganisms, increasing the number of bacteria and fungi with enhanced adhesive properties in the population of microorganisms on the surface of the dental implant abutment and on the oral mucosa, which is in direct contact with them. Such changes may remain subcompensated for a long time due to the adaptation mechanisms of bacterial survival in biofilms, but sooner or later they will lead to the accumulation of pathogenic potential of microorganisms, changes in the qualitative composition of microflora, colonizing the dental implant neck and the oral mucosa around it. Involvement in the process of initially potentially pathogenic streptococci, which include *Streptococcus gordoni* and a number of other microorganisms isolated from patients of the control group, will inevitably lead to an increase in the adhesive ability of other microorganisms, in particular, having proven pathogenic action, which is confirmed by the data described in the scientific literature [4, 7, 9]. Involvement in the process of colonization and change of the dominant microbial population of enterobacteria, staphylococci, fungi can be considered a serious risk factor for the development of post-implantation complications.

CONCLUSIONS

Implantologic and orthopedic types of treatment performed for patients of the 1st index group using collapsible dental implants supported removable prosthetic appliances with metal frame and fixing elements, telescopic crowns and clasps (patent of Russian Federation № 2593349) less changed the qualitative composition of the microflora of the oral mucosa around the dental implant neck compared to other methods of orthopedic treatment. In this group of patients, microflora was detected in a small amount, participating in the adhesion of paradontopathogenic microorganisms to oral mucosa, reducing the risk of periimplantitis.

The data obtained in the study indicate the influence of the type of prosthetic appliances and dental implants on the oral cavity microbiocenosis. Further research in this field will minimize the negative impact of orthopedic treatment on the qualitative composition of oral microflora, reduce the risk of complications, of the development of mucositis and periimplantitis.

References

1. Gvetadze RSh, Uzunjan NA, Lebedenko Iyu, et al. Osseointegration of superelastic alloys of titanium and niobium. In the collection: Actual issues of dentistry Collection of scientific papers dedicated to the founder of the Department of Prosthetic Dentistry KSMU Professor Isaak M. Oksman, Kazan. 2018; 89–93.
2. Tlustenko VP, Tlustenko VS, Golovina ES, Koshelev VA. Effect of chronic localized periodontitis and dental periimplantitis on oral homeostasis. Journal of Scientific Articles Health and Education in the XXI Century. 2017; 19 (11): 102–6.
3. Utjuzh AS, Jumashev AV, Mihajlova MP. Prosthetic appliances made of titanium alloys with intolerance to traditional dentures. Doctor. 2016; (7): 62–64.
4. Gorobec SM, Romanenko IG, Dzherelej AA, et al. Risk factors for the development of inflammatory complications after the implantation. Tavrichesky Medical-Biological Journal. 2017; 20 (2): 208–14.
5. Alkan EA, Tüter G, Parlar A, et al. Evaluation of peri-implant crevicular fluid prostaglandin levels in augmented extraction sockets by different biomaterials. Acta Odontol. Scand. 2016; 74 (7): 532–8.
6. Salivonchik MS, Kalivradzhiyan ES, Ryzhova IP. Results of microscopy of basic polymers. Modern prosthetic dentistry. 2014; (22): 66–7.
7. Ryzhova IP, Prisnyj AA, Shinkarenko NN, Salivonchik MS. The state of the oral microflora under the influence of removable dentures. Intern journals applied and basic research. 2014; (2): 151–3.
8. Riega-Torres JC, Villarreal-Gonzalez AJ, Ceceñas-Falcon LÁ, Salas-Alanis JC. Sjögren's syndrome (SS), a review of the subject and saliva as a diagnostic method. Gac Med Mex. 2016; 152 (3): 371–80.
9. Habilov NL, Akbarov AN, Salimov OR, et al. Influence of removable laminar prostheses on the oral microbiocenosis. Medicus. 2016; 6 (12): 82–5.
10. Zekij AO, Zekij OE. Pathogenic microflora and the state of peri-implantable tissues in patients with fixed prosthetic appliances with support on intraosseous implants using a silicone sealing matrix. Institute of Dentistry. 2018; (1): 37–9.
11. Shishkova YuS, Babikova MS, Orner Iyu, et al. Features of the microbial spectrum of the oral fluid of persons using dental prosthetic appliances. Medical science and education of the Urals. 2017; 1 (89): 32–6.

Литература

1. Гветадзе Р. Ш., Узунян Н. А., Лебеденко И. Ю. и др. Остеоинтеграция сверхупругих сплавов титана и ниобия. В сборнике: Актуальные вопросы стоматологии. Сборник научных трудов, посвященный основателю кафедры ортопедической стоматологии КГМУ профессору Исааку Михайловичу Оксману, Казань. 2018; 89–93.
2. Тлустенко В. П., Тлустенко В. С., Головина Е. С., Кошелев В. А. Влияние хронического локализованного пародонтита и дентального периимплантита на гомеостаз полости рта. Здоровье и образование в XXI веке. 2017; 19 (11): 102–6.
3. Утюж А. С., Юмашев А. В., Михайлова М. П. Ортопедические конструкции из сплавов титана при непереносимости традиционных зубных протезов. Врач. 2016; (7): 62–4.
4. Горобец С. М., Романенко И. Г., Джерелей А. А. и др. Факторы риска развития воспалительных осложнений дентальной имплантации. Таврический медико-биологический вестник. 2017; 20 (2): 208–14.
5. Alkan EA, Tüter G, Parlar A, et al. Evaluation of peri-implant crevicular fluid prostaglandin levels in augmented extraction sockets by different biomaterials. Acta Odontol. Scand. 2016; 74 (7): 532–8.
6. Саливончик М. С., Каливраджиян Э. С., Рыжова И. П. Результаты микроскопии базисных полимеров. Современная ортопедическая стоматология. 2014; (22): 66–7.
7. Рыжова И. П., Присный А. А., Шинкаренко Н. Н., Саливончик М. С. Состояние микрофлоры полости рта под влиянием съемных конструкций зубных протезов. Международный журнал прикладных и фундаментальных исследований. 2014; (2): 151–3.
8. Riega-Torres JC, Villarreal-Gonzalez AJ, Ceceñas-Falcon LÁ, Salas-Alanis JC. Sjögren's syndrome (SS), a review of the subject and saliva as a diagnostic method. Gac Med Mex. 2016; 152 (3): 371–80.
9. Хабилов Н. Л., Акбаров А. Н., Салимов О. Р. и др. Влияние съемных пластиночных протезов на микробиоценоз полости рта. Medicus. 2016; 6 (12): 82–5.
10. Зекий А. О., Зекий О. Е. Патогенная микрофлора и состояние периимплатационных тканей у пациентов с несъемными ортопедическими конструкциями с опорой на внутрикостные имплантаты при использовании герметизирующей силиконовой матрицы. Институт стоматологии. 2018; (1): 37–9.
11. Шишкова Ю. С., Бабикова М. С., Орнер И. Ю. и др. Особенности микробного спектра ротовой жидкости лиц, использующих стоматологические ортопедические конструкции. Медицинская наука и образование Урала. 2017; 1 (89): 32–6.

A STUDY OF THE TYPE OF ANTIMICROBIAL ACTION OF NOVEL COMPOUNDS SYNTHESIZED FROM SUBSTITUTED BENZAMINOINDOLES

Stepanenko IS[1]✉, Yamashkin SA[2], Kostina YuA[1], Slastnikov ED[1], Batarsheva AA[1]

[1] Institute of Medicine, National Research Mordovia State University, Saransk, Russia

[2] Evseviev Mordovia State Institute of Pedagogy, Saranks, Russia

The antimicrobial activity of novel compounds is tested by determining the minimum inhibitory concentration of the agent in question and investigating a few other parameters, including the type of antimicrobial action the drug exhibits. The aim of this study was to determine the type of antimicrobial action of the compounds synthesized from the substituted benzaminoindoles. The strain of *Staphylococcus aureus ATCC 6538-P* was briefly exposed to the compounds with laboratory codes 5D, 7D, HD, and S3. Bacterial growth was evaluated macroscopically under transmitted light. Additionally, photoelectric colorimetry was applied to monitor changes in the optical density of the culture medium. The minimum inhibitory concentrations of the studied compounds delayed bacterial growth for 2–3 days and had a bacteriostatic effect on *S. aureus*.

Keywords: benzaminoindole, pyrroloquinoline, antimicrobial activity, antimicrobial activity type

Author contribution: Stepanenko IS conducted the experiment and analyzed its results; Yamashkin SA helped to design the experiment and synthesized the tested compounds; Kostina YuA analyzed the results of the experiment and wrote the article; Batarsheva AA and Slastnikov ED conducted the experiment.

✉ **Correspondence should be addressed:** Irina S. Stepanenko
Ulianova 26, Saranks, 430032; ymahkina@mail.ru

Received: 21.11.2018 **Accepted:** 07.04.2019 **Published online:** 21.04.2019

DOI: 10.24075/brsmu.2019.030

ИЗУЧЕНИЕ ТИПА ПРОТИВОМИКРОБНОГО ДЕЙСТВИЯ НОВЫХ СОЕДИНЕНИЙ, СИНТЕЗИРОВАННЫХ НА ОСНОВЕ ЗАМЕЩЕННЫХ БЕНЗАМИНОИНДОЛОВ

И. С. Степаненко[1]✉, С. А. Ямашкин[2], Ю. А. Костина[1], Е. Д. Сластников[1], А. А. Батаршева[1]

[1] Медицинский институт, Национальный исследовательский Мордовский государственный университет имени Н. П. Огарёва, Саранск, Россия

[2] Мордовский государственный педагогический институт имени М. Е. Евсевьева, Саранск, Россия

Исследование противомикробной активности новых соединений включает изучение как минимальной подавляющей концентрации вещества, так и других показателей, в том числе — определение типа противомикробного действия. Целью работы было определить тип противомикробного действия новых соединений, синтезированных на основе замещенных бензаминоиндолов. Тип противомикробного действия определяли при воздействии исследуемых соединений с лабораторными шифрами 5D, 7D, HD и S3 в коротких экспозициях с использованием тест-штамма микроорганизма *Staphylococcus aureus ATCC 6538-P*. Рост микроорганизмов в присутствии исследуемых соединений определяли невооруженным глазом в проходящем свете и по изменению оптической плотности культуральной среды фотоколориметрически. Исследуемые соединения задерживали рост тест-штамма *S. aureus* в течение 2–3 и более суток и оказывали бактериостатическое действие в минимальных подавляющих концентрациях.

Ключевые слова: бензаминоиндолы, пирролохинолоны, противомикробная активность, тип противомикробного действия

Информация о вкладе авторов: И. С. Степаненко — участие в реализации эксперимента, анализ полученных результатов; С. А. Ямашкин — синтез тестируемых соединений и консультирование по идее исследования; Ю. А. Костина — разработка дизайна статьи и анализ полученных результатов; А. А. Батаршева и Е. Д. Сластников — участие в реализации эксперимента.

✉ **Для корреспонденции:** Ирина Семеновна Степаненко
ул. Ульянова, д. 26, г. Саранск, 430032; ymahkina@mail.ru

Статья получена: 21.11.2018 **Статья принята к печати:** 07.04.2019 **Опубликована онлайн:** 21.04.2019

DOI: 10.24075/vrgmu.2019.030

For centuries humanity has been fighting a battle against infectious diseases. Discovery of antimicrobial agents was a crucial milestone in treating and eliminating infections, but it also yielded understanding that bacteria have mechanisms promoting resistance to antibiotics [1–3]. Today, drug resistance in bacteria is a mounting concern. Research into the mechanisms underlying this phenomenon is fundamentally important for developing novel approaches to countering bacterial infections [4, 5]. Resistance to a wide range of drugs seen in major clinically important microorganisms is a global threat [6, 7].

Microbiological surveillance conducted over the past few years has revealed an alarming increase in the number of multidrug-resistant bacterial strains. For example, in comparison with methicillin-susceptible strains, methicillin-resistant *S. aureus* do not respond to gentamicin, clindamycin, rifampicin, tetracycline, chloramphenicol, ceftaroline, ciprofloxacin, and erythromycin more frequently; *P. aeruginosa* are resistant to cephalosporins, such as cefepime and ceftazidime, and piperacillin-tazobactam, imipenem, and meropenem; *Enterobacteriaceae* are resistant to at least three classic antibiotics, such as cefotaxime, ceftazidime, cefepime, aztreonam, etc. [8–10].

The search for and the development of novel antimicrobial agents are crucial for overcoming antibiotic resistance. The need for highly effective and safe antibacterial agents has been emphasized by the government of the Russian Federation [11].

Previously, we synthesized a few indolilamides and pyrroloquinolines from substituted 4-, 5-, 6-, 7-aminoindoles that representing the compounds, which contain cyclic or noncyclic *N*-(indolyl)amides and pyrroloquinolines, exhibit antimicrobial activity against gram-positive and gram-negative microorganisms [12–14].

This study sought to identify the type of antimicrobial activity exhibited by the novel compounds synthesized from substituted aminoindoles.

METHODS

The type of antimicrobial action of the synthesized compounds was tested on the test strain of *Staphylococcus aureus* ATCC 6538-P from the Museum of Live Cultures (State Research Center for Applied Microbiology & Biotechnology). The microorganisms were exposed to the studied compounds for different time periods at room temperature as described in [15]. The compounds were diluted to a number of different concentrations in the physiological saline and then poured into test tubes (1 ml per tube). The control tubes did not contain the studied compounds. The microorganisms were suspended in the physiological saline; 1 ml of the resulting suspension was added to each test tube (a final concentration of $1.5 \cdot 10^8$ CFU/ml). At this concentration, the turbidity of the bacterial suspension was 0.5 McFarland [16, 17]. Turbidity was measured using a commercial kit (Sensititre; UK). The optical density of the suspension was determined spectrophotometrically. The bacterial suspension was prepared from a colony grown on slant agar for 24 h. One hundred µl of the physiological solution containing bacteria and one of the studied compounds were pipetted into the tubes filled with 1 ml of a Mueller Hinton broth (MHB) (M391; HiMedia Laboratories Pvt. limited; India) after 5, 10, 15, 30, 60, 120, and 240 min following the preparation of the bacterial suspension. By varying the time of the exposure to a fixed concentration of a studied agent, one can assess the potential and actual effects of the latter, including the effect produced by a minimum inhibitory concentration or its dynamics over time. The properties of antimicrobial compounds can change depending on the medium used and the bacteria themselves [15].

The final concentration of *S. aureus* in the suspension was approximately $5 \cdot 10^5$ CFU/ml in each test tube. The following concentrations of the synthesized compounds were tested: 25 µg/ml for the cyclic amide 5D, 125 µg/ml for the cyclic amide 7D, 62.5 µg/ml for the amide S3, 59 µg/ml for the cyclic amide HD, and 1 µg/ml for azithromycin [11–13]. Azithromycin chosen for comparison is a classic drug with a bacteriostatic effect; its MIC_{90} for *S. aureus* is 0.01–2 µg/ml [18]. The test tubes were placed into an incubator and left there for 5 days at 37 °C. The growth of the microorganisms was regularly monitored by examining the tubes macroscopically under transmitted light. Additionally, the optical density of the culture media was measured using a photoelectric colorimeter Apel AP-101 (Energopromavtomatika; Russia). The measurements were performed in 1 ml sterile cuvettes at 600 nm wavelength. The optical density of the microorganisms cultured in the presence of an antimicrobial compound was compared to the optical density of the microorganisms cultured in the absence of thereof. In total, 4 series of experiments were carried out.

The compounds tested in this work were derived from substituted 4-, 6- and 7-aminoindoles. Their structural formulas are provided below.

1. The cyclic amide with the laboratory code 5D is a derivative of the substituted 4-amino-2-phenylindole 4-hydroxy-8-phenyl-4-(trifluoromethyl)-1,3,4,7-tetrahydro-2*H*-pyrrolo[2,3-h] quinoline-2-on

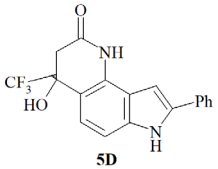

5D

2. The noncyclic amide with the laboratory code S3 is a derivative of substituted 6-aminoindole:

N-(1,5-dimethyl-2-phenyl-1*H*-indole-6-yl)-4,4,4-trifluoro-3-oxobutanamide

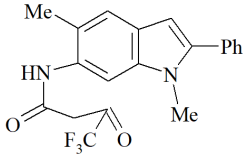

S3

3. The cyclic amide with the laboratory code 7D is a derivative of substituted 6-aminoindole: 9-hydroxy-5-methyl-2-phenyl-9-(trifluoromethyl)-1,6,8,9-tetrahydro-7*H*-pyrrolo[2,3-*f*] quinoline-7-on

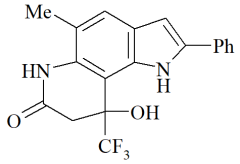

7D

4. The cyclic amide with the laboratory code HD is a derivative of substituted 7-aminoindole 6-hydroxy-2,3-dimethyl-6-(trifluoromethyl)-1,6,7,9-tetrahydro-8*H*-pyrrolo[3,2-*h*] quinoline-8-on

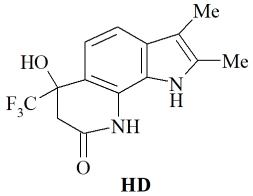

HD

The names for the studied compounds were generated by ACD/LABS Name Generator MarvinSketch 4.7.7.0. (ChemAxon Ltd.; Hungary) according to the IUPAC nomenclature. The structural formulas of the compounds were drawn in ISIS Draw 2.4. (MDL Information Systems; USA).

The obtained data were processed using the analysis of variance. Significance of differences was measured by Student's *t*-test [16].

RESULTS

Bacterial growth was observed when the optical density (*D*) of the culture media exceeded 0.21. The culture medium used as a negative control ($5 \cdot 10^5$ CFU/ml) was stored in a refrigerator and had $D = 0.003$.

In the control tubes, bacterial growth was visible to the unaided eye 24 h following inoculation (Fig. 1). The optical density of the culture medium (0.26 and above) was also indicative of bacterial growth after 24 h of incubation (Table). After two days of incubation, *D* reached 0.39; after 3 days, 0.51; after 4 days, 0.56; after 5 days, it was 0.6. Summing up, the bacterial mass increased by 50%, 30%, 9%, and 7% after 2, 3, 4 and 5 days of incubation, respectively (Fig. 2). A decline in growth rates can be explained by the depletion of nutrients in the culture medium.

Azithromycin inhibited the growth of *S. aureus* for 3 days. After 4 days of culture in the presence of azithromycin taken at its MIC, visible bacterial growth was noticed macroscopically under transmitted light (Fig. 3). The optical density of the culture medium started to increase after 2 days of incubation (see Table). The *D* value of the culture medium samples with azithromycin differed significantly from that of the control ($p < 0.05$). After 4 days of culture, the optical density of the culture medium increased to 0.23–0.25, relative to its initial value, but

bacterial growth still was significantly delayed throughout the experiment in comparison with the control samples. Delayed growth, which became noticeable only after day 4, suggests the absence of a bactericidal effect. At the minimum inhibitory concentration, azithromycin delays bacterial growth and has a bacteriostatic effect.

During the first 24 h of incubation, no visible growth was observed under transmitted light in the bacterial cultures exposed to the cyclic amide HD. After 2 days of incubation, the situation did not change. After 3 days, turbidity appeared in all the cultures exposed to the HD compound. The optical density of the samples measured 24 h after inoculation suggests the inhibition of *S. aureus* growth following exposure to the HD compound (Table; Fig. 4). After 2 days of incubation, this cyclic amide significantly inhibited bacterial growth ($p < 0.05$). Throughout the entire experiment, the optical density of the samples containing HD at the minimum inhibitory concentration was lower than that of the control samples. This means that

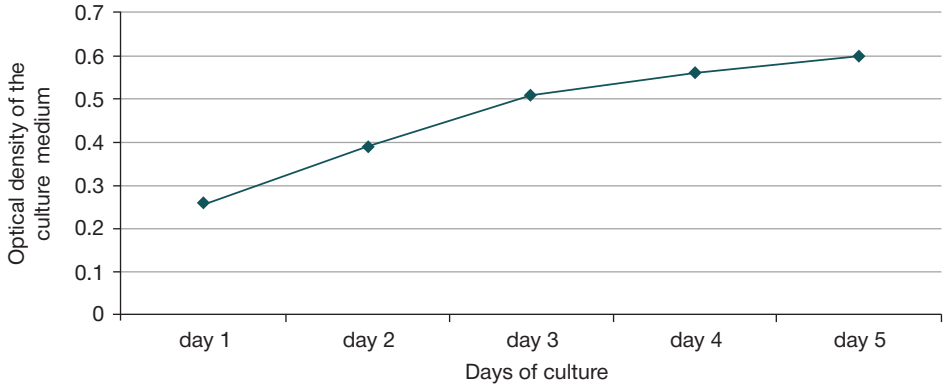

Fig. 1. The optical density of the culture medium with *S. aureus ATCC 6538-P* throughout 5 days of culture

Table. The growth of *S. aureus ATCC 6538-P* that studied by the optical density of the culture medium

		Exposure time							
Days of measurements	Control	Compounds	5 min	10 min	5 min	30 min	1 h	2 h	4 h
Day 1	0.26 ± 0.03	Control	0.22 ± 0.01	0.22 ± 0.02	0.25 ± 0.04	0.26 ± 0.02	0.23 ± 0.05	0.27 ± 0.03	0.25 ± 0.02
		Azithromycin	0.05 ± 0.01*	0.05 ± 0.01*	0.05 ± 0.01*	0.05 ± 0.01*	0.07 ± 0.03*	0.07 ± 0.02*	0.06 ± 0.01*
		HD	0.07 ± 0.01*	0.07 ± 0.02*	0.07±0.01*	0.08 ± 0.03*	0.07 ± 0.01*	0.06 ± 0.02*	0.05 ± 0.001*
		S3	0.12 ± 0.02*	0.12 ± 0.02*	0.10 ± 0.01*	0.10 ± 0.02*	0.09 ± 0.03*	0.09 ± 0.02*	0.09 ± 0.02*
		7D	0.07 ± 0.02*	0.07 ± 0.02*	0.07 ± 0.01*	0.08 ± 0.02*	0.06 ± 0.01*	0.06 ± 0.01*	0.06 ± 0.01*
		5D	0.010 ± 0.001*	0.010 ± 0.001*	0.010 ± 0.001*	0.010 ± 0.003*	0.010 ± 0.001*	0.010 ± 0.001*	0.010 ± 0.002*
Day 2	0.39 ± 0.06	Control	0.38 ± 0.07	0.38 ± 0.09	0.38 ± 0.12	0.37 ± 0.08	0.43 ± 0.09	0.39 ± 0.04	0.44 ± 0.01
		Azithromycin	0.09 ± 0.06*	0.09 ± 0.05*	0.12 ± 0.04*	0.15 ± 0.02*	0.15 ± 0.01*	0.15 ± 0.04*	0.11 ± 0.02*
		HD	0.18 ± 0.04*	0.18 ± 0.02*	0.15 ± 0.03*	0.14 ± 0.03*	0.09 ± 0.01*	0.08 ± 0.01*	0.07 ± 0.02*
		S3	0.25 ± 0.02	0.27 ± 0.02	0.24 ± 0.03	0.20 ± 0.01*	0.19 ± 0.03*	0.20 ± 0.01*	0.20 ± 0.01*
		7D	0.15 ± 0.04*	0.15 ± 0.02*	0.14 ± 0.03*	0.19 ± 0.04*	0.15 ± 0.02*	0.15 ± 0.01*	0.13 ± 0.03*
		5D	0.011 ± 0.002*	0.012 ± 0.001*	0.012 ± 0.002*	0.011 ± 0.002*	0.011 ± 0.001*	0.011 ± 0.003*	0.011 ± 0.002*
Day 3	0.51 ± 0.05	Control	0.45 ± 0.02	0.45 ± 0.04	0.48 ± 0.02	0.49 ± 0.08	0.51 ± 0.03	0.46 ± 0.02	0.51±0.01
		Azithromycin	0.13 ± 0.07*	0.13 ± 0.05*	0.17 ± 0.02*	0.20 ± 0.01*	0.20 ± 0.01*	0.19 ± 0.02*	0.18 ± 0.02*
		HD	0.28 ± 0.11	0.28 ± 0.08	0.28 ± 0.02	0.24 ± 0.05*	0.22 ± 0.03*	0.21 ± 0.04*	0.23 ± 0.02*
		S3	0.32 ± 0.1	0.32 ± 0.07	0.34 ± 0.04	0.29 ± 0.5	0.29 ± 0.04	0.27 ± 0.05	0.26 ± 0.03
		7D	0.18 ± 0.03*	0.18 ± 0.02*	0.17 ± 0.01*	0.25 ± 0.04	0.20 ± 0.01*	0.19 ± 0.01*	0.18 ± 0.01*
		5D	0.014 ± 0.002*	0.013 ± 0.003*	0.014 ± 0.003*	0.02 ± 0.007*	0.014 ± 0.002*	0.02 ± 0.002*	0.02±0.002*
Day 4	0.56 ± 0.02	Control	0.53 ± 0.01	0.53 ± 0.03	0.56 ± 0.03	0.56 ± 0.01	0.58 ± 0.01	0.54 ± 0.01	0.57 ± 0.01
		Azithromycin	0.24 ± 0.05*	0.25 ± 0.03*	0.27 ± 0.07	0.33 ± 0.03	0.34 ± 0.02	0.25 ± 0.03	0.23 ± 0.03*
		HD	0.35 ± 0.09	0.35 ± 0.12	0.36 ± 0.09	0.36 ± 0.10	0.32 ± 0.07	0.36 ± 0.09	0.30 ± 0.06
		S3	0.42 ± 0.03	0.42 ± 0.04	0.39 ± 0.02	0.36 ± 0.03	0.35 ± 0.06	0.35 ± 0.04	0.33 ± 0.04
		7D	0.27 ± 0.02	0.27 ± 0.04	0.27 ± 0.06	0.33 ± 0.03	0.33 ± 0.04	0.25 ± 0.03	0.23 ± 0.01*
		5D	0.03 ± 0.007*	0.03 ± 0.008*	0.03 ± 0.003*	0.04 ± 0.011*	0.07 ± 0.013*	0.07 ± 0.01*	0.09 ± 0.01*
Day 5	0.60 ± 0.02	Control	0.54 ± 0.03	0.54 ± 0.05	0.57 ± 0.03	0.57 ± 0.01	0.59 ± 0.01	0.55 ± 0.04	0.58 ± 0.03
		Azithromycin	0.25 ± 0.05*	0.26 ± 0.02*	0.28 ± 0.09	0.38 ± 0.1	0.36 ± 0.06	0.26 ± 0.02*	0.25 ± 0.01*
		HD	0.43 ± 0.05	0.43 ± 0.09	0.43 ± 0.06	0.53 ± 0.05	0.43 ± 0.09	0.46 ± 0.04	0.37 ± 0.9
		S3	0.43 ± 0.06	0.43 ± 0.05	0.40 ± 0.13	0.37 ± 0.11	0.36 ± 0.07	0.35 ± 0.04	0.35 ± 0.03
		7D	0.31 ± 0.12	0.31 ± 0.09	0.31 ± 0.04	0.42 ± 0.05	0.35 ± 0.02	0.31 ± 0.03	0.25 ± 0.02*
		5D	0.04 ± 0.009*	0.04 ± 0.01*	0.06 ± 0.012*	0.07 ± 0.011*	0.08 ± 0.002*	0.09 ± 0.01*	0.11 ± 0.01*

Note: * — differences from the control samples are significant at $p < 0.05$.

MIC of the HD compound delays bacterial growth and has a bacteriostatic effect.

On day 1 of incubation, no visible growth was observed under transmitted light in the samples exposed to the S3 compound. After two days of incubation, there was visible growth in the tubes containing cultures exposed to amide S3 for 5, 10 and 15 min; no visible macroscopic growth was observed in the remaining tubes. On day 3, turbidity was noticed in the tubes. The S3 amide significantly delayed bacterial growth on days 1 and 2 of culture ($p < 0.05$) (Table; Fig. 5). In the following few days, the rates of *D* growth demonstrated a gradual decline in comparison with the control samples. A 2-day delay in the bacterial growth suggested the absence of a bactericidal effect. Thus, the S3 compound used at the minimum inhibitory concentration delays bacterial growth and has a bacteriostatic effect.

The cultures exposed to the 7D compound demonstrated no visible growth under transmitted light during the first 24 h of incubation. After 2 days of culture, the situation did not change. After 3 days of culture, turbidity was noticed in the colonies exposed to the 7D compound for 30 min. After 4 days, turbidity became macroscopically visible in all the cultures from this series of samples. The optical density of the samples exposed to the 7D compound was decreasing significantly for 3 days following the onset of incubation, as compared to the controls (Table; Fig. 6). Throughout the experiment, bacterial growth was significantly delayed in the samples exposed to the 7D compound. Thus, the MIC of the cyclic amide 7D delays bacterial growth and has a bacteriostatic effect.

Throughout the experiment, no bacterial growth was noticed under transmitted light in the colonies exposed to the compound 5D. The optical density of the inoculated culture medium indicated inhibition of the tested *S. aureus* strain throughout 5 days of incubation (Table; Fig. 7). The *D* value of the samples was significantly different from that of the control tubes ($p < 0.05$) throughout the experiment, but still tended to increase. Perhaps, the concentration of the 5D compound in the culture was close to bactericidal. We conclude that the cyclic amide 5D delays bacterial growth and has a bacteriostatic effect.

Summing up, the cyclic amide 5D derived from 4-amino-phenylindole, the amide S3 and the cyclic amide 7D derived from substituted 6-aminoindoles, as well as the cyclic amide HD derived from substituted 7-aminoindoles, delayed the growth of *S. aureus ATCC 6538-P* for at least 1 day. Apart from the S3 compound, the studied compounds continued to inhibit bacterial growth on day 2 of culture. Visible bacterial growth and an increase in the optical density of the culture medium were observed after 48 h of incubation in the tubes exposed to the compound S3 for 5, 10 and 15 min. After 3

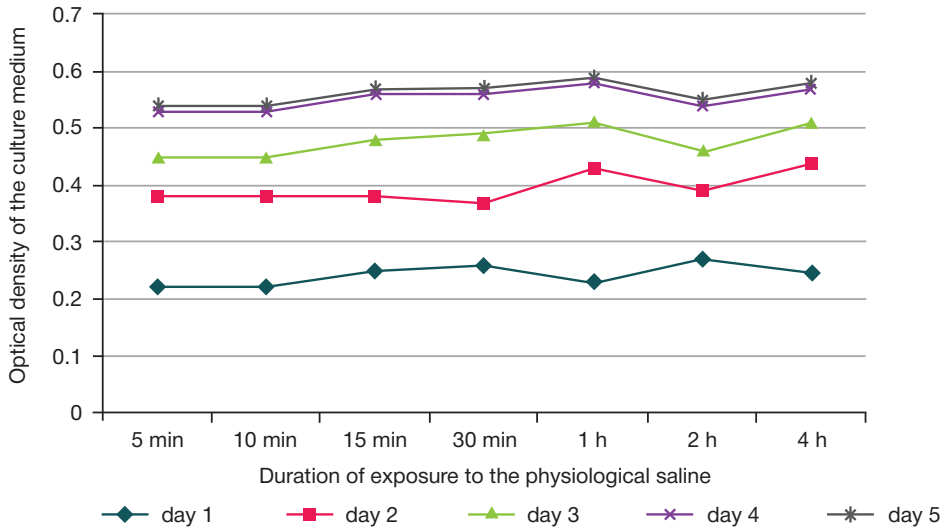

Fig. 2. The optical density of the culture medium with *S. aureus ATCC 6538-P* after exposure in the physiological saline during 5 days of culture

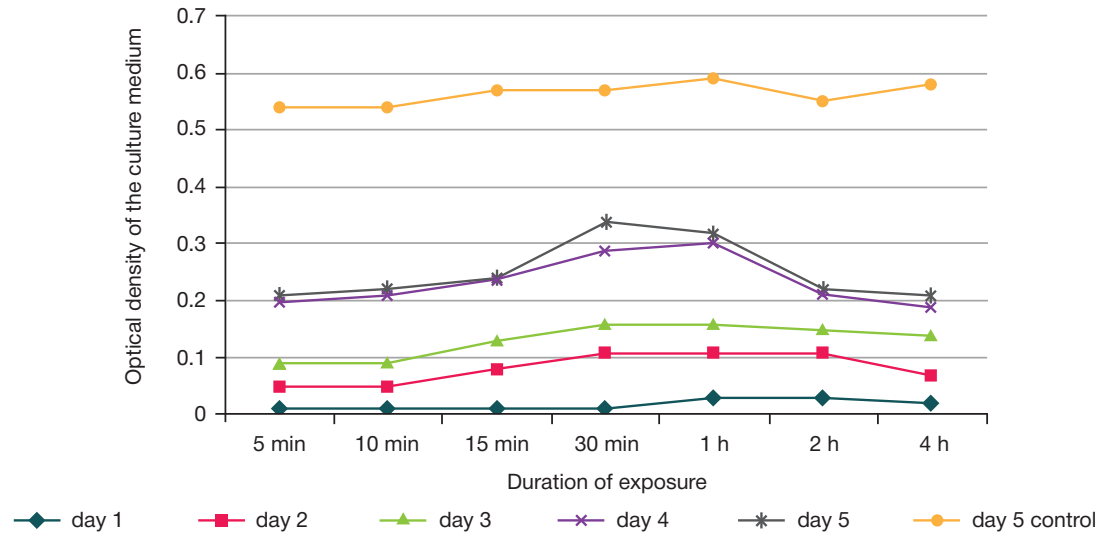

Fig. 3. The optical density of the culture medium with *S. aureus ATCC 6538-P* after exposure to azithromycin

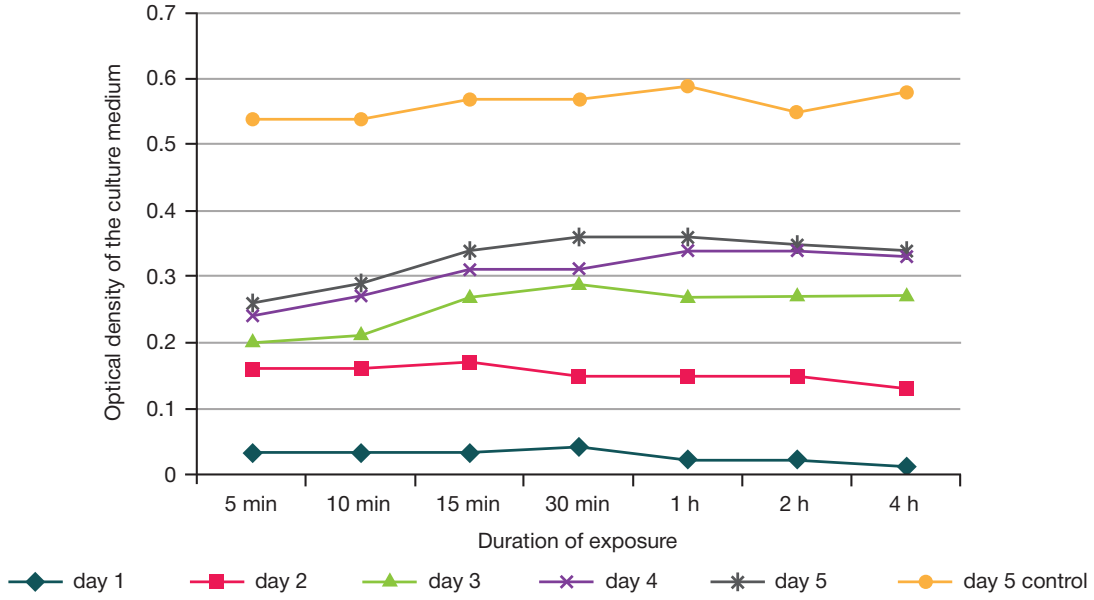

Fig. 4. The optical density of the culture medium with *S. aureus ATCC 6538-P* after exposure to the compound HD

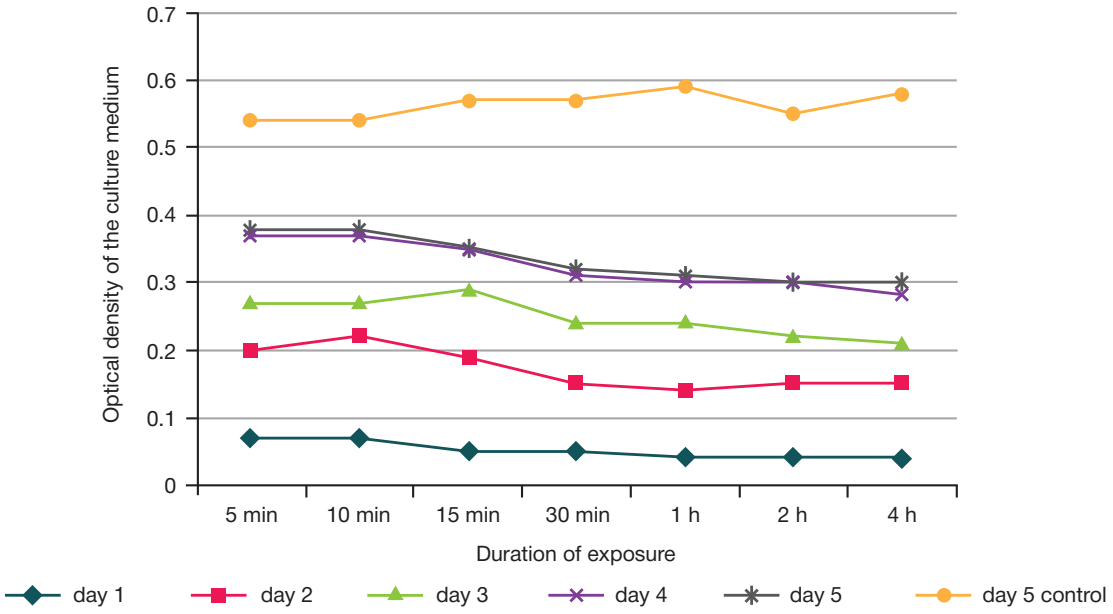

Fig. 5. The optical density of the culture medium with *S. aureus ATCC 6538-P* after exposure to the compound S3

days of incubation, visible bacterial growth was observed in all the tubes exposed to the compounds HD and S3. After 4 days of incubation, visible bacterial growth was observed in the samples exposed to the compound 7D. No visible growth of *S. aureus ATCC 6538-P* was noticed throughout 5 days of the experiment in the samples exposed to the compound 5D, although the optical density dynamics suggested an increase in the bacterial population.

The type of antimicrobial action of the studied compounds synthesized from substituted 4-, 6-, 7-aminoindoles that have the strongest antimicrobial effect is comparable to that of azithromycin, a classic antibiotic with a bacteriostatic effect.

DISCUSSION

Over the past decades, the chemistry of indoles and their derivatives has been in the focus of experimental research. Indoles are basic components of many natural and synthetic compounds that possess a physiological activity, such as tryptophan or serotonin, a biogenic amine. Aminoindoles with an amino group in the benzene ring arouse particular interest. Like any other aromatic amines, these compounds have a lot of derivatives with an amino group component [12–13]. Previously, we studied interactions between β-dioxycompounds and substituted aminoindoles with different positions of the amino group in the benzene ring. We developed methods for the synthesis of 16 aminoindoles and their 32 derivatives — indolilamides, enamines and pyrroloquinolines. Their MIC and spectra of antimicrobial activity were also determined.

While studying a novel antimicrobial compound, it is important to determine its minimum inhibitory concentration, identify the type of antimicrobial activity or its range, explore the mechanism underlying the biological effect, etc. The type of antimicrobial activity is usually determined by comparing MIC and minimum bactericidal concentrations (MBC); such method allows researchers to only arbitrarily classify a new compound based on its effect on the bacterial cell [16]. The method applied in this study involves the use of brief exposures to the compound in question [15]; it allowed us not only to identify the type of antimicrobial activity but also to prove that

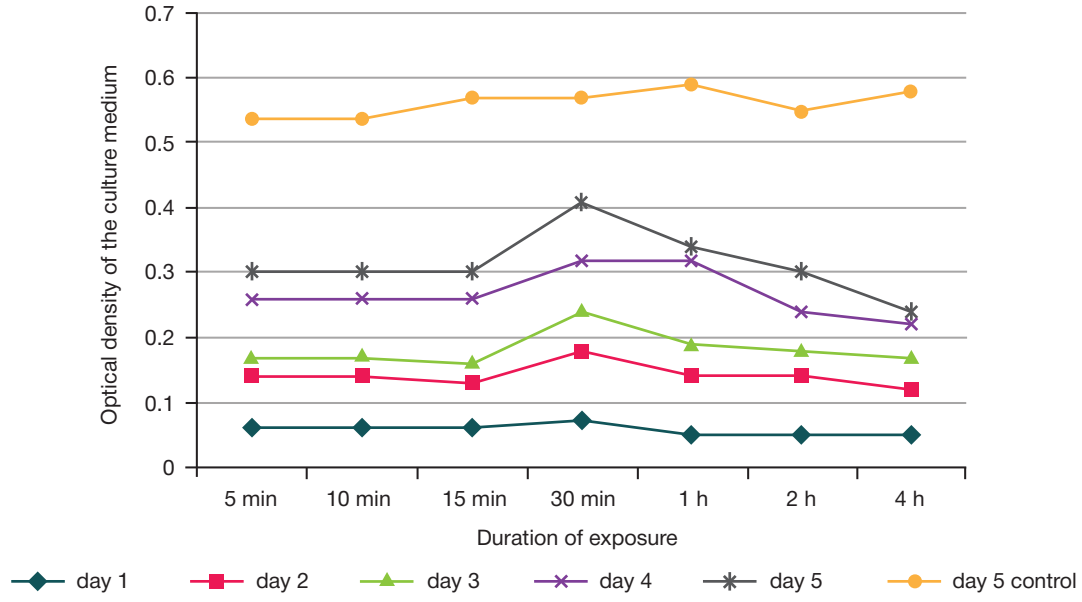

Fig. 6. The optical density of the culture medium with *S. aureus ATCC 6538-P* after exposure to the compound 7D

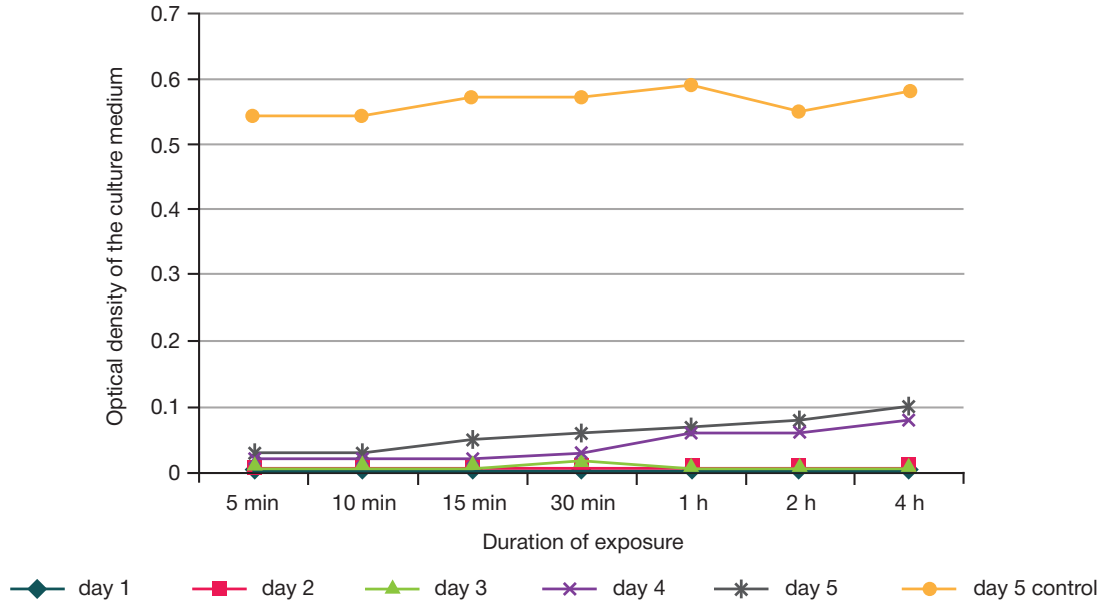

Fig. 7. The optical density of the culture medium with *S. aureus ATCC 6538-P* after exposure to the compound 5D

the synthesized compounds retain their antimicrobial properties regardless of the duration of exposure, the properties of the medium or the activity of microorganisms themselves. Throughout the experiment, the growth of *S. aureus ATCC 6538-P* was generally delayed following exposure to any of the studied compounds, although the optical density of the bacterial population may have been increasing. Considering the proven bacteriostatic effect of the compounds used at minimum inhibitory concentrations, we hypothesize that the mechanism underlying the antimicrobial effect of 4-, 6-, 7-aminoindole derivatives does not involve a possible effect on the cell wall or the cytoplasmic membrane that eventually leads to cell death. Perhaps, the studied compounds have a certain effect on the DNA of the bacterial cell (DNA damage or any additional mechanism that is not accompanied by DNA breaks) or on protein synthesis. In the next step, we are planning to study the mechanisms underlying the antimicrobial activity of 4-, 6-, 7-aminoindole derivatives.

CONCLUSIONS

We have proven that derivatives of substituted benzaminoindoles used at minimum inhibitory concentrations produce a bacteriostatic effect and delay the growth of *S. aureus ATCC 6538-P*. Our findings encourage us to continue research into the synthetic derivatives of 4-, 6-, 7-aminoindoles and the feasibility of their application as antimicrobial agents in clinical practice.

References

1. Parhizgari N, Gouya MM, Mostafavi E. Emerging and re-emerging infectious diseases in Iran. Iranian Journal of Microbiology. 2017; 9 (3): 122–42.
2. Yokoyama M, Stevens E, Laabei M, Bacon L, Heesom K, Bayliss S et al. Epistasis analysis uncovers hidden antibiotic resistance-associated fitness costs hampering the evolution of MRSA. Genome Biology. 2018; 19 (1): 94.
3. Kumarasamy KK, Toleman MA, Walsh TR, Bagaria J, Butt F, Balakrishnan R et al. Emergence of a new antibiotic resistance mechanism in India, Pakistan, and the UK: a molecular, biological, and epidemiological study. The Lancet Infectious Diseases. 2010; 10 (9): 597–602.
4. McKeegan KS, Borges-Walmsley MI, Walmsley AR. Microbial and viral drug resistance mechanisms. Trends in Microbiology. 2002; (10): 8–14.
5. Savjani JK, Gajjar AK, Savjani KT. Mechanisms of resistance: useful tool to design antibacterial agents for drug — resistant bacteria. Mini-Reviews in Medicinal Chemistry. 2009; 9 (2): 194–205.
6. Yadav N, Dubey A, Shukla S, Saini CP, Gupta G, Priyadarshini R et al. Graphene Oxide-Coated Surface: Inhibition of Bacterial Biofilm Formation due to Specific Surface-Interface Interactions. ACS Omega. 2017; 2 (7): 3070–82.
7. Obayiuwana A, Ogunjobi M, Yang M, Ibekwe M. Characterization of Bacterial Communities and Their Antibiotic Resistance Profiles in Wastewaters Obtained from Pharmaceutical Facilities in Lagos and Ogun States. Nigeria International Journal of Environmental Research and Public Health. 2018; 15 (7): 1365.
8. Kozlov RS. Antibiotic resistance of gram-positive pathogens of complicated intra-abdominal infections in Russia. Clinical microbiology and antimicrobial chemotherapy. 2015; 17 (3): 227–34.
9. Romanov AV. Antibiotic resistance of nosocomial strains of *Staphylococcus aureus* in hospitals in Russia: results of the Marathon 2013–2014 multicenter epidemiological study. Clinical microbiology and antimicrobial chemotherapy. 2017; 19 (1): 57–62.
10. Sukhorukova MV. Antibiotic resistance of nosocomial *Enterobacteriaceae* strains in hospitals in Russia: the results of the Marathon 2013–2014 multicenter epidemiological study. Clinical microbiology and anti-microbial chemotherapy. 2017; 19 (1): 49–56.
11. Rasporyazheniye Pravitel'stva RF ot 25 sentyabrya 2017 g. № 2045-r «O strategii preduprezhdeniya rasprostraneniya antimikrobnoy rezistentnosti v RF na period do 2030 g.». Available from: https://www.garant.ru/products/ipo/prime/doc/71677266/. Russian.
12. Alyamkina EA, Stepanenko IS, Yamashkin SA, Yurovskaya MA. Soedineniya s potencial'noj antimikrobnoj aktivnost'yu na osnove 4-amino-2-fenilindola. Vestnik Moskovskogo universiteta. 2016; 57 (6): 410–7. Russian.
13. Alyamkina EA, Yamashkin SA, Stepanenko IS, Yurovskaya MA. 4-amino-2-phenylindole-based compounds with potential antibacterial activity. Moscow University Chemistry Bulletin. 2017; 72 (1): 24–8.
14. Stepanenko IS. A new group of compounds derived from 4-, 5-, 6- and 7-aminoindoles with antimicrobial activity. Research Results in Pharmacology. 2018; 4 (3): 17–26.
15. Pershin GN, redaktor. Prakticheskoe rukovodstvo. Metody ehksperimental'noj himioterapii. M.: Medicina, 1971; 541 s. Russian.
16. Mironov AN, Bunyatyan ND, Vasilyev AN, Verstakova OL, Zhuravleva VV, Lepakhin VK, i dr. Rukovodstvo po provedeniju doklinicheskih issledovanij lekarstvennyh sredstv. M.: Grif i K, 2012; 944 s. Russian.
17. Opredelenie chuvstvitel'nosti mikroorganizmov k antibakterial'nym preparatam. Metodicheskie ukazanija MUK 4.2.1890-04. Klinicheskaja mikrobiologija i antimikrobnaja himioterapija. 2004; 6 (4): 303–402. Russian.
18. Kozlov RS, Sukhorukova MV, Eidelstein MV, Ivanchik NV, Skleenova EYu, Timokhova AV, et al. Determination of the sensitivity of microorganisms to antimicrobial drugs: clinical recommendations. Smolensk: Interregional Association of Clinical Microbiology and Antimicrobial Chemotherapy. 2018; 206 p.

Литература

1. Parhizgari N, Gouya MM, Mostafavi E. Emerging and re-emerging infectious diseases in Iran. Iranian Journal of Microbiology. 2017; 9 (3): 122–42.
2. Yokoyama M, Stevens E, Laabei M, Bacon L, Heesom K, Bayliss S et al. Epistasis analysis uncovers hidden antibiotic resistance-associated fitness costs hampering the evolution of MRSA. Genome Biology. 2018; 19 (1): 94.
3. Kumarasamy KK, Toleman MA, Walsh TR, Bagaria J, Butt F, Balakrishnan R et al. Emergence of a new antibiotic resistance mechanism in India, Pakistan, and the UK: a molecular, biological, and epidemiological study. The Lancet Infectious Diseases. 2010; 10 (9): 597–602.
4. McKeegan KS, Borges-Walmsley MI, Walmsley AR. Microbial and viral drug resistance mechanisms. Trends in Microbiology. 2002; (10): 8–14.
5. Savjani JK, Gajjar AK, Savjani KT. Mechanisms of resistance: useful tool to design antibacterial agents for drug — resistant bacteria. Mini-Reviews in Medicinal Chemistry. 2009; 9 (2): 194–205.
6. Yadav N, Dubey A, Shukla S, Saini CP, Gupta G, Priyadarshini R et al. Graphene Oxide-Coated Surface: Inhibition of Bacterial Biofilm Formation due to Specific Surface-Interface Interactions. ACS Omega. 2017; 2 (7): 3070–82.
7. Obayiuwana A, Ogunjobi M, Yang M, Ibekwe M. Characterization of Bacterial Communities and Their Antibiotic Resistance Profiles in Wastewaters Obtained from Pharmaceutical Facilities in Lagos and Ogun States. Nigeria International Journal of Environmental Research and Public Health. 2018; 15 (7): 1365.
8. Козлов Р. С. Антибиотикорезистентность грамположительных возбудителей осложненных интраабдоминальных инфекций в России. Клиническая микробиология и антимикробная химиотерапия. 2015; 17 (3): 227–34.
9. Романов А. В. Антибиотикорезистентность нозокомиальных штаммов *Staphylococcus aureus* в стационарах России: результаты многоцентрового эпидемиологического исследования «Марафон» 2013–2014. Клиническая микробиология и антимикробная химиотерапия. 2017; 19 (1): 57–62.
10. Сухорукова М. В. Антибиотикорезистентность нозокомиальных штаммов *Enterobacteriaceae* в стационарах России: результаты многоцентрового эпидемиологического исследования «Марафон» 2013–2014. Клиническая микробиология и антимикробная химиотерапия. 2017; 19 (1): 49–56.
11. Распоряжение Правительства РФ от 25 сентября 2017 г. № 2045-р «О стратегии предупреждения распространения антимикробной резистентности в РФ на период до 2030 г.». Доступно по ссылке: https://www.garant.ru/products/ipo/prime/doc/71677266/.
12. Алямкина Е. А., Степаненко И. С., Ямашкин С. А., Юровская М. А. Соединения с потенциальной антимикробной активностью на основе 4-амино-2-фенилиндола. Вестник Московского университета. 2016; 57 (6): 410–17.
13. Alyamkina EA, Yamashkin SA, Stepanenko IS, Yurovskaya MA. 4-amino-2-phenylindole-based compounds with potential antibacterial activity. Moscow University Chemistry Bulletin. 2017; 72 (1): 24–8.
14. Stepanenko IS. A new group of compounds derived from 4-, 5-, 6- and 7-aminoindoles with antimicrobial activity. Research Results in Pharmacology. 2018; 4 (3): 17–26.
15. Першин Г. Н. редактор. Практическое руководство. Методы экспериментальной химиотерапии. М.: Медицина, 1971; 541 с.
16. Миронов А. Н., Бунятян Н. Д., Васильев А. Н., Верстакова О. Л., Журавлева М. В., Лепахин В. К. и др. Руководство по

проведению доклинических исследований лекарственных средств. М.: Гриф и К, 2012; 944 с.
17. Определение чувствительности микроорганизмов к антибактериальным препаратам. Методические указания МУК 4.2.1890-04. Клиническая микробиология и антимикробная химиотерапия. 2004; 6 (4): 303–402.
18. Козлов Р. С., Сухорукова М. В., Эйдельштейн М. В., Иванчик Н. В., Склеенова Е. Ю., Тимохова А. В. и др. Определение чувствительности микроорганизмов к антимикробным препаратам: клинические рекомендации. Смоленск: Межрегиональная ассоциация по клинической микробиологии и антимикробной химиотерапии. 2018; 206 с.

DYNAMICS OF HEMOSTASIS PARAMETERS AND ENDOTHELIAL DYSFUNCTION MARKERS IN PATIENTS WITH THERMAL INJURY

Morrison VV[1], Bozhedomov AYu[2] ✉

[1] Saratov State Medical University, Saratov, Russia

[2] Pirogov Russian National Research Medical University, Moscow, Russia

Burn injuries kill thousands of people. The aim of this study was to investigate the dynamics of systemic inflammatory response parameters, endothelial dysfunction markers and hemostasis impairment in patients with thermal burn injuries. The study was conducted in 51 patients aged 16 to 80 years presenting with moderate to severe thermal burns. The systemic inflammatory response was assessed based on the levels of tumor necrosis factor α (TNFα), a number of interleukins (IL6, IL12), the C-reactive protein, and the monocyte chemoattractant protein 1 (MCP-1). Hemostatic impairments were inferred from the results of coagulation tests that measured the activated partial thromboplastin time (APTT), the prothrombin index (PI), the prothrombin time (PT) and the platelet count. Endothelial dysfunction was analyzed based on the levels of vascular endothelial growth factor (VEGF), total endothelin (TE) and circulating endothelial cells. The dynamics of the listed parameters were studied over 45 days following the injury. Endothelial dysfunction markers peaked on days 3–15 (VEGF 828.9 ± 993.2 pg/mL, TE 3.0 ± 1.7 fmol/mL, CEC 6.4 ± 6.0 • 10^4/l, IL6 264.4 ± 131.2 pg/mL, TNFα 41.4 ± 111.9 pg/ml, C-reactive protein 128.3 ± 52.4 nmol/mL). Coagulation was significantly impaired during the same period (APTT 41.4 ± 17.7 s, PI 83.6 ± 15.4%, PT 22.3 ± 10.0 s). By day 30–35, blood concentrations of proinflammatory cytokines and inflammation mediators had declined (TNFα 3.9 ± 9.6 pg/mL, IL6 49.0 ± 35.9 pg/mL, C-reactive protein 81.9 ± 341 nmol/ml); in that phase, the coagulation potential was continuing to decrease (APTT 51.8 ± 34.1 s, PI 82.9 ± 19.4%, PT 24.9 ± 21.4 s). The study demonstrates that damage to the endothelium results from both injured tissue breakdown and inflammation mediators. The risk of thromboembolic and hemorrhagic complications is the highest on days 7 through 15 following thermal injury. Further research is needed to study the mechanisms of endothelial damage in patients with thermal burns.

Keywords: burns, endothelial dysfunction, hemostasis, hypocoagulation, systemic inflammatory response

Author contribution: Morrison VV — design of the experiment, data analysis, manuscript revision; Bozhedomov AYu — data collection and statistical analysis, manuscript draft.

Compliance with ethical standards: the study was approved by the Ethics Committee of Saratov State Medical University (Protocol No. 5 dated May 27, 2010); the patients gave informed consent to participate in the study and to disclose information about their medical condition and treatment on the Internet for the sake of science.

✉ **Correspondence should be addressed:** Alexey Yu. Bozhedomov
Ostrovityanova 1, Moscow, 117997; alecso_84@mail.ru

Received: 28.12.2018 **Accepted:** 26.03.2019 **Published online:** 07.04.2019

DOI: 10.24075/brsmu.2019.021

ДИНАМИКА ПОКАЗАТЕЛЕЙ ГЕМОСТАЗА И ЭНДОТЕЛИАЛЬНОЙ ДИСФУНКЦИИ ПРИ ТЕРМИЧЕСКОЙ ТРАВМЕ

В. В. Моррисон[1], А. Ю. Божедомов[2] ✉

[1] Саратовский государственный медицинский университет имени В. И. Разумовского, Саратов, Россия

[2] Российский национальный исследовательский медицинский университет имени Н. И. Пирогова, Москва, Россия

Ожоги остаются причиной смертности сотен тысяч людей. Целью работы было изучить динамику изменений показателей системной воспалительной реакции, эндотелиальной дисфункции и нарушений гемостаза у пострадавших от ожогов. У 51 пациента в возрасте 16–80 лет с термическими ожогами средней и тяжелой степеней изучали выраженность системного воспаления по уровням фактора некроза опухоли α (ФНОα), интелейкинов (IL6, IL12), С-реактивного протеина, моноцитарного хемоаттрактантного протеина-1 (MCP-1). Состояние гемостаза оценивали на основании коагулометрических исследований (активированное парциальное тромбопластиновое время (АПТВ), протромбиновый индекс (ПТИ), протромбиновое время (ПТВ) и др.), количества тромбоцитов; дисфункцию эндотелия — по уровням васкулоэндотелиального ростового фактора (VEGF), общего эндотелина (ЭТ), циркулирующих эндотелиальных клеток. Показатели изучали в динамике на 1–45-е сутки с момента получения травмы. Наибольшую выраженность дисфункции эндотелия и воспалительной реакции выявили на 3–15-е сутки (VEGF 828,9 ± 993,2 пг/мл, общий эндотелин 3,0 ± 1,7 фмоль/мл, ЦЭК 6,4 ± 6,0 • 10^4/л, IL6 264,4 ± 131,2 пг/мл, ФНОα 41,4 ± 111,9 пг/мл, С-реактивный белок 128,3 ± 52,4 нмоль/мл). В этот же период было отмечено выраженное угнетение коагуляции (АЧТВ 41,4 ± 17,7 с, ПТИ 83,6 ± 15,4%, ПТВ 22,3 ± 10,0 с). К 30–45-м суткам происходило уменьшение концентрации провоспалительных цитокинов и медиаторов воспаления в крови (ФНОα 3,9 ± 9,6 пг/мл, IL6 49,0 ± 35,9 пг/мл, С-реактивный белок 81,9 ± 34,1 нмоль/мл) и дальнейшее снижение коагуляционного потенциала крови (АЧТВ 51,8 ± 34,1 с, ПТИ 82,9 ± 19,4%, ПТВ 24,9 ± 21,4 с). Отмечено снижение показателей гемокоагуляции. Показано, что происходит повреждение эндотелия сосудов как продуктами, попадающими из ожоговых ран, так и медиаторами воспалительной реакции. Риск тромбоэмболических и геморрагических осложнений максимален с 7-х по 15-е сутки ожоговой болезни. Требуются дальнейшие более детальные исследования механизмов повреждения эндотелия при ожогах.

Ключевые слова: ожоги, эндотелиальная дисфункция, гемостаз, гипокоагуляция, системная воспалительная реакция

Информация о вкладе авторов: Моррисон В. В. — планирование эксперимента, анализ материала, редактирование статьи; Божедомов А. Ю. — сбор и анализ материала, статистическая обработка, написание текста статьи.

Соблюдение этических стандартов: исследование одобрено этическим комитетом Саратовского государственного медицинского университета им. В. И. Разумовского (протокол № 5 от 27 мая 2010 г.); пациенты, включенные в исследование, подписали согласие на публикацию и размещение в интернете информации о характере заболевания, проведенном лечении и его результатах с научной и образовательной целями.

✉ **Для корреспонденции:** Алексей Юрьевич Божедомов
ул. Островитянова, д. 1, г. Москва, 117997; alecso_84@mail.ru

Статья получена: 28.12.2018 **Статья принята к печати:** 26.03.2019 **Опубликована онлайн:** 07.04.2019

DOI: 10.24075/vrgmu.2019.021

There is increasing evidence of a complex interplay between systemic inflammation, hemostasis and endothelial dysfunction observed in severe pathology [1]. Burn injuries are not an exception, especially when the burn size exceeds 10% of total body surface area. The primary cause of death in burned patients is multiple organ dysfunction syndrome (MODS) resulting from the inability of adaptation mechanisms to cope with severe trauma-induced stress, hypermetabolism and damage done by the toxic products of tissue destruction [2, 3]. Although the pathophysiology of burn injury is relatively well studied, burns still kill thousands of people each year, posing a significant economic burden.

MODS is driven by a cytokine storm resulting from hyperproduction of cytokines. This phenomenon leads to systemic endothelial damage, disrupts microcirculation and transcapillary exchange [4, 5]. Therefore, endothelial dysfunction should be regarded as an important MODS manifestation and its contributor [6].

This study aimed to investigate the dynamics of hemostasis, systemic inflammatory response and endothelial dysfunction markers in patients with thermal injury.

METHODS

This prospective study was conducted in 51 patients (37 males and 14 females) aged 16 to 80 years undergoing treatment at Saratov Center of Thermal Injuries. The mean age of the participants was 40.5 ± 36.2 years (M ± σ). The study included patients with fire or scald burns with a prognostic index over 30 calculated as an area of small first to third degree burns + 3 areas of deep third to fourth degree burns (the index was proposed by G. Frank in 1960). On average, the Frank index was 80.1 ± 63.2 (M ± σ). The following exclusion criteria were applied: age under 16 and over 80 years (age significantly affects the organism's response to thermal injury); electrical or inhalation injury (the lesion size did not correlate with the severity of the condition); pregnancy; clinically uncompensated comorbidities at the time of admission. The death rate among the patients was 37%.

The patients were brought to the hospital within 1 h to 3 days after sustaining injury. Their serum samples were collected and assayed for endothelial dysfunction biomarkers, including vascular endothelial growth factor (VEGF) (reagents by Biosource, EuropeS.A; Belgium), monocyte chemoattractant protein 1 (MCP-1) (reagents by Vector Best; Novosibirsk) and total endothelin (reagents by BiomedicaGruppe; Austria). ELISA assays were performed in a StatFax 2100 microplate reader (Awareness Technology Inc.; USA). We also measured the levels of IL6, IL12 and tumor necrosis factor α (TNFα) using the kits by Biosource, EuropeS.A, Belgium. Circulating endothelial cells (CEC) were counted by phase-contrast microscopy using a method proposed by J. Hladovec and modified by N. Petrischev [7]. The severity of inflammation was inferred from C-reactive protein (CRP) levels measured by solid-phase enzyme immunoassay (Vector Best; Novosibirsk). Hemostasis dynamics were assessed based on fibrinogen levels, the prothrombin time (PT), the prothrombin index (PI), the activated partial thromboplastin time (APTT), and platelet count. Some factors of endothelial dysfunction are described in Table 1.

Fasting blood samples were collected from central or peripheral veins at 8 am. The tests were performed on days 1, 3, 5, 15, 30, and 45 following the injury. The number of patients fluctuated at different stages of the study because some of them were admitted to the hospital later than 1 day after the injury, some were discharged when their condition had improved, and some died. All of them received treatment according to the standard procedures for burn care adopted in the hospital.

Blood samples of 20 healthy volunteers were used as a control. Of those individuals, 12 were men and 8 women with a mean age of 37.5 ± 18.4 years.

Statistical analysis

The obtained data were processed in Statistica v10.0 (StatSoft; USA) and expressed as a mean and a standard deviation from the mean (M ± σ). The groups were compared using Student's t-test, which is usually applied to the samples with normal distribution. Differences were considered significant at $p \leq 0.05$, a standard value used in medical and biological research. The distribution type was determined by the Shapiro-Wilk test. The distribution in the sample was considered normal at $p > 0.05$.

RESULTS

Coagulation parameters were quite stable during the entire post-injury period. Over time, though, PI started to decline gradually, whereas PT and APTT started to grow. This may have been caused by the depletion of protein reserve, infusion therapy and antithrombotic agents.

The levels of fibrinogen, one of the acute-phase proteins, peaked on day 7 (5.6 ± 2.2 g/L) during the acute autointoxication phase.

The dynamics of platelet levels were different. The highest platelet count was observed on days 15 through 30 (555.3 ± 344.9 • 10^9/L). Platelets were also significantly elevated in the survivors, in contrast to non-survivors.

The most pronounced hemostatic changes were seen during the acute autointoxication phase or sepsis (days 7 through 15). That period was marked by hypercoagulation and an increasing risk of thromboembolic complications (Table 2).

The highest concentrations of proinflammatory cytokines and acute-phase mediators (TNFα, CRP, IL6) were observed on days 3 through 7, corresponding to the acute autointoxication phase of the burn injury (Table 3).

In contrast, the levels of IL12, which stimulates proliferation and differentiation of lymphocytes, reached their peak in the recovering patients (131.3 ± 70.7 pg/mL) and demonstrated the lowest values in the acute autointoxication phase or sepsis (35.7 ± 22.9 pg/mL).

Table 1. Markers of endothelial dysfunction

Name	Description
VEGF	A potent angiogenic and mitogenic factor; its levels rise in response to hypoxia or cancer, during wound healing or gestosis. It is secreted by endothelial cells, macrophages, fibroblasts, and some other cells [8]
CEC	CEC levels rise in response to vascular endothelial damage, increased necrosis of endothelial cells, hypoxia, sepsis, sever intoxication, atherosclerosis, other cardiovascular diseases, and gestosis [9]
Endothelin	ET is involved in the local regulation of vascular tone. It is an antagonist of endothelium-derived relaxing factor NO and an indirect indicator of its activity. Contributes to the progression of cardiovascular pathology and is involved into blood flow centralization during massive blood loss. ET is secreted by endothelial cells [10, 11]

Monocyte chemoattractant protein 1 (chemokine) is secreted by a variety of cells, including fibroblasts, endothelial cells and macrophages and recruits monocytes to an inflammation site. MCP-1 had two peaks: during acute autointoxication (381.7 ± 560.49 pg/mL) and during recovery (514.7 ± 740.9 pg/mL). The second peak was more pronounced.

The highest concentrations of endothelial dysfunction markers were observed on days 3–7. On day 7, VEGF rose 30-fold, in comparison with the controls (828.9 ± 993.2 pg/mL). That period was also marked by an elevated blood plasma count of desquamated endothelial cells (as high as 5.9 ± 6.0 • 10^9/L; Table 4). This suggests acute hypoxia of the endothelium, its intense desquamation and increased apoptosis or necrosis.

The concentrations of cytokines and endothelial dysfunction markers were compared in the patients with normal coagulation and coagulopathy. Hypocoagulation was inferred from APTT > 35 s and PI < 85% (Tables 5, 6). Decreased coagulation co-occurred with significantly increased levels of acute-phase proteins (CRP, IL6, TNFα), VEGF, CEC, and low (in comparison with patients with normal coagulation) IL12, MCP-1, and endothelin.

DISCUSSION

We have found that a rise in the levels of proinflammatory cytokines co-occurs with coagulopathy and an increase in endothelial dysfunction markers. Previously, we studied cytokine concentrations in patients with thermal burn injuries of different severity and noticed that endothelial dysfunction markers followed a phase pattern. Those markers rose significantly in patients with mild and moderate burns, peaked in patients with severe but not fatal burn injuries, and declined in the end stage of MODS in non-survivors [12]. It is known that endothelial dysfunction triggers activation of prothrombotic mechanisms and increases coagulability, promoting disseminated intravascular blood coagulation. Compromised vessel wall integrity results in the hyperproduction of endothelin, which stimulates activation of all phases of hemostasis; endothelin levels rise in patients with severe trauma [13, 14].

Our findings suggest that the levels of proinflammatory cytokines and endothelial dysfunction factors in severe burn injuries are inversely proportional.

Table 2. Hemostasis dynamics in patients with burn injuries, M ± σ

Parameter	Day 1 $n = 50$	Day 3 $n = 51$	Day 7 $n = 49$	Day 15 $n = 40$	Day 30 $n = 36$	Day 45 $n = 19$	Controls $n = 20$
APTT, s	39.6 ± 25.4 ($p_к = 0.02$)^к	41.4 ± 17.7 ($p = 0.5$; $p_к = 0.05$)	41.9 ± 25.3 ($p = 0.88$; $p_к = 0.03$)^к	40.2 ± 27.0 ($p = 0.48$; $p_к = 0.27$)	50.4 ± 31.4 ($p = 0.001$; $p_к = 0.03$)*^{к}	51.8 ± 34.1 ($p = 0.80$; $p_к = 0.04$)^к	26.2 ± 2.8
PI, %	90.9 ± 14.1 ($p_к = 0.25$)	86.5 ± 13.3 ($p = 0.03$; $p_к = 0.02$)*^{к}	83.6 ± 15.4 ($p = 0.09$; $p_к = 0.01$)^к	83.1 ± 16.5 ($p = 0.86$; $p_к = 0.01$)^к	82.3 ± 17.5 ($p = 0.07$; $p_к = 0.01$)^к	82.9 ± 19.4 ($p = 0.82$; $p_к = 0.03$)^к	101.1 ± 6.3
PT, s	19.5 ± 6.3 ($p_к = 0.04$)^к	22.2 ± 17.6 ($p = 0.22$; $p_к = 0.04$)^к	22.3 ± 10.0 $p = 0.82$; $p_к = 0.03$)	21.8 ± 8.0 ($p = 0.96$; $p_к = 0.01$)^к	24.9 ± 21.4 ($p = 0.11$; $p_к = 0.04$)^к	22.9 ± 13.5 ($p = 0.52$; $p_к = 0.04$)^к	12.6 ± 0.9
Fibrinogen, g/L	3.4 ± 1.4 ($p_к = 0.11$)	5.2 ± 2.0 ($p = 0.001$; $p_к = 0.04$)*^{к}	5.6 ± 2.2 ($p = 0.43$; $p_к = 0.001$)^к	5.0 ± 2.1 ($p = 0.06$; $p_к = 0.001$)^к	4.7 ± 1.8 ($p = 0.22$; $p_к = 0.001$)^к	4.2 ± 1.7 ($p = 0.03$; $p_к = 0.05$)	3.3 ± 0.69
Platelets, • 10^9/L	319.6 ± 197.0 ($p_к = 0.27$)	209 ± 122.9 ($p = 0.001$; $p_к = 0.47$)*	316.0 ± 214.6 ($p = 0.001$; $p_к = 0.09$)*	555.3 ± 344.9 ($p = 0.001$; $p_к = 0.04$)*^{к}	467.8 ± 237.9 ($p = 0.04$; $p_к = 0.03$)*^{к}	454.3 ± 294.4 ($p = 0.03$; $p_к = 0.03$)^к	230.4 ± 224.9

Note: p — the specified and the previous stages of the study are compared; * — the differences between the specified and the previous stages of the study are significant ($p < 0.05$); $p_к$ — the patients compared to the controls at the specified stage of the study; ^{к} — the differences between the patients and the controls are significant ($p < 0.05$).

Table 3. Cytokine dynamics in patients with burn injuries, M ± σ

Parameter	Day 1 $n = 50$	Day 3 $n = 51$	Day 7 $n = 49$	Day 15 $n = 40$	Day 30 $n = 36$	Day 45 $n = 19$	Controls $n = 20$
TNFα, pg/mL	42.3 ± 46.6 ($p_к = 0.04$)^к	32.2 ± 99.3 ($p = 0.79$; $p_к = 0.03$)^к	41.4 ± 111.9 ($p = 0.85$; $p_к = 0.02$)^к	17.8 ± 47.9 ($p = 0.45$; $p_к = 0.03$)^к	3.9 ± 9.6 ($p = 0.26$; $p_к = 0.003$)^к	8.2 ± 12.1 ($p = 0.30$; $p_к = 0.01$)^к	0.2 ± 0.3
IL6, pg/mL	114.1 ± 172.8 ($p_к = 0.008$)^к	264.4 ± 131.2 ($p = 0.05$; $p_к = 0.001$)^к	203.8 ± 180.9 ($p = 0.39$; $p_к = 0.001$)^к	67.8 ± 63.4 ($p = 0.07$; $p_к = 0.001$)^к	49.0 ± 35.9 ($p = 0.51$; $p_к = 0.001$)^к	68.9 ± 66.3 ($p = 0.51$; $p_к = 0.001$)^к	4.2 ± 3.1
IL12, pg/mL	46.9 ± 53.8 ($p_к = 0.001$)^к	39.4 ± 32.9 ($p = 0.63$; $p_к = 0.001$)^к	35.7 ± 22.9 ($p = 0.45$; $p_к = 0.001$)^к	54.9 ± 41.0 ($p = 0.03$; $p_к = 0.001$)*^{к}	81.3 ± 50.0 ($p = 0.06$; $p_к = 0.001$)^к	131.3 ± 70.7 ($p = 0.02$; $p_к = 0.001$)^к*	3.1 ± 3.2
C-reactive protein, nmol/mL	43.2 ± 46.6 ($p_к = 0.001$)^к	128.1 ± 49.6 ($p = 0.001$; $p_к = 0.001$)*^{к}	128.3 ± 52.4 ($p = 0.93$; $p_к = 0.001$)^к	85.1 ± 41.7 ($p = 0.001$; $p_к = 0.001$)*^{к}	81.9 ± 34.1 ($p = 0.79$; $p_к = 0.001$)^к	110.3 ± 57.7 ($p = 0.08$; $p_к = 0.001$)^к	1.2 ± 1.1
MCP-1, pg/ml	198.9 ± 191.7 ($p_к = 0.001$)^к	319.1 ± 238.3 ($p = 0.04$; $p_к = 0.001$)*^{к}	381.7 ± 560.49 ($p = 0.5$; $p_к = 0.009$)^к	229.9 ± 210.3 ($p = 0.11$; $p_к = 0.001$)^к	287.1 ± 231.9 ($p = 0.29$; $p_к = 0.001$)^к	514.7 ± 740.9 ($p = 0.11$; $p_к = 0.009$)^к	44.1 ± 36.5

Note: p — the specified and the previous stages of the study are compared; * — the differences between the specified and the previous stages of the study are significant ($p < 0.05$); $p_к$ — the patients compared to the controls at the specified stage of the study; ^{к} — the differences between the patients and the controls are significant ($p < 0.05$).

Table 4. Dynamics of endothelial dysfunction markers in patients with burn injuries, M ± σ

Parameter	Day 1 $n = 50$	Day 3 $n = 51$	Day 7 $n = 49$	Day 15 $n = 40$	Day 30 $n = 36$	Day 45 $n = 19$	Controls $n = 20$
VEGF, pg/mL	546.4 ± 692.8 ($p_к = 0.02$)^к	476.4 ± 626.9 ($p = 0.68$; $p_к = 0.003$)^к	828.9 ± 993.2 ($p = 0.06$; $p_к = 0.001$)^к	544.4 ± 570.9 ($p = 0.11$; $p_к = 0.001$)^к	505.6 ± 551.1 ($p = 0.77$; $p_к = 0.001$)^к	958.1 ± 1025.6 ($p = 0.04$; $p_к = 0.001$)*^{к}	28.7 ± 15.7
Endothelin, fmol/mL	3.2 ± 3.2 ($p_к = 0.001$)^к	3.0 ± 1.7 ($p = 0.88$; $p_к = 0.001$)^к	2.97 ± 1.32 ($p = 0.76$; $p_к = 0.001$)^к	2.4 ± 1.2 ($p = 0.11$; $p_к = 0.001$)^к	2.3 ± 1.1 ($p = 0.71$; $p_к = 0.001$)^к	2.4 ± 1.3 ($p = 0.93$; $p_к = 0.001$)^к	0.42 ± 0.4
CEC, 10^4/L	3.3 ± 2.5 ($p_к = 0.48$)	4.7 ± 3.3 ($p = 0.09$; $p_к = 0.05$)	5.9 ± 4.9 ($p = 0.28$; $p_к = 0.03$)^к	6.4 ± 6.0 ($p = 0.62$; $p_к = 0.04$)^к	3.7 ± 3.1 ($p = 0.02$; $p_к = 0.29$)*	2.9 ± 1.6 ($p = 0.33$; $p_к = 0.78$)	2.8 ± 1.9

Note: p — the specified and the previous stages of the study are compared; * — the differences between the specified and the previous stages of the study are significant ($p < 0.05$); $p_к$ — the patients compared to the controls at the specified stage of the study; ^{к} — the differences between the patients and the controls are significant ($p < 0.05$).

Table 5. Differences in the values of blood coagulation parameters in burn patients with normal coagulation and coagulopathy, M ± σ

Group	APTT, s	PT, s	PI, %	Fibrinogen, g/L	Platelets, • 10^9/L
Normal coagulation	31.3 ± 2.9	19.0 ± 3.6	89.1 ± 13.4	4.2 ± 1.2	391.5 ± 215.4
Hypocoagulation	54.5 ± 27.9 (p = 0.001)*	20.9 ± 5.0 (p = 0.01)*	81.8 ± 12.8 (p = 0.001)*	4.9 ± 1.4 (p = 0.001)*	391.2 ± 216.9 (p = 0.99)

Note: * — the difference between the two groups is significant ($p < 0.05$).

Table 6. Differences in the levels of cytokines and endothelial dysfunction markers in burn patients with normal coagulation and coagulopathy, M ± σ

Group	CRP, nmol/mL	IL6, pg/mL	TNF, pg/mL	IL12, pg/mL	MCP-1, pg/mL	VEGF, pg/mL	ET, fmol/mL	CEC, • 10^4/L
Normal coagulation	75.0 ± 49.1	50.3 ± 63.9	9.1 ± 28.5	68.6 ± 55.6	308.2 ± 231.6	578.5 ± 523.9	2.96 ± 2.7	4.4 ± 3.6
Hypocoagulation	97.4 ± 47.7 (p = 0.04)*	145.2 ± 138.3 (p = 0.35)	45.5 ± 114.3 (p = 0.10)	48.3 ± 46.4 (p = 0.08)	252.8 ± 238.2 (p = 0.26)	712.3 ± 745.0 (p = 0.35)	2.41 ± 1.3 (p = 0.21)	5.0 ± 4.9 (p = 0.37)

Note: * — the difference between the two groups is significant ($p < 0.05$).

Cytokines stimulate production of free radicals, lysosomal enzymes and cationic proteins by phagocytes and cytotoxic lymphocytes and activate humoral factors (complement components, properdin, kinins), causing endothelial dysfunction. In response, endothelial cells secrete autocrine and paracrine regulatory factors, such as VEGF and endothelin. When activated by proinflammatory cytokines, endothelial cells increase expression of adhesion molecules and launch degranulation of Weibel-Palade bodies (vesicles inside a vascular endothelial cells), thereby destabilizing the endothelial lining, reducing resistance to blood clotting and increasing permeability of blood vessels [15]. Damage to the vascular endothelium results in excessive cell desquamation. Growing VEGF concentrations aim to regulate neoangiogenesis in response to the endothelial damage induced by hypoxia in the acute autointoxication phase of burn injury and to promote tissue regeneration in the recovery period (days 30–45) [13]. Most likely, the function of the inducible NO synthase is also altered significantly, because there is evidence that blood NO metabolites decline following thermal injury [16]. Therefore, a rise in endothelin levels could be compensatory. Also, there are reports that this factor participates in blood flow centralization in other severe pathologies [10].

Growing concentrations of those damaging factors promote endothelial dysfunction and energy deficit, impair protein synthesis and contribute to the inhibition of procoagulant properties of proteins, eventually leading to hypercoagulation. The syndrome of disseminated intravascular blood coagulation developed by most patients with severe burns leads to a reduction in the plasma levels of coagulation factors. Besides, a deficit of amino acids is observed that are increasingly utilized to maintain tissue regeneration.

CONCLUSIONS

Our findings demonstrate that thermal burns affect the structure and function of the vascular endothelium. Those changes are a manifestation of the systemic inflammatory response accompanied by the presence of highly specific markers of endothelial dysfunction in the blood. In patients with severe burns, the correlation between the levels of proinflammatory cytokines and functional parameters of hemostasis is inversely proportional. Further research is needed to investigate the relationship between hemostatic impairment and endothelial dysfunction in patients with severe trauma in general and burn injury in particular.

References

1. Dumnicka P, Maduzia D, Ceranowicz P, et al. The Interplay between Inflammation, Coagulation and Endothelial Injury in the Early Phase of Acute Pancreatitis: Clinical Implications. Int J Mol Sci. 2017; 18 (2): E354. DOI: 10.3390/ijms18020354. PubMed PMID: 28208708.
2. Alekseev AA, Ushakova TA, Krutikov MG, Bobrovnikov AYe. Markery sepsisa v diagnostike adaptivnogo vospalenija pri ozhogovoj travme. Lechenie i profilaktika. 2015; 2 (14): 84–91. Russian.
3. Ushakova TA. Adaptacija k ozhogovoj travme: problemy i perspektivy. Kombustiologija. 2009; 39. Dostupno po ssylke: www.combustiolog.ru (data obrashhenija 23.06.2018). Russian.
4. Chousterman BG, Swirski FK, Weber GF. Cytokine storm and sepsis disease pathogenesis. Semin Immunopathol. 2017; 39 (5): 517–28.
5. Ince C, Mayeux PR, Nguyen T, et al. The endothelium in sepsis. Shock. 2016; 45 (3): 259–70.
6. Abdel-Hafez NM, Saleh Hassan Y, El-Metwally TH. A study on biomarkers, cytokines, and growth factors in children with burn injuries. Ann Burns Fire Disasters. 2007; 20 (2): 89–100.
7. Petrishhev NN, Berkovich OA, Vlasov TD i dr. Diagnosticheskaja cennost' opredelenija deskvamirovannyh jendotelial'nyh kletok v krovi. Klinicheskaja laboratornaja diagnostika. 2001; (1): 50–2. Russian.
8. Gavrilenko TI, Ryzhkova NA, Parhomenko AN. Sosudistyj jendotelial'nyj faktor rosta v klinike vnutrennih zabolevanij i ego patogeneticheskoe znachenie. Ukraïns'kij kardiologichnij zhurnal. 2011; (4): 87–95. Russian.
9. Erdbruegger U, Haubitez M, Woywodt A. Circulating endothelial cells: a novel marker of endothelial damage. Clinica Chimica Acta. 2006; (373): 17–26.
10. Dremina NN, Shurygin MG, Shurygina IA. Jendoteliny v norme i patologii. Mezhdunarodnyj zhurnal prikladnyh i fundamental'nyh issledovanij. 2016; (10): 210–14. Russian.
11. Yanagisawa M, Masaki T. Molecular biology and biochemistry of the endothelins. Trends Pharmacol Sci. 1989; 10 (9): 374–8.
12. Morrison VV, Bozhedomov AYu. Disfunkcija jendotelija pri sindrome poliorgannoj nedostatochnosti u bol'nyh s termicheskoj travmoj. Regionarnoe krovoobrashhenie i mikrocirkuljacija. 2013; 2 (46): 43–8. Russian.
13. Iba T, Kidokoro A, Fukunaga M, et al. Association between the severity of sepsis and the changes in hemostatic molecular markers and vascular endothelial damage markers. Shock. 2005; 23 (1): 25–9.
14. Firsov SA, Matveev RP. Jendotelial'naja disfunkcija i ee prognosticheskoe znachenie pri kriticheskih sostojanijah v rezul'tate dorozhno-transportnogo travmatizma. Sovremennye problemy nauki i obrazovanija. 2014; 6. Dostupno po ssylke: http://science-education.ru/ru/article/view?id=16629 (data obrashhenija: 24.03.2019). Russian.

15. Scharpfenecker M, Fiedler U, Reiss Y, Augustin HG. The Tie-2 ligandangiopoietin-2 destabilizes quiescent endothelium through an internal autocrine loop mechanism. J Cell Sci. 2005; 118 (4): 771–80.
16. Abo El-Noor MM, Elgazzar FM, Alshenawy HA. Role of inducible nitric oxide synthase and interleukin-6 expression in estimation of skin burn age and vitality. J Forensic Leg Med. 2017; (52): 148–53.

Литература

1. Dumnicka P, Maduzia D, Ceranowicz P, et al. The Interplay between Inflammation, Coagulation and Endothelial Injury in the Early Phase of Acute Pancreatitis: Clinical Implications. Int J Mol Sci. 2017; 18 (2): E354. DOI: 10.3390/ijms18020354. PubMed PMID: 28208708.
2. Алексеев А. А., Ушакова Т. А., Крутиков М. Г., Бобровников А. Э. Маркеры сепсиса в диагностике адаптивного воспаления при ожоговой травме. Лечение и профилактика. 2015; 2 (14): 84–91.
3. Ушакова Т. А. Адаптация к ожоговой травме: проблемы и перспективы. Комбустиология. 2009; 39. Доступно по ссылке: www.combustiolog.ru (дата обращения 23.06.2018).
4. Chousterman BG, Swirski FK, Weber GF. Cytokine storm and sepsis disease pathogenesis. Semin Immunopathol. 2017; 39 (5): 517–28.
5. Ince C, Mayeux PR, Nguyen T, et al. The endothelium in sepsis. Shock. 2016; 45 (3): 259–70.
6. Abdel-Hafez NM, Saleh Hassan Y, El-Metwally TH. A study on biomarkers, cytokines, and growth factors in children with burn injuries. Ann Burns Fire Disasters. 2007; 20 (2): 89–100.
7. Петрищев Н. Н., Беркович О. А., Власов Т. Д. и др. Диагностическая ценность определения десквамированных эндотелиальных клеток в крови. Клиническая лабораторная диагностика. 2001; (1): 50–2.
8. Гавриленко Т. И., Рыжкова Н. А., Пархоменко А. Н. Сосудистый эндотелиальный фактор роста в клинике внутренних заболеваний и его патогенетическое значение. Український кардіологічний журнал. 2011; (4): 87–95.
9. Erdbruegger U, Haubitez M, Woywodt A. Circulating endothelial cells: a novel marker of endothelial damage. Clinica Chimica Acta. 2006; (373): 17–26.
10. Дремина Н. Н, Шурыгин М. Г., Шурыгина И. А. Эндотелины в норме и патологии. Международный журнал прикладных и фундаментальных исследований. 2016; (10): 210–14.
11. Yanagisawa M, Masaki T. Molecular biology and biochemistry of the endothelins. Trends Pharmacol Sci. 1989; 10 (9): 374–8.
12. Моррисон В. В., Божедомов А. Ю. Дисфункция эндотелия при синдроме полиорганной недостаточности у больных с термической травмой. Регионарное кровообращение и микроциркуляция. 2013; 2 (46): 43–8.
13. Iba T, Kidokoro A, Fukunaga M, et al. Association between the severity of sepsis and the changes in hemostatic molecular markers and vascular endothelial damage markers. Shock. 2005; 23 (1): 25–9.
14. Фирсов С. А., Матвеев Р. П. Эндотелиальная дисфункция и ее прогностическое значение при критических состояниях в результате дорожно-транспортного травматизма. Современные проблемы науки и образования. 2014; 6. Доступно по ссылке: http://science-education.ru/ru/article/view?id=16629 (дата обращения: 24.03.2019).
15. Scharpfenecker M, Fiedler U, Reiss Y, Augustin HG. The Tie-2 ligandangiopoietin-2 destabilizes quiescent endothelium through an internal autocrine loop mechanism. J Cell Sci. 2005; 118 (4): 771–80.
16. Abo El-Noor MM, Elgazzar FM, Alshenawy HA. Role of inducible nitric oxide synthase and interleukin-6 expression in estimation of skin burn age and vitality. J Forensic Leg Med. 2017; (52): 148–53.

OSTEOARTHRITIS OF THE KNEE IN THE ELDERLY: IS KNEE REPLACEMENT ALWAYS JUSTIFIED?

Lychagin AV, Garkavi AV ✉, Meshcheryakov VA, Kaykov VS

Faculty of General Medicine, I. M. Sechenov First Moscow State Medical University, Moscow, Russia

Osteoarthritis is a condition that mostly affects the elderly population and tends to be localized to the knee joint. At old age, active treatment options are limited by co-morbidities and a higher risk for surgical complications. Therefore, the search for strategies that could become a temporary alternative to knee replacement is a pressing concern. The aim of this study was to analyze how justifiable is total knee replacement in elderly patients with knee osteoarthritis and to propose a less aggressive therapeutic alternative to this surgery. The study included 178 patients over 60 years of age with clinically established knee osteoarthritis who had been previously recommended knee replacement but chosen not to undergo it. The choice of a treatment strategy tested in the study was based on the original grading scale for the evaluation of the knee joint dislocation syndrome. The treatment consisted of therapeutic arthroscopy and intraarticular injections of hyaluronic acid and platelet-rich plasma (PRP). The data were processed in Statistica 12. Data analysis revealed that 39.3% of the participants did not have compelling indications for knee replacement. The proposed combination therapy with intraarticular PRP injections and arthroscopy allowed all the patients to delay knee replacement for at least a year; unaided by arthroscopy, intraarticular injections worked well for only 40%.

Keywords: knee arthroplasty, total knee replacement, arthroscopy of the knee, intraarticular injection

Author contribution: Lychagin AV devised a KJDS scale, planned the study, performed arthroscopy and follow-up observation, processed and analyzed the data. Garkavi AV planned the study and proposed its design, performed arthroscopy, intraarticular injections and follow-up observation, processed and analyzed the data, and wrote the manuscript. Meshcheryakov VA performed arthroscopy, intraarticular injections and follow-up observation, surveyed the patients. Kaykov VS performed arthroscopy, intraarticular injections, and follow-up observation, surveyed the patients.

Compliance with ethical standards: this study was approved by the Ethics Committee of I. M. Sechenov First Moscow State Medical University (Protocol No. 17–18 dated 2018); the patients gave informed consent to participate.

✉ **Correspondence should be addressed:** Andrey V. Garkavi
Trubetskaya 8, bld. 2, Moscow, 119991; Avgar22@yandex.ru

Received: 13.09.2018 **Accepted:** 25.03.2019 **Published online:** 06.04.2019

DOI: 10.24075/brsmu.2019.020

ОСТЕОАРТРОЗ КОЛЕННОГО СУСТАВА У ПОЖИЛЫХ — ВСЕГДА ЛИ ОПРАВДАНО ЭНДОПРОТЕЗИРОВАНИЕ?

А. В. Лычагин, А. В. Гаркави ✉, В. А. Мещеряков, В. С. Кайков

Лечебный факультет, Первый московский государственный медицинский университет имени И. М. Сеченова (Сеченовский Университет), Москва, Россия

Остеоартроз — заболевание преимущественно пожилых людей, и по локализации первое место уверенно удерживает коленный сустав. Именно в пожилом и старческом возрасте возможность активного лечения пациентов с гонартрозом ограничена их полиморбидностью, а также повышенным операционным риском. Поэтому весьма актуален поиск методик лечения, способных хотя бы на время стать альтернативой эндопротезированию коленного сустава. Целью исследования было проанализировать оправданность операции эндопротезирования коленного сустава у пациентов пожилого и старческого возраста с гонартрозом и разработать комплексную систему лечения, сохраняющую сустав. В исследовании участвовали 178 пациентов старше 60 лет, которым ранее было предложено, но не выполнено эндопротезирование коленного сустава по поводу верифицированного гонартроза. Для определения лечебной тактики использовали оригинальную балльную систему оценки дислокационного синдрома коленного сустава. Применяли сочетание санационной артроскопии с внутрисуставным введением гиалуроновой кислоты и обогащенной тромбоцитами аутоплазмы (PRP). Для анализа результатов определяли статистическую значимость отмеченных отличий по стандартному пакету программ «Statistica 12.0». Показано, что 39,3% пациентов эндопротезирование было предложено без достаточных объективных оснований. Проведение комплексного лечения, сочетающего внутрисуставную PRP-терапию с предварительно проведенной санационной артроскопией, стало альтернативой эндопротезированию для всех пациентов как минимум на год, а внутрисуставная терапия без артроскопии — только для 40%.

Ключевые слова: эндопротезирование коленного сустава, артроскопия, внутрисуставная инъекционная терапия

Информация о вкладе авторов: А. В. Лычагин — создание шкалы оценки степени ДСКС, планирование исследования, выполнение операций артроскопии, послеоперационное наблюдение, систематизация и анализ результатов; А. В. Гаркави — планирование и создание дизайна исследования, операции артроскопии, внутрисуставные инъекции, наблюдение пациентов в динамике, систематизация и анализ результатов, оформление статьи; В. А. Мещеряков — артроскопия, внутрисуставные инъекции, наблюдение и анкетирование пациентов; В. С. Кайков — артроскопия, внутрисуставные инъекции, наблюдение и анкетирование пациентов.

Соблюдение этических стандартов: исследование одобрено этическим комитетом ФГАОУ ВО Первый МГМУ им. И. М. Сеченова (протокол № 17–18, 2018 г.); все пациенты подписали добровольное информированное согласие на участие в проводимом исследовании.

✉ **Для корреспонденции:** Андрей Владимирович Гаркави
ул. Трубецкая, д. 8, стр. 2, г. Москва, 119991; Avgar22@yandex.ru

Статья получена: 13.09.2018 **Статья принята к печати:** 25.03.2019 **Опубликована онлайн:** 06.04.2019

DOI: 10.24075/vrgmu.2019.020

Osteoarthritis of the knee is one of the most common orthopedic conditions. Presenting with pain and the loss of joint function, it debilitates the patient leaving them unable to engage in the usual daily activities. Most typically, osteoarthritis affects the elderly, causing a dramatic impact on their social life, making them dependent on others and leading to depression [1–5].

On the one hand, conservative treatment of knee osteoarthritis in elderly patients with marked age-related changes in the joint merely seeks to achieve temporary relief. On the other hand, advances in arthroplasty techniques have made knee replacement safer, less traumatic and more available [6–12].

In recent years, arthroplasty in the elderly has been on the rise because the indications for this procedure have been expanded [13–15]. Sometimes, the severity of medically diagnosed knee osteoarthritis seems to leave no other option for an aging patient but a knee replacement; other, less aggressive treatments, such as arthroscopy, systemic medication therapy, intraarticular injections, or physical rehabilitation, are not even considered by the physician. But if we really think about it, doesn't it deprive patients of the chance to avoid a surgical intervention that, in spite of the advances in the medical science, still poses certain health risks [16, 17]?

Unfortunately, there is no universal approach to establishing compelling indications for endoprosthetic knee replacement; therefore, this surgery may not always be a reasonable or adequate therapeutic option.

The aim of this study was to analyze how justifiable is total knee replacement (TKR) in elderly patients with knee osteoarthritis and to propose a less aggressive alternative to this surgery.

METHODS

We had 178 retired patients aged 60 to 82 years in our care who had been previously offered to undergo TKR but chosen not to for a variety of reasons (fear of surgery, a long waiting list, etc.). The patients agreed to try an alternative treatment strategy and then revisit the idea of surgery. The study included patients aged over 60 years with a previously established diagnosis of knee osteoarthritis and a recommendation to have knee replacement surgery, who gave written informed consent to try a different treatment strategy developed by the authors of this work. The treatment course and the follow-up observation period lasted for 1 year each. The following exclusion criteria were applied: severe comorbidities that significantly limited patients' ability to walk or were a direct contraindication for the offered rehabilitation; intraarticular fractures with persisting joint incongruence; failure to cooperate.

The grading scale proposed by Lychagin AV [18] was applied to determine the severity of the knee joint dislocation syndrome (KJDS) in the examined patients. The following parameters were evaluated: degeneration of the articular cartilage, paraarticular bone damage, joint instability, the narrowing of the joint space, and the total WOMAC score. Each parameter was scored on a scale of 0 to 4; the maximum total score was 20 points.

The total of 0–5 points scored on this scale suggested that a patient could benefit from a conservative medication therapy; 6–12 points, a complex treatment including arthroscopy and intraarticular injections should be offered; 13–20 points, a patient should be advised to undergo TKR.

Of 178 patients with stage II/III knee osteoarthritis (according to Kellgren–Lawrence classification) who had been recommended to undergo TKR, only 108 (60.7%) scored 13 points

Table 1. The evaluation of the severity of the knee joint dislocation syndrome (KJDS) expressed in points

Changes to the anatomy or function	Severity of pathology	Score (points)
Articular cartilage (classification by ICRS) evaluated by MRI or arthroscopy	normal	0
	Grade 1–2	1
	Grade 3	2
	Grade 4 (slight defect < 2.5 cm^2)	3
	Grade 4 (significant defect > 2.5 cm^2)	4
Paraarticular bone region	– normal	0
	– osteoporosis	1
	– cysts	2
	– mild bone deformity	3
	– pronounced bone deformity	4
Joint instability	No instability detected	0
	Compensated (grade 1)	1
	Subcompensated (grade 2)	2
	Uncompensated (grade 3)	3
	Arthrogenic contractures	4
Narrowing of the joint space (%)	0–5	0
	6–30	1
	31–50	2
	51–75	3
	76–100	4
WOMAC score (points)	≤ 30	0
	31–50	1
	51–70	2
	71–90	3
	> 90	4

and above; this confirms that surgery is justifiable for such patients (Fig. 1).

The patients were distributed into 3 groups. Group 1 consisted of 54 patients who received intraarticular platelet-rich plasma (PRP) injections; group 2 was constituted by 64 individuals who received intraarticular injections of hyaluronic acid. The patients from group 3 received systemic medication therapy (chondroprotective agents + non-steroidal anti-inflammatories).

Knee arthroscopy was performed on 118 patients who had scored 6 or more points on the KJDS scale. Of them 32 (59.3%) were from group 1, 44 (68.8%) from group 2, and 42 (70.0%) from group 3 (Fig. 2).

RESULTS

The patients were divided into several groups based on the severity of osteoarthritis. The severity of the condition was inferred from their total KJDS scores that reliably showed whether the patient needed knee replacement; unlike this scale, radiographic findings do not always correlate with patients' complaints of pain and decreasing lifestyle, so we did not use them as a criterium. Of 178 patients who had been recommended TKR, as many as 70 turned to have no compelling indication for surgery (Table 2).

This, however, does not mean that by the end of observation the patients were fully determined to never revisit the idea of a surgical intervention, but rather suggests that they were satisfied with the outcomes of an alternative treatment strategy for the time being and did not intend to have TKR in the nearest future.

Of 70 patients who had been offered to undergo TKR without having a compelling indication for it (KJDS < 13 points), only 15 (21.4%) still thought that surgery would be beneficial for them, even after completing the treatment course. Those were mostly patients from group 3 (no intraarticular injections administered): 13 individuals out of 28, or 46.4%. All patients from group 1 (100%) and 22 patients from group 2 (91.7%) decided they no longer wanted knee replacement (Fig. 3).

Of 108 patients with severe articular damage and indications for TKR (KJDS ≥ 13 points), 39 (36.1%) still thought about having surgery after completing the treatment course. Therefore, it can be assumed that 69 (63.9%) patients believed that their condition had significantly improved (Fig. 4).

The patients receiving intraarticular injection therapy benefited the most from the treatment course and saw it as a real alternative to surgery (86.1% in group 1 and 77.5% in group 2). At the same time in group 3, 25 of 32 patients (78.1%) still considered TKR as an option because they were not satisfied with the result, although 90.6% of those patients had received therapeutic arthroscopy.

DISCUSSION

The efficacy of intraarticular injections and therapeutic arthroscopy at the onset of treatment can be assessed separately or in combination with each other.

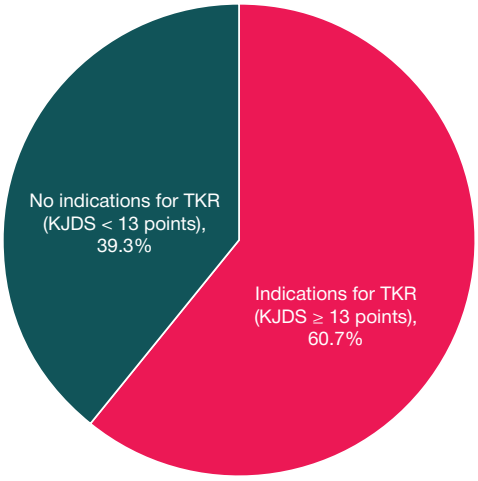

Fig. 1. Indications for knee replacement based on the KJDS score in patients who had been previously recommended to undergo TKR

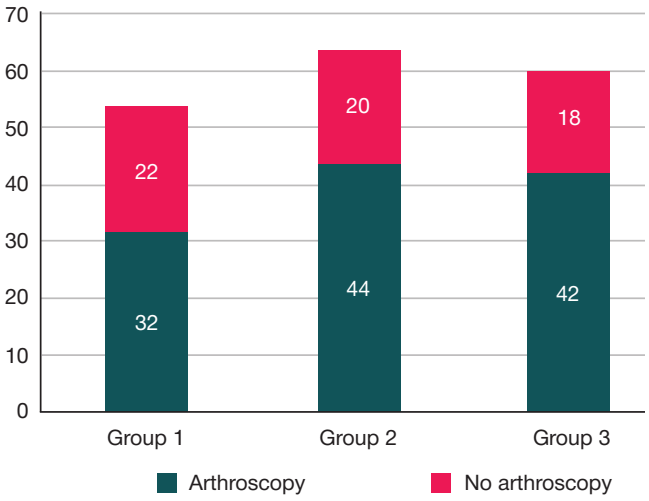

Fig. 2. The distribution of patients based on therapeutic arthroscopy

Table 2. Patients' attitude to TKR a year after completing the suggested treatment course

	Number of patients who agreed to try a different treatment strategy instead of TKR		Number of patients who received therapeutic arthroscopy		Number of patients who did not receive therapeutic arthroscopy	
			Total	Of them, number of patients willing to reconsider TKR after completing the treatment course	Total	Of them, number of patients willing to reconsider TKR after completing the treatment course
Group 1 (*n* = 54)	No compelling indication for TKR	18	5	0	13	0
	TKR justified	36	27	0	9	5 (55.6%)
Group 2 (*n* = 64)	No compelling indication for TKR	24	15	0	9	2 (22.2%)
	TKR justified	40	29	2 (6.9%)	11	7 (63.6%)
Group 3 (*n* = 60)	No compelling indication for TKR	28	13	4 (30.8%)	15	9 (60.0%)
	TKR justified	32	29	22 (75.9%)	3	3 (100%)
Total (*n* = 178)	No compelling indication for TKR	70	33	4 (12.1%)	37	11 (29.7%)
	TKR justified	108	85	24 (28.2%)	23	15 (65.2%)

If we look at the efficacy of intraarticular injections alone, we should note that of 118 patients from groups 1 and 2, who had previously considered a possibility of surgical intervention, 42 had no compelling indications for surgery. After completing a course of intraarticular PRP or hyaluronic acid injections, only 2 (4.8%) patients still thought of undergoing TKN versus 13 (46.4%) out of 28 patients in group 3 who had no injection therapy.

Seventy-six patients from groups 1 and 2 had serous indications for surgery and received intraarticular injections. Of them, only 14 (18.4%) did not give up the idea of surgery after completing the treatment course.

In group 1, 32 of 54 patients received therapeutic arthroscopy. If we look at the efficacy of this procedure performed at the beginning of the treatment course, we will see that none of those 32 patients was still willing to undergo TKR a year after completing the treatment course. In group 2, 44 of 64 patients received arthroscopy, and only 2 (4.5%) of them decided they were satisfied with the result. In group 3, 42 of 60 patients received therapeutic arthroscopy, and TKR was still considered by 18 of them (42.9%) a year later, whereas 14 (77.8%) of 18 "arthroscopy-free" patients still thought they would benefit from TKR (Table 2).

Unsurprisingly, in patients who had no compelling indications for TKR, our treatment course tended to be a good alternative to surgery. After arthroscopy, 29 (87.9%) of 33 patients said they had benefited from it. The proportion of such patients in groups 1 and 2 was 100%. Thirty-seven (77.1%) of 48 patients who had not received arthroscopy were able to delay or avoid TKR; the proportion of such patients was 100% in group 1, 81.8% in group 2 and 62.5% in group 3 (Fig. 5).

Of all the patients who had objective indications for TKR, 71.7% (61 of 85 individuals) decided against after the treatment course. The proportion of such patients was 100% in group 1, 93.1% in group 2 and only 24.1% in group 3, which confirms the efficacy of intraarticular PRP injections included into the complex therapy of knee osteoarthritis. Arthroscopy was not performed in 23 patients who had objective indications for TKR. Of them, only 8 (34.8%) benefited temporarily from the suggested therapy course, more specifically intraarticular injections: 4 (44.4%) of 9 patients in group 1 and 4 (36.4%) of 11 patients in group 2 (Fig. 6).

CONCLUSIONS

1) Endoprosthetic knee replacement is often overused in elderly patients with osteoarthritis who do not have compelling indications for this surgical procedure. The KJDS grading scale proposed by Lychagin AV shows that only 60.7% of

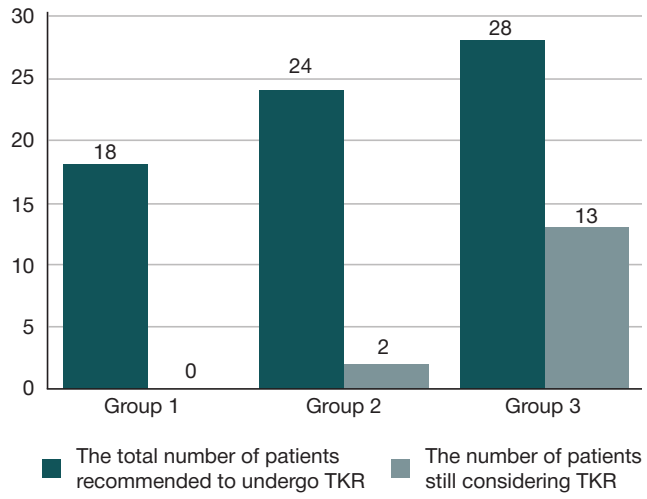

Fig. 3. The attitude of patients who had no compelling indications for TKR to this surgical intervention after completing the suggested treatment course

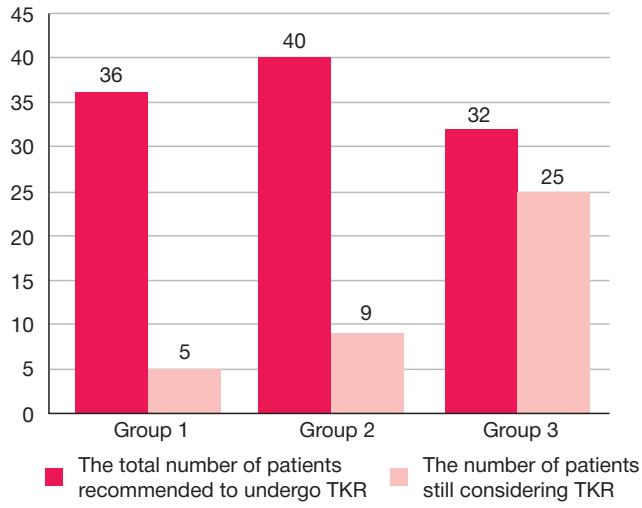

Fig. 4. The attitude of patients who had compelling indications for TKR to this surgical intervention after completing the suggested treatment course

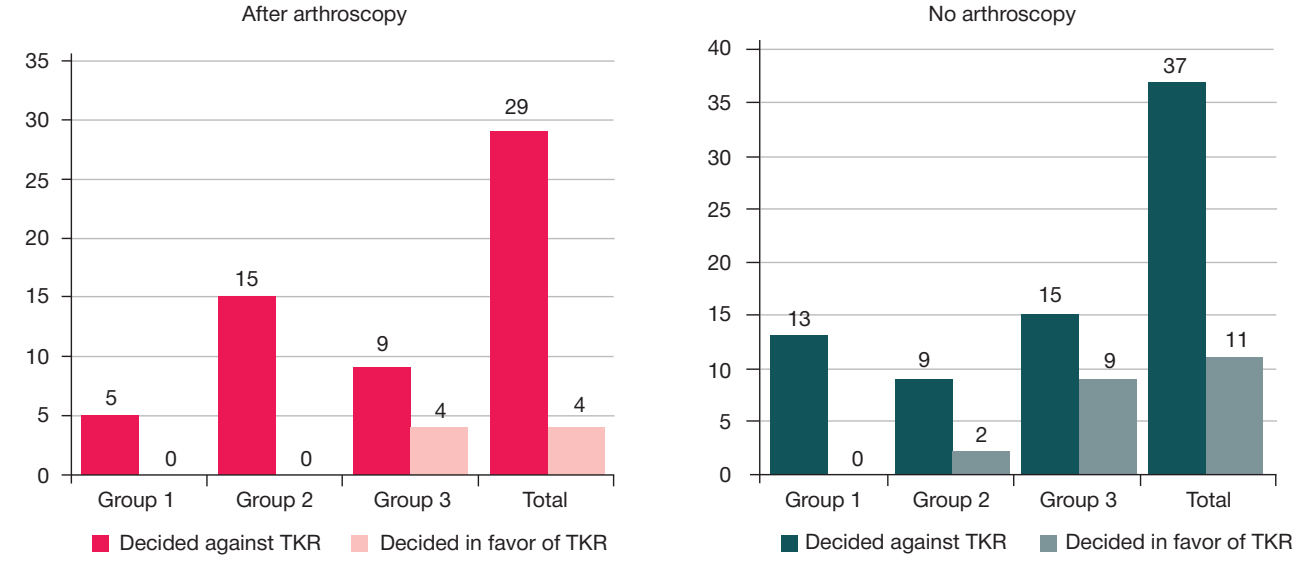

Fig. 5. The impact of arthroscopy on the attitude to TKR in patients with no compelling indication for TKR

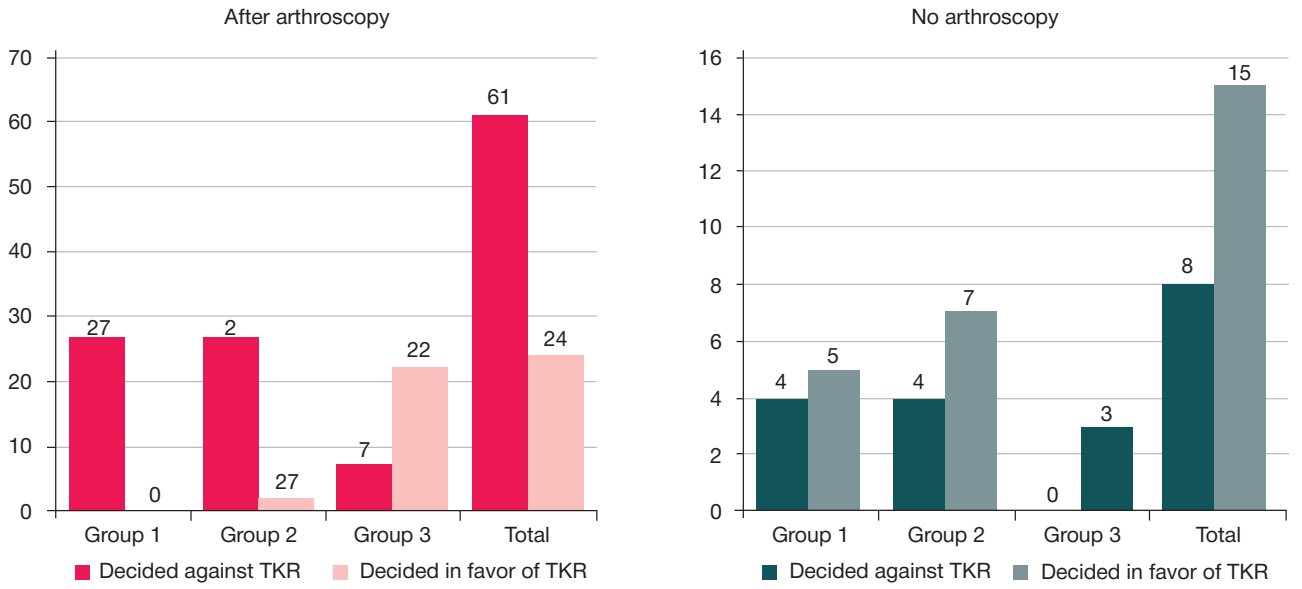

Fig. 6. The impact of arthroscopy on the attitude to TKR in patients with compelling indications for TKR

such patients have objective indications for surgery. 2) A combination therapy with arthroscopy and intraarticular PRP injections ensures durable improvement that can delay TKR for at least a year. 3) Unaided by arthroscopy, intraarticular injectins can be an alternative to knee replacement in 40.0% of patients with compelling indications for TKR.

References

1. Bragina SV, Matveev RP. Struktura stojkoj utraty trudosposobnosti u pacientov s gonartrozom. Genij ortopedii. 2011; (4): 96–100.
2. Savelova EE, Majko OYu. Kachestvo zhizni bol'nyh gonartrozom po ankete ER-50. Materialy II Vserossijskogo kongressa revmatologov Rossii. Yaroslavl', 2011 g; 68.
3. Hamroeva ZD. Ocenka klinicheskogo techeniya i osobennostej lecheniya osteoartroza u lic pozhilogo i starcheskogo vozrasta. [dissertacya]. Dushanbe, 2016.
4. Curko VV, Egorov IV, Krasnoselskij MYA. Sustavnoj sindrom u pozhilyh: Patofi-ziologiya boli i kliniko-vozrastnye aspekty terapii. Consilium Medicum. 2009; 11 (2): 2–10.
5. Shukurova SM, Hamroeva ZD, SHodiev BR. Osteoartroz kak vazhnaya problema geriatrii. Vestnik Avicenny. 2015; (1): 137–143.
6. Vignon E, Valat JP, Rossignol M, et al. Osteoarthritis of the knee and hip and activity: a systematic international review and synthesis (OASIS). Joint Bone Spine. 2006; (73): 442–55.
7. Alekseeva LI, Cvetkova ES. Osteoartroz: iz proshlogo v budushchee. Nauchno-prakticheskaya revmatologiya. 2009; (2): 31–39.
8. Batpenov ND, Bajmagambetov ShA i dr. Artroskopiya kolennogo sustava pri osteoart-roze kolennogo sustava. Materialy VII Kongressa Rossijskogo artroskopicheskogo obshchestva. M., 2007; 49.
9. Dubrov VEh, Yarema IV, Rebrov VN. Kompleksnoe lechenie degenerativno-vospalitel'nyh porazhenij kolennogo sustava u pozhilyh bol'nyh. Travmatologiya i ortopediya Rossii. 2005; (35): 49.
10. Zabolotnyh II, Zabolotnyh VA. Bolezni sustavov v pozhilom vozraste. SPb.: “Petropolis”, 2000; 144.
11. Karateev DE. Farmakoterapiya osteoartroza: ehffektivnost' i bezopasnost'. Poliklinika. 2010; (5): 74–9.
12. Sinusas K. Osteoarthritis: diagnosis and treatment. Am Fam Physician. 2012; 85 (1): 49–56.
13. Kavalerskij GM, Lychagin AV, Smetanin SM i dr. Istoricheskoe razvitie koncepcii ehndoprotezirovaniya kolennogo sustava. Kafedra travmatologii i ortopedii. 2016; (3): 16–20.
14. Tarbushkin AA. Ocenka strukturno-funkcional'nyh narushenij kolennogo sustava dlya opredeleniya pokazaniya k ehndoprotezirovaniyu pri gonartrozah [dissertaciya]. M., 2013.
15. Tihilov RM, Shubnyakov II, Kovalenko AN i dr. Dannye registra ehndoprotezirovaniya tazobedrennogo sustava RNIITO im. R. R. Vredena za 2007–2012 gody. Travmatologiya i ortopediya Rossii. 2013; (3): 167–90.
16. Sereda AP, Gricyuk AA, Zelenyak KB, Serebryakov AB. Faktory riska infekcionnyh oslozhnenij posle ehndoprotezirovaniya kolennogo sustava. Infekcii v hirurgii. 2010; 8 (4): 67–76.
17. Gioe TJ, Killeen KK, Grimm K, et al. Why are total knee replacements revised? Analysis of early revision in a community knee implant registry. Clin Orthop Relat Res. 2004; (428): 100–6.
18. Lychagin AV. Hirurgicheskoe lechenie strukturno-funkcional'nyh narushenij pri gonartroze [dissertaciya]. M., 2017.

Литература

1. Брагина С. В., Матвеев Р. П. Структура стойкой утраты трудоспособности у пациентов с гонартрозом. Гений ортопедии. 2011; (4): 96–100.
2. Савелова Е. Е., Майко О. Ю. Качество жизни больных гонартрозом по анкете ЕР-50. В сборнике: Материалы II Всероссийского конгресса ревматологов России; 26–29 апреля; Ярославль, 2011 г.; 68.
3. Хамроева З. Д. Оценка клинического течения и особенностей лечения остеоартроза у лиц пожилого и старческого возраста [диссертация]. Душанбе, 2016.
4. Цурко В. В., Егоров И. В., Красносельский М. Я. Суставной синдром у пожилых: Патофизиология боли и клинико-возрастные аспекты терапии. Consilium Medicum. 2009; 11 (2): 2–10.
5. Шукурова С. М., Хамроева З. Д., Шодиев Б. Р., Каримова Г. Н.

Остеоартроз как важная проблема гериатрии. Вестник Авиценны. 2015; (1): 137–43.
6. Vignon E, Valat JP, Rossignol M, et al. Osteoarthritis of the knee and hip and activity: a systematic international review and synthesis (OASIS). Joint Bone Spine. 2006; (73): 442–55.
7. Алексеева Л. И., Цветкова Е. С. Остеоартроз: из прошлого в будущее. Научно-практическая ревматология. 2009; (2): 31–39.
8. Батпенов Н. Д., Баймагамбетов Ш. А. и др. Артроскопия коленного сустава при остеоартрозе коленного сустава. В сборнике: Материалы VII Конгресса Российского артроскопического общества; 17–19 декабря 2007 г.; Москва. М.: 49.
9. Дубров В. Э., Ярема И. В., Ребров В. Н. Комплексное лечение дегенеративно-воспалительных поражений коленного сустава у пожилых больных. Травматология и ортопедия России. 2005; (35): 49.
10. Заболотных И. И., Заболотных В. А. Болезни суставов в пожилом возрасте. СПб.: Петрополис, 2000; 144 с.
11. Каратеев Д. Е. Фармакотерапия остеоартроза: эффективность и безопасность. Поликлиника. 2010; (5): 74–9.
12. Sinusas K. Osteoarthritis: diagnosis and treatment. Am Fam Physician. 2012; 85 (1): 49–56.
13. Кавалерский Г. М., Лычагин А. В., Сметанин С. М. и др. Историческое развитие концепции эндопротезирования коленного сустава. Кафедра травматологии и ортопедии. 2016; (3): 16–20.
14. Тарбушкин А. А. Оценка структурно-функциональных нарушений коленного сустава для определения показания к эндопротезированию при гонартрозах [диссертация] М., 2013.
15. Тихилов Р. М., Шубняков И. И., Коваленко А. Н. и др. Данные регистра эндопротезирования тазобедренного сустава РНИИТО им. Р. Р. Вредена за 2007–2012 годы. Травматология и ортопедия России. 2013; (3): 167–90.
16. Середа А. П., Грицюк А. А., Зеленяк К. Б., Серебряков А. Б. Факторы риска инфекционных осложнений после эндопротезирования коленного сустава. Инфекции в хирургии. 2010; 8 (4): 67–76.
17. Gioe TJ, Killeen KK, Grimm K, et al. Why are total knee replacements revised? Analysis of early revision in a community knee implant registry. Clin Orthop Relat Res. 2004; (428): 100–6.
18. Лычагин А. В. Хирургическое лечение структурно-функциональных нарушений при гонартрозе [диссертация]. М., 2017.

THE NEW METHOD OF PELVIC PACKING AGAINST CONTINUING INTRAPELVIC BLEEDING RESULTING FROM THE UNSTABLE PELVIC RING FRACTURES

Egiazaryan KA[1], Gordienko DI[1], Starchik DA[2], Lysko AM[1]✉

[1] Pirogov Russian National Research Medical University, Moscow, Russia

[2] Mechnikov North-Western State Medical University, Saint-Peterburg, Russia

Unstable pelvic ring fractures are one of the common causes of death of patients with concomitant injuries. The existing methods applied to treat such conditions can cause a number of complications and have contraindications. We have described a successful clinical case of intrapelvic hemorrhage arrest in a patient with multiple injuries. in this case, we applied the new method combining minimally invasive angioembolization and easily applicable and effective balloon tamponade.

Keywords: concomitant injury, multiple injury, polytrauma, intrapelvic bleeding, pelvic packing

Author contribution: Egiazaryan KA, Gordienko DI — study organization and planning; Starchik DA — study planning, anatomical examination; Lysko AM — literature analysis, data collection, analysis, interpretation, surgery.

Compliance with ethical standards: the study was approved by the Ethics Committee of Pirogov City Clinical Hospital № 1 (minutes № 5 of May 28, 2018) and Ethics Committee of Pirogov Russian National Research Medical University (minutes № 170 of December 18, 2017).

✉ **Correspondence should be addressed:** Artyom M. Lysko
Khachaturiana 12–3, Moscow, 127562; ArtLysko@gmail.com

Received: 03.03.2019 **Accepted:** 16.04.2019 **Published online:** 29.04.2019

DOI: 10.24075/brsmu.2019.031

НОВЫЙ СПОСОБ ТАМПОНАДЫ ТАЗА ПРИ ПРОДОЛЖАЮЩЕМСЯ ВНУТРИТАЗОВОМ КРОВОТЕЧЕНИИ

К. А. Егиазарян[1], Д. И. Гордиенко[1], Д. А. Старчик[2], А. М. Лыско[1]✉

[1] Российский национальный исследовательский медицинский университет имени Н. И. Пирогова, Москва, Россия

[2] Северо-Западный государственный медицинский университет имени И. И. Мечникова, Санкт-Петербург, Россия

Нестабильные повреждения тазового кольца продолжают оставаться одной из наиболее частых причин летального исхода у пациентов с сочетанной травмой, а существующие способы имеют ряд осложнений и противопоказаний. Нами описан успешный клинический случай остановки внутритазового кровотечения у пациента с множественными травмами, в котором с целью объединения преимуществ малой инвазивности ангиоэмболизации, простоты исполнения и воздействия на основную причину кровопотери тампонады таза применен новый способ внутритазовой остановки кровотечения при помощи баллонных устройств.

Ключевые слова: сочетанная травма, множественная травма, политравма, переломы костей таза, внутритазовое кровотечение, тампонада таза

Информация о вкладе авторов: К. А. Егиазарян, Д. И. Гордиенко — организация и планирование исследования; Д. А. Старчик — планирование исследования, выполнение анатомического исследования; А. М. Лыско — анализ литературы, сбор, анализ, интерпретация данных, выполнение оперативного вмешательства.

Соблюдение этических стандартов: исследование одобрено этическим комитетом городской клинической больницы № 1 имени Н. И. Пирогова (протокол № 5 от 28 мая 2018 г.) и этическим комитетом РНИМУ имени Н. И. Пирогова (протокол № 170 от 18 декабря 2017 г.).

✉ **Для корреспонденции:** Артём Михайлович Лыско
ул. Хачатуряна, д. 12, корп. 3, г. Москва, 127562; ArtLysko@gmail.com

Статья получена: 03.03.2019 **Статья принята к печати:** 16.04.2019 **Опубликована онлайн:** 29.04.2019

DOI: 10.24075/vrgmu.2019.0xx

The considerably high mortality rate, medical and social consequences associated with unstable pelvic ring injuries make the problem of arresting intrapelvic hemorrhage an urgent one [1]. Latest research shows that in 25% of cases pelvic ring damage is concomitant with other injuries [2–4]. Up to 60% of such situation end in death; in every third case the, the reason is unarrested pelvic hemorrhage [5–9].

Over the years, practitioners and scholars have developed and improved a number of methods to arrest pelvic hemorrhage, including angioembolization, pelvic tamponade and REBOA (Resuscitative Endovascular Balloon Occlusion of the Aorta) [10–16]. All of them are unique, and each has both positive and negative aspects. Pelvic tamponade arrests venous bleeding, which is a more common condition; the procedure is invasive, implies considerable blood loss and poses a risk of infection. Angioembolization can cause ischemic damage, which leads to necrosis and intracranial hemorrhage [17–22]. We have developed a new pelvic hemorrhage arrest method that combines minimal invasiveness of angioembolization and pelvic tamponade's ease of application and blood stopping properties. The idea behind the new method is a derivative of the uterine balloon tamponade commonly used in obstetrics and gynecology to arrest uncontrolled intrauterine hemorrhages [23].

Description of the clinical case

Patient S., 26 years old, a construction worker, suffered a fall from the 2nd floor (height of about 12 meters) onto a concrete slab. Pre-hospital, the patient received infusions and analgesics. On admission, he was intubated, his bladder and veins catheterized, emergency infusions and analgesics replaced with more adequate solutions; his arterial blood pressure (ABP) was

of 107/70 mmHg, heart rate — 113 beats per minute, diuresis rate normal. The patient's Glasgow Coma Scale score was 9. Laboratory tests have shown that his hemoglobin and hemotacritis were normal with pronounced leukocytosis (up to 29.9 • 10^9/l), alkalipenia (9.8 mmol/l) and lactate of 4.8 mmol/l in the background. Ultrasound examination revealed no fluid in pleural and abdominal cavities and a small amount in the pelvic cavity. The patient's hemodynamics at admission was stable, his pelvic ring showed clinical signs of mechanical instability, therefore, he received a pelvic bandage and was sent to the PAN CT examination (whole body computed tomography), which revealed a C1 concomitant pelvic ring injury according to AO (Arbeitsgemeinschaft für Osteosynthesefragen) / OTA (Orthopedic Trauma Association) classification (Fig. 1). Also, he suffered a closed head injury, parietal brain lobe contusion (right), fractures of the nose bones, left orbit walls, closed fractures of the right shoulder's large tubercle with slight displacement of the fragments, Lisfranc injury (right foot), scrotal hematoma (ISS = 29 points).

During the CT examination, the patient's ABP dropped abruptly to 60/30 mmHg and heart rate increased to 150 beats per minute; he was given 0.3 μg/kg/min of 0.2% norepinephrine (vasopressor support) and urgently taken to the operating room to stabilize the front of the pelvic ring with an external fixation device placed over acetabulum and to apply a C-shaped frame to the back of the pelvic ring. The emergency measures taken to stabilize the pelvic ring raised the patient's ABP to 85/40 mmHg and reduced his heart rate to 130 beats per minute. The vasopressor support was continued. After mechanical stabilization of the pelvic ring, hemodynamic instability persisted for 15 minutes, which lead us to a decision to arrest hemorrhage therein with the help of a balloon (balloon tamponade). We injected anesthetic solutions into the soft tissues of the access incision area and made a puncture-cut measuring 2–3 cm directly above the pubic symphysis and along the anterior midline of the body. Using blunt instruments, we separated subcutaneous tissue, reached the pyramidal muscle and separated its fibers the same way, then introduced a trocar with a mandrin into retropubic space. Next, the trocar was guided paravesically towards left or right sacroiliac joint in the corresponding lateral cellular tissue space (Fig. 2). Once the mandrin was removed, we inserted the balloon device along the trocar, which was a Zhukovsky balloon (Ginamed, Russia) used to arrest intrauterine bleeding. The device includes a plastic frame up to 25 cm long and up to 8 mm in diameter, and a rubber balloon measuring up to 11.5 cm. Then the trocar was removed, and the protocol was repeated in the opposite direction. The balloons were filled with sterile saline simultaneously. During filling, the resistance felt on the piston of the Janet's syringe was gradually increasing; when the balloons received 110 ml, the piston started moving backwards, which we took as a sign of sufficiency of the inflation. To monitor position and integrity of the balloon devices we made intraoperative X-ray scans with the help of Phillips BV Endura (Netherlands) imaging system (Fig. 3). The ends of the balloon devices were kept outside; the wound was layer sutured (Fig. 4). The minimally invasive pelvis tamponade done as described above raised the patient's ABP to 110/47 mmHg and decreased his heart rate to 115 beats per minute. The patient was transferred to the intensive care unit soon after surgery. in the course of the first 24 hours, his hemodynamics stabilized at 115/70 mmHg, heart rate — at 100–110 beats per minute. By the end of the first day vasopressor support was gradually discontinued. Table describes the dynamics of the patient's condition indicators. Diuresis was at a sufficient level, with no signs of bleeding. Forty-eight hours after admission, with the patient's hemodynamic and laboratory test indicators stable, we decided to deflate the balloons by 50 ml while continuing to monitor his condition. Since his condition was stable, on the third day it was decided to dismantle the C-shaped frame and lock the posterior sections of the pelvis with a screw, as well as to remove the balloons from the true pelvis cavity (Fig. 5). On the fifth day after admission, the patient was transferred to the specialized traumatology and orthopedics department for further treatment with daily checkups of the operative wound. It was healing with primary intention and showing no signs of inflammation and pathological discharge, which allowed final stabilization of the pelvic ring on the 10th day and transferring the patient to outpatient care on 16th day (Fig. 6, 7).

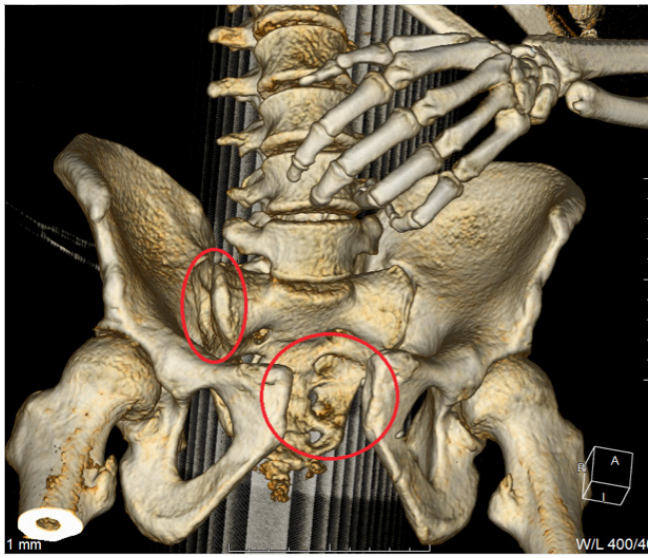

Fig. 1. 3D CT model of the pelvic ring injury: *red* ovals show the right sacroiliac joint rupture and the pubic symphysis rupture

Table. Dynamics of the patient's condition indicators before and after surgery

Indicator/time	Admission	First hour after surgery	End of the first 24 hours from admission
ABP (mmHg)	60/30	110/47	115/70
Heart rate (beats/min)	150	115	100–110
Hemoglobin (g/l)	149	128	92
Hematocrit (%)	44.2	38.4	27.2
Leukocytosis (10^9/l)	29.9	33	11
Lactate (mmol/l)	4.8	7.4	2.8
Alkalipenia (mmol/l)	–9.8	–14	–2.7

Discussion of the clinical case

International community issues guidelines covering treatment of patients with unstable pelvic ring injuries on a regular basis. The most relevant of such guidelines recommend mechanical stabilization of the pelvic ring by external fixation devices as the first step and intrapelvic hemorrhage arrest as the second one, with preference given to tamponade since venous bleeding occurs in 8 out of 10 cases while arterial bleeding is registered in every 2 out of 10 cases only [24]. If pelvic tamponade does not stabilize the patient's hemodynamics, it is recommended to perform angioembolization of the bleeding vessels through a catheter [24]. According to the guidelines, if the patient's injuries cause both mechanical and hemodynamic instability, it is necessary to first stabilize the pelvic ring mechanically and then tamponade the cavity, as we did in the clinical case described above. In that case, this intervention was sufficient to stabilize hemodynamics. Another advantage of the developed method is the ability to control inflation of the balloon devices, which allows gradually deflating them as soon as 24 hours after deployment while monitoring hemodynamic indicators and learning the source of bleeding. Use of sterile and neutral saline solution is an equally important aspect: if the balloon breaks, the solution flowing out of it into the body will do no harm, which reduces the risk of complications.

It should be noted that the global trend to minimize invasion during medical interventions is obvious in pelvic surgery, too. A paper published in 2015 describes a clinical case of a small pelvic tamponade through bladder catheterization and inflation with 500–600 ml of normal saline [25]. There was an absolute contraindication to this method, however: violation of the urinary tract's integrity. Tamponade with a filled bladder in the early postoperative period allowed stabilization of the patient's hemodynamics, but, with the signs of renal failure becoming more vivid, bladder had to be deflated, which lead to destabilization of the patient's hemodynamics and laparotomy. in December 2016, a group of researchers conducted an animal experiment and published the results

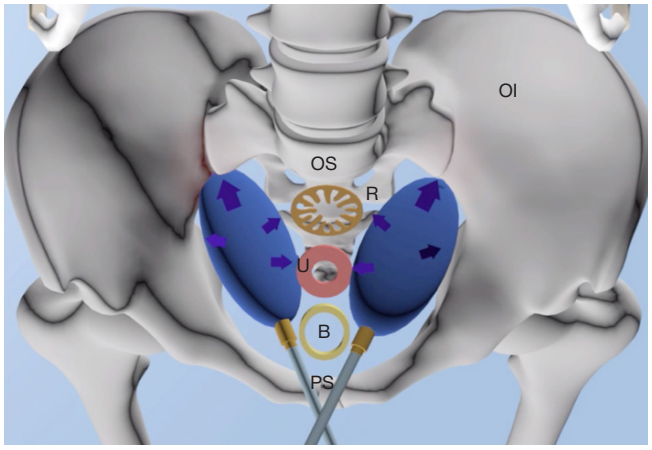

Fig. 2. Schematic representation of the direction of installation of balloon devices in the pelvic cavity: B — bladder, U — uterus, R — rectum, OS — sacrum, Oi — os innominatum, PS — pubic symphysis. The balloons deployed in the lateral space of the pelvis is in blue

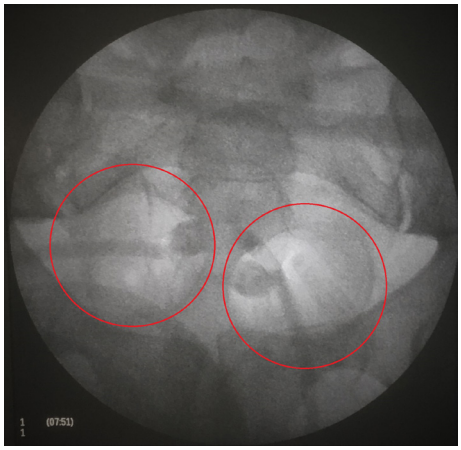

Fig. 3. Intraoperative patient's pelvis X-ray scan, unstable pelvic ring damage and development of intrapelvic hemorrhage after stabilization by external fixation devices and deployment of the balloon devices in the pelvic cavity (balloons circled by red)

Fig. 4. External appearance of the patient's pelvic region with unstable pelvic ring injury and development of intrapelvic hemorrhage after stabilization by external fixation devices and deployment of the balloon devices in pelvic cavity: C — C-shaped frame for the back of the ring, IFD — External Fixation Device for the front, B — balloon devices

Fig. 5. Appearance of the patient's wound with tubes of balloon devices, before removal, 3rd day. The wound has no signs of inflammation; there is no pathological discharge along the balloon devices. in the right half of the picture — external fixation device on the front of the pelvic ring

Fig. 6. Postoperative wound, first day after removal of the balloon devices. The postoperative wound heals by primary intention, without signs of inflammation and pathologic discharge; the sutures are consistent. In the left half of the picture — external fixation device on the front of the pelvic ring

thereof, suggesting to tamponade pelvis with a balloon device in the perivascular space [26]. The test group in this experiment was compared to the regular pelvis tamponade group and the control group (no pelvic bleeding arrest); the comparison proved balloon tamponade to be a minimally invasive and effective method. However, it should be noted that placing the

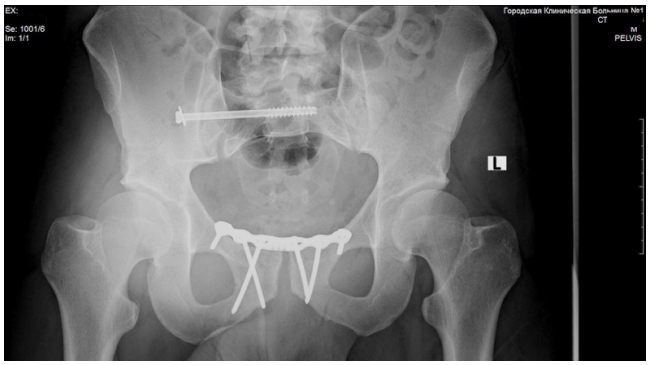

Fig. 7. X-rau scan of the patient's pelvis after the final stabilization of the pelvic ring (10th day): right sacroiliac joint fixed with a spongy screw with partial cutting and a washer, pubic symphysis — with plate and screws

balloon in the anterior small pelvis can cause displacement of the floating bone ring fragments that cannot be immobilized externally, as well as push the internal organs into the back sections of the pelvis where they can be punctured by bone fragments, and the excessive pressure applied to the bladder can rupture and damage urethra. We believe that twin balloons placed symmetrically in the lateral cellular spaces can prevent development of such complications.

CONCLUSIONS

The method we developed shows promise because it is minimally invasive, offers limited damage and control over the pressure. We hope that this method will be practiced to treat patients with unstable pelvic ring injuries.

References

1. Smoljar AN. Diagnostic and treatment of traumatic retroperitoneal hemorrhages [dissertation]. M., 2012–272. In Russian.
2. Burkhardt M, Kristen A, Culemann U, Koehler D, Histing T, Holstein J, et al. Pelvic fracture in multiple trauma: Are we still up-to-date with massive fluid resuscitation? Injury. 2014; (45): S70–5.
3. Esmer E, Esmer E, Derst P, Schulz M, Siekmann H, Delank K. Einfluss der externen Beckenstabilisierung bei hämodynamisch instabilen Beckenfrakturen. Der Unfallchirurg. 2015; 120 (4): 312–9.
4. Wohlrath B, Trentzsch H, Hoffmann R, Kremer M, Schmidt-Horlohè K, Schweigkofler U. Preclinical and clinical treatment of instable pelvic injuries: Results of an online survey. Der Unfallchirurg. 2014; 119 (9): 755–62. In German.
5. Holcomb J, del Junco D, Fox E, Wade C, Cohen M, Schreiber M, et al. The Prospective, Observational, Multicenter, Major Trauma Transfusion (PROMMTT) Study. JAMA Surgery. 2013; 48 (2): 27.
6. Guerado E, Bertrand M, Valdes L, Cruz E, Cano J. Resuscitation of Polytrauma Patients: The Management of Massive Skeletal Bleeding. The Open Orthopaedics Journal. 2015; 9 (1): 283–95.
7. Costantini T, Coimbra R, Holcomb J, Podbielski J, Catalano R, Blackburn A, et al. Current management of hemorrhage from severe pelvic fractures. Journal of Trauma and Acute Care Surgery. 2016; 80 (5): 717–25.
8. Burlew C, Moore E, Stahel P, Geddes A, Wagenaar A, Pieracci F, et al. Preperitoneal pelvic packing reduces mortality in patients with life-threatening hemorrhage due to unstable pelvic fractures. Journal of Trauma and Acute Care Surgery. 2017; 82 (2): 233–42.
9. Tesoriero R, Bruns B, Narayan M, Dubose J, Guliani S, Brenner M, et al. Angiographic embolization for hemorrhage following pelvic fracture. Journal of Trauma and Acute Care Surgery. 2017; 82 (1): 18–26.
10. Fajn AM. Diagnostic and treatment of severe pelvic fractures by patients with concomitant and multiple injuries. [dissertation]. M., 2017–238. Russian.
11. Guerado E, Medina A, Mata M, Galvan J, Bertrand M. Protocols for massive blood transfusion: when and why, and potential complications. European Journal of Trauma and Emergency Surgery. 2015; 42 (3): 283–95.
12. Margolies M, Ring E, Waltman A, Kerr W, Baum S. Arteriography in the Management of Hemorrhage from Pelvic Fractures. New England Journal of Medicine. 1972; 287 (7): 317–21.
13. Pohlemann T, Gansslen A, Bosch U, Tscherne H. The Technique of Packing for Control of Hemorrhage in Complex Pelvic Fractures. Techniques in Orthopaedics. 1994; 9 (4): 267–70.
14. Smith W, Moore E, Osborn P, Agudelo J, Morgan S, Parekh A, et al. Retroperitoneal Packing as a Resuscitation Technique for Hemodynamically Unstable Patients with Pelvic Fractures: Report of Two Representative Cases and a Description of Technique. The Journal of Trauma: Injury, Infection, and Critical Care. 2005; 59 (6): 1510–4.
15. Hughes C. W. Use of an intra-aortic balloon catheter tamponade for controlling intra-abdominal hemorrhage in man. Surgery. 1954; 36 (1): 65–8.
16. DuBose J, Scalea T, Brenner M, Skiada D, Inaba K, Cannon J, et al. The AAST prospective Aortic Occlusion for Resuscitation in Trauma and Acute Care Surgery (AORTA) registry. Journal of Trauma and Acute Care Surgery. 2016; 81 (3): 409–19.
17. Matityahu A, Marmor M, Elson J, Lieber C, Rogalski G, Lin C et al. Acute Complications of Patients With Pelvic Fractures After Pelvic Angiographic Embolization. Clinical Orthopaedics and Related Research. 2013; 471 (9): 2906–11.
18. Salcedo E, Brown I, Corwin M, Galante J. Pelvic angioembolization

in trauma — Indications and outcomes. International Journal of Surgery. 2016; 33: 231–6.
19. Rudloff M, Triantafillou K. Management of Pelvic Ring Injuries in Unstable Patients. Orthopedic Clinics of North America. 2016; 47 (3): 551–63.
20. Saito N, Matsumoto H, Yagi T, Hara Y, Hayashida K, Motomura T, et al. Evaluation of the safety and feasibility of resuscitative endovascular balloon occlusion of the aorta. Journal of Trauma and Acute Care Surgery. 2015; 78 (5): 897–904.
21. Davidson A, Russo R, Reva V, Brenner M, Moore L, Ball C, et al. The pitfalls of resuscitative endovascular balloon occlusion of the aorta. Journal of Trauma and Acute Care Surgery. 2018; 84 (1): 192–202.
22. Uchino H, Tamura N, Echigoya R, Ikegami T, Fukuoka T. "REBOA" — Is it Really Safe? A Case with Massive Intracranial Hemorrhage Possibly due to Endovascular Balloon Occlusion of the Aorta (REBOA). American Journal of Case Reports. 2016; (17): 810–3.
23. Charoenkwan K. Effective use of the Bakri postpartum balloon for posthysterectomy pelvic floor hemorrhage. American Journal of Obstetrics and Gynecology. 2014; 210 (6): 586.
24. Coccolini F, Stahel P, Montori G, Biffl W, Horer T, Catena F, et al. Pelvic trauma: WSES classification and guidelines. World Journal of Emergency Surgery. 2017; 12 (1): 5.
25. Huang S, Vohora A, Russ M, Mathew J, Johnny C, Stevens J, et al. Delaying urinary catheter insertion in the reception and resuscitation of blunt multitrauma and using a full bladder to tamponade pelvic bleeding. Injury. 2015; 46 (6): 1081–3.
26. Sokol K, Black G, Willey S, Song M, Marko S, Eckert M, et al. Preperitoneal balloon tamponade for lethal closed retroperitoneal pelvic hemorrhage in a swine model. Journal of Trauma and Acute Care Surgery. 2016; 81 (6): 1046–55.

Литература

1. Смоляр А. Н. Диагностика и лечение травматических забрюшинных кровоизлияний [диссертация]. М.: 2012–272.
2. Burkhardt M, Kristen A, Culemann U, Koehler D, Histing T, Holstein J et al. Pelvic fracture in multiple trauma: Are we still up-to-date with massive fluid resuscitation? Injury. 2014; (45): 70–5.
3. Esmer E, Esmer E, Derst P, Schulz M, Siekmann H, Delank K. Einfluss der externen Beckenstabilisierung bei hämodynamisch instabilen Beckenfrakturen. Der Unfallchirurg. 2015; 120 (4): 312–9.
4. Wohlrath B, Trentzsch H, Hoffmann R, Kremer M, Schmidt-Horlohè K, Schweigkofler U. Preclinical and clinical treatment of instable pelvic injuries: Results of an online survey. Der Unfallchirurg. 2014; 119 (9): 755–62. In German.
5. Holcomb J, del Junco D, Fox E, Wade C, Cohen M, Schreiber M, et al. The Prospective, Observational, Multicenter, Major Trauma Transfusion (PROMMTT) Study. JAMA Surgery. 2013; 48 (2): 27.
6. Guerado E, Bertrand M, Valdes L, Cruz E, Cano J. Resuscitation of Polytrauma Patients: The Management of Massive Skeletal Bleeding. The Open Orthopaedics Journal. 2015; 9 (1): 283–95.
7. Costantini T, Coimbra R, Holcomb J, Podbielski J, Catalano R, Blackburn A, et al. Current management of hemorrhage from severe pelvic fractures. Journal of Trauma and Acute Care Surgery. 2016; 80 (5): 717–25.
8. Burlew C, Moore E, Stahel P, Geddes A, Wagenaar A, Pieracci F, et al. Preperitoneal pelvic packing reduces mortality in patients with life-threatening hemorrhage due to unstable pelvic fractures. Journal of Trauma and Acute Care Surgery. 2017; 82 (2): 233–42.
9. Tesoriero R, Bruns B, Narayan M, Dubose J, Guliani S, Brenner M, et al. Angiographic embolization for hemorrhage following pelvic fracture. Journal of Trauma and Acute Care Surgery. 2017; 82 (1): 18–26.
10. Файн А. М. Диагностика и лечение тяжелых переломов костей таза у пострадавших с сочетанной и множественной травмой [диссертация]. М., 2017–238.
11. Guerado E, Medina A, Mata M, Galvan J, Bertrand M. Protocols for massive blood transfusion: when and why, and potential complications. European Journal of Trauma and Emergency Surgery. 2015; 42 (3): 283–95.
12. Margolies M, Ring E, Waltman A, Kerr W, Baum S. Arteriography in the Management of Hemorrhage from Pelvic Fractures. New England Journal of Medicine. 1972; 287 (7): 317–21.
13. Pohlemann T, Gansslen A, Bosch U, Tscherne H. The Technique of Packing for Control of Hemorrhage in Complex Pelvic Fractures. Techniques in Orthopaedics. 1994; 9 (4): 267–70.
14. Smith W, Moore E, Osborn P, Agudelo J, Morgan S, Parekh A, et al. Retroperitoneal Packing as a Resuscitation Technique for Hemodynamically Unstable Patients with Pelvic Fractures: Report of Two Representative Cases and a Description of Technique. The Journal of Trauma: Injury, Infection, and Critical Care. 2005; 59 (6): 1510–4.
15. Hughes C. W. Use of an intra-aortic balloon catheter tamponade for controlling intra-abdominal hemorrhage in man. Surgery. 1954; 36 (1): 65–8.
16. DuBose J, Scalea T, Brenner M, Skiada D, Inaba K, Cannon J et al. The AAST prospective Aortic Occlusion for Resuscitation in Trauma and Acute Care Surgery (AORTA) registry. Journal of Trauma and Acute Care Surgery. 2016; 81 (3): 409–19.
17. Matityahu A, Marmor M, Elson J, Lieber C, Rogalski G, Lin C, et al. Acute Complications of Patients With Pelvic Fractures After Pelvic Angiographic Embolization. Clinical Orthopaedics and Related Research. 2013; 471 (9): 2906–11
18. Salcedo E, Brown I, Corwin M, Galante J. Pelvic angioembolization in trauma — Indications and outcomes. International Journal of Surgery. 2016; (33): 231–6.
19. Rudloff M, Triantafillou K. Management of Pelvic Ring Injuries in Unstable Patients. Orthopedic Clinics of North America. 2016; 47 (3): 551–63.
20. Saito N, Matsumoto H, Yagi T, Hara Y, Hayashida K, Motomura T, et al. Evaluation of the safety and feasibility of resuscitative endovascular balloon occlusion of the aorta. Journal of Trauma and Acute Care Surgery. 2015; 78 (5): 897–904.
21. Davidson A, Russo R, Reva V, Brenner M, Moore L, Ball C, et al. The pitfalls of resuscitative endovascular balloon occlusion of the aorta. Journal of Trauma and Acute Care Surgery. 2018; 84 (1): 192–202.
22. Uchino H, Tamura N, Echigoya R, Ikegami T, Fukuoka T. "REBOA" — Is it Really Safe? A Case with Massive Intracranial Hemorrhage Possibly due to Endovascular Balloon Occlusion of the Aorta (REBOA). American Journal of Case Reports. 2016; 17: 810–3.
23. Charoenkwan K. Effective use of the Bakri postpartum balloon for posthysterectomy pelvic floor hemorrhage. American Journal of Obstetrics and Gynecology. 2014; 210 (6): 586.
24. Coccolini F, Stahel P, Montori G, Biffl W, Horer T, Catena F, et al. Pelvic trauma: WSES classification and guidelines. World Journal of Emergency Surgery. 2017; 12 (1): 5.
25. Huang S, Vohora A, Russ M, Mathew J, Johnny C, Stevens J, et al. Delaying urinary catheter insertion in the reception and resuscitation of blunt multitrauma and using a full bladder to tamponade pelvic bleeding. Injury. 2015; 46 (6): 1081–3.
26. Sokol K, Black G, Willey S, Song M, Marko S, Eckert M, et al. Preperitoneal balloon tamponade for lethal closed retroperitoneal pelvic hemorrhage in a swine model. Journal of Trauma and Acute Care Surgery. 2016; 81 (6): 1046–55.

INTERRELATION OF NON-DRUG CORRECTION OF MENOPAUSAL DISORDERS AND FUNCTIONING OF THE PITUITARY-THYROID SYSTEM IN WOMEN WITH METABOLIC SYNDROME

Berihanova RR[1]✉, Minenko IA[2]

[1] Central clinical hospital of civil aviation, Moscow, Russia

[2] Sechenov First Moscow State Medical University, Moscow, Russia

In perimenopausal women, the frequency of thyroid diseases and metabolic syndrome (MS) increases. In this work, the effect of non-drug correction programs for menopausal disorders on the structural and functional state of the thyroid gland in patients with MS was evaluated. For that, five groups of women (330 people total) aged 45–50 years with climacteric syndrome (CS) against the background of MS were examined. For the index group and the experimental groups the following was used: basic treatment, exercise therapy, drinking balneotherapy, additional oral intake of multivitamins and minerals, as well as physical therapy — vibrotherapy, chromotherapy, music therapy, aromatherapy, aeroionotherapy in various combinations. In the control group, only basic treatment was used. The levels of thyroid-stimulating hormone (TSH) and free thyroxine (free T4) in serum were determined, a sonographic study of the thyroid gland was performed. According to the study results, the use of correction programs using physical therapy methods improved the functioning parameters of the pituitary-thyroid system in the surveyed patients. In women with moderate-severity CS, the best results were obtained while simultaneously using all the mentioned above physiotherapy methods: during the transition period the TSH decreased by 6.5%, during the postmenopausal period — by 5.6%, the level of free T4 increased by 6.5% and 6,6% respectively ($p < 0.05$, applied to both parameters). It can be concluded that non-drug programs, including physical therapy, have a protective effect on the thyroid gland function. In case of moderate-severity climacteric syndrome, the program with simultaneous use of vibrotherapy, chromotherapy, music therapy, aromatherapy, aeroionotherapy has priority.

Keywords: climacteric syndrome, metabolic syndrome, thyroid status, physical therapy modalities

Author contribution: Berihanova RR — collection and processing of materials, obtained data analysis, writing of the text; Minenko IA — study concept and design.

Compliance with ethical standards: the study was conducted according to international ethical requirements of WHO (GCP — Good Clinical Practice standard) and to Declaration of Helsinki: Ethical Principles for Medical Research Involving Human Subjects; the study was approved by the Ethics Committee of I.M. Sechenov First Moscow State Medical University (protocol No 01-13 dated January 23, 2013).

✉ **Correspondence should be addressed:** Rumisa R. Berihanova
Severnyy boulevard 1, Moscow, 127566; rumiska07@mail.ru

Received: 16.10.2018 **Accepted:** 29.03.2019 **Published online:** 11.04.2019

DOI: 10.24075/brsmu.2019.023

ВЗАИМОСВЯЗЬ НЕМЕДИКАМЕНТОЗНОЙ КОРРЕКЦИИ КЛИМАКТЕРИЧЕСКИХ РАССТРОЙСТВ И ФУНКЦИОНИРОВАНИЯ ГИПОФИЗАРНО-ТИРЕОИДНОЙ СИСТЕМЫ У ЖЕНЩИН С МЕТАБОЛИЧЕСКИМ СИНДРОМОМ

Р. Р. Бериханова[1]✉, И. А. Миненко[2]

[1] Центральная клиническая больница гражданской авиации, Москва, Россия

[2] Первый Московский государственный медицинский университет имени И. М. Сеченова, Москва, Россия

У женщин в перименопаузе частота тиреоидной патологии и метаболического синдрома (МС) увеличивается. В данной работе оценивали влияние нелекарственных программ коррекции климактерических расстройств на структурно-функциональное состояние щитовидной железы (ЩЖ) у пациенток с МС. Для этого обследовали пять групп женщин (всего 330 человек) 45–50 лет с климактерическим синдромом (КС) на фоне МС. У основной группы и групп сравнения применяли: базовое лечение, лечебную физкультуру, питьевую бальнеотерапию, дополнительный пероральный прием поливитаминов и минералов, а также физиотерапию — вибротерапию, хромотерапию, мелотерапию, ароматерапию, аэроионотерапию в различных сочетаниях. В группе контроля применяли только базовое лечение. Определяли уровни тиреотропного гормона (ТТГ) и свободного тироксина (Т4св) в сыворотке крови, проводили эхографическое исследование ЩЖ. Согласно результатам исследования, применение программ коррекции с использованием физиотерапевтических методов улучшило параметры функционирования гипофизарно-тиреоидной системы у обследованных. У женщин с КС средней степени тяжести лучшие результаты получили при одновременном использовании всех перечисленных методов физиотерапии: в переходном периоде ТТГ снизился на 6,5%, в период постменопаузы — на 5,6%, уровень Т4св увеличился соответственно на 6,5% и 6,6% ($p < 0,05$, относится к обоим параметрам). Можно сделать вывод, что нелекарственные программы, включающие физиотерапию, обладают протективным влиянием на функцию ЩЖ. При КС средней степени тяжести преимущество имеет программа с одновременным применением вибротерапии, хромотерапии, мелотерапии, ароматерапии и аэроионотерапии.

Ключевые слова: климактерический синдром, метаболический синдром, тиреоидный статус, физиотерапия

Информация о вкладе авторов: Р. Р Бериханова — сбор и обработка материалов, анализ полученных данных, написание текста; И. А. Миненко — концепция и дизайн исследования.

Соблюдение этических стандартов: исследование проводили согласно международным этическим требованиям ВОЗ (правила GCP — Good Clinical Practice) и Хельсинкской декларации Всемирной медицинской ассоциации по проведению биометрических исследований на людях; исследование одобрено комитетом по этике Первого Московского государственного медицинского университета имени И. М. Сеченова (протокол № 01–13 от 23 января 2013 г.). Все пациентки подписали информированное добровольное согласие на включение в исследование.

✉ **Для корреспонденции:** Румиса Рамзановна Бериханова
ул. Северный бульвар, д. 1, г. Москва, 127566; rumiska07@mail.ru

Статья получена: 16.10.2018 **Статья принята к печати:** 29.03.2019 **Опубликована онлайн:** 11.04.2019

DOI: 10.24075/vrgmu.2019.023

At the stage of extinction of ovarian function, conditions are created for the formation of polymorbid pathology [1–3]. Often a woman enters the menopause having the background of somatic ill-being, in particular, having metabolic syndrome (MS), the prevalence of which in the overall population in developed countries is 25–40% [4]. In the period of aging estrogen deficiency, the frequency of occurrence of MS increases [5–7]. Involutional changes in the body are also associated with an increase in the frequency of thyroid diseases [8–10]. Perimenopausal thyroid dysfunction in the thyroid gland is found in 19.5% of women living in the iodine-deficient region, and hypothyroidism is most often detected — 16.7% [11]. The presence of conjugation points in the pathogenetic chains of menopause, MS and thyroid diseases determines the aggravation of metabolic-endocrine disorders by the principle of mutual complication of comorbid conditions [12, 13]. At the forefront of therapeutic measures aimed to stop age disorders, the menopausal hormone therapy of systemic and local action is worth [14]. However, the presence of contraindications to menopausal hormone therapy, the use of a large number of medicines for comorbid pathology, hormonophobia, characteristic for many women, preclude the appointment of estrogen preparations [15]. The need to search for effective non-drug technologies aimed to correct metabolic and endocrine disorders and maintain a decent quality of life in women with MS in peri- and postmenopausal period becomes obvious. The aim of the work was to assess the impact of complex non-drug correction programs for menopausal disorders in patients with MS on the structural and functional state of the thyroid gland.

METHODS

Clinical study of 330 women was performed. The duration of the observation was six months.

Using randomization method the five groups of surveyed patients were formed (see below). Each group was divided into two subgroups depending on the total modified menopausal index level: subgroup 1 — patients with mild climacteric syndrome (CS), subgroup 2 — patients with moderate severity CS. Index group (A) — 60 women, who used the «A» treatment complex; first experimental group (B) — 59 women, who used the «B» complex; second experimental group (C) — 66 women, who used the «C» complex; third experimental group (D) — 70 women, who used the «D» complex; control group (E) — 75 women, who used the «E» complex (Table 1). At the stage of assessment of endocrine profile in dynamics, it was expedient to divide the subgroups into subsubgroups according to the period of the woman's life: perimenopausal period (P) and postmenopause (M).

The groups had no statistically significant differences in age, social status, level of education, region of residence, genital and extragenital pathology spectrum.

Inclusion criteria: 45–50 year old women (average age 47.2 ± 3.2 years) in the perimenopausal period or early natural postmenopause (up to two years); the presence of the original MS, diagnosed according to the recommendations of experts of the Russian Scientific Society of Cardiologists on diagnosis and treatment of metabolic syndrome (second revision, 2009); duration of MS from two to five years; the presence of CS of mild or moderate severity, typical complicated form (against the MS background); no menopausal hormone therapy in the personal medical history; no thyroid gland dysfunction initially.

Non-inclusion criteria: the presence of gross mental disorders, alcohol and drug addiction, acute diseases of the cardiovascular system, acute inflammatory diseases, hemorrhage and liability to it, malignant or unverified neoplasms, tumors in growth stage or in a condition requiring surgical treatment; signs of severe organ failure; presence of original thyroid dysfunction according to hormonal tests; presence of 3rd degree intestinal dysbacteriosis; diabetes mellitus presence; vaginitis presence.

Exclusion criteria: individual intolerance to physical factors; individual intolerance to the components of the vitamin and mineral preparations. There were no such patients.

Basic treatment was used in all groups. It included the normalization of lifestyle and sleep, nutritional treatment, increased physical activity. The patients controlled the components of the treatment themselves. Principles of treatment: personalized approach, consisting in the individual calculation of the basal metabolism, physical exercises in the comfort zone for each patient, temperature conditions also in the comfort zone for the patients, carrying out of antihypertensive therapy for hypertensia; nutritional therapy during the entire observation time; lifestyle correction (all study participants were motivated to quit smoking). In the index

Table 1. The number of patients and the applied methods of treatment in groups

		Index group (A), $n = 60$		First experimental group (B), $n = 59$		Second experimental group (C), $n = 66$		Third experimental group (D), $n = 70$		Control group (E), $n = 75$	
Subgroup 1 population	P	32	17	30	17	34	18	36	19	38	20
	M		15		13		16		17		18
Subgroup 2 population	P	28	13	29	15	32	17	34	18	37	20
	M		15		14		15		16		17
Applied methods		Complex «A»		Complex «B»		Complex «C»		Complex «D»		Complex «E»	
		Basic treatment		Basic treatment		Basic treatment		Basic treatment		Basic treatment	
		Exercise therapy		Exercise therapy		Exercise therapy		Exercise therapy		–	
		Drinking balneotherapy		Drinking balneotherapy		Drinking balneotherapy		Drinking balneotherapy		–	
		Additional oral use of multivitamin and mineral preparation		Additional oral use of multivitamin and mineral preparation		Additional oral use of multivitamin and mineral preparation		Additional oral use of multivitamin and mineral preparation		–	
		vibrotherapy, full-spectrum and selective chromotherapy, music therapy, aromatherapy, aeroionotherapy		vibrotherapy, – – – music therapy, aromatherapy, aeroionotherapy		– full-spectrum and selective chromotherapy, music therapy, aromatherapy, aeroionotherapy		–		–	

group there were 12 smokers (20.0%), in the first experimental group 11 smokers (18.6%), in the second experimental group 14 smokers (21.2%), in the third experimental group 14 smokers (20.0%), in the control group 16 smokers (21.3%). Of them 6 women (10.0%) from the index group, 5 women (8.5%) from the first experimental group, 6 women (9.1%) from the second experimental group, 7 women (10.0%) from the third experimental group and 7 women (9.3%) from the control group smoked more than 10 sigarettes a day. These patients either quit smoking or reduced the number of cigarettes smoked per day to five. There were no patients among those who constantly took antihypertensive drugs before being included in the study. When a cardiologist diagnosed arterial hypertension during the study period, patients received standard antihypertensive therapy — moxonidine (Physiotens) 200 μg orally 1 time a day (Order of the Ministry of Health of the Russian Federation dated November 9, 2012, № 708н «On approval of the standard of primary health care for primary arterial hypertension (hypertensive disease)»). Antihypertensive therapy in the index group was received by 11 (34.4%) patients from A1 subgroup and 13 (46.4%) patients from A2 subgroup; in the first experimental group — 11 (36.7%) patients from B1 subgroup and 14 (48.3%) patients from B2 subgroup; in the second experimental group — 12 (35.3%) patients from C1 subgroup and 15 (46.9%) patients from C2 subgroup; in the third experimental group — 13 (36.1%) patients from D1 subgroup and 16 (47.1%) patients from D2 subgroup; in the control group — 14 (36.8%) %) patients from E1 subgroup and 17 (46.0%) patients from E2 subgroup. Of these, in the index group during the observation period only for one patient (3.6%) of the A2 subgroup there was a need to double the daily dose of moxonidine (from 200 to 400 μg), in the second subgroups of the first, second and third experimental groups there were 2 (6.9%), 3 (9.4%) and 3 (8.8%) such patients respectively. In the control group in E2 subgroup, it was necessary to increase the dose of moxonidine for 4 (10.8%) patients, and for one of them up to 600 μg per day.

Basic treatment

Basic treatment was performed during the whole observation period. *Nutritional treatment*. To calculate the individual daily caloric need, the basal metabolic rate was calculated using the formula recommended by WHO: BM = (0,0342 • M + 3,5377) • 240, where BM was basal metabolism value (kcal), M was body mass (kg). Then determined the total energy consumption, adjusted for the coefficient of physical activity: E = F • BM, where E was total energy consumption (kcal), F was correction factor (1,1 — low, 1,3 — moderate, 1,5 — high activity), BM was basal metabolism value (kcal). For a gradual decrease in body weight, a diet with a lower energy value was taken, subtracting 600 kcal from the total energy consumption value. Split meals were recommended, 5–6 times per day, taking small portions at the same time. The diet included foods containing complex carbohydrates (cereals, fruit, vegetables), rich in dietary fiber; the use of simple carbohydrates, saturated fats, salt (up to 3 g per day) was limited, coffee and alcohol were not allowed. *Physical activity* was recommended considering the state of health and tolerance. Daily walking in the fresh air for 30 minutes was offered. In addition to quitting smoking, all patients were motivated to keep up the work-rest regime.

Excercise therapy

Was used during the entire observation time. A daily morning hygienic gymnastics (10–15 min) was conducted in the form of a set of exercises aimed to improve the overall tone of the cardiovascular system and to remove muscle hypertonia, as well as daily training of the pelvic floor muscles (Kegel Exercises), focused on strengthening the periureteral and perivaginal muscles, the anal sphincter, the increase in the functional volume of the bladder without the participation of the abdominal, gluteal and femoral muscles [16].

Drinking balneotherapy

A balneotherapy course was performed from the very beginning of the study, repeated after three months. The duration of each course was four weeks. The ingestion of Essentuki No. 4 mineral water in a volume of 180–300 ml (3 ml per 1 kg of body weight) at room temperature 30 minutes before main meals (3 times a day) was prescribed.

Additional oral use of multivitamin and mineral preparation

The oral intake of vitamin and mineral preparation was prescribed: 22 balanced components, including iodine in the form of potassium iodide in the amount of 225 μg (Menopace®, registration number № П N015844/01; Vitabiotics Ltd; UK) and calcium carbonate with colecalciferol (D3 vitamin) (Calcium-D3 Nycomed, registration number № П N013478/01; Nycomed Pharma; Norway). Menopace® was taken daily in 1 capsule with or after a meal. The treatment course duration was six months. Calcium-D3 Nycomed, containing 1250 mg of calcium carbonate (equivalent to 500 mg of elemental calcium) and 5 μg (200 IU) of colecalciferol (D3 vitamin) was taken orally 1 tablet twice a day for one month, the course was repeated after three months.

Physical therapy

For the complex health effects the multifactor physical therapy unit Spectra Color SPA System (Sybaritic Inc., USA, registration certificate of the Ministry of Health of the Russian Federation № 97/532 dated May 22, 1997) was used. When combining physical factors and procedures, their compatibility was taken into account in accordance with the Annex to «The list of necessary medical services and procedures available in specialized sanatoriums to the patient according to the profile of his disease. Methodical instructions» (approved by the Ministry of Health of the Russian Federation on December 22, 1999, № 99/229). The exact dosage of each influencing factor according to the degree of intensity and time of exposure was carried out. *General vibrotherapy* was carried out for 15 minutes: with the help of multipoint vibration transmitters mounted in the capsule bed, the effect of a manual massage was created, providing anesthetic and relaxing effect, as well as contributing to the rapid removal of fatigue and restoration of muscle performance. A vibration mode with a varying frequency from 10 to 60 Hz and an increasing amplitude up to 7 mm was used, the vibration frequency increased during 8–10 s. *Full-spectrum chromotherapy* was carried out for 30 minutes, using wavelength from 760 to 400 nm. *Selective chromotherapy* was applied (the green light was used for 30 minutes, wavelength 530 nm). Through a stereo sound system with a CD player, passive (receptive) musical therapy was carried out using relaxing melodies for 30 minutes. Aromatherapy oils were sprayed through the four-channel system inside the capsule for *aromatherapy*: lavender (*Lavandula officinalis*) and common fennel (*Foeniculum vulgare*). *Aeroionotherapy* (cooling the face with ionized cool air with a predominance of negative

ions) was applied for 30 minutes. Sessions in the conditions of the Spectra Color SPA System physical therapy unit were performed twice a week for 30 minutes, the course consisted of 10 sessions. The course was repeated after three months. A total of 20 procedures were performed during the observation.

Measurement methods

Assessment of the severity of climacteric disorders was performed using the modified menopausal Kupperman index (version by Uvarova EV, 1983) [17]. Using the automated IFA processor NEXgen (Adaltis S.r.l.; Italy) and the hormone diagnostic reagents (Alkor Bio; Russia) the serum levels of thyroid stimulating hormone (TSH) (reference values: 0.23–3.4 μIU/ml) and free thyroxine (free T4) (reference values: 9.5–22.6 mmol/l) were determined. Ultrasound examination of the thyroid gland was performed on the expert class multifunctional system MyLab 70 (Esaote; Italy) using the 4–13 MHz linear sensor with color flow mapping. When performing the sonography of the thyroid gland the size and structure of the gland was assessed, as well as the presence, size and type of blood flow of the nodules.

Methods of statistical data analysis

Sample size was not previously calculated. Statistical analysis of the research results was carried out using a standard software package STATISTICA® for Windows 6.0 (StatSoft Inc; USA). Quantitative indicators are presented as the number of cases (n) and the average error of the arithmetic mean (m). The significance of differences in the mean values was determined by Student's t-test. For comparison of relative indicators characterizing the frequency of a particular characteristic the non-parametric method according to the Pearson $\chi 2$ criterion was used. Differences were considered statistically significant when $p < 0.05$.

RESULTS

Structural changes on the part of the thyroid gland, according to sonography, were more common in women with moderately severe CS than in women with mild CS: 105 (65.7%) and 90 (52.9%) women respectively ($p < 0.05$). The structure of the deviations according to the thyroid sonography data of the examined patients is reflected in Table. 2.

After six months of observation, according to the sonography data, two patients of the E2-M subgroup (control group) were first diagnosed with nodules. In the remaining groups, the number of patients with structural changes in the thyroid gland according to the sonography data remained unchanged.

In most patients initially the thyroid gland had normal size. Sonographic monitoring was performed after six months of treatment. The Table. 3 presents the average values of the volume of the gland in the subgroups of examined patients in the dynamics, before treatment and after six months of therapy. It should be noted that in patients with moderately severe CS the volume of the thyroid gland was significantly higher than in patients with mild CS. After six months of therapy, the average volume of the thyroid gland significantly decreased in patients with mild CS in subgroups A1, B1 and C1 — by 11.3%, 7.2% and 7.6% respectively ($p < 0.05$ compared with pre-treatment rates; $p > 0.05$ when comparing rates between subgroups). Among patients with moderate-severity CS, a significant decrease in the average thyroid volume was found only in A2 subgroup — by 10.7 % ($p < 0.05$). In subgroups 2 of all three experimental groups, a slight decrease in thyroid volume was noted, but it was not reliable. The tendency for this indicator to increase in the E1 and E2 subgroups of the control group attracted attention, but the changes were not statistically significant ($p > 0.05$).

By the time of the beginning of the study, patients of all groups had no abnormal thyroid function — the mean values of free T4, TSH were within the reference intervals, however, in participants of the study with moderately severe CS the free T4 level was lower, and the TSH level was higher than the corresponding indicators of patients with mild CS. In addition, it was noted that in patients in the period of early postmenopause, the level of free T4 was lower, and the level of TSH was higher in comparison with patients in the perimenopausal period ($p < 0.05$). After six months of treatment, the average values of TSH and free T4 in all subgroups corresponded to the euthyroid state. However, after six months of therapy, subclinical hypothyroidism was detected in one (6.3%) patient of the D2-M subgroup, and in the control group the greatest increase in the frequency of hypothyroidism was demonstrated — it was observed in 2 (11.1%) patients of the E1-M subgroup, in 3 (16.7%) patients of the E2-P subgroup and in 4 (23.5%) patients of the E2-M subgroup.

The dynamics of changes of the levels of TSH and free T4 in the groups of surveyed patients is presented in Table. 4. After six months of therapy in all subgroups of the index group the level of TSH decreased significantly — in A1-P by 10.0%, in A2-P — by 6.5%, in A1-M — by 7.3%, in A2-M — by 5.6% ($p < 0.05$), and the level of free T4 increased by 8.1%, 6.5%, 7.7%, 6.6% respectively ($p < 0.05$). Patients in the perimenopausal period with mild CS from the first and second experimental groups also demonstrated a significant decrease in TSH and the increase in free T4: in subgroup B1-P, the level of TSH decreased by 5.1%, in subgroup C1-P by 8.8%, and the level of free T4 increased by 6.5% and 7.1% respectively ($p < 0.05$). It should be noted that there were no statistically significant differences between the subgroups A1-P, B1-P and C1-P. In other subgroups of the experimental groups, there was a slight decrease in the level of TSH and an increase in the level of free T4, however, changes of characteristics relative to baseline were not reliable. In all subgroups of the control group, there was a decrease in the level of free T4 and an increase in

Table 2. Structural changes of the thyroid gland in the groups of surveyed patients according to the results of ultrasound investigation

Nature of change	Index group, $n = 36$, abs (%)		First experimental group, $n = 34$, abs (%)		Second experimental group, $n = 39$, abs (%)		Third experimental group, $n = 41$, abs (%)		Control group, $n = 45$, abs (%)	
	A1, $n = 17$	A2, $n = 19$	B1, $n = 16$	B2, $n = 18$	C1, $n = 18$	C2, $n = 21$	D1, $n = 18$	D2, $n = 23$	E1, $n = 21$	E2, $n = 24$
Diffuse changes	5 (29.4)	5 (26.3)	5 (31.3)	6 (33.3)	6 (33.3)	7 (33.3)	6 (33.3)	8 (34.8)	7 (33.3)	8 (33.3)
Palpable abnormalities	6 (35.3)	7 (36.8)	5 (31.3)	6 (33.3)	5 (27.8)	6 (28.6)	6 (33.3)	7 (30.4)	6 (28.6)	7 (29.2)
Overlapping changes	6 (35.3)	7 (36.8)	6 (37.5)	6 (33.3)	7 (38.9)	8 (38.1)	6 (33.3)	8 (34.8)	8 (38.1)	9 (37.5)

the level of TSH, and in the subgroups E2-P, E1-M and E2-M, the changes were statistically significant: Accordingly, the level of TSH increased by 5.5%, 5.6% and 6.3%, and the free T4 level regressed by 4.4%, 5.1% and 7.8% ($p < 0.05$), which indicated a decrease in thyroid function.

DISCUSSION

We found a high frequency of structural changes in the thyroid gland according to the results of ultrasound investigation in women with MS; in women with a moderately severe CS, sonographic abnormalities in the structure of the thyroid were more common than in women with a mild CS. According to literature data, in peri- and postmenopausal women, the thyroid diseases increase by 2–2.5 times [18]. A higher incidence of thyroid diseases in patients with MS compared with persons not suffering from MS was indicated [19, 20]. Our results suggest a decrease in thyroid function in women with ageing, which is consistent with literature data [21].

Therapeutic programs were formed taking into account the mechanism of action of each applied factor and the pathogenesis of disorders characteristic for CS and MS. The programs were based on diet and normalization of lifestyle, which corresponds to the recommendations of experts from Russian Scientific Society of Cardiologists on diagnosis and treatment of metabolic syndrome (2009) [22], as well as recommendations of Russian Society of Obstetricians and Gynecologists for the management of women in menopause (2016) [23].

The use of drinking mineral waters is justified by their stimulating effect on metabolism by improving functional interactions in the entero insular system, increasing the sensitivity of tissues to insulin, enhancing the utilization of glucose by the liver, activating antioxidant defence enzymes.

Table 3. The average volume of the thyroid gland in the groups of surveyed patients (M ± m, ml)

Control point	Index group, $n = 60$		First experimental group, $n = 59$		Second experimental group, $n = 66$		Third experimental group, $n = 70$		Control group, $n = 75$	
	A1, $n = 32$	A2, $n = 28$	B1, $n = 30$	B2, $n = 29$	C1, $n = 34$	C2, $n = 32$	D1, $n = 36$	D2, $n = 34$	E1, $n = 38$	E2, $n = 37$
Before treatment	16.69 ± 0.44	18.07 ± 0.50°	16.17 ± 0.42	18.14 ± 0.54°	16.26 ± 0.33	18.25 ± 0.54°	16.22 ± 0.29	18.21 ± 0.55°	16.29 ± 0.27	18.22 ± 0.51°
After six months of treatment	14.81 ± 0.32#	16.14 ± 0.35°#	15.0 ± 0.36#	17.79 ± 0.35°*	15.03 ± 0.28#	17.63 ± 0.28°*	15.78 ± 0.27*	17.85 ± 0.24°*	16.61 ± 0.34*	18.71 ± 0.28°*

Note: * — $p < 0.05$ compared with the index group rates; # — $p < 0.05$ compared with pre-treatment rates; ° — $p < 0.05$ when comparing rates between subgroups 1 and 2.

Table 4. The results of hormonal studies in the groups of surveyed patients (M ± m)

Subgroup	TSH, μIU/l (0,23–3,4 μME/ml)		Free T4, pmol /l (9,5–22,6 mmol /l)	
	Before treatment	After six months of treatment	Before treatment	After six months of treatment
Index group, $n = 60$				
A1-P, $n = 17$	2.61 ± 0.06	2.35 ± 0.05#	13.81 ± 0.35	14.93 ± 0.34#
A2-P, $n = 13$	2.76 ± 0.05°	2.58 ± 0.03#°*	12.59 ± 0.36°	13.41 ± 0.30#°
A1-M, $n = 15$	2.87 ± 0.04	2.66 ± 0.03#	12.36 ± 0.18	13.31 ± 0.15#
A2-M, $n = 15$	3.04 ± 0.04°	2.87 ± 0.03#°*	11.83 ± 0.16°	12.61 ± 0.14#°
First experimental group, $n = 59$				
B1-P, $n = 17$	2.55 ± 0.05	2.42 ± 0.04#	13.83 ± 0.31	14.73 ± 0.38#
B2-P, $n = 15$	2.78 ± 0.07°	2.69 ± 0.03°*	12.61 ± 0.28°	13.03 ± 0.20°*
B1-M, $n = 13$	2.90 ± 0.04	2.75 ± 0.4#	12.28 ± 0.17	13.11 ± 0.13#
B2-M, $n = 14$	3.01 ± 0.04°	2.90 ± 0.04°*	11.87 ± 0.11°	12.2 ± 0.09°*
Second experimental group, $n = 66$				
C1-P, $n = 18$	2.61 ± 0.02	2.38 ± 0.03#	13.88 ± 0.20	14.86 ± 0.20#
C2-P, $n = 17$	2.76 ± 0.05°	2.71 ± 0.03°*	12.68 ± 0.19°	12.86 ± 0.16°*
C1-M, $n = 16$	2.85 ± 0.02	2.73 ± 0.02#	12.34 ± 0.11	13.19 ± 0.07#
C2-M, $n = 15$	3.03 ± 0.02°	2.96 ± 0.03°*	11.88 ± 0.11°	12.13 ± 0.09°*
Third experimental group, $n = 70$				
D1-P, $n = 19$	2.64 ± 0.02	2.51 ± 0.03#*	13.75 ± 0.18	14.01 ± 0.16*
D2-P, $n = 18$	2.77 ± 0.06°	2.75 ± 0.03°*	12.69 ± 0.16°	12.8 ± 0.15°*
D1-M, $n = 17$	2.86 ± 0.02	2.77 ± 0.02#*	12.36 ± 0.10	12.48 ± 0.08*
D2-M, $n = 16$	3.01 ± 0.02°	2.99 ± 0.05°*	11.99 ± 0.10°	12.11 ± 0.17°*
Control group, $n = 75$				
E1-P, $n = 20$	2.62 ± 0.02	2.64 ± 0.03*	13.72 ± 0.22	13.52 ± 0.23*
E2-p, $n = 20$	2.74 ± 0.05°	2.89 ± 0.06#°*	12.63 ± 0.17°	12.07 ± 0.33#°*
E1-M, $n = 18$	2.86 ± 0.02	3.02 ± 0.07#*	12.36 ± 0.09	11.73 ± 0.24#*
E2-M, $n = 17$	3.01 ± 0.02°	3.20 ± 0.07#°*	11.91 ± 0.10°	10.98 ± 0.28#°*

Note: * — $p < 0.05$ compared with the index group rates; # — $p < 0.05$ compared with pre-treatment rates; ° — $p < 0.05$ when comparing rates between subgroups 1 and 2.

Drinking balneotherapy is pathogenetically justified in patients with MS and CS. It has been shown that its use in comprehensive rehabilitation programs for combined pathology in MS patients normalizes the carbohydrate and lipid metabolism [24].

The need for taking vitamins is determined by their performance as biocatalysts and antioxidants. Vitamins are involved in the formation of hormones, have the ability to change the sensitivity of the receptors to them, thereby contributing to the normal functioning of the endocrine, nervous, cardiovascular systems of the woman's body [25]. The importance of adequate daily iodine intake can hardly be overestimated. Iodine is necessary for the synthesis of triiodothyronine and thyroxine, which affect all types of metabolism, regulate the balance of reproductive sex hormones [26]. The feasibility of iodine prophylaxis in mature women is also indicated in the literature [27].

The use of low-frequency vibrotherapy is based on its ability to reduce vascular tone, improve microcirculation, tissue trophism due to stimulation of skin mechanoreceptors, primary endings of muscle spindles, and effects on the autonomic nervous system [28]. The use of full-spectrum and selective (green light) chromotherapy is based on their ability to coordinate the activities of the hypothalamic-pituitary system and the endocrine glands due to the effect on melatonin production by affecting the visual analyzer, the extraocular photoneuroendocrine system and the skin [29]. Musical therapy was included in the treatment complex due to the presence of a sedative effect, realized due to the rhythmic effect of melodies on various brain regions. It is shown that it increases the effectiveness of complex therapy for patients with cardiovascular pathology [30]. The use of aromatherapy is based on its ability to regulate the functioning of the endocrine system, to reduce the effects of psycho-emotional stress through the effects on the olfactory sensory system [31]. Aeroionotherapy was included in the program, taking into account the biological effects of negative aeroions realized by reflex, such as stabilization of the processes of vegetative regulation, beneficial effects on the cardiovascular and endocrine systems.

Thus, in our study, complex programs, including physical therapy effects — A, B and C complexes, were required to preserve the structure and maintain the normal function of the thyroid gland in patients with CS and MS. For patients with moderately severe CS to maintain the functioning of the pituitary-thyroid system, the need for a combined use of the whole range of physical therapy factors (vibrotherapy, chromotherapy, music therapy, aromatherapy, aeroionotherapy — A complex) has been identified. It was found that the standard approach does not reduce the incidence of thyroid diseases.

We explain the positive effect on the thyroid status of the applied programs by a decrease in the load on the thyroid gland as a result of the regression of body mass [32], prophylactic effect of iodine-containing vitamin and mineral preparations, improvement of microcirculation as a cumulative effect of preformed physical factors (vibrotherapy, chromotherapy, music therapy, aeroionotherapy, aromatherapy), which increases with their simultaneous use, that is especially significant for patients with moderately severe CS.

CONCLUSIONS

The use of complex programs, including physical therapy effects, has a protective effect on the thyroid status in patients with CS and MS. For patients with moderate-severity CS, the programs with simultaneous use of vibrotherapy, chromotherapy, music therapy, aromatherapy, aeroionotherapy have priority.

The developed complex non-drug treatment technology can be applied in practical healthcare in inpatient, outpatient, sanatorium and resort conditions, in the centers of restorative medicine and rehabilitation.

References

1. Krasnikova NV, Shemetova GN. Somaticheskaya patologiya u zhenshchin v razlichnye dekady klimaktericheskogo perioda. Byulleten' medicinskih internet-konferencij. 2013; 3 (3): 537–539. Russian.
2. Chazova IE, Smetnik VP, Balan VE, Zajdieva YaZ, Majchuk EYu, Mychka VB i dr. Vedenie zhenshchin s serdechno-sosudistym riskom v peri- i postmenopauze: konsensus rossijskih kardiologov i ginekologov. Consilium medicum. 2008; 1 (6): 5–18. Russian.
3. Konsensus Ehkspertov po mezhdisciplinarnomu podhodu k vedeniyu, diagnostike i lecheniyu bol'nyh s metabolicheskim sindromom. Kardiovaskulyarnaya terapiya i profilaktika. 2013; 12 (6): 41–81.
4. Lyashuk RP, Lyashuk PM. Metabolicheskij sindrom kak mezhdisciplinarnaya problema (obzor literatury). Mezhdunarodnyj ehndokrinologicheskij zhurnal. 2017; 13 (7) : 499–502. Russian.
5. Halmuhamedov BT. Metabolicheskij sindrom u zhenshchin v zavisimosti ot prodolzhitel'nosti menopauzy. Evrazijskij kardiologicheskij zhurnal. 2017; (3): 10. Russian.
6. Shishkin AN, Hudyakova NV, Smirnov VV. Menopauzal'nyj metabolicheskij sindrom. Sovremennye predstavleniya. Vestnik SPbGU. Seriya 11. Medicina. 2013; (2): 17–27. Russian.
7. Nikolenko LA, Alyohin DI, Nikolenko ES. Postmenopauza, metabolicheskij sindrom i IBS (obzor literatury). Problemy reprodukcii. 2015; 21 (3): 117–121. Russian.
8. Uygur MM, Yoldemir T, Yavuz DG. Thyroid disease in the perimenopause and postmenopause period. Climacteric. 2018; 21 (6): 542–548. DOI: 10.1080/13697137.2018.1514004.
9. Panda S, Das A. Analyzing Thyroid Dysfunction in the Climacteric. J Midlife Health. 2018; 9 (3): 113–116. DOI: 10.4103/jmh.JMH_21_18.
10. Glembockaya GT, Zaharova AS. Obosnovanie neobhodimosti i vozmozhnostej optimizacii farmacevticheskoj pomoshchi zhenshchinam s patologiej shchitovidnoj zhelezy. Farmaciya i farmakologiya. 2015; 3 (4): 37–42. Russian.
11. Deryabina EG, Bashmakova NV. Funkcional'noe sostoyanie shchitovidnoj zhelezy v perimenopauzal'nyj period u zhenshchin, prozhivayushchih v jododeficitnom regione. Klinicheskaya i ehksperimental'naya tireoidologiya. 2007; 3 (3): 46–49. Russian.
12. Ruyatkina LA, Ruyatkin DS. Integral'nyj serdechno-sosudistyj risk: metabolicheskij sindrom i disfunkciya shchitovidnoj zhelezy. Sibirskoe medicinskoe obozrenie. 2010; 64 (4): 11–16. Russian.
13. Madyanov IV, Kichigin VA, Markova TN, Semakina SM, Bashkova IB. Osobennosti funkcional'nogo sostoyaniya kory nadpochechnikov i shchitovidnoj zhelezy pri metabolicheskom sindrome. Ozhirenie i metabolizm. 2011; (3): 46–50. Russian.
14. De Villiers TJ, Gass MLS, Haines CJ, Hall JE, Lobo RA, Pierroz DD et al. Global Consensus Statement on Menopausal Hormone Therapy. Climacteric. 2013; (16): 203–204.
15. Dobrohotova YuEh, Saprykina LV. Tofizopam: vozmozhnost' negormonal'noj terapii nejrovegetativnyh i psihoehmocional'nyh narushenij pri klimaktericheskom sindrome. Medicinskij sovet. 2017; (2): 88–91. Russian.
16. Kegel A. Stress Incontinence and Genital Relaxation: A non-surgical Method of Increasing the Tone of Sphincters and Supporting Structures. CIBA Symposium; 1952.
17. Cmetnik V. P. Meditsina klimakteriya. Yaroslavl': Litera, 2006. 848 s. Russian.
18. Krasnikova NV, Shemetova GN. Komorbidnaya patologiya u

zhenshchin v klimaktericheskom periode. Problemy zhenskogo zdorov'ya. 2013; 8 (2): 31–35. Russian.
19. Porksheyan KA. Vyyavlyaemost' porazhenij shchitovidnoj zhelezy u bol'nyh metabolicheskim sindromom i saharnym diabetom 2 tipa po dannym ul'trazvukovogo issledovaniya. Kardiovaskulyarnaya terapiya i profilaktika. 2011; 4 (1): 22–23. Russian.
20. Kanavec NS, Levina LI, Vasilenko VS, Karpovskaya EB, Rybka TG, Ivanov SN. Strukturno-funkcional'noe sostoyanie arterij u zhenshchin s metabolicheskim sindromom, associirovannym s autoimmunnym tireoiditom. Pediatr. 2016; 17 (4): 90–95. Russian.
21. Deryabina EG, Bashmakova NV. Rasprostranennost' i struktura tireopatij posle estestvennoj i hirurgicheskoj menopauzy u zhenshchin 45–55 let v regione s legkim deficitom joda. Ural'skij medicinskij zhurnal. 2008; 12 (52): 24–27. Russian.
22. Rekomendacii ehkspertov Vserossijskogo nauchnogo obshchestva kardiologov po diagnostike i lecheniyu metabolicheskogo sindroma (vtoroj peresmotr). Prakticheskaya medicina. 2010; 5 (44): 81–101. Russian.
23. Klinicheskie rekomendacii Ministerstva zdravoohraneniya Rossijskoj Federacii «Menopauza i klimaktericheskoe sostoyanie u zhenshchiny», 2016: Rossijskoe obshchestvo akusherov-ginekologov, Rossijskaya associaciya po menopauze. https://bz.medvestnik.ru/nosology/Menopauza-i-klimaktericheskoe-sostoyanie-u-jenshiny.html. Russian.
24. Zhernov VA, Frolkov VK, Zubarkina MM. Mekhanizmy lechebnogo dejstviya akupunktury i pit'evyh mineral'nyh vod pri metabolicheskom sindrome. Voprosy kurortologii, fizioterapii i lechebnoj fizicheskoj kul'tury. 2017; 94 (2): 36–41. DOI: 10.17116/kurort201794236-41. Russian.
25. Shih EV, Mahova AA. Kliniko-farmakologicheskie aspekty ispol'zovaniya v klimaktericheskij period gormonopodobnyh ehffektov mikonutrientov. Medicinskij sovet. 2016; (2): 68–73. Russian.
26. Begaliev ShS, Abdullabekova RM. Biologicheskaya rol' joda v organizme cheloveka. Aktual'nye problemy sovremennosti. 2017; 2: 201–204.
27. Deryabina EG, Bashmakova NV. Novye sluchai zabolevanij shchitovidnoj zhelezy u zhenshchin v postmenopauzal'nyj period. Ural'skij medicinskij zhurnal. 2009; 3 (57): 103–107. Russian.
28. Ivanova IV. Vliyanie vibro-termo-aromaterapii na organizm pozhilogo cheloveka v processe lecheniya sochetannyh patologij serdechno-sosudistoj sistemy i oporno-dvigatel'nogo apparata. V sbornike: Kotelnikov GP, Zakharova NO, redaktory. Klinicheskie i fundamental'nye aspekty gerontologii. Samara: Samar. gos. med. un-t, 2015. S160–163. Russian.
29. Bogolyubov VM, redaktor. Fizioterapiya i kurortologiya. Kniga I. M.: BINOM. Laboratoria znanij, 2015. S381–392. Russian.
30. Yakupov EhZ, Nalbat AV, Semyonova MV, Tlegenova KA. Ehffektivnost' muzykoterapii v reabilitacii bol'nyh insul'tom. Zhurnal nevrologii i psihiatrii. 2017; 117 (5): 14–21. DOI: 10.17116/jnevro20171175114-21. Russian.
31. Shutova SV. Aromaterapiya: fiziologicheskie ehffekty i vozmozhnye mekhanizmy (obzor literatury). Vestnik Tambovskogo universiteta. Seriya: Estestvennye i tekhnicheskie nauki. 2013; 4 (1): 1330–6. Russian.
32. Berihanova RR, Minenko IA. Antropometricheskie pokazateli u pacientok s metabolicheskim sindromom i klimaktericheskimi rasstrojstvami: vliyanie nelekarstvennoj korrekcii. Novaya nauka: Ot idei k rezul'tatu. 2016; 8–2 (96): 18–20. Russian.

Литература

1. Красникова Н. В., Шеметова Г. Н. Соматическая патология у женщин в различные декады климактерического периода. Бюллетень медицинских интернет-конференций. 2013; 3 (3): 537–39.
2. Чазова И. Е., Сметник В. П., Балан В. Е., Зайдиева Я. З., Майчук Е. Ю., Мычка В. Б. и др. Ведение женщин с сердечно-сосудистым риском в пери- и постменопаузе: консенсус российских кардиологов и гинекологов. Consilium medicum. 2008; 1 (6): 5–18.
3. Консенсус Экспертов по междисциплинарному подходу к ведению, диагностике и лечению больных с метаболическим синдромом. Кардиоваскулярная терапия и профилактика. 2013; 12 (6): 41–81.
4. Ляшук Р. П., Ляшук П. М. Метаболический синдром как междисциплинарная проблема (обзор литературы). Международный эндокринологический журнал. 2017; 13 (7): 499–502.
5. Халмухамедов Б. Т. Метаболический синдром у женщин в зависимости от продолжительности менопаузы. Евразийский кардиологический журнал. 2017; (3): 10.
6. Шишкин А. Н., Худякова Н. В., Смирнов В. В. Менопаузальный метаболический синдром. Современные представления. Вестник СПбГУ. Серия 11. Медицина. 2013; (2): 17–27.
7. Николенко Л. А., Алёхин Д. И., Николенко Е. С. Постменопауза, метаболический синдром и ИБС (обзор литературы). Проблемы репродукции. 2015; 21 (3): 117–121.
8. Uygur MM, Yoldemir T, Yavuz DG. Thyroid disease in the perimenopause and postmenopause period. Climacteric. 2018; 21 (6): 542–548. DOI: 10.1080/13697137.2018.1514004.
9. Panda S, Das A. Analyzing Thyroid Dysfunction in the Climacteric. J Midlife Health. 2018; 9 (3): 113–116. DOI: 10.4103/jmh.JMH_21_18.
10. Глембоцкая Г. Т., Захарова А. С. Обоснование необходимости и возможностей оптимизации фармацевтической помощи женщинам с патологией щитовидной железы. Фармация и фармакология. 2015; 3 (4): 37–42.
11. Дерябина Е. Г., Башмакова Н. В. Функциональное состояние щитовидной железы в перименопаузальный период у женщин, проживающих в йододефицитном регионе. Клиническая и экспериментальная тиреоидология. 2007; 3 (3): 46–49.
12. Руяткина Л. А., Руяткин Д. С. Интегральный сердечно-сосудистый риск: метаболический синдром и дисфункция щитовидной железы. Сибирское медицинское обозрение. 2010; 64 (4): 11–16.
13. Мадянов И. В., Кичигин В. А., Маркова Т. Н., Семакина С. М., Башкова И. Б. Особенности функционального состояния коры надпочечников и щитовидной железы при метаболическом синдроме. Ожирение и метаболизм. 2011; (3): 46–50.
14. De Villiers TJ, Gass MLS, Haines CJ, Hall JE, Lobo RA, Pierroz DD et al. Global Consensus Statement on Menopausal Hormone Therapy. Climacteric. 2013; (16): 203–204.
15. Доброхотова Ю. Э., Сапрыкина Л. В. Тофизопам: возможность негормональной терапии нейровегетативных и психоэмоциональных нарушений при климактерическом синдроме. Медицинский совет. 2017; (2): 88–91.
16. Kegel A. Stress Incontinence and Genital Relaxation: A non-surgical Method of Increasing the Tone of Sphincters and Supporting Structures. CIBA Symposium; 1952.
17. Сметник В. П. Медицина климактерия. Ярославль: Литера, 2006. 848 с.
18. Красникова Н. В., Шеметова Г. Н. Коморбидная патология у женщин в климактерическом периоде. Проблемы женского здоровья. 2013; 8 (2): 31–35.
19. Поркшеян К. А. Выявляемость поражений щитовидной железы у больных метаболическим синдромом и сахарным диабетом 2 типа по данным ультразвукового исследования. Кардиоваскулярная терапия и профилактика. 2011; 4 (1): 22–23.
20. Канавец Н. С., Левина Л. И., Василенко В. С., Карповская Е. Б., Рыбка Т. Г., Иванов С. Н. Структурно-функциональное состояние артерий у женщин с метаболическим синдромом, ассоциированным с аутоиммунным тиреоидитом. Педиатр. 2016; 17 (4): 90–95.
21. Дерябина Е. Г., Башмакова Н. В. Распространенность и структура тиреопатий после естественной и хирургической менопаузы у женщин 45–55 лет в регионе с легким дефицитом йода. Уральский медицинский журнал. 2008; 12 (52): 24–27.
22. Рекомендации экспертов Всероссийского научного общества кардиологов по диагностике и лечению метаболического

синдрома (второй пересмотр). Практическая медицина. 2010; 5 (44): 81–101.
23. Клинические рекомендации Министерства здравоохранения Российской Федерации «Менопауза и климактерическое состояние у женщины», 2016: Российское общество акушеров-гинекологов, Российская ассоциация по менопаузе. https://bz.medvestnik.ru/nosology/Menopauza-i-klimaktericheskoe-sostoyanie-u-jenshiny.html
24. Жернов В. А., Фролков В. К., Зубаркина М. М. Механизмы лечебного действия акупунктуры и питьевых минеральных вод при метаболическом синдроме. Вопросы курортологии, физиотерапии и лечебной физической культуры. 2017; 94 (2): 36–41. DOI: 10.17116/kurort201794236-41.
25. Ших Е. В., Махова А. А. Клинико-фармакологические аспекты использования в климактерический период гормоноподобных эффектов микронутриентов. Медицинский совет. 2016; (2): 68–73.
26. Бегалиев Ш. С., Абдуллабекова Р. М. Биологическая роль йода в организме человека. Актуальные проблемы современности. 2017; (2): 201–204.
27. Дерябина Е. Г., Башмакова Н. В. Новые случаи заболеваний щитовидной железы у женщин в постменопаузальный период. Уральский медицинский журнал. 2009; 3 (57): 103–107.
28. Иванова И. В. Влияние вибро-термо-ароматерапии на организм пожилого человека в процессе лечения сочетанных патологий сердечно-сосудистой системы и опорно-двигательного аппарата. В сборнике: Котельников Г. П., Захарова Н. О., редакторы. Клинические и фундаментальные аспекты геронтологии. Самара: Самар. гос. мед. ун-т, 2015. С.160.
29. Боголюбов В. М., редактор. Физиотерапия и курортология. Книга I. М.: БИНОМ. Лаборатория знаний, 2015. С. 381–392.
30. Якупов Э. З., Налбат А. В., Семёнова М. В., Тлегенова К. А. Эффективность музыкотерапии в реабилитации больных инсультом. Журнал неврологии и психиатрии. 2017; 117 (5): 14–21. DOI: 10.17116/jnevro20171175114-21.
31. Шутова С. В. Ароматерапия: физиологические эффекты и возможные механизмы (обзор литературы). Вестник Тамбовского университета. Серия: Естественные и технические науки. 2013; 4 (1): 1330–1336.
32. Бериханова Р. Р., Миненко И. А. Антропометрические показатели у пациенток с метаболическим синдромом и климактерическими расстройствами: влияние нелекарственной коррекции. Новая наука: от идеи к результату. 2016; 8–2 (96): 18–20.

A RATIONALE FOR THE USE OF ANTHROPOMETRIC MEASUREMENTS AND BIOELECTRICAL IMPEDANCE ANALYSIS AS EFFICACY CRITERIA FOR SUMMER CAMP HEALTHCARE

Gavryushin MYu ✉, Sazonova OV, Gorbachev DO, Borodina LM, Frolova OV, Tupikova DS

Samara State Medical University, Samara, Russia

The proportion of obese and overweight children is alarmingly high. This dictates the need for promoting healthy lifestyle and eating habits in children. Summer camps provide a wide range of activities to improve children's health. However, methods used to assess children's nutritional status during a camp session need to be analyzed in depth, and a rationale should be provided for the use of bioelectrical impedance analysis (BIA) and anthropometric measurements as efficacy criteria for summer camp healthcare. We examined 125 boys and 221 girls aged 8–15 years spending their summer holidays at 3 different camps. Measurements were taken twice: on days 1 and 2 upon arrival to a camp and 2 days before leaving for home. In each camp, both positive and negative health weight dynamics were observed. The overall weight dynamics in children from camps 1 and 2 were statistically insignificant ($p = 0.415$ and $p = 0.585$), in contrast to camp 3 where those changes were significant ($p = 0.025$). BIA revealed that less than 44.34% of children had gained skeletal muscle mass during their stay at the camp, whereas weight loss was associated with both decreased fat and skeletal muscle masses. BIA confirms the results of anthropometric measurements and also provides information about the diet offered to children and their level of physical activity. Therefore, the use of anthropometric measurements and BIA could be an informative method for assessing the efficacy of healthcare in summer camps.

Keywords: hygiene of children and adolescents, physical development, anthropometry, bioimpedance analysis, nutritional status, diet

Author contribution: Gavryushin MYu — study design, data acquisition and analysis, interpretation of the results; Sazonova OV — study design, interpretation of the results; Gorbachev DO — literature analysis, manuscript draft; Borodina LM — data analysis, interpretation of the results; Frolova OV — manuscript revision, literature analysis; Tupikova DS — manuscript draft.

Compliance with ethical standards: this study was approved by the Ethics Committee of Samara State Medical University (Protocol No. 8 dated September 13, 2018). Informed consent was obtained from all the participants or their legal representatives.

✉ **Correspondence should be addressed:** Mikhail Yu. Gavryushin
Chapaevskaya 87, Samara, 443099; m.yu.samara@mail.ru

Received: 10.12.2018 **Accepted:** 29.03.2018 **Published online:** 12.04.2019

DOI: 10.24075/brsmu.2019.024

НАУЧНОЕ ОБОСНОВАНИЕ ПРИМЕНЕНИЯ РЕЗУЛЬТАТОВ АНТРОПОМЕТРИЧЕСКИХ ИССЛЕДОВАНИЙ И БИОИМПЕДАНСНОГО АНАЛИЗА В КАЧЕСТВЕ КРИТЕРИЕВ ОЦЕНКИ ЭФФЕКТИВНОСТИ ОЗДОРОВЛЕНИЯ ДЕТЕЙ В ЛЕТНИХ ЛАГЕРЯХ

М. Ю. Гаврюшин ✉, О. В. Сазонова, Д. О. Горбачев, Л. М. Бородина, О. В. Фролова, Д. С. Тупикова

Самарский государственный медицинский университет, Самара, Россия

В современных условиях жизни высока доля детей с избыточной массой тела и ожирением. Очевидна необходимость оздоровления детей, способствующего коррекции пищевого статуса. На выполнение этой задачи направлена работа детских организаций отдыха и оздоровления, в том числе летних лагерей. Необходимы анализ различных методов оценки изменений пищевого статуса детей в течение лагерной смены и научное обоснование возможности применения результатов биоимпедансного анализа состава тела (БИА) и антропометрических измерений в качестве критериев оценки эффективности оздоровления детей в лагерях. Обследованы 125 мальчиков и 221 девочка в возрасте 8–15 лет, отдыхающие в трех детских лагерях. Исследования проводили в 2 этапа: на 1-й, 2-й дни заезда и за 2 дня до окончания лагерной смены. В каждой организации выявлены дети, у которых за период лагерной смены отмечена как положительная, так и отрицательная тенденция изменения массы тела. Общая тенденция к изменению массы тела среди детей в лагерях № 1 и № 2 была статистически незначима ($p = 0{,}415$ и $p = 0{,}585$), а в лагере № 3 отмечена достоверная тенденция к изменению массы тела отдыхающих ($p = 0{,}025$). По данным БИА, повышение массы тела в течение лагерной смены не более чем в 44,34% случаев сопровождалось должным повышением скелетно-мышечной составляющей, а снижение массы тела включало потерю как жировой, так и скелетно-мышечной составляющих. БИА не только дополняет результаты антропометрических исследований, но и позволяет сделать предположение о фактическом питании и уровне двигательной активности детей. Соответственно, применение антропометрических исследований в совокупности с данными БИА может служить в качестве информативного методического подхода к оценке эффективности оздоровления детей в летних лагерях.

Ключевые слова: гигиена детей и подростков, физическое развитие, антропометрия, биоимпедансный анализ, пищевой статус, рацион питания

Информация о вкладе авторов: М. Ю. Гаврюшин — планирование исследования, сбор данных, анализ данных, интерпретация результатов; О. В. Сазонова — планирование исследования, интерпретация результатов; Д. О. Горбачев — анализ литературы, подготовка черновика рукописи; Л. М. Бородина — анализ данных, интерпретация результатов; О. В. Фролова — редактирование статьи, анализ литературы; Д. С. Тупикова — подготовка черновика рукописи.

Соблюдение этических стандартов: исследование одобрено экспертной комиссией ФГБОУ ВО СамГМУ Минздрава России (протокол № 8 от 13 сентября 2018 г.). Все участники исследования (или их законные представители) подписали информированное согласие на участие в исследовании.

✉ **Для корреспонденции:** Михаил Юрьевич Гаврюшин
ул. Чапаевская, д. 87, г. Самара, 443099; m.yu.samara@mail.ru

Статья получена: 10.12.2018 **Статья принята к печати:** 29.03.2018 **Опубликована онлайн:** 12.04.2019

DOI: 10.24075/vrgmu.2019.024

Harmonious physical development is a critical indicator of a child's health [1, 2]. Unfortunately, over 25% of school-age children and adolescents cannot boast physical fitness [3–5], and the proportion of obese and overweight children is alarmingly high [1, 3, 6–9]. This situation is largely attributed to a contemporary lifestyle and diet that would ideally promote normal growth and development, protect against diseases and help children to adapt to the environment [10, 11].

Unbalanced diet and unhealthy eating habits in the critical periods of child development delay growth and may promote disease [12–14]. In recent years, the incidence of obesity in the Samara region has been stably high, reaching 54.1 cases

per 10,000 children in 2016. These figures are well above the average rate of 36.7 reported in the Russian Federation [15].

This dictates the need for instilling healthy lifestyle and eating habits in children. Summer may be a good time for taking measures, as many children spend their holidays in summer camps. The camps are expected to provide a wide range of activities, as well as improve a child's health. Nutrition is a crucial factor that affects the overall health, growth and development, contributing to the efficacy of health programs [16].

Advances in modern science have been instrumental in elaborating the efficacy criteria for summer camp healthcare. The guidelines on the *Methods for the assessment of the efficacy of health initiatives in health resorts for children* (2.4.4.0127-18; adopted instead of 2.4.4.0011-10), recommend using a grading scale for measuring the dynamics of height, body weight, muscular strength, and respiratory function in children during a summer camp session [17]. The expert panel of the Ministry of Healthcare of the Russian Federation on the hygiene in children and adolescents has approved a protocol ROSHUMZ-15-2014 on the *Comprehensive assessment of the efficacy of health initiatives in health resorts for children* (Protocol No. 4 dated May 6, 2014). The protocol proposes a method for assessing the efficacy of health programs for children based on the dynamics of height, weight, cardiovascular and respiratory function, physical fitness, and morbidity rates during a camp session. Some researchers also recommend using a cardiac exercise test [18] and tests of physical [19] and mental activity [20].

We believe that such protocols should also focus on the assessment of a child's nutritional status and the analysis of its dynamics during a summer camp session. This can help to reduce the incidence of nutrition-related diseases [21].

The methods proposed earlier are intended to analyze changes to anthropometric parameters in children with a variety of physical statuses. Recently, other approaches have been introduced, involving the use of diagnostic equipment for the assessment of a child's nutritional status [21, 22], including bioelectrical impedance analysis (BIA). However, the feasibility of BIA for such tasks still needs to be investigated.

The objective of this study was to provide a rationale for the use of bioimpedance analysis and anthropometric measurements as efficacy criteria for summer camp healthcare.

METHODS

The study was conducted in 346 children and teenagers (125 boys and 221 girls) aged 8 to 15 years from 3 summer camps located in the Samara region. The camps were selected from those recreational organizations whose directors agreed to cooperate. More than one camp was included in the study to ensure the probability of encountering different patterns of changes to the anthropometric and bioimpedance parameters. Each camp had playgrounds, sports facilities and dining halls. Specialized sports camps were not included in the study. The daily schedules were standard. The study enrolled the residents of the Samara region whose medical histories placed them into health groups I or II. Children who had chronic conditions or pronounced peripheral edemas, were undergoing medication therapy at the time of the study, permanently resided outside of the Samara region, or whose parents refused to give their consent to participate were excluded.

Measurements were performed twice: on the first and second days upon arrival to the camp, and two days before leaving for home. A camp session lasted 21 days. Anthropometric measurements were taken following a standard unified method [23]: height was measured using an anthropometer (Kafa; Russia) with a 0.5 cm precision; body weight was measured on the electronic medical scales EMS-150-Massa-K (Massa-K; Russia) with a 60 g precision. The children's physical development was assessed using a modified regression scale for the Samara region [24]. Body composition was estimated on the ABC-01 analyzer (Medass; Russia) operated at 50 kHz frequency. A standard tetrapolar method was applied; it is based on 4 electrodes placed over the hand and ankle of a child lying in the supine position. During the procedure, the angle between the right shoulder and the vertical body axis was 45°; the right forearm was parallel to the vertical body axis; the feet were positioned shoulder width apart. Bioimpedance measurements were taken in the morning before meal or 2.5–3 hours after meal. No vigorous physical activity or physiotherapy preceded the procedure. The following parameters were estimated: total fat mass (FM), skeletal muscle mass (SMM), and the basal metabolic rate (BMR) [25, 26]. The obtained data were saved in Microsoft Excel 2010 (Microsoft; USA) and later processed in Statistica ver. 13.1 (StatSoft Inc.; USA). Body weight dynamics during a camp session were analyzed using the Wilcoxon test for paired samples. Changes in the total proportion of children with normal physical development (NPD), body weight deficit (BWD) and excess body weight (EBW) were analyzed using McNemar's chi-squared test. Between the camps, the dynamics were compared using Pearson's chi-squared test. Differences ($M \pm m$, where M is an arithmetic mean, m is an arithmetic mean error) were considered significant at $p < 0,05$.

RESULTS

Changes in the physical development during a camp session were analyzed and compared between children from 3 different camps. Data on camp 1 are shown in Table 1.

In camp 1, 62 children with NPD (47.7%), 19 children with BWD (14.6%) and 31 children with EBW (23.8%) retained their physical status. A positive trend was observed in 8 children with BWD (6.2%) and 5 children with EBW (3.8%), whose physical development could be described as normal by the end of the session. Negative dynamics were observed in 4 children (3.1%): although their physical health was normal when they arrived at the camp, they lost weight and developed BWD during their stay. One more child (0.8%) was physically fit upon arrival, but later gained weight and thus joined the EBW group. The general trend in weight change was nevertheless insignificant ($p = 0.415$).

The analysis of changes in the proportion of children with NPD, BWD and EBW in camp 1 did not reveal any significant differences inside those groups (Table 2).

In camp 2, 56 children with NPD (48.7%), 16 children with BWD (13.9%) and 31 children with EBW (27%) retained their health status (Table 3).

A positive change was observed in 5 children with BWD (4.3%) and 2 children with EBW (1.7%), whose physical development was characterized as normal at the end of their stay at the camp. Three children (2.6%) had developed BWD and 2 children (1.7%) had gained weight, thus moving to the EBW group by the end of the camp session (Table 4). Similarly to camp 1, the overall body weight dynamics were insignificant ($p = 0.585$).

Weight trends in each separate health group (NPD, BWD, EBW) were also insignificant (Table 4).

In camp 3, 62 children with NPD (61.4%), 13 children with BWD (12.9%) and 6 children with EBW (5.9%) retained their health status. Positive changes were observed in 6 children with BWD (5.9%) and 5 children with EBW (5.0%), who had

moved into the NPD group. Negative dynamics were observed in 9 children who had developed body mass deficit by the end of their stay. In camp 3, the overall weight dynamics were reliable ($p = 0.025$) (Table 5).

There were more children in camp 3 who had lost weight during their stay than those who had gained it ($p = 0.025$). Of 14 children (12.2%) who had lost weight, 9 had BWD at the end of the camp session and 5 had moved into the NPD group. Six children with initial BWD had gained weight and moved into the NPD group by the end of their stay. Importantly, weight loss during a camp session can be regarded as a positive health effect only for initially overweight children. For children with NPD and BWD such changes are not beneficial.

We analyzed the dynamics of body weight in children with different physical statuses during their stay at a summer camp (Table 6). For children who were initially fit or overweight, the changes were statistically insignificant. For example, in camp 1 the children with NPD weighed 47.05 ± 1.1 kg upon arrival and 47.34 ± 1.12 kg ($p = 0.347$) before leaving for home. At the same time, the children with weight deficit demonstrated a significant increase in their body weight by the end of a camp session. In camp 2, such children weighed 39.78 ± 1.48 kg upon arrival and 41.37 ± 1.66 kg ($p = 0.002$) at the end of the camp session.

Bioimpedance analysis is expected to confirm such positive body weight dynamics. During their stay at camp, children are supposed to receive a balanced diet and enough physical exercise, which will be reflected in their bioimpedance results. Fat mass will decrease, whereas skeletal muscle mass and the basal metabolism rate will grow. In camps 1 and 2, the average

Table 1. Analysis of overall body weight dynamics in camp 1

Beginning of session		End of session			Total
		NPD	BWD	EBW	
NPD	Абс.	62	4	1	67
	%	47.7	3.1	0.8	51.5
BWD	Абс.	8	19	0	27
	%	6.2	14.6	0	20.8
EBW	Абс.	5	0	31	36
	%	3.8	0	23.8	27.7
Total	Абс.	75	23	32	130
	%	57.7	17.7	24.6	100

Table 2. Changes in the proportion of children with NPD, BWD and EBW during a camp session in camp 1

Dynamics	NPD		BWD		EBW	
	n	%	*n*	%	*n*	%
Increase	13	10	4	3.1	1	0.8
Decline	5	3.8	8	6.2	5	3.8
No changes	112	86.2	118	90.8	124	95.4
Total	130	100	130	100	130	100
Statistical significance, *p*	0.096		0.388		0.219	

Table 3. Analysis of overall body weight dynamics in camp 2

Beginning of session		End of session			Total
		NPD	BWD	EBW	
NPD	Abs.	56	3	2	61
	%	48.7	2.6	1.7	53
BWD	Abs.	5	16	0	21
	%	4.3	13.9	0	18.3
EBW	Abs.	2	0	31	33
	%	1.7	0	27	28.7
Total	Abs.	63	19	33	115
	%	54.8	16.5	28.7	100

Table 4. Changes in the proportion of children with NPD, BWD and EBW during a camp session in camp 2

Dynamics	NPD		BWD		EBW	
	n	%	*n*	%	*n*	%
Increase	8	7	3	2.6	2	1.7
Decline	5	4.3	6	5.2	2	1.7
No changes	102	88.7	106	92.2	111	96.5
Total	115	100	115	100	115	100
Statistical significance, *p*	0.581		0.508		1	

values of those bioimpedance parameters increased slightly, suggesting that the children had been receiving a balanced diet and sufficient physical exercise throughout their stay, but those changes were statistically insignificant. In camp 3, both fat and skeletal muscle masses decreased significantly. This may have been due to the inadequate diet, insufficient physical activity or a poorly structured daily schedule. Insignificant changes in the metabolism rate confirm our hypothesis (Table 7).

FM, SMM and BMR were measured in each child. Based on the measurement results, 7 groups were distinguished (Table 8). Groups 1 and 3 consist of the children who received enough exercise and healthy diet. In group 2, the children were physically active, but food intake did not compensate for energy expenditures. In group 4, the children were also quite active, but their diet was too rich in calories. The children from groups 5, 6 and 7 lacked physical activity and consumed too many calories (Table 8).

The largest proportion of children who demonstrated positive changes in their body composition (groups 1–3) was observed in camps 1 and 2 (44.61% and 44.34%, respectively). At the same time, the number of children whose fat mass had increased while their skeletal mass had not was also quite high in camps 1 and 2. In camp 3, 19.8% of children had gained FM by the end of their stay but lost SMM or retained it at the initial level. Body weight dynamics in camp 3 inferred from the anthropometric measurements are confirmed by the presence of a significant proportion of children constituting groups 1–3.

DISCUSSION

The anthropometric measurements identified children with negative body weight dynamics observed during their stay at a summer camp: the initially fit children had developed body weight deficit or gained weight by the end of the camp session. This is an alarming trend, especially because it was observed in all three studied camps. In camp 3, body weight dynamics were statistically significant and were not always positive. Some physically fit children and their weight-deficient peers

Table 5. Analysis of overall body weight dynamics in camp 3

Beginning of session		End of session			Total
		NPD	BWD	EBW	
NPD	Abs.	62	9	0	71
	%	61.4	8.9	0	70.3
BWD	Abs.	6	13	0	19
	%	5.9	12.9	0	18.8
EBW	Abs.	5	0	6	11
	%	5	0	5.9	10.9
Total	Abs.	73	22	6	101
	%	72.3	21.8	5.9	100

Table 6. A summary table of children's body weight dynamics during a camp session in camps 1–3

Camp	Upon arrival	Beginning of session			End of session			Difference[4]		p^6
		M[1]	SD[2]	m^3	M	SD	m	M	SE[5]	
Camp 1	NPD	47.05	9.03	1.1	47.34	9.16	1.12	0.29	0.3	0.347
	BWD	40.49	6.64	1.28	41.56	7.72	1.49	1.07	0.4	**0.014**
	EBW	61.92	10.3	1.72	62.59	10.5	1.75	0.67	0.55	0.228
Camp 2	NPD	47.47	8.26	1.06	47.33	8.67	1.11	–0.14	0.29	0.627
	BWD	39.78	6.77	1.48	41.37	7.63	1.66	1.6	0.46	**0.002**
	EBW	61.16	10.18	1.77	61.51	10.83	1.89	0.35	0.46	0.458
Camp 3	NPD	42.94	7.02	0.83	43.14	6.9	0.82	0.2	0.32	0.543
	BWD	35.73	5.12	1.17	37.28	5.69	1.31	1.55	0.36	**<0.001**
	EBW	57.66	12.21	3.68	57.07	12.85	3.87	–0.59	0.9	0.524

Table 7. Bioimpedance parameters in children from camps 1–3

Camp	BIA parameter	Beginning of session		End of session		Difference[4]		p^6
		M[1] ± m^2	$P_{25–75}$[3]	M ± m	$P_{25–75}$	M	SE[5]	
Camp 1	FM (kg)	10.89 ± 0.44	7.7 – 13.9	11.29 ± 0.49	7.3 – 14.3	0.4	0.29	0.473
	SMM (kg)	21.23 ± 0.46	17.5 – 25.1	21.35 ± 0.45	18 – 25.1	0.12	0.4	0.687
	BMR (kcal/m^2)	857.04 ± 4.98	824 – 888	865.27 ± 5.38	835 – 894	8.23	0.65	0.262
Camp 2	FM (kg)	12.32 ± 0.56	8.1 – 16.5	13.09 ± 0.38	8.3 – 17.9	0.77	0.35	0.198
	SMM (kg)	20.45 ± 0.34	16.6 – 24.3	20.84 ± 0.56	17.2 – 24.5	0.39	0.46	0.478
	BMR (kcal/m^2)	832.54 ± 5.34	798 – 867	846.01 ± 4.78	813 – 879	13.47	0.58	0.061
Camp 3	FM (kg)	12.35 ± 0.55	8.7 – 15.9	10.89 ± 0.44	7.3 – 14.3	–1.46	0.46	**0.039**
	SMM (kg)	23.43 ± 0.57	19.3 – 27.5	21.81 ± 0.55	18.5 – 25.3	–1.62	0.42	**0.041**
	BMR (kcal/m^2)	873.32 ± 5.45	849 – 897	862.51 ± 5.29	836 – 889	–10.81	0.51	0.155

Table 8. Dynamics of bioimpedance parameters in children from camps 1–3 during a camp session

Group	Dynamics	Number of children (%)		
		Camp 1	Camp 2	Camp 3
1	Decreasing FM, stable SMM, increasing BMR	17 (13.07)	14(12.17)	12 (11.89)
2	Decreasing FM, increasing SMM, decreasing BMR	12 (9.23)	16 (13.91)	11 (10.89)
3	Decreasing FM, increasing SMM, increasing BMR	29 (22.31)	21 (18.26)	17 (16.83)
4	Increasing FM, SMM, BMR	14 (10.77)	14 (12.17)	13 (12.87)
5	Increasing FM, stable SMM, decreasing BMR	20 (15.39)	17(14.79)	19 (18.81)
6	Increasing FM, decreasing SMM, decreasing BMR	24 (18.46)	14 (12.17)	20 (19.8)
7	Increasing FM, decreasing SMM, increasing BMR	14 (10.77)	19 (16.53)	9 (8.91)

gained weight, which can be regarded as a positive effect, but there was also a big proportion of children who lost weight during their stay. BIA confirms the results of the conducted anthropometric measurements. Based on the dynamics of fat mass, skeletal muscle mass and basal metabolism rates measured in each child, we can assess the quality of nutrition at camps and its impact of children's health. Weight gain that serves as a criterium of healthy physical development and therefore suggests a positive effect of a health program can also result from an increase in fat content [17, 20, 25]. If children receive a balanced diet and are provided with physical activities that match food intake, changes in the body composition will not be manifested as an increase in fat mass. Skeletal muscle mass can grow or remain stable throughout a camp session [18, 19, 25]. In our study, weight gain was accompanied by a healthy increase in skeletal muscle mass, as well as by an unhealthy increase in fat mass in many children. At the same time, weight loss during the camp session was not always associated with a drop in fat mass, but in some cases was indicative of skeletal muscle mass loss, indicating the absence of a positive effect on children's health. Anthropometric measurements and BIA conducted in camp 1 suggest that the children were provided with a balanced diet and energy intake matched energy expenditures. In camp 2, the diet was probably too rich in calories and energy intake exceeded energy expenditures. In camp 3, food intake could not compensate for energy expenditures.

CONCLUSIONS

During a summer camp session, a child's anthropometric parameters and body composition undergo certain changes that can reflect his/her nutritional status. The dynamics of the anthropometric parameters and bioelectrical impedance analysis can provide information about the diet a child receives and the physical activity he/her is provided with. Therefore, anthropometric measurements and BIA can be used as efficacy criteria for summer camp healthcare.

References

1. Baranov AA, Kuchma VR, Skoblina NA, Milushkina OYu, Bokareva NA, Yampolskaya YuA. Physical development of children and adolescents of the Russian Federation. M., 2013. 192 p.
2. Skoblina NA, Fedotov DM, Milushkina OYu, Bokareva NA, Tatarinchik AA. Characteristics of physical development of children and adolescents in Arkhangelsk and Moscow: history aspects. Vestnik Severnogo (Arkticheskogo) federal'nogo universiteta. 2016. (2): 110–22.
3. Baranov AA, Kuchma VR, Skoblina NA, Milushkina OYu, Bokareva NA. The main mechanisms of morphofunctional development of children and adolescents in modern conditions. Vestnik Rossijskoj akademii medicinskih nauk. 2012; (12): 35–40.
4. Kuchma VR. Inter-sectoral collaboration in the formation of a healthy lifestyle of children and teenagers: problems and solutions. Voprosy shkol'noj i universitetskoj mediciny i zdorov'ya. 2014; (3): 4–9.
5. Zigitbaev RN, Ahmadullina GH, Povargo EA, Zulkarnaev TR. Sravnitel'naya ocenka sostoyaniya zdorov'ya shkol'nikov v usloviyah promyshlennyh gorodov respubliki Bashkortostan. Medicinskij vestnik Bashkortostana. 2017; 12 (5): 15–20.
6. Gricinskaja VL. Characteristics of physical development and nutrition of schoolchildren of urban and rural population of Krasnoyarsk region. Pediatric Nutrition. 2012; (5): 8–11.
7. Malceva EA, Chesnokova LL, Mihajlova LA. Anthropometrical indicators of children of prepubertatny age of the industrial city. Sovremennye problemy nauki i obrazovanija. 2016; (6): 22.
8. Skoblina NA, Milushkina OYu, Gudinova ZhV, Bokareva NA, Gavryushin MYu, Sazonova O.V., et al. The scientific-methodical substantiation of norms of body weight and the standards for physical development of children''s population. Zdorov'e naseleniya i sreda obitaniya. 2018; 9 (306): 19–22.
9. Tenfold increase in childhood and adolescent obesity in four decades: new study by Imperial College London and WHO. Available from: http://www.who.int/mediacentre/news/releases/2017/increase-childhood-obesity/ru/ (Data obrashcheniya: 22.12.2018).
10. Baturin AK, Pogozheva AV, Martinchik AN, Safronova AM, Keshbyants EE, Denisova NN, et al. Study of nutrition peculiarities of the population of the European and Asian part of the Arctic zone of Russia. Problems of nutrition. 2016; 85 (2): 83.
11. Kotelnikov GP, Krjukov NN, Gridasov GN, Baturin AK, Gilmiyarova FN, Berezin II, et al. The rationale for the implementation of the principles of state policy of healthy nutrition of the population of Samara region for the period till 2020. Problems of nutrition. 2011; (2): 52–7.
12. Tapeshkina NV, Klishina MN. The organization of school in the modern conditions: problems and solutions. Sibirskij meditsinskij zhurnal (Irkutsk). 2013. 122 (7): 113–7.
13. Kon IYa, Tutelyan VA, Uglickij AK, Volkova LYu. Racional'noe pitanie rossijskih shkol'nikov: problemy i ih puti preodoleniya. Zdorov'e naseleniya i sreda obitaniya. 2008; 7 (184): 4–5
14. Gorelova ZhYu, Kuchma VR, Solovyeva YuV, Letuchaya TA, Plats-Koldobenko AN, Uglov SYu. Scientific substantiation and working out of a school menu options (12 day daily rations), taking into account domestic supply. The basic principles, features and benefits. Evrazijskoe Nauchnoe Ob"edinenie. 2017; 3 (25): 71–7.
15. Samarskij statisticheskij ezhegodnik: Stat. sbornik. Samara: Samarastat, 2016. 345 s.
16. Sedova AS, Sokolova SB, Laponova ED. Dynamics of functional state of children's body in conditions of shortened shifts of stationary recreation. Voprosy shkol'noj i universitetskoj mediciny i zdorov'ya. 2016; (4): 41–7.

17. Metodicheskie rekomendacii MR 2.4.4.0127-18 «Metodika ocenki ehffektivnosti ozdorovleniya v stacionarnyh organizaciyah otdyha i ozdorovleniya detej». Utverzhdeny Glavnym gosudarstvennym sanitarnym vrachom RF 11 maya 2018 g. Available from: https://www.garant.ru/products/ipo/prime/doc/71875014/.
18. Tanina NA. Evaluation of healthcare measures efficiency in summer out-of-town recreational and rehabilitation facilities for children. Medicinskij al'manah. 2015; 2 (37): 77–9.
19. Platonova AG, Podrigalo LV. Application of motor activity for the evaluation of the effectiveness of children's rehabilitation. Voprosy shkol'noj i universitetskoj mediciny i zdorov'ya. 2014; (3): 51–2.
20. Novikova II, Vejnih PA. Metodicheskie aspekty ocenki ehffektivnosti ozdorovleniya detej i podrostkov v sovremennyh usloviyah. Vesti MANEB v Omskoj oblasti. 2013; 3 (3): 30–3
21. Blinova EG, Akimova IS, Chesnokova MG, Demakova LV. The results of the analysis of the anthropometric and bioimpendancemetria studies of students of Omsk city. Sovremennye problemy nauki i obrazovanija. 2014; (3): 543 p.
22. Mok E, Letellier G, Cuisset JM, et al. Assessing change in body composition in children with Duchenne muscular dystrophy: anthropometry and bioelectrical impedance analysis versus dual-energy X-ray absorptiometry. Clin Nutr. 2010; 29 (5): 633–8.
23. Kuchma VR, Vishneveckaya TYu, Yamshchikova NL. Issledovanie fizicheskogo razvitiya detej i podrostkov v sisteme social'no-gigienicheskogo monitoringa. Metodicheskie ukazaniya. Utverzhdeny zamestitelem glavnogo gosudarstvennogo sanitarnogo vracha g. Moskvy 12.07.99 g. M., 1999. 37 p.
24. Vdovenko SA, Sazonova OV, Ponomarev VA, Mazur LI, Gavryushin MYu, Borodina LM. Ocenochnye tablicy fizicheskogo razvitiya detej i podrostkov shkol'nogo vozrasta Samarskoj oblasti. Metodicheskie rekomendacii. Samara, 2018. 46 p.
25. Nikolaev DV, Shchelykalina SP. Bioimpedance analysis of the human body composition: Lectures. M., 2016. 152 p.
26. Rudnev SG, Soboleva NP, Sterlikov SA, Nikolaev DV, Starunova OA, Chernykh SP, et al. Bioimpedance study of body composition in the Russian population. M., 2014. 493 p.

Литература

1. Баранов А. А., Кучма В. Р., Скоблина Н. А., Милушкина О. Ю., Бокарева Н. А., Ямпольская Ю. А. Физическое развитие детей и подростков Российской Федерации. М., 2013. 192 с.
2. Скоблина Н. А., Федотов Д. М., Милушкина О. Ю., Бокарева Н. А., Татаринчик А. А. Характеристика физического развития детей и подростков Архангельска и Москвы: исторические аспекты. Вестник Северного (Арктического) федерального университета. 2016; (2): 110–22.
3. Баранов А. А., Кучма В. Р., Скоблина Н. А., Милушкина О. Ю., Бокарева Н. А. Основные закономерности морфо-функционального развития детей и подростков в современных условиях. Вестник Российской академии медицинских наук. 2012; (12): 35–40.
4. Кучма, В. Р. Межсекторальное взаимодействие при формировании здорового образа жизни детей и подростков: проблемы и пути решения. Вопросы школьной и университетской медицины и здоровья. 2014; (3): 4–9.
5. Зигитбаев Р. Н., Ахмадуллина Г. Х., Поварго Е. А., Зулькарнаев Т. Р. Сравнительная оценка состояния здоровья школьников в условиях промышленных городов республики Башкортостан. Медицинский вестник Башкортостана. 2017; 12 (5): 15–20.
6. Грицинская В. Л. Характеристика физического развития и питания школьников городского и сельского населения Красноярского края. Вопросы детской диетологии. 2012; (5): 8–11.
7. Мальцева Е. А., Чеснокова Л. Л., Михайлова Л. А. Антропометрические показатели детей препубертатного возраста промышленного города. Современные проблемы науки и образования. 2016; (6): 22.
8. Скоблина Н. А., Милушкина О. Ю., Гудинова Ж. В., Бокарева Н. А., Гаврюшин М. Ю., Сазонова О. В. и др. Научно-методическое обоснование границ нормы массы тела, используемых при разработке нормативов физического развития детского населения. Здоровье населения и среда обитания. 2018; 9 (306): 19–22.
9. ВОЗ. Ожирение и избыточный вес. Десятикратный рост числа детей и подростков с ожирением за последние сорок лет: новое исследование Имперского колледжа в Лондоне и ВОЗ. Доступно по ссылке: http://www.who.int/mediacentre/news/ releases/2017/increase-childhood-obesity/ru/ (дата обращения: 22.12.2018).
10. Батурин А. К., Погожева А. В., Мартинчик А. Н., Сафронова А. М., Кешабянц Э. Э., Денисова Н. Н., Кобелькова И. В. Изучение особенностей питания населения Европейской и Азиатской части арктической зоны России. Вопросы питания. 2016; 85 (2): 83.
11. Котельников Г. П., Крюков Н. Н., Гридасов Г. Н., Батурин А. К., Гильмиярова Ф. Н., Березин И. И. и др. Обоснование программы реализации основ государственной политики здорового питания населения Самарской области на период до 2020 года. Вопросы питания. 2011; (2): 52–7.
12. Тапешкина Н. В., Клишина М. Н. Организация школьного питания в современных условиях: проблемы и пути решения. Сибирский медицинский журнал (Иркутск). 2013; 122 (7): 113–7.
13. Конь И. Я., Тутельян В. А., Углицкий А. К., Волкова Л. Ю. Рациональное питание российских школьников: проблемы и их пути преодоления. Здоровье населения и среда обитания. 2008; 7 (184): 4–5.
14. Горелова Ж. Ю., Кучма В. Р., Соловьева Ю. В., Летучая Т. А., Плац-Колдобенко А. Н., Углов С. Ю. Научное обоснование и разработка вариантов школьного меню (12 дневных суточных рационов) с учетом домашнего питания. Основные принципы, особенности и преимущества. Евразийское Научное Объединение. 2017; 3 (25): 71–7.
15. Самарский статистический ежегодник: Стат. сборник. Самара: Самарастат, 2016. 345 с.
16. Седова А. С., Соколова С. Б., Лапонова Е. Д. Динамика функционального состояния организма детей в условиях укороченной смены стационарной организации отдыха. Вопросы школьной и университетской медицины и здоровья. 2016; (4): 41–7.
17. Методические рекомендации МР 2.4.4.0127-18 «Методика оценки эффективности оздоровления в стационарных организациях отдыха и оздоровления детей». Утверждены Главным государственным санитарным врачом РФ 11 мая 2018 г. Доступно по ссылке: https://www.garant.ru/products/ipo/prime/doc/71875014/.
18. Танина Н. А. Оценка эффективности оздоровительных мероприятий в летних загородных учреждениях отдыха и оздоровления детей. Медицинский альманах. 2015; 2 (37): 77–9.
19. Платонова А. Г., Подригало Л. В. Использование двигательной активности для оценки эффективности оздоровления детей. Вопросы школьной и университетской медицины и здоровья. 2014; (3): 51–2.
20. Новикова И. И., Вейних П. А. Методические аспекты оценки эффективности оздоровления детей и подростков в современных условиях. Вести МАНЭБ в Омской области. 2013; 3 (3): 30–3.
21. Блинова Е. Г., Акимова И. С., Чеснокова М. Г., Демакова Л. В. Результаты анализа антропометрических и биоимпедансометрических исследований у студентов города Омска. Современные проблемы науки и образования. 2014; (3): 543.
22. Mok E, Letellier G, Cuisset JM, et al., Assessing change in body composition in children with Duchenne muscular dystrophy: anthropometry and bioelectrical impedance analysis versus dual-energy X-ray absorptiometry. Clin Nutr. 2010; 29 (5): 633–8.
23. Кучма В. Р., Вишневецкая Т. Ю., Ямщикова Н. Л. Исследование физического развития детей и подростков

в системе социально-гигиенического мониторинга. Методические указания. Утверждены заместителем главного государственного санитарного врача г. Москвы 12.07.99 г. М., 1999. 37 с.
24. Вдовенко С. А., Сазонова О. В., Пономарев В. А., Мазур Л. И., Гаврюшин М. Ю., Бородина Л. М. Оценочные таблицы физического развития детей и подростков школьного возраста Самарской области. Методические рекомендации. Самара, 2018. 46 с.
25. Николаев Д. В., Щелыкалина С. П. Лекции по биоимпедансному анализу состава тела человека. М., 2016. 152 с.
26. Руднев С. Г., Соболева Н. П., Стерликов С. А., Николаев Д. В., Старунова О. А., Черных С. П. и др. Биоимпедансное исследование состава тела населения России. М., 2014. 493 с.

COMBINATION LASER THERAPY FOR EPIRETINAL MEMBRANE: A PHYSICO-MATHEMATICAL MODEL

Takhchidi KP[1,2], Zheltov GI[4], Kachalina GF[2], Kasminina TA[2], Tebina EP[3] ✉

[1] Pirogov Russian National Research Medical University, Moscow, Russia

[2] Research Center for Ophthalmology, Pirogov Russian National Research Medical University, Moscow, Russia

[3] Faculty of Pediatrics, Pirogov Russian National Research Medical University, Moscow, Russia

[4] Stepanov Institute of Physics, Minsk, Belarus

An epiretinal membrane (ERM) is a product of abnormal cell proliferation on the inner surface of the retina and at the vitreomacular interface. Laser therapy is an interesting modality for treating pathologies of the vitreomacular interface. The wise choice of laser settings (wavelength, exposure time, power) minimizes damage to the retina and ensures a good therapeutic effect. This could be a serious impetus to the development and refinement of laser technologies for treating ERM. This work investigates the biophysical response of structural retinal components, including the dynamics of temperatures and acoustic oscillations, protein denaturation, and stimulation of tissue regeneration, to a quasi-cw laser beam and a subsequent series of laser micropulses. The manuscript also analyzes the mechanisms underlying the therapeutic effect of the proposed laser therapy in patients with ERM.

Keywords: epiretinal membrane, subthreshold micropulse laser photocoagulation, combination laser therapy, optical coherence tomography

Author contribution: Takhchidi KP and Kachalina GF conceived and designed the study; Tebina EP collected and analyzed the data; Kasminina TA performed laser therapy; Zheltov GI, Kasminina TA, and Tebina EP wrote the manuscript; Zheltov GI and Takhchidi KP revised the manuscript.

Compliance with ethical standards: the study was approved by Russian National Research Medical University (Protocol № 160 of December 19, 2016).

✉ **Correspondence should be addressed:** Ekaterina P. Tebina
Volokolamskoe shosse 30, bl. 2, 123182; ekaterinatebina@mail.ru

Received: 01.03.2019 **Accepted:** 15.03.2019 **Published online:** 30.04.2019

DOI: 10.24075/brsmu.2019.032

ТЕХНОЛОГИЯ КОМБИНИРОВАННОГО ЛАЗЕРНОГО ЛЕЧЕНИЯ ЭПИРЕТИНАЛЬНОГО ФИБРОЗА: ФИЗИКО-МАТЕМАТИЧЕСКАЯ МОДЕЛЬ

Х. П. Тахчиди[1,2], Г. И. Желтов[4], Г. Ф. Качалина[2] , Т. А. Касмынина[2], Е. П. Тебина[3] ✉

[1] Российский национальный исследовательский медицинский университет имени Н. И. Пирогова, Москва, Россия

[2] Научно-исследовательский центр офтальмологии, Российский национальный исследовательский медицинский университет имени Н. И. Пирогова, Москва, Россия

[3] Педиатрический факультет, Российский национальный исследовательский медицинский университет имени Н. И. Пирогова, Москва, Россия

[4] Институт физики имени Б. И. Степанова НАН Беларуси, Минск, Беларусь

Эпиретинальная мембрана (ЭРМ) возникает в результате пролиферативно-дистрофического процесса во внутренних слоях сетчатки и витреомакулярном интерфейсе. Особый интерес в лечении витреоретинальной патологии представляет применение лазерного излучения в макулярной зоне. При адекватном выборе режимов облучения (длины волны, длительности экспозиции и мощности излучения) лечебный эффект достигается при минимальном повреждающем действии на структуры сенсорной сетчатки. Этот фактор явился серьезным стимулом для развития и совершенствования лазерных технологий в лечении ЭРМ. В представленной работе проведен анализ биофизического отклика структурных элементов сетчатки (динамики температурных и акустических полей, термоденатурация, стимуляция репаративных процессов) при последовательном воздействии лазерного квазинепрерывного излучения и серии микроимпульсов с дальнейшей оценкой основных механизмов лечебного эффекта разработанной комбинированной лазерной технологии у пациентов с ЭРМ.

Ключевые слова: эпиретинальный фиброз, субпороговое микроимпульсное лазерное воздействие, комбинированная лазерная технология, оптическая когерентная томография

Информация о вкладе авторов: Х. П. Тахчиди, Г. Ф. Качалина — концепция и дизайн исследования; Е. П. Тебина — сбор и обработка материала; Т. А. Касмынина — лазерное лечение пациента; Г. И. Желтов, Т. А. Касмынина, Е. П. Тебина — написание текста; Г. И. Желтов, Х. П. Тахчиди — редактирование.

Соблюдение этических стандартов: исследование одобрено этическим комитетом РНИМУ имени Н. И. Пирогова (протокол № 160 от 19 декабря 2016 г.).

✉ **Для корреспонденции:** Екатерина Павловна Тебина
Волоколамское шоссе, д. 30, корп. 2, 123182; ekaterinatebina@mail.ru

Статья получена: 01.03.2019 **Статья принята к печати:** 15.03.2019 **Опубликована онлайн:** 30.04.2019

DOI: 10.24075/vrgmu.2019.032

Ever more people across the world are affected by fibrotic scarring of the retina that can cause significant visual impairment or even blindness [1]. An epiretinal membrane (ERM) is a product of abnormal cell proliferation on the inner surface of the retina and at the vitreomacular interface [2]. It is a fibrous tissue that contracts, causing the retina to pucker and promoting formation of a macular hole [2, 3].

The major contributors to this ocular disorder are posterior vitreous detachment (PVD), the anatomy of the internal limiting membrane (ILM), which has microscopic pores, and abnormal blood supply to the macula [4–6]. According to the literature, ERM is constituted by various cell types, including glial cells (Müller cells, astrocytes and microglial cells), hyalocytes, macrophages, retinal pigment epithelial cells, and fibroblasts

[7–8]. ERM formation is initiated when these cells, regardless of their origin, transdifferentiate into myofibroblast-like cells that abundantly secrete transforming growth factor beta 1, causing the membrane to contract [9–10]. The most intense cell proliferation takes place long before ERM becomes symptomatic. Once the membrane has been formed on the retinal surface, cell proliferation stops [11].

In the early stages of the disease, cell proliferation can be inhibited using a variety of different methods, such as intravitreal injections of high doses of glucocorticoids, radiation therapy or administration of cytostatic agents [12]. These methods, however, have a high risk of adverse effects and therefore are not popular in clinical practice. At present, two strategies are normally used in patients with ERM: surgery to remove the membrane (vitrectomy) and monitoring without treatment [13].

In spite of significant advances in the understanding of the mechanisms underlying ERM formation, the conditions under which vitreoretinal cells transdifferentiate into myofibroblasts are unknown. It is also unclear whether surgical removal of the membrane should be performed in asymptomatic patients or can be safely delayed until visual acuity starts to deteriorate or a patient develops metamorphopsia. Unfortunately, there is no guarantee that the lost vision will be restored after surgery. In addition, post-operative relapses are not a rare thing [12].

Laser therapy is an interesting modality for treating pathologies of the vitreomacular interface [14–15]. The wise choice of laser settings (wavelength, exposure time, power) minimizes damage to the retina and ensures a good therapeutic effect [16–17]. Recently, the authors of this work have patented a new, clinically tested method for treating patients with early stages of preretinal macular fibrosis; the method is a combination of selective photocoagulation of the ERM by a yellow laser and subsequent stimulation of tissue regeneration by a series of subthreshold laser micro-pulses [18]. Such laser therapy induces ERM regression, improves visual acuity and increases light sensitivity of the retina.

Further evolution and clinical application of the proposed method will largely depend on the understanding of its therapeutic mechanisms. Research into biological and physical interactions between the laser beam and structural retinal components can significantly expand our knowledge in this field. a useful tool here is mathematical modeling that accounts for the laser settings needed to achieve a therapeutic effect [17–20].

We have developed a physico-mathematical model that predicts biophysical effects of laser exposure on retinal tissues. The aim of this study was to investigate and analyze the biophysical response (the dynamics of temperatures and acoustic oscillations, protein denaturation, and stimulation of tissue regeneration) of structural retinal components to a quasi-continuous-wave laser beam and a subsequenta series of laser micropulses.

METHODS

Based on the experiments conducted in animal models (rabbits and primates), we determined the conditions required to induce local changes to intact chorioretinal tissue by laser radiation and identified the underlying mechanisms [17, 19].

These findings, coupled with the knowledge of spectral, optical and physical properties of intraocular structures, laid a basis for developing a physical model of the interactions between the laser beam and ocular fundus tissues (Fig.1) [19]. The mathematical description of this model was used to determine and optimize laser settings needed to preserve the

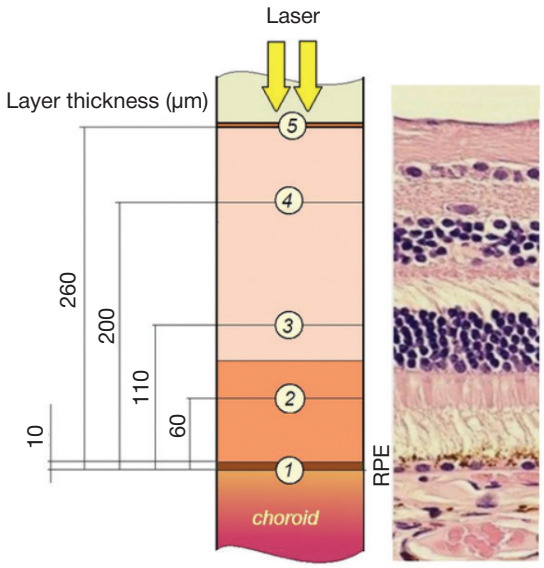

Fig. 1. A topographic representation of the chorioretinal complex. 1— the retinal pigment epithelium (10 μm in thickness), 2 — the layer of photoreceptors (60 μm), 3 — the outer nuclear layer (110 μm), 4 — the inner nuclear layer (200 μm), 5 — the inner limiting membrane (260 μm)

healthy structure of the retina and inhibit cell proliferation in the early stages of ERM.

The model is a multilayer system in which the geometrical dimensions and physical/optical properties of the layers correspond to those of major anatomical structures of the ocular fundus [21]. It accounts for the patterns of laser beam propagation in the anterior part of the eye, light absorption and scattering in the neuroepithelium and the choroid, and some other factors, including the presence of blood flow in the choroid with a speed gradient in the zone extending from Bruch's membrane to the sclera. Laser beam energy is absorbed by melanin granules and converts into heat. In the model, the optical properties of the intraocular structures located in the anterior part of the eyeball corresponded to those found in individuals above 40 years of age. The concentration of the pigment in the retinal pigment epithelium (RPE) was assumed to be 0.2, which is a typical concentration for a Caucasian patient.

The proposed method for treating ERM uses a combination of grid laser photocoagulation (577 nm wavelength, power of 50 mW, pulse duration of 0.05 s, spot size of 100 μm, distance between the coagulates of 150 μm) and subthreshold laser micropulses (577 nm wavelength, burst length of 30 ms, micropulse duration of 50 μs, duty cycle of 4.7%, repetition rate of 1,000 Hz, spot size of 100 μm, power of 50 mW) [18]. These parameters were used as initial conditions for further computations.

The distribution of temperatures in the chorioretinal complex was determined by a numerical solution of a two-dimensional

$$\rho(Z)\mathrm{Cp}(Z)\frac{\partial T}{\partial t} + F^{(k)}(U,V) = \frac{1}{r}\frac{\partial}{\partial r}\left[r\varkappa(Z)\frac{\partial T}{\partial r}\right] + \frac{\partial}{\partial Z}\left[\varkappa(Z)\frac{\partial T}{\partial Z}\right] + Q(t)q(r,Z,k,s);$$

$$q_i(r,Z) = \frac{E_{i-1}\,(k_i + s_i)R_{i-1}^2}{r_{i-1}^2}\exp\left[-k_i\,(Z - Z_i) - \frac{r^2}{r_s^2}\right]$$

Fig. 2. The heat equation for layer *i* of the model. *T* (*r*, *Z*, *t*) is a temperature rise above the physiological norm (37 °C); *Cp* (*Z*), *p* (*Z*), ϰ (*Z*), are specific heat capacity, density and thermal conductivity, respectively; *Q*(*t*) is time-dependent intensity of the absorbed radiation; *q* is volumetric heat generation, *k* and *s* are light absorption and scattering; $F^{(k)}$ is a function determined by the rates of radial (*V*) and axial (*U*) convective heat transfer; R_{i-1} and E_{i-1} are spot size (*exp* (-1)) and Gaussian beam irradiance at the interface between two adjacent layers

heat equation [19, 22] Fig. 2 shows the equation applied to describe each layer of the model. The size of the irradiated area of the pigment epithelium was assumed to be 100 μm, corresponding to the spot size. Radial irradiance distribution was considered to be Gaussian. The laser wavelength was 577 nm. Given the age of patients and the typical optical loss in the anterior part of the eye, the power of the laser beam absorbed by the chorioretinal complex was assumed to be 0.035 W [21, 23]. Then, given that the beam radius R was 50 μm, irradiance received by the inner limiting membrane was $E \approx 4.5 \cdot 10^6$ W/m^2. The pulse shape, which defines the $Q(t)$ function, was rectangular.

RESULTS AND DISCUSSION

Below, we describe the temperature profile of the retina irradiated by laser pulses with the parameters specified above. The distribution of temperatures along the laser beam axis ($r = 0$) is shown in Fig 3. Curve 1 in Fig. 3 reflects the degree of tissue heating ($T(Z, r = 0)$) by the end of the pulse. The averaged value k_{RPE} of yellow light absorption by RPE is 3–10^{-4}m^{-1}. About 30% of energy of the incident light is absorbed by pigment granules of RPE, whereas 70% propagates further into the capillaries and the choroid, and is absorbed by blood hemoglobin, causing tissue heating (Curve 1 in Fig. 3).

The part of the choroid adjacent to RPE is heated to the temperatures that exceed that of RPE. This area acts as a buffer, ensuring propagation of heat to the inner layers of the neuroepithelium and preventing the heat flow from traveling deeper into the choroid. Attenuated heat reaches the internal limiting membrane 0.3 s after the onset of exposure. Cooling continues for a few more seconds, stimulating photothermal tissue regeneration in all structural components of the neuroepithelium.

The relatively low absorption value k_{RPE} (in comparison with k_i of the green spectrum) means that the degree of a patient's retinal pigmentation has only a mild effect on the damage threshold. This fact, as well as the lack of absorption of the yellow spectrum by macular pigments, makes the proposed treatment modality especially beneficial for patients [20, 21, 24].

Fig. 4 shows the dynamics of tissue cooling and heating $T(t, Z, r = 0)$ in the retinal layers lying in the proximity to the laser beam axis; the colored areas on the graph indicate a dominating optical and thermal effect of laser radiation on the retinal tissues.

Exposure to 0.05-second-long laser pulses results in a temperature rise by about 35 °C and causes denaturation (coagulation) of RPE and proteins of the retina [19, 25]. Under such conditions, about 70% of the protein molecules undergo irreversible damage; therefore, the temperature specified above is considered to be a critical threshold. A temperature rise above the threshold value aggravates damage to tissues. In Fig. 3. The area heated above the threshold value is designated as the area of *denaturation*.

Laser-induced heating of tissue by 10 to 25 °C does not cause irreversible damage, but instead has a therapeutic effect that involves stimulation of retinal tissue regeneration [26]. In the picture, this area is referred to as the area of *photothermal stimulation*.

Laser-induced heating of tissue by 25 to 35 °C is characterized by a competition between tissue destruction and regeneration. It is difficult to tell which process is dominating; mathematical modelling cannot give an accurate answer. In the figure, this area is termed *the staging area*.

Summing up, our model predicts denaturation of RPE protein structures and total or partial local coagulation of the retina in the described irradiation modes (Curve 1, Fig. 4).

The most pronounced photothermal therapeutic effect on the tissues is observed in the area of inner and outer nuclear layers and part of the inner plexiform layer and ganglia. Here, exposure time is determined by the rate of tissue cooling. It takes the tissues a few seconds to cool down, which is many times longer than the duration of irradiation itself. In the retinal region close to the internal limiting membrane where ERM is formed, the probability of photothermal stimulation remains finite but still decreases considerably (see Curve 5 in Fig. 4). This means that laser-induced direct stimulation of ERM growth is highly unlikely. Figure 5 shows 10, 25 and 35 °C isotherms in the r, Z plane; they are given to illustrate radial distribution of temperatures under the studied conditions. The temperature ranges correspond to the data provided in Fig. 3.

Thus, the reduction of pulse duration down to 0.03 s shifts the zone of effective photothermal stimulation closer toward the inner nuclear layer. By contrast, an increase in the pulse

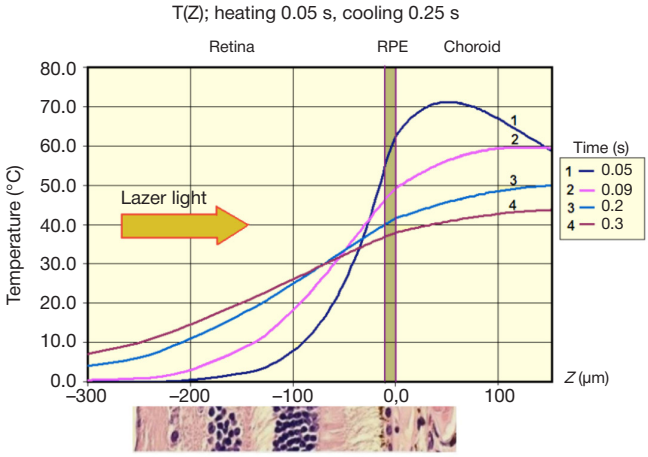

Fig. 3. A relationship between the degree of retinal tissue heating and the thickness Z ($r = 0$) of the chorioretinal complex by the end of the pulse, $t = 0.05$ s (**1**) and during tissue cooling 0.09 s (**2**), 0.2 s (**3**) and 0.3 s (**4**) after the onset of irradiation

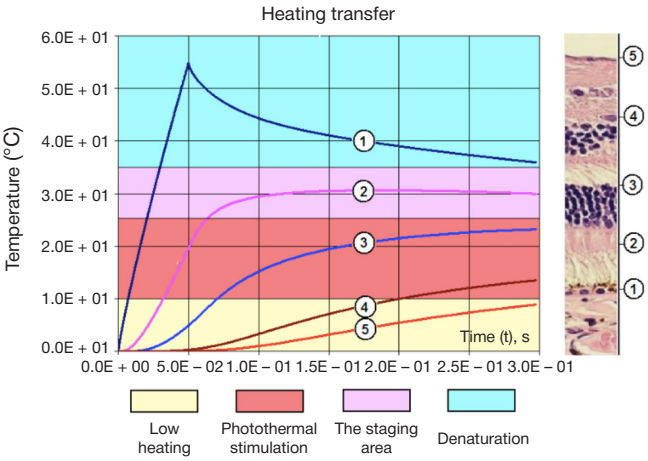

Fig. 4. Heating and cooling dynamics $T(t, Z_i, r = 0)$ in the retinal zones corresponding to the thickness Z_i of layer **1** (the retinal pigment epithelium, 10 μm), **2** (the layer of photoreceptors, 60 μm), **3** (the outer nuclear layer, 110 μm), **4** (the inner nuclear layer, 200 μm), and **5** (the inner limiting membrane, 260 μm). The *blue color* marks the area of irreversible protein denaturation at temperatures that exceed the physiological norm by 25 °C. The area of photothermal stimulation with the temperature rise ranging between 10 and 25 °C is shown in *red*; at these temperatures the therapeutic effect is achieved, and irreversible protein denaturation is almost negligible. The staging area marked in *purple* is where tissue regeneration stops and irreversible protein denaturation begins

length up to 0.07 s promotes heating of deeper layers and ERM and, therefore, can directly stimulate its growth.

Thermomechanical effects of laser micropulses on biological tissue

More intricate mathematical modeling is required to predict the thermomechanical effect of short laser pulses on biological tissue [27, 28]. Short pulses induce mechanical (acoustic) oscillations. For yellow laser pulses of 50 μs in length generated at 50 mW, the amplitude of mechanical oscillations approximates decimal fractions of a bar (1 bar ≈ 1 atm). Mechanical (cavitation-induced) damage to biological tissue occurs above the threshold value of 30–40 bar [28, 29].

At power set to 50 mW and a pulse duration of 50 μs, the temperature rise in the hottest spot of the pigment epithelium (along the beam axis) does not exceed 0.15 °C. Given that the repetition rate is 1,000 Hz, the next short pulse arrives in 10^{-3} s (1 ms). Regardless of the degree of heating, cooling occurs slowly. RPE does not cool down completely in the intervals between the pulses, and, therefore, accumulates heat from pulse to pulse. The interval of 0.03 s is enough to ensure a steady temperature rise of 2 °C. The critical rise above the physiological temperature is 30–35 °C. Generally, the heating and cooling of the retina follow the patterns shown in Fig. 2–4. However, in this case the temperature rise is 20 times lower.

Thus, at the selected stimulation mode, the thermomechanical effect of laser radiation on retinal tissues is very mild. We can almost rule out the probability of inducing thermal damage to the neuroepithelium. The therapeutic effect is determined by the thermomechanical impact of low-intensity laser radiation with the specified parameters.

The efficacy and safety of the proposed method can be illustrated by the following clinical case. Patient I., 68 years of age, presented with complains of decreased visual acuity and distorted vision in the right eye. During the examination, uncorrected visual acuity was 0.6; best-corrected visual acuity was 1.0. Biomicroscopy of the right eye revealed clear optical media. The optic disc was pale-pink, with sharp edges. a “cellophane” membrane was noticed in the macular zone.

The patient underwent multispectral imaging of the retina in the Multicolor mode with the following monochromatic filters: blue (BR; 488 nm), green (GR; 515 nm) and infrared (IR; 820 nm); spectral optical coherence tomography (SOCT), En Face optical coherence tomography angiography (OCT-A) (Spectralis OCT; Heidelberg Engineering, Inc., Germany) and microperimetry (MAIA, CenterVue; Italy). Multispectral imaging revealed the yellow-green foci indicative of ERM prominence (Fig. 6A). Measured by microperimetry, the average light sensitivity of the central retina was 26,3 dB (Fig. 6B). An OCT scan through the fovea discovered a hyperreflective line intimately associated with the internal limiting membrane; the foveal pit was flat. The thickness of the central retina was increased (257 μm). The outer limiting membrane, the junction between the inner and outer photoreceptor segments, the retinal pigment epithelium, and the choroid were intact (Fig. 6C).

Based on those findings, the patient was diagnosed with stage 0–1 preretinal macular fibrosis of the right eye. The patient was offered to undergo laser therapy: a combination of grid laser photocoagulation at 577 nm wavelength and subthreshold laser micropulses at 577 nm wavelength (3 sessions, separated by a month).

The first stage of treatment included grid laser photocoagulation of the retina excluding the avascular zone. The following laser settings were applied: wavelength of 577 nm, power of 50 mW, pulse duration of 0.05 s, spot size of 100 μm, distance between the coagulated spots of 150 μm. Two weeks after the session, a follow-up examination was conducted; uncorrected visual acuity improved to 0.7, best-corrected visual acuity was 1.0.

Multispectral imaging in the Multicolor mode revealed thinner, blurred ERM contours along its entire length, apart from the avascular zones, where coagulation spots remained (Fig. 7A). Measured by microperimetry, the average light sensitivity of the retina was 26.5 dB (Fig.7 B). SOCT visualized the flat fovea and the same hyperreflective line fused to the retinal surface (ERM). The thickness of the central retina had decreased to 253 μm. The outer limiting membrane, the junction between the inner and outer photoreceptor segments, the choroid, and the retinal pigment epithelium were intact (Fig. 7C).

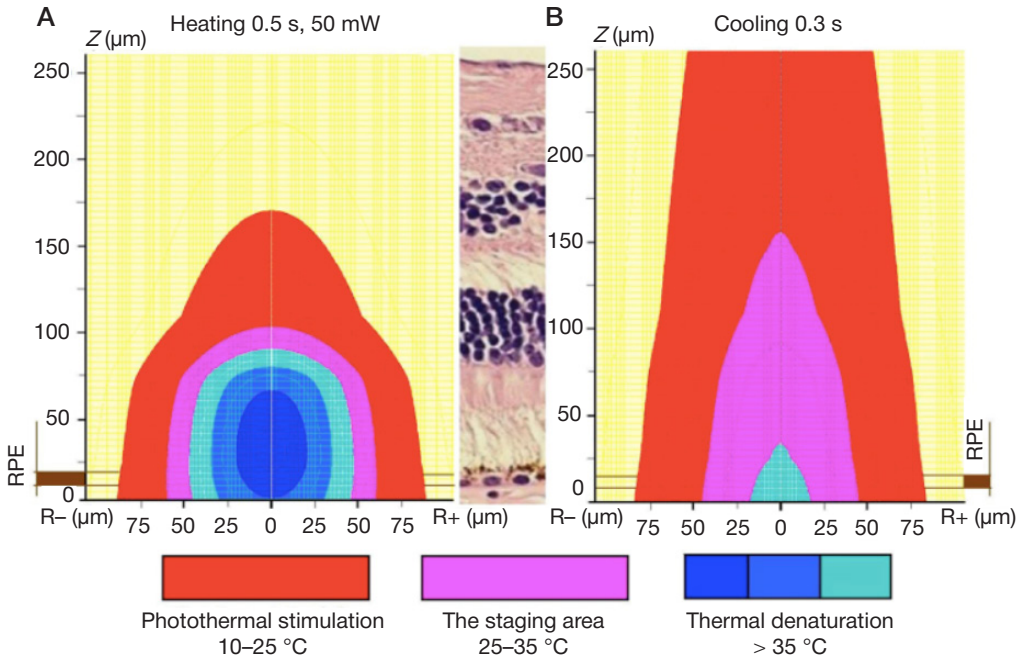

Fig. 5. Distribution of temperatures $T(r, Z)$ in retinal tissues during heating (**A**) and cooling (**B**) by the end of the laser pulse (t = 0.05 s) and at t = 0.3 s (cooling) in the sagittal plane

Six months after completing the second part of the treatment course that included 3 sessions of subthreshold laser micropulses (with a month interval between each two sessions), the patient underwent a follow-up examination; uncorrected visual acuity became 0.9, whereas best-corrected acuity was 1.0.

Multispectral imaging conducted in the Multicolor mode revealed regression of the central part of ERM (Fig. 8A). Measured by microperimetry, the average light sensitivity of the retina 26.6 dB (Fig. 8B). SOCT images revealed formation of the foveal pit; the thickness of the central retina had decreased to 246 μm. The outer limiting membrane, the junction between the inner and outer photoreceptor segments, the choroid, and the retinal pigment epithelium were intact (Fig. 8C). Post-operative SOCT images demonstrated that coagulation sites corresponded to the sites of photothermal stimulation showed in Figures 3 and 4.

CONCLUSIONS

We have developed a new laser combination therapy for treating the early stages of ERM. The first clinical tests have confirmed its efficacy and safety. Mathematical modeling allowed us to study the dynamics of thermomechanical effects of laser radiation on the structural components of the neuroepithelium during the exposure. We have also described the major mechanisms underlying the therapeutic effect of laser radiation in patients with ERM.

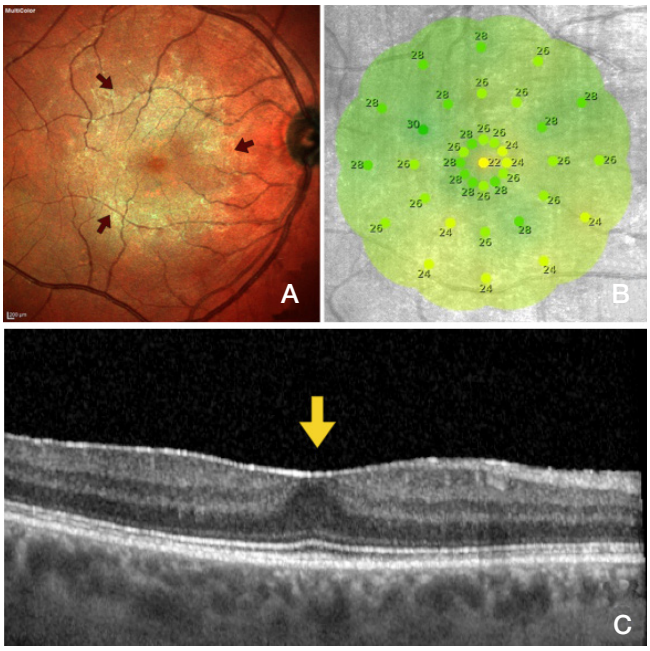

Fig. 6. The ocular fundus before the treatment: (**A**) a Multicolor photo showing the surface and the boundaries of ERM in yellow and green (*marked by red arrows*); (**B**) microperimetry of the macular zone, the average light sensitivity was 26.3 dB; (**C**) SOCT of the retinal membrane surface showing a hyperreflective line fused to the inner limiting membrane; the foveal pit is flat (*the yellow arrow*); the thickness of the central retina is 257 μm (c)

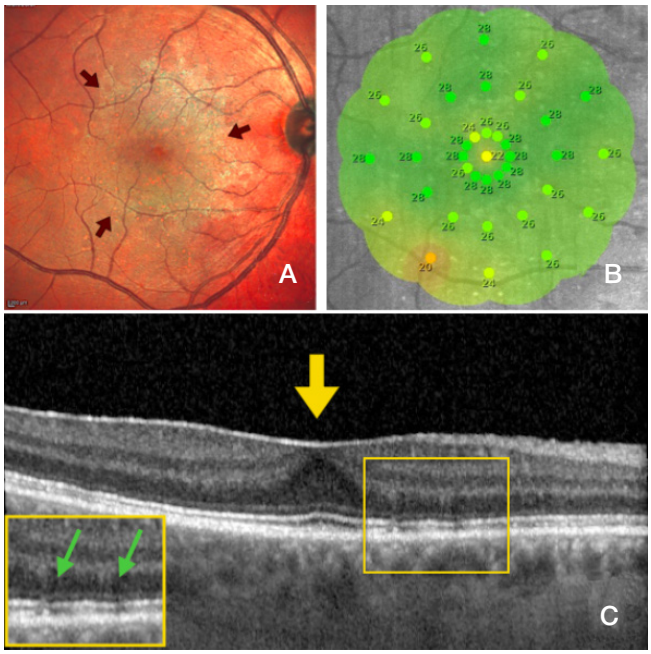

Fig. 7. The ocular fundus after the first session of grid laser photocoagulation; (**A**) a Multicolor photo of the fundus shows thinner, blurred ERM contours in the macular zone (*the red arrow*); (**B**) microperimetry of the macular zone: the average light sensitivity is 26.5 Db; (**C**) SOCT reveals a hyperreflective line fused to ILM, the foveal pit is flat (*the yellow arrow*), the thickness of the central retina is slightly decreased (253 μm). *The green arrow* on the OCT image marks laser coagulates; the retinal layers are structurally unchanged

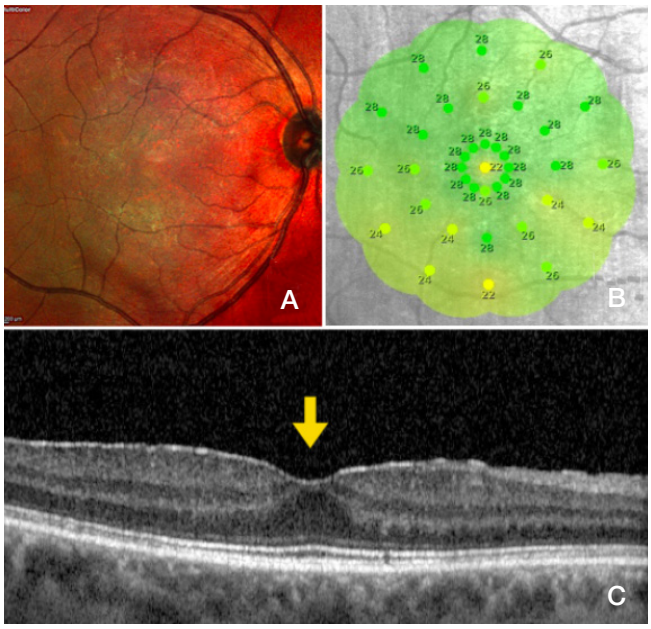

Fig. 8. The ocular fundus after the completed treatment course: (**A**) a Multicolor photo of the fundus showing ERM regression; (**B**) microperimetry: the average light sensitivity is 26.6 dB; (**C**) an OCT image showing a thinner hyperreflective line (ERM) and formation of the foveal pit (*the yellow arrow*); the thickness of the central retina is 246 μm

References

1. Leask A, Abraham D. TGF-β signaling and the fibrotic response. The FASEB Journal. 2004; 18 (7): 816–27.
2. Kachalina GF, Kasminina TA, Ivanova EV, Kuranova OI. Laser treatment of transudative maculopathy caused by the epiretinal membrane. Modern technologies of treatment of vitreoretinal pathology. S. Fyodorov Eye Microsurgery Federal State Institution. 2012; 94–6.
3. Patronas M, Kroll A, Lou P, Ryan E. a Review of Vitreoretinal

Interface Pathology. International Ophthalmology Clinics. 2009; 49 (1): 133–43.
4. Ponomareva EN, Kazaryan AA. The electroretinogram and the pattern of optical coherence tomography in patients with idiopathic epiretinal membrane. Russian Ophthalmological Journal. 2013; (2): 66–9.
5. Guidry C. The role of Müller cells in fibrocontractive retinal disorders. Progress in Retinal and Eye Research. 2005; 24 (1): 75–86.
6. Harada C, Mitamura Y, Harada T. The role of cytokines and trophic factors in epiretinal membranes: Involvement of signal transduction in glial cells. Progress in Retinal and Eye Research. 2006; 25 (2): 149–64.
7. Zhao F, Gandorfer A, Haritoglou C, Scheler R, Schaumberger M, Kampik a et al. Epiretinal Cell Proliferation in Macular Pucker and Vitreomacular Traction Syndrome. Retina. 2013; 33 (1): 77–88.
8. Joshi M, Agrawal S, Christoforidis J. Inflammatory Mechanisms of Idiopathic Epiretinal Membrane Formation. Mediators of Inflammation. 2013; (2013): 1–6.
9. Hinz B, Phan SH, Thannickal VJ, et al. The myofibroblast: one function, multiple origins. Am J Pathol. 2007; (170): 1807–16.
10. Zakharov VD, Borzenok SA, Gorshkov IM, Kolesnik SV, Kolesnik AI, Miridonova AV. Etiological and pathogenetic aspects and role of vitreoretinal interface structures in idiopathic epiretinal membranes formation. Practical medicine. 2018; (114): 71–76.
11. Kachalina GF, Doga AV, Kasmynina TA, Kuranova OI. Epiretinal fibrosis: pathogenesis, outcomes, treatment methods. Ophthalmosurgery. 2013; 4: 108–10.
12. Kuranova OI. The study of the effectiveness of micropulse laser irradiation with a wavelength of 577 nm in macular edema after surgical removal of idiopathic epiretinal membrane [dissertation]. 2014.
13. Bu S, Kuijer R, Li X, Hooymans J, Los L. Idiopathic epiretinal membrane. Retina. 2014; 34 (12): 2317–35.
14. Bolshunov AV. Questions of laser ophthalmology. M., 2013; 316.
15. Krasnov MM, Saprykin PI, Doronin PP, Nikolskaya GM, Akopyan VS, Mamedov NG. Electron-microscopic examination of the fundus tissue during laser coagulation. Bulletin of Ophthalmology. 1973; (2): 9–12.
16. Fedoruk NA, Fedorov AA, Bol'shunov AV. Morphological and histochemical effects of subthreshold laser therapy on the chorioretinal complex/ Bulletin of Ophthalmology. 2013; (5): 73–81.
17. Zheltov GI, Romanov GS, Romanov OG, Ivanova EV. Selective effect of laser pulses on the retinal pigment epithelium. Physical basis. New in ophthalmology. 2012; (3): 37–43.
18. Tahchidi HP, Kachalina GF, Kasmynina TA, Tebina EP. The method of combined laser treatment of the initial stage of epiretinal fibrosis RF № 2634684. 02.11.2017.
19. Zheltov GI. Effect of intense optical radiation on eye tissue: research and applications. Extended abstract of candidate's thesis [dissertation]. 1996.
20. Zheltov GI. Biophysics of the destructive action of the above-threshold laser radiation on the fundus tissue. II All Russian seminar: "MAKULA 2006". Report in the conference proceedings. 2006; 71–85.
21. Jacobs S. Safety with Lasers and Other Optical Sources, by D. Sliney and M. Wolbarsht. Medical Physics. 1981; 8 (5): 725–6.
22. Karslow G, Eger D. Thermal conductivity of solids. M.: Science, 1964; 488.
23. Linnik LA, Zheltov GI, Glazkov VN, Puhlik ES, Privalov AP. Change of energy thresholds of laser coagulation of retinal tissues with the age of patients. Ophthalmological journal. 1988; 6 (302): 355–8.
24. Zheltov GI. Effects of above-threshold laser radiation on the fundus tissue. Ophthalmology in Belarus. 2009; 3 (03): 24–40.
25. Barnes FS. Bological Damage Resulting from Thermal Pulses. In: Wolbarsht ML, Ed. Laser Application in Medicine and Biology. Ntw York: Plenum Press, 1984; 205–22.
26. Klepinina OB Subthreshold micropulse laser treatment with a wavelength of 577 nm in the treatment of central serous chorioretinopathy.Tambov, 2014; 61.
27. Romanov OG, Romanov GS, Zheltov GI. Numerical modelling of photo-thermal and photo-mechanical effects in absorbing biological structures under action of short laser pulses Proceedings of SPIE. 2013; (8803). DOI: 10.1117/12.2032462
28. Zheltov G, Lisinetskii V, Grabtchikov A, Orlovich V. Low-threshold cavitation in water using IR laser pulse trains. Applied Optics. 2008; 47 (20): 3549–54.
29. Oraevsky A, Jacques S, Esenaliev R, Tittel F. Pulsed laser ablation of soft tissues, gels, and aqueous solutions at temperatures below 100 °C. Lasers in Surgery and Medicine. 1996; 18 (3): 231–40.

Литература

1. Leask A, Abraham D. TGF-β signaling and the fibrotic response. The FASEB Journal. 2004; 18 (7): 816–27.
2. Качалина Г. Ф., Касмынина Т. А., Иванова Е. В., Куранова О. И. Лазерное лечение транссудативной макулопатии, вызванной наличием эпиретинальной мембраны. Современные технологии лечения витреоретинальной патологии. В сборнике тезисов. ФГБУ «МНТК «Микрохирургия глаза». 2012; 94–6.
3. Patronas M, Kroll A, Lou P, Ryan E. A Review of Vitreoretinal Interface Pathology. International Ophthalmology Clinics. 2009; 49 (1): 133–43.
4. Пономерёва Е. Н., Казарян А. А. Структурно-функциональные особенности макулярной зоны сетчатки при идиопатической эпиретинальной мембране. Российский офтальмологический журнал. 2013; (2): 66–9.
5. Guidry C. The role of Müller cells in fibrocontractive retinal disorders. Progress in Retinal and Eye Research. 2005; 24 (1): 75–86.
6. Harada C, Mitamura Y, Harada T. The role of cytokines and trophic factors in epiretinal membranes: Involvement of signal transduction in glial cells. Progress in Retinal and Eye Research. 2006; 25 (2): 149–64.
7. Zhao F, Gandorfer A, Haritoglou C, Scheler R, Schaumberger M, Kampik A, et al. Epiretinal Cell Proliferation in Macular Pucker and Vitreomacular Traction Syndrome. Retina. 2013; 33 (1): 77–88.
8. Joshi M, Agrawal S, Christoforidis J. Inflammatory Mechanisms of Idiopathic Epiretinal Membrane Formation. Mediators of Inflammation. 2013; (2013): 1–6.
9. Hinz B, Phan SH, Thannickal VJ, et al. The myofibroblast: one function, multiple origins. Am J Pathol. 2007; (170): 1807–16.
10. Захаров В. Д., Борзенок С. А., Горшком И. М., Колесник С. В., Колесник А. И., Миридонова А. В. Этиопатогенетические аспекты и роль структур витреоретинального интерфейса в формировании идиопатических эпиретинальных мембран. Практическая медицина. 2018; (114): 71–6.
11. Качалина Г. Ф., Дога А. В., Касмынина Т. А., Куранова О. И. Эпиретинальный фиброз: патогенез, исходы, способы лечения. Офтальмохирургия. 2013; (4): 108–10.
12. Куранова О. И. Изучение эффективности микроимпульсного лазерного воздействия длиной волны 577 нм при макулярном отеке после хирургического удаления идиопатической эпиретинальной мембраны [диссертация]. 2014.
13. Bu S, Kuijer R, Li X, Hooymans J, Los L. Idiopathic epiretinal membrane. Retina. 2014; 34 (12): 2317–35.
14. Большунов А. В. Вопросы лазерной офтальмологии. М., 2013; 316 с.
15. Краснов М. М., Сапрыкин П. И., Доронин П. П., Никольская Г. М., Акопян В. С., Мамедов Н. Г. Электронно-микроскопическое изучение тканей глазного дна при лазеркоагуляции. Вестник офтальмологии. 1973; (2): 9–12.
16. Федорук Н. А., Федоров А. А., Большунов А. В. Морфологические и гистохимические особенности субпорогового лазерного воздействия на структуры хориоретинального комплекса. Вестник офтальмологии. 2013; (5): 73–81.
17. Желтов Г. И., Романов Г. С., Романов О. Г., Иванова Е. В. Селективное действие лазерных импульсов на ретинальный пигментный эпителий. Физические основы. Новое в офтальмологии. 2012; (3): 37–43.

18. Тахчиди Х. П., Качалина Г. Ф., Касмынина Т. А., Тебина Е. П. Способ комбинированного лазерного лечения начальной стадии эпиретинального фиброза. Патент РФ №2634684. 02.11.2017.
19. Желтов Г. И. Воздействие интенсивного оптического излучения на ткани глаз: исследования и приложения [диссертация]. 1996.
20. Желтов Г. И. Биофизика деструктивного действия надпорогового лазерного излучения на ткани глазного дна. II Всероссийский семинар: «МАКУЛА 2006». Доклад в сборнике материалов конференции. 2006; 71–85.
21. Jacobs S. Safety with Lasers and Other Optical Sources, by D. Sliney and M. Wolbarsht. Medical Physics. 1981; 8 (5): 725–6.
22. Карслоу Г., Егер Д. Теплопроводность твердых тел. М.: Наука,1964; 488.
23. Линник Л. А., Желтов Г. И., Глазков В. Н. Пухлик Е. С., Привалов А. П. Изменение энергетических порогов лазерокоагуляции тканей сетчатки с возрастом больных. Офтальмологический журнал. 1988; 6 (302), 355–8.
24. Желтов Г. И. Действие надпорогового лазерного излучения на ткани глазного дна. Офтальмология в Беларуси. 2009; 3 (03): 24–40.
25. Barnes FS. Bological Damage Resulting from Thermal Pulses. In: Wolbarsht ML, Ed. Laser Application in Medicine and Biology. Ntw York: Plenum Press, 1984; 205–22.
26. Клепинина О. Б. Субпороговое микроимпульсное лазерное воздействие длиной волны 577 нм при лечении центральной серозной хориоретинопатии. Тамбов, 2014; 61.
27. Romanov OG, Romanov GS, Zheltov GI. Numerical modelling of photo-thermal and photo-mechanical effects in absorbing biological structures under action of short laser pulses Proceedings of SPIE. 2013; (8803). DOI: 10.1117/12.2032462.
28. Zheltov G, Lisinetskii V, Grabtchikov A, Orlovich V. Low-threshold cavitation in water using IR laser pulse trains. Applied Optics. 2008; 47 (20): 3549–54.
29. Oraevsky A, Jacques S, Esenaliev R, Tittel F. Pulsed laser ablation of soft tissues, gels, and aqueous solutions at temperatures below 100 °C. Lasers in Surgery and Medicine. 1996; 18 (3): 231–40.

COMBINED LASER TREATMENT OF EARLY IDIOPATHIC EPIRETINAL MEMBRANE: CLINICAL EVALUATION OF THE DEVELOPED TECHNIQUE

Takhchidi KP[1,2], Kachalina GF[2], Kasminina TA[2], Tebina EP[3] ✉

[1] Pirogov Russian National Research Medical University, Moscow, Russia

[2] Research Center for Ophthalmology, Pirogov Russian National Research Medical University, Moscow, Russia

[3] Faculty of Pediatrics, Pirogov Russian National Research Medical University, Moscow, Russia

Process of development of epiretinal membrane (ERM) on the retinal surface of macular area is one of the important problems associated with vitreoretinal pathologies. Up to the present day, there has not been developed an effective method to arrest fibrosis at the early stages of its development. This study aimed to evaluate efficacy and safety of the new combined laser technique designed to treat early idiopathic ERM (stages 0–1). Ninety-two patients aged 64.7 ± 9.6 years (mean) participated in the clinical research. They were divided into three groups: treatment group (n = 32), patients whose ERM was treated following the new combined laser technique; comparison group (n = 30), patients who underwent grid laser coagulation; control group (n = 30), no treatment, observation of the natural course. Based on the results of examination of the patients, we assessed uncorrected visual acuity, best corrected visual acuity, central retinal thickness, central retinal sensitivity. Assessed against the results registered in comparison and control groups, the developed combined laser treatment technique applied in the treatment group proved to be highly effective in maintaining/improving visual functional indicators and stabilizing/improving morphofunctional indicators throughout the entire period of observation. As pertains to the morphological and functional structures of sensory retina, the technique enabled retinal sensitivity improvement at different stages of observation, which reflects its safety and efficacy.

Keywords: idiopathic epiretinal membrane, subthreshold micropulse laser exposure, combined laser technology, optical coherent tomography

Author contribution: Takhchidi KP and Kachalina GF conceived and designed the study; Tebina EP collected and analyzed the data; Kasminina TA performed laser therapy; Kasminina TA, and Tebina EP wrote the manuscript; Takhchidi KP revised the manuscript.

Compliance with ethical standards: the study was approved by Russian National Research Medical University (Protocol № 160 of December 19, 2016).

✉ **Correspondence should be addressed:** Ekaterina P. Tebina
Volokolamskoe shosse 30, bld. 2, 123182; ekaterinatebina@mail.ru

Received: 18.03.2019 **Accepted:** 02.04.2019 **Published online:** 30.04.2019

DOI: 10.24075/brsmu.2019.033

КЛИНИЧЕСКАЯ ОЦЕНКА РАЗРАБОТАННОЙ ТЕХНОЛОГИИ КОМБИНИРОВАННОГО ЛАЗЕРНОГО ЛЕЧЕНИЯ ПРИ НАЧАЛЬНЫХ СТАДИЯХ ИДИОПАТИЧЕСКОЙ ЭПИРЕТИНАЛЬНОЙ МЕМБРАНЫ

Х. П. Тахчиди[1,2], Г. Ф. Качалина[2] , Т. А. Касмынина[2], Е. П. Тебина[3] ✉

[1] Российский национальный исследовательский медицинский университет имени Н. И. Пирогова, Москва, Россия

[2] Научно-исследовательский центр офтальмологии, Российский национальный исследовательский медицинский университет имени Н. И. Пирогова, Москва, Россия

[3] Педиатрический факультет, Российский национальный исследовательский медицинский университет имени Н. И. Пирогова, Москва, Россия

Одной из актуальных проблем витреоретинальной патологии является процесс формирования эпиретинальной мембраны (ЭРМ) на ретинальной поверхности макулярной зоны. До настоящего времени не существует эффективных методов, оказывающих антипролиферативное и антиконстрикторное действие на фиброзный процесс на начальных этапах его развития. Целью исследования являлась оценка эффективности и безопасности технологии комбинированного лазерного лечения пациентов с начальными стадиями (0–1 стадия) идиопатической ЭРМ. В клиническое исследование были включены 92 пациента (64,7 ± 9,6 лет). Основную группу составили 32 пациента (32 глаза), которым было проведено лазерное лечение по комбинированной технологии. Группу сравнения составили 30 пациентов (30 глаз), лечение которых осуществлялось с применением лазерной коагуляции по типу «решетки». В контрольную группу были включены 30 пациентов (30 глаз), у которых было установлено динамическое наблюдение за естественным течением пролиферативного процесса без лазерного и консервативного лечения. По результатам офтальмологического обследования проводилась оценка некоррегированной остроты зрения, максимально коррегированной остроты зрения, центральной толщины сетчатки и центральной светочувствительности сетчатки. Разработанная технология комбинированного лазерного лечения показала высокую эффективность, заключающуюся в сохранении/увеличении зрительно-функциональных показателей и стабилизации/улучшении морфофункциональных показателей сетчатки в течение всего периода наблюдения. Безопасность и эффективность разработанной лазерной технологии в отношении морфофункциональных структур сенсорной сетчатки отражалась в увеличении показателей светочувствительности сетчатки в различные сроки наблюдения.

Ключевые слова: идиопатическая эпиретинальная мембрана, субпороговое микроимпульсное лазерное воздействие, комбинированная лазерная технология, оптическая когерентная томография

Информация о вкладе авторов: Х. П. Тахчиди, Г. Ф. Качалина — концепция и дизайн исследования; Е. П. Тебина — сбор и обработка материала; Т. А. Касмынина — лазерное лечение пациента; Т. А. Касмынина, Е. П. Тебина — написание текста; Х. П. Тахчиди — редактирование.

Соблюдение этических стандартов: исследование одобрено этическим комитетом РНИМУ имени Н. И. Пирогова (протокол № 160 от 19 декабря 2016 г.).

✉ **Для корреспонденции:** Екатерина Павловна Тебина
Волоколамское шоссе, д. 30, корп. 2, г. Москва, 123182; ekaterinatebina@mail.ru

Статья получена: 18.03.2019 **Статья принята к печати:** 02.04.2019 **Опубликована онлайн:** 30.04.2019

DOI: 10.24075/vrgmu.2019.033

In the recent years, numerous researchers studied the problem of formation of connective tissue in the eye [1–4]. However, there is one special vitreoretinal pathology, macular fibrosis, which causes significant deterioration and even irreversible loss of visual function in working age population.

Despite the considerable progress in understanding etiological, pathological and genetic mechanisms of formation of epiretinal membrane (ERM), some questions pertaining to the development idiopathic ERM remain unanswered [5]. The main factors contributing to the development of this pathology are:

impaired biomechanical processes at the vitreoretinal interface, namely, posterior vitreous detachment (PVD); micropores in the internal limiting membrane (ILM); pathological changes of the macular microvasculature [6–8]. Regardless of the pathogenetic mechanism of ERM development, migration and proliferation of various cell types play a key role in its formation and progression, the cells being glial cells (Muller retinal cells, astrocytes and microglia), hyalocytes, macrophages, retinal pigment epithelium (RPE) and retinal surface fibroblasts [9, 10]. Influenced by cytokines and growth factors, these cells transdifferentiate into a phenotype similar to myofibroblasts [11]. With aseptic inflammation in the background, myofibroblasts undergo apoptosis [11, 12]. In fibrosis, myofibroblasts activate and, when persisting for a long period of time, cause excessive deposition of collagen followed by its remodeling [13]. Evidence obtained through ophthalmoscope examination [14] and with the help of a number of current fundus pathology investigation methods allows isolating three main stages (grades) of ERM development: stage 0 — cellophane maculopathy, stage 1 — crinkled cellophane maculopathy, and stage 2 — macular puckering. Depending on the stage, clinical manifestations of the disease vary from total lack of symptoms to a significant visual function deterioration [15]. To date, there are no safe and effective methods that allow slowing down cell proliferation and progression of fibrosis in its early stages.

Globally, medical researchers and practitioners successfully subject late-stage ERM to vitreoretinal surgery, having accumulated significant related experience. However, despite the positive surgery results, numerous histological studies have shown that ILM peeling damages Muller cells and compromises retina architectonics and biomechanical strength [16, 17]. As a result, complete restoration of vision after such surgery occurs in 5–25% of cases only [18]. Moreover, this kind of treatment is prescribed in case the clinical symptoms, i.e. visual function alteration and/or deterioration, are pronounced. Up to the present, the main tactic for managing ERM patients has been dynamic observation [19].

Thus, development of an effective and safe early-stage ERM treatment technique yielding stabilization and/or improvement of vision and functional indicators is an urgent problem.

Given the urgency, such a technique was developed in the Research Center for Ophthalmology of Pirogov Russian National Research Medical University. The technique combines grid laser photocoagulation and exposure to 577 nm subthreshold micropulse laser light (RF patent №. 2634684, 02.11.2017), the two techniques that differ in their mechanism of action [20]. This study aimed to evaluate efficacy and safety of the combined laser technique designed to treat early idiopathic ERM (stages 0–1).

METHODS

Ninety-two patients aged 64.7 ± 9.6 years (mean) participated in the clinical research. The inclusion criteria were: early idiopathic epiretinal membrane (stage 0–1) with concomitant lens pathology: pseudophakia or early cataract.

All patients were randomized into three groups depending on the treatment tactics. The treatment group included 32 patients (32 eyes); they underwent laser treatment following the combined technique developed at the Research Center for Ophthalmology of Pirogov Russian National Research Medical University. The comparison group consisted of 30 patients (30 eyes); their treatment was laser coagulation, "lattice" type. The control group included 30 patients (30 eyes); they received neither laser nor conservative treatment, and natural proliferation of their fibroses was under dynamic observation.

The new technique is a combination of grid laser photocoagulation and subthreshold micropulse laser irradiation [20]. We used IRIDEX IQ 577 retinal surgery laser (IRIDEX Corporation, Mountain View; USA) that works in continuous and micropulse modes.

Grid laser photocoagulation was the first stage of the treatment. We irradiated the entire surface of ERM except for the avascular zone; the wavelength was 577 nm, power — 50 mW, pulse duration — 0.05 s, spot diameter — 100 μm, distance between coagulates — 150 μm. After two weeks, ERM was exposed to subthreshold laser micropulses (second stage of the combined laser treatment technique); the wavelength was 577 nm, pulse packet duration — 30 ms, micropulse duration — 50 μs, pulse ratio — 4.7%, spot diameter — 100 μm, power — 50 mW (Table 1). Since we registered no significant changes after the 4th session, treatment group patients had only 3 sessions of subthreshold micropulse laser treatment, each a month apart.

All patients underwent standard ophthalmic and special examinations: multispectral with various filters (Blue, Green, Infrared Reflectance, MultiColor), spectral optical coherent tomography (SOCT) «Spectralis OCT» (Heidelberg Engineering, Inc; Germany) and microperimetry MAIA (CenterVue; Italy).

All participants were examined before treatment and 3 months, 6 months, 1 year, 2 years, 3 years, 4 years and 5 years after treatment. Treatment and comparison group patients also underwent examination after each stage of laser treatment.

Table 1. Protocol of the developed combined laser treatment technique for idiopathic ERM

Energy parameters	**Grid laser coagulation**	
	Wavelength (nm)	577
	Spot diameter (μm)	100
	Emission power (mW)	50
	Micropulse duration (μs)	50
	Number of applicates	60–90
	Subthreshold micropulse laser exposure	
	Wavelength (nm)	577
	Spot diameter (μm)	100
	Emission power (mW)	50
	Micropulse duration (μs)	50
	Micropulse packet duration (ms)	30
	Pulse ratio (%)	4.7

Central retinal sensitivity was used as the basis for clinical assessment of safety of laser treatment.

We assessed uncorrected visual acuity (UVA), best corrected visual acuity (BCVA), central retinal thickness (CRT), central retinal sensitivity (CRS). These indicators were subjected to normal distribution; methods of parametric statistics (paired sample *t*-test) were applied to the data acquired to compare benchmark figures and results of treatment at different observation timepoints. Single-factor analysis of variance (ANOVA) was used to assess the significance of differences in comparison of results from more than two independent groups. The differences were considered statistically significant at $p < 0.05$.

RESULTS

Results of initial examination of patients from the treatment group (32 eyes): UVA — 0.45 ± 0.31, BCVA — 0.9 ± 0.13, CRS (microperimetry data) — 26.3 ± 1.65 dB, CRT (OCT data, mean) — 282.8 ± 27.1 μm.

In the comparison group (30 eyes), the pre-surgery indicators were: UVA — 0.44 ± 0.26, BCVA (mean) — 0.86 ± 0.15, CRT (mean) — 26.3 ± 1.57, CRT (mean) — 292.4 ± 62.2 μm.

Initial indicators registered in the control group (30 eyes) were as follows: UVA (mean) — 0.64 ± 0.23, BCVA — 0.87 ± 0.14, CRS (mean, microperimetry data) — 27.1 ± 1.52 dB, CRT (mean) — 301.4 ± 44.8 μm.

Table 2. Clinical and functional results of treatment of patients (clinical groups)

Observation period	Treatment group	Comparison group	Control group	ANOVA, *p*
Mean uncorrected visual acuity				
Before treatment	0.45 ± 0.31	0.44 ± 0.26	0.64 ± 0.23	0.01
3 months	0.57 ± 0.3*	0.47 ± 0.27*	0.63 ± 0.23*	0.08
6 months	0.59 ± 0.31*	0.43 ± 0.27*	0.6 ± 0.24*	0.13
Year 1	0.61 ± 0.31*	0.42 ± 0.27*	0.56 ± 0.26*	0.04
Year 2	0.61 ± 0.3*	0.42 ± 0.27*	0.53 ± 0.25*	0.03
Year 3	0.6 ± 0.3*	0.42 ± 0.27*	0.48 ± 0.26*	0.03
Year 4	0.61 ± 0.2*	0.42 ± 0.27*	0.45 ± 0.27*	0.01
Year 5	0.61 ± 0.29*	0.41 ± 0.27*	0.43 ± 0.28*	0.01
Mean best corrected visual acuity				
Before treatment	0.9 ± 0.13	0.86 ± 0.15	0.87 ± 0.14	0.53
3 months	0.95 ± 0.1*	0.85 ± 0.16	0.85 ± 0.14*	0.007
6 months	0.95 ± 0.1*	0.85 ± 0.16	0.85 ± 0.14*	0.007
Year 1	0.95 ± 0.1*	0.83 ± 0.17*	0.83 ± 0.17*	0.001
Year 2	0.95 ± 0.1*	0.81 ± 0.18*	0.8 ± 0.17*	0.000
Year 3	0.94 ± 0.1*	0.78 ± 0.19*	0.75 ± 0.2*	0.000
Year 4	0.94 ± 0.1*	0.76 ± 0.19*	0.7 ± 0.23*	0.000
Year 5	0.94 ± 0.1*	0.73 ± 0.21*	0.68 ± 0.24*	0.000
Mean central retinal sensitivity				
Before treatment	26.3 ± 1.65	26.3 ± 1.57	27.1 ± 1.52	0.13
3 months	27.0 ± 1.5*	26.6 ± 1.68	26.8 ± 1.56*	0.61
6 months	27.1 ± 1.5*	26.5 ± 1.73	26.6 ± 1.62*	0.51
Year 1	27.1 ± 1.5*	26.2 ± 1.5	26.2 ± 1.68*	0.06
Year 2	27.1 ± 1.5*	25.9 ± 1.52*	26 ± 1.68*	0.01
Year 3	27.1 ± 1.5*	25.7 ± 1.69*	25.7 ± 1.78*	0.002
Year 4	27.1 ± 1.5*	25.6 ± 1.71*	25.5 ± 1.92*	0.000
Year 5	27.1 ± 1.5*	25.5 ± 1.79*	25.4 ± 1.88*	0.000
Mean central retinal thickness				
Before treatment	282.8 ± 27.1	292.4 ± 62.2	301.4 ± 44.8	0.37
3 months	277.6 ± 42.9	291.7 ± 63.6	308.8 ± 45.1*	0.06
6 months	277.5 ± 42.5	293.6 ± 64.6	316.6 ± 43.2*	0.01
Year 1	277.7 ± 44.4	300 ± 65.6*	323.6 ± 43.6*	0.003
Year 2	277.1 ± 41.5	303.9 ± 65.1*	331.5 ± 49*	0.000
Year 3	274.9 ± 41.2*	304 ± 63.9*	338.1 ± 48.1*	0.000
Year 4	274.9 ± 41.8*	306.5 ± 63.4*	345.9 ± 48.1*	0.000
Year 5	275.1 ± 42.2*	309.7 ± 63.2*	349.7 ± 49.1*	0.000

Note: * — significant difference from benchmark data, paired sample *t*-test ($p < 0.05$), ANOVA ($p < 0.05$).

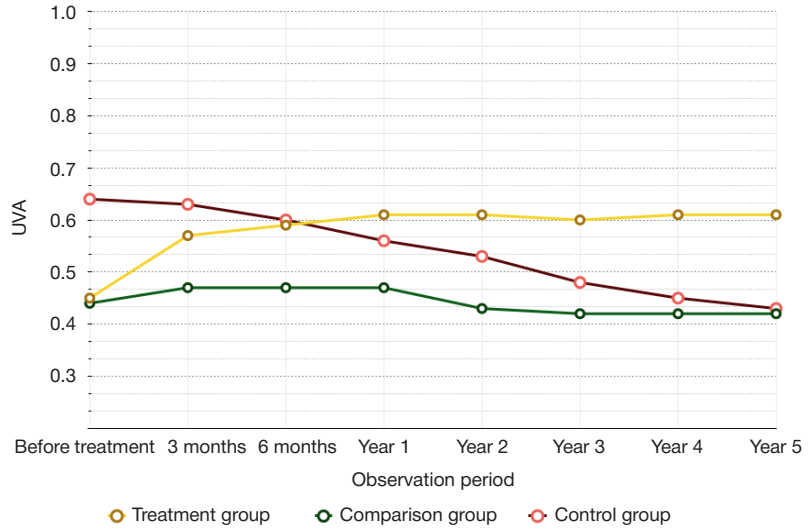

Fig. 1. Mean UVA dynamics, all groups. Treatment group — *yellow line*; UVA increased significantly from the 3rd to the 12th month of observation, results persisted throughout the observation period. Comparison group — *green line*; mean UVA was increasing significantly up to the 3rd month, from the 6th month onward to the end of the observation period the indicators were decreasing significantly. Control group — *red line*; mean UVA was falling significantly throughout the observation period

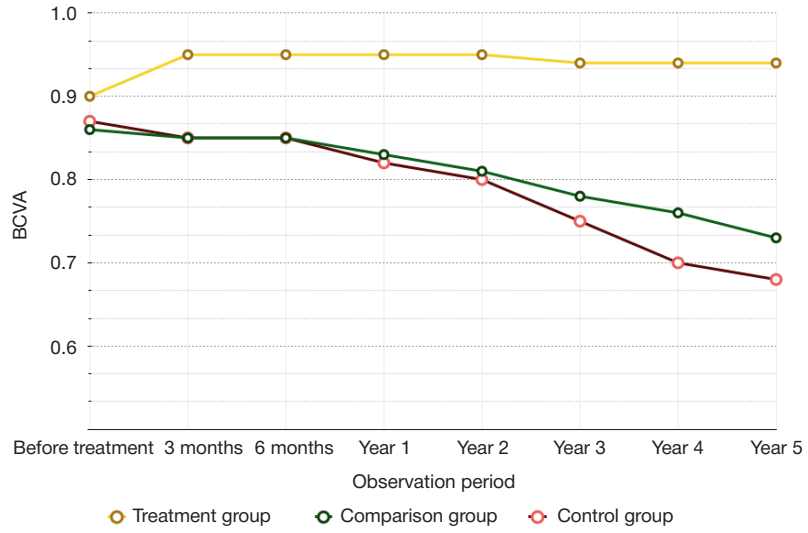

Fig. 2. Mean BCVA dynamics, all groups. Treatment group — *yellow line*; BCVA increased significantly from the 3rd to the 12th month of observation, results persisted throughout the observation period. Comparison group — *green line*; within the first 3 months of observation, mean BCVA changes were insignificant, but from the 12th month on this indicator was decreasing gradually, the difference being significant. Control group — *red line*; mean BCVA was falling significantly throughout the observation period

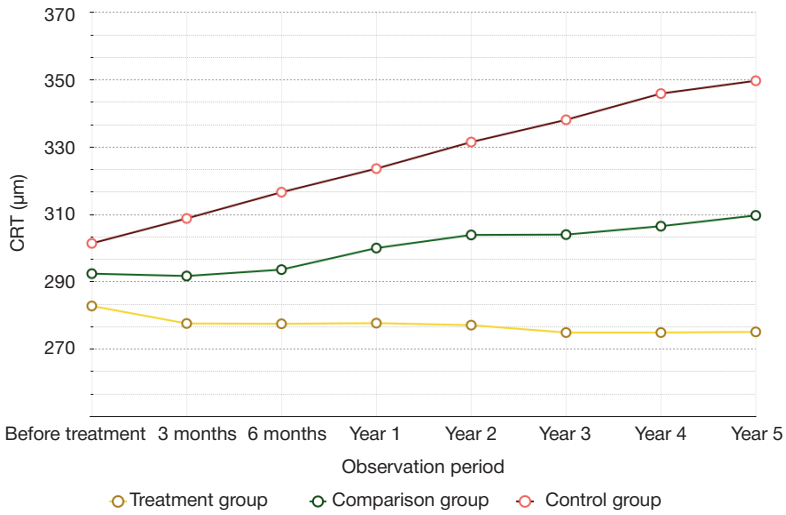

Fig. 3. Mean CRT dynamics, all groups. Treatment group — *yellow line*; the analysis of mean CRT did not reveal significant differences from the benchmark data within the first 6 months, but from the 12th month on, this indicator was increasing significantly. Comparison group — *green line*; the analysis of mean CRT did not reveal significant differences from the benchmark data within the first 6 months, but from the 12th month on, this indicator was increasing significantly. Control group — *red line*; mean CRT was increasing significantly from the 3rd month on to the end of the observation period

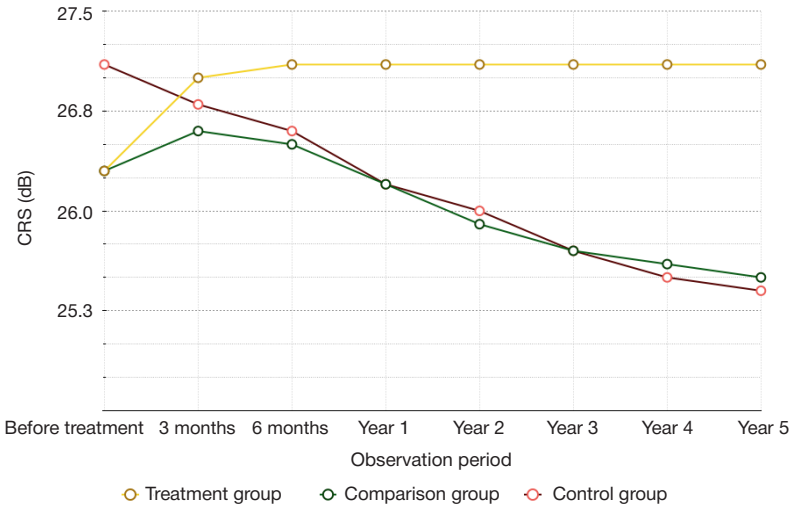

Fig. 4. Mean CRS dynamics, all groups. Treatment group — *yellow line*; mean CRS increased significantly from the 3rd to the 12th month of observation, results persisted throughout the observation period. Comparison group — *green line*; within the first 12 months of observation, mean CRS changes were insignificant, but from the 2nd to the 5th year of observation the indicator decreased significantly. Control group — *red line*; mean CRS was decreasing significantly from the 3rd month on to the end of the observation period

Table 2 presents analysis of clinical and functional results of treatment and dynamic observation of patients with idiopathic ERM.

In the control group, mean UVA and BCVA were decreasing significantly throughout the observation period (Fig. 1, 2). According to the OCT data, mean CRT was increasing significantly from the 3rd month on (Fig. 3), while mean CRS, on the contrary, was significantly increasing from the 3rd month on (Fig. 4). Multispectral imaging revealed continued proliferation on the retinal surface (Fig. 5A, B).

In the comparison group, the mean UVA was increasing significantly up to the 3rd month and decreasing from the 6th month on (Fig. 1). Within the first 3 months of observation, mean BCVA changes were insignificant, but from the 12th month on this indicator was decreasing gradually, the difference being significant (Fig. 2). The analysis of mean CRT did not reveal significant differences from the benchmark data within the first 6 months, but from the 12th month on, this indicator was increasing significantly (Fig. 3) and ERM was developing (Fig. 6A, B). Computer microperimetry did not register significant changes of mean CRS within the first 12 months, but from the 2nd to the 5th years it was decreasing, and these changes were significant (Fig. 4).

Comparing the results registered in treatment, comparison and control groups we established that only patients of the treatment group enjoyed significant improvement of visual and functional indicators (UVA, BCVA and CRS) combined with decreasing CRT and idiopathic ERM involution, these results staying stable throughout observation (Fig. 7A, B). In the comparison group, the indicators improved for a short period of time (up to the 3rd month), and then began to gradually deteriorate; in the control group, such deterioration, significant, was registered at all observation timepoints (Fig. 1–4).

Laser treatment did not inflict biomechanical damage to the retina in treatment and comparison groups, as confirmed by the results of computer microperimetry and SOCT.

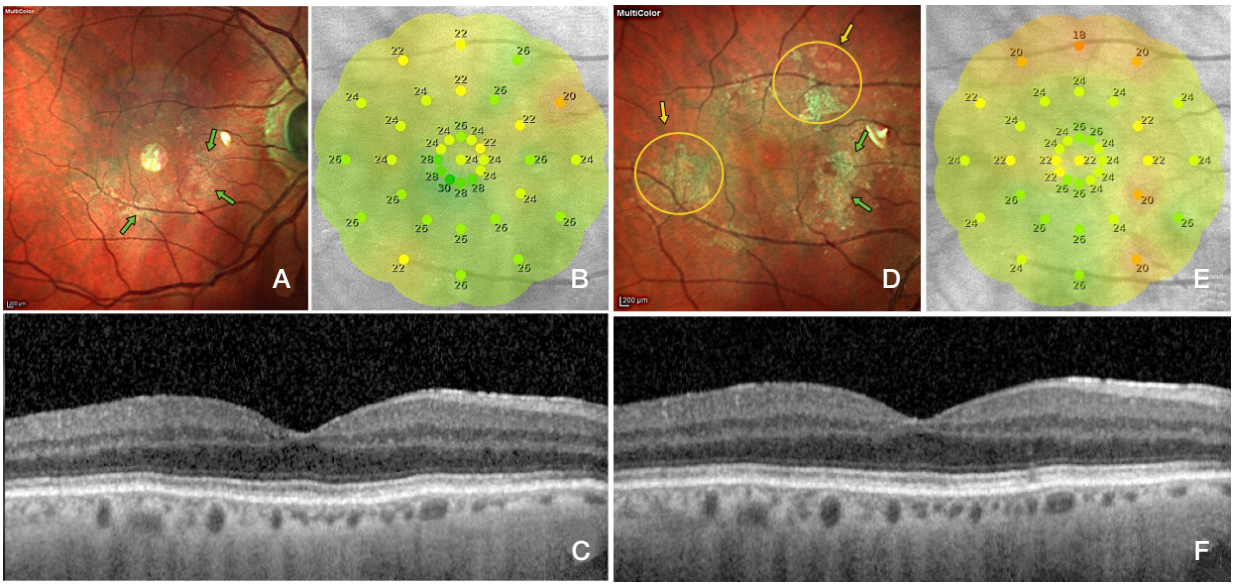

Fig. 5. Control group. Patient E, 58 years old. Results of the initial examinations: ERM surface and boundaries visualized yellow-green through multispectral imaging (Multicolor) (**A**); mean CRS (computer microperimetry data) — 24.9 dB (**B**); SOCT revealed a hyperreflective line on the ILM surface corresponding to the ERM, foveal pit morphology preserved (**C**). Results of examinations at the end of the 1st year of observation: multispectral imaging showed continued proliferation of ERM with new foci (*yellow arrow*) and continued growth of the fibrosis area (*green arrow*) (**D**); Mean CRS — 23.5 dB (**E**); SOCT revealed persistence of ERM on the ILM surface, foveal pit morphology preserved (**F**)

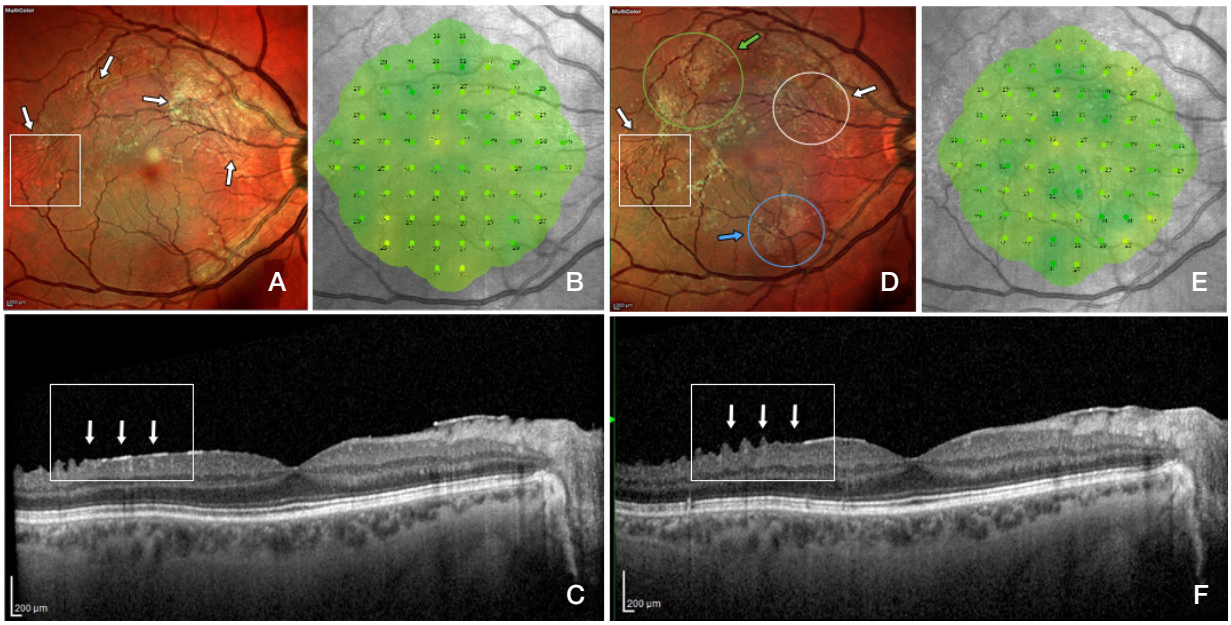

Fig. 6. Comparison group. Patient S., 56 years old. Results of the initial examinations: ERM surface and boundaries visualized yellow-green through multispectral imaging (Multicolor; *white arrow*) (**A**); mean CRS (computer microperimetry data) — 28.2 dB (**B**); SOCT revealed a hyperreflective line on the ILM surface corresponding to the ERM (*white arrow*), foveal pit morphology preserved, CRT — 239 µm (**C**). Results of examinations at the end of the 2nd year of observation: multispectral imaging showed laser coagulates and the resulting ERM involution spots (*white arrow*), ERM activation spots (*green arrow*) and new fibrosis foci (*blue arrow*) (**D**); mean CRS — 27.8 dB (**E**); SOCT revealed an almost complete absence of hyperreflective line (ERM) (*white arrow*), corresponding to the Multicolor visualized zone (*white rectangle*), foveal pit morphology preserved, CRT — 237 µm (**F**)

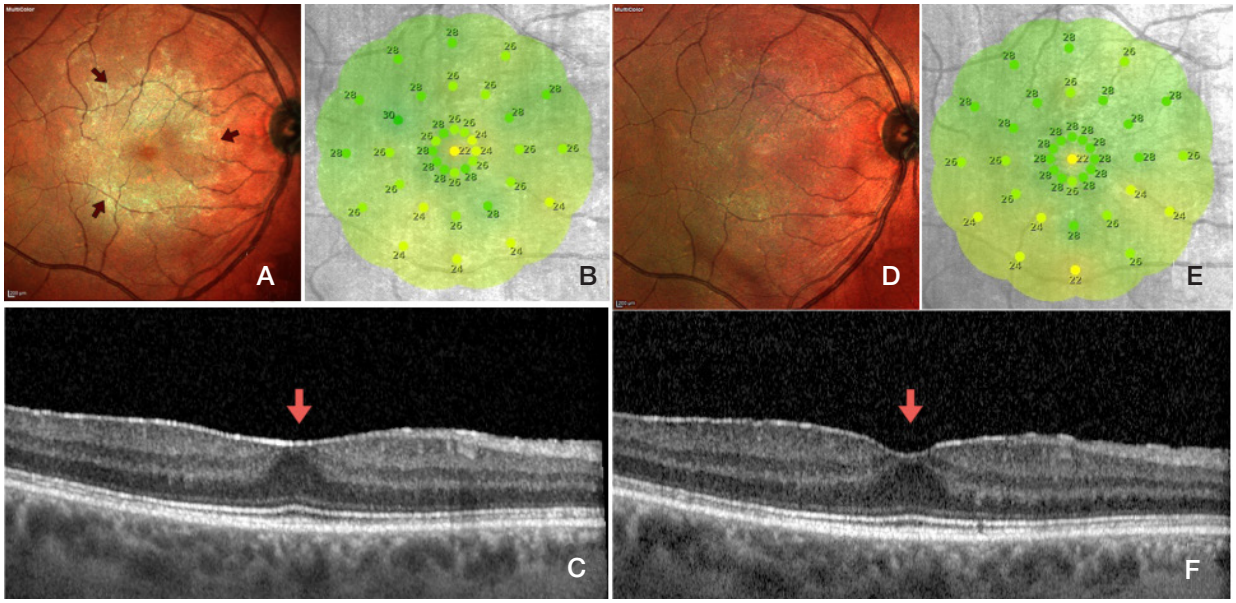

Fig. 7. Treatment group, Patient I, 68 years old. Results of the initial examinations: ERM surface and boundaries visualized yellow-green through multispectral imaging (Multicolor; *red arrow*) (**A**); mean CRS (computer microperimetry data) — 26.3 dB (**B**); SOCT revealed a hyperreflective line on the ILM surface corresponding to the ERM, foveal pit morphology flat (*red arrow*), CRT — 257 µm (**C**). Results of examinations at the end of the 5th year of observation: multispectral imaging showed total involution of ERM (**D**); mean CRS — 26.6 dB (**E**); SOCT revealed a less "solid" hyperreflective line (ERM) and forming foveal pit morphology (*red arrow*), CRT — 234 µm (**F**)

CONCLUSIONS

Assessed against the results registered in comparison and control groups, the suggested combined laser treatment technique applied in the treatment group proved to be highly effective in maintaining/improving visual functional indicators and stabilizing/improving morphofunctional indicators throughout the entire period of observation. As for the morphological and functional structures of sensory retina, the combined laser treatment technique is a safe option, which is proved by the retinal sensitivity improvements registered at the different timepoints of the observation period.

References

1. Balashova LM, Zaĭceva NS, Saksonova EO i dr. Patogeneticheskie faktory razvitiya proliferativnoĭ vitreoretinopatii pri distroficheskoĭ otsloĭke setchatki. Proliferativnyĭ sindrom v oftal'mologii. 2000; (1): 12–3.
2. Campochiaro PA. Pathogenic mechanisms in proliferative vitreoretinopathy. Archives of ophthalmology. 1997; 115 (2): 407–8.
3. Pastor JC. Proliferative vitreoretinopathy: an overview. Survey of Ophthalmology. 1998; 43 (1): 3–18.
4. Kachalina GF, Doga AV, Kasmynina TA, Kuranova OI. Epiretinal'nyi fibroz: patogenez, iskhody, sposoby lecheniya. Oftal'mohirurgiya. 2013; (4): 108–10.
5. Zaharov VD, Borzenok SA, Gorshkom IM, Kolesnik SV, Kolesnik AI, Miridonova AV. Etiopatogeneticheskie aspekty i rol' struktur vitreoretinal'nogo interfejsa v formirovanii idiopaticheskih epiretinal'nyh membran. Prakticheskaya medicina. 2018; 114 (3): 71–6.
6. Ponomeryova EN, Kazaryan AA. Strukturno-funkcional'nye osobennosti makulyarnoj zony setchatki pri idiopaticheskoj epiretinal'noj membrane. Rossijskij oftal'mologicheskij zhurnal. 2013; 6 (2): 66–9.
7. Guidry C. The role of Muller cells in fibrocontractive retinal disorders. Progress in Retinal and Eye Research. 2005; 24 (1): 75–86.
8. Harada C, Mitamura Y, Harada T. The role of cytokines and trophic factors in epiretinal membranes: Involvement of signal transduction in glial cells. Progress in Retinal and Eye Research. 2006; 25 (2): 149–64.
9. Zhao F, Gandorfer A, Haritoglou C. Epiretinal cell proliferation in macular pucker and vitreomacular traction syndrome: analysis of flat-mounted internal limiting membrane specimens. Retina. 2013; 33 (1): 77–88.
10. Joshi M, Agrawal S, Christoforidis JB. Inflammatory mechanisms of idiopathic epiretinal membrane formation. Mediators Inflammation. 2013; DOI: 10.1155/2013/192582.
11. Speca S, Giusti I, Rieder F, Latella G. Cellular and molecular mechanisms of intestinal fibrosis. World Journal of Gastroenterology. 2012; 18 (28): 3635–61.
12. Shurygina IA i dr. Fibroblasty I ih rol' v razvitii soedinitel'noj tkani. Sibirskiĭ medicinskiĭ zhurnal. 2012; 110 (3): 8–12.
13. Hinz B, Gabbiani G. Fibrosis: recent advances in myofibroblast biology and new therapeutic perspectives. Molecular Biology Reports. 2010; (2): 78.
14. Gass JDM. Macular dysfunction caused by epiretinal membrane contraction. In: Stereoscopic Atlas of Macular Diseases: Diagnosis and Treatment. 1997; 2 (4): 938–50.
15. Kuranova OI. Izuchenie effektivnosti mikroimpul'snogo lazernogo vozdejstviya dlinoj volny 577 nm pri makulyarnom oteke posle hirurgicheskogo udaleniya idiopaticheskoj epiretinal'noj membrany (dissertation). 2014; 33.
16. Zaharov VD, Borzenok SA, Gorshkov IM, Kolesnik SV, Kolesnik AI, Kupriyanova AG, Ostrovskij DS, Miridonova AV. Kliniko-eksperimental'naya ocenka rannego hirurgicheskogo lecheniya idiopaticheskih epiretinal'nyh membran u pacientov s nachal'nymi priznakami patologicheskogo processa. Sovremennye tekhnologii v oftal'mologii. 2018; 21 (1): 127–30.
17. Pichi F, Lembo A, Morara M, Veronese C, Alkabes M, Nucci P, Ciardella A. Early and late inner retinal changes after inner limiting membrane peeling. International Ophthalmology. 2013; 34 (2): 437–46.
18. Mazit C, Scholtes F. Assessment of macular profile using optical coherens tomography after epiretinal membrane surgery. Journal Français D'Ophtalmologie. 2008; 31 (7): 667–72.
19. Bu S, Kuijer R, Li X, Hooymans J, Los L. Idiopathic epiretinal membrane. Retina. 2014; 34 (12): 2317–35.
20. Tahchidi HP, Kachalina GF, Kasmynina TA, Tebina EP. Sposob kombinirovannogo lazernogo lecheniya nachal'noj stadii epiretinal'nogo fibroza. Russian Federation Patent RF № 2634684. 02.11.2017.

Литература

1. Балашова Л. М., Зайцева Н. С., Саксонова Е. О. и др. Патогенетические факторы развития пролиферативной витреоретинопатии при дистрофической отслойке сетчатки. Пролиферативный синдром в офтальмологии. 2000; (1): 12–3.
2. Campochiaro PA. Pathogenic mechanisms in proliferative vitreoretinopathy. Archives of ophthalmology. 1997; 115 (2): 407–8.
3. Pastor JC. Proliferative vitreoretinopathy: an overview. Survey of Ophthalmology. 1998; 43 (1): 3–18.
4. Качалина Г. Ф., Дога А. В., Касмынина Т. А., Куранова О. И. Эпиретинальный фиброз: патогенез, исходы, способы лечения. Офтальмохирургия. 2013; (4): 108–10.
5. Захаров В. Д., Борзенок С. А., Горшком И. М., Колесник С. В., Колесник А. И., Миридонова А. В. Этиопатогенетические аспекты и роль структур витреоретинального интерфейса в формировании идиопатических эпиретинальных мембран. Практическая медицина. 2018; 114 (3): 71–6.
6. Пономерёва Е. Н., Казарян А. А. Структурно-функциональные особенности макулярной зоны сетчатки при идиопатической эпиретинальной мембране. Российский офтальмологический журнал. 2013; 6 (2): 66–9.
7. Guidry C. The role of Muller cells in fibrocontractive retinal disorders. Progress in Retinal and Eye Research. 2005; 24 (1): 75–86.
8. Harada C, Mitamura Y, Harada T. The role of cytokines and trophic factors in epiretinal membranes: Involvement of signal transduction in glial cells. Progress in Retinal and Eye Research. 2006; 25 (2): 149–64.
9. Zhao F, Gandorfer A, Haritoglou C. Epiretinal cell proliferation in macular pucker and vitreomacular traction syndrome: analysis of flat-mounted internal limiting membrane specimens. Retina. 2013; 33 (1): 77–88.
10. Joshi M, Agrawal S, Christoforidis JB. Inflammatory mechanisms of idiopathic epiretinal membrane formation. Mediators Inflammation. 2013; DOI: 10.1155/2013/192582.
11. Speca S, Giusti I, Rieder F, Latella G. Cellular and molecular mechanisms of intestinal fibrosis. World Journal of Gastroenterology. 2012; 18 (28): 3635–61.
12. Шурыгина И. А. и др. Фибробласты и их роль в развитии соединительной ткани. Сибирский медицинский журнал (Иркутск). 2012; 110 (3): 8–12.
13. Hinz B, Gabbiani G. Fibrosis: recent advances in myofibroblast biology and new therapeutic perspectives. Molecular Biology Reports. 2010; (2): 78.
14. Gass JDM. Macular dysfunction caused by epiretinal membrane contraction. In: Stereoscopic Atlas of Macular Diseases: Diagnosis and Treatment. 1997; 2 (4): 938–50.
15. Куранова О. И. Изучение эффективности микроимпульсного лазерного воздействия длиной волны 577 нм при макулярном отеке после хирургического удаления идиопатической эпиретинальной мембраны (диссертация). 2014; 33.
16. Захаров В. Д., Борзенок С. А., Горшков И. М., Колесник С. В., Колесник А. И., Куприянова А. Г., Островский Д. С., Миридонова А. В. Клинико-экспериментальная оценка раннего хирургического лечения идиопатических эпиретинальных мембран у пациентов с начальными признаками патологического процесса. Современные технологиив офтальмологии. 2018; 21 (1): 127–30.
17. Pichi F, Lembo A, Morara M, Veronese C, Alkabes M, Nucci P, Ciardella A. Early and late inner retinal changes after inner limiting membrane peeling. International Ophthalmology. 2013; 34 (2): 437–46.
18. Mazit C, Scholtes F. Assessment of macular profile using optical coherens tomography after epiretinal membrane surgery. Journal Français D'Ophtalmologie. 2008; 31 (7): 667–72.
19. Bu S, Kuijer R, Li X, Hooymans J, Los L. Idiopathic epiretinal membrane. Retina. 2014; 34 (12): 2317–35.
20. Тахчиди Х. П., Качалина Г. Ф., Касмынина Т. А., Тебина Е. П. Способ комбинированного лазерного лечения начальной стадии эпиретинального фиброза. Патент РФ № 2634684. 02.11.2017.